Volume 14, No. 2

December, 1963

SOVIET ATOMIC ENERGY

АТОМНАЯ ЭНЕРГИЯ
(ATOMNAYA ÉNERGIYA)

TRANSLATED FROM RUSSIAN

CONSULTANTS BUREAU

JOURNALS: METALLURGY
in cover-to-cover translation

METALLURGIST
(METALLURG)

A technical journal of the Soviet Ministry of the Metallurgical Industry. Reviews new techniques, at Russian and foreign factories, for improving output and quality. Publishes articles on new inventions and suggestions for improvement of existing equipment. Includes all aspects of the most recent Soviet metallurgical research from ore to finished product and application. Covers: smelting; refining; processing; internal structure; applications of radioactive isotopes; etc. Typical sample sections include articles on blast furnaces, steel making, rolling and pipes, organization of production and economy, power and mechanical equipment. Translation Editor: Professor Bruce Chalmers. Published in cover-to-cover translation by the Board of Governors of ACTA METALLURGICA and distributed by CONSULTANTS BUREAU.

Annual Subscription: 12 issues bound in six volumes, $25.00
(Special price to members of ASM and AIME and other cooperating Societies of Acta Metallurgica.)

METAL SCIENCE AND HEAT TREATMENT OF METALS
(METALLOVEDENIE I TERMICHESKAYA OBRABOTKA METALLOV)

Reports the results of research in metallography and thermal treatment of metals both in the USSR and abroad. This journal publishes papers on production of alloys; research into phase transformations, corrosion, surface and metal strength, the influence of varied processes on properties of metals; and synthesis of new steels and alloys with special properties. Extensive consideration is given to research in heat treatment of metals; other features include surveys on metallographic problems, book reviews, abstracts of non-Soviet literature, and discussions of technical problems. Translation Editor: Professor Bruce Chalmers. Published in cover-to-cover translation by the Board of Governors of ACTA METALLURGICA and distributed by CONSULTANTS BUREAU.

Annual Subscription: 12 issues bound in six volumes, $24.00
(Special price to members of ASM and AIME and other cooperating Societies of Acta Metallurgica.)

REFRACTORIES
(OGNEUPORY)

Published by the State Scientific and Technical Commission of the Council of Ministers of the USSR, and the Central Administration of the Scientific and Technical Society of Ferrous Metallurgy. Covers subjects dealing with the production and technology of refractory materials and their applications in industry. Papers from the USSR and abroad on research and testing methods involving these materials are included in the journal coverage. Regular sections include: production; mechanics of production; practical application of refractories; research; news and foreign science. Translation Editor: Professor William D. Kingery. Published in cover-to-cover translation by the Board of Governors of ACTA METALLURGICA and distributed by CONSULTANTS BUREAU.

Annual Subscription: 12 issues bound in six volumes, $16.00
(Special price to members of ASM and AIME and other cooperating Societies of Acta Metallurgica.)

SOVIET POWDER METALLURGY AND METAL CERAMICS
(POROSHKOVAYA METALLURGIYA)

The results of theoretical and applied research in powder metallurgy (metal ceramics, cermets) and practical plant experience in the Soviet Union and abroad. The journal is the official organ of the Institute of Metal Ceramics and Special Alloys of the Ukrainian Academy of Sciences, and reports advances in the following areas: theoretical; metal powders; powder metal materials for machine parts; alloys and products with special physical properties; refractory compounds and hard metals; refractory and rare metals; design, economics and equipment; control methods, tests and standardization; safety engineering; and technical information.

Annual Subscription: 6 issues, $80.00

SEND FOR SAMPLE ISSUES

CONSULTANTS BUREAU 227 W. 17 ST., NEW YORK 11, N.Y.

SOVIET ATOMIC ENERGY

A translation of **ATOMNAYA ÉNERGIYA**
A publication of the Academy of Sciences of the USSR

Vol. 14, No. 2 December, 1963

CONTENTS

Annual Subscription: $95 **Single Issue: $30** **Single Article: $15**

CONTENTS (continued)

NOTE

The Table of Contents lists all materials that appear in Atomnaya Énergiya. Those items that originated in the English language are not included in the translation and are shown enclosed in brackets. Whenever possible, the English-language source containing the omitted reports will be given.

Consultants Bureau Enterprises, Inc.

DIFFUSION OF A PLASMA IN A MAGNETIC FIELD DUE TO COLLISIONS

S. G. Alikhanov, V. E. Zakharov, and G. L. Khorasanov

Translated from Atomnaya Énergiya, Vol. 14, No. 2,
pp. 137-142, February, 1963
Original article submitted February 10, 1962

A microwave method has been used to study diffusion in the afterglow of a helium plasma. The investigation has been carried out for experimental parameters such that the diffusion across the magnetic field is due to electron-ion collisions. The measured diffusion coefficients in magnetic fields ranging from 700-800 Oe are in agreement with those computed on the basis of classical Coulomb collision theory. At magnetic fields ranging from 1000 to 5000 Oe there is an appreciable deviation from theory, in which case the diffusion coefficient is proportional to 1/H. We have obtained an asymptotic solution of the diffusion equation describing the density decay in the afterglow of a completely ionized plasma in the axially symmetric case.

Introduction

In recent years there has been a great deal of interest in the nature of the diffusion of a fully ionized plasma in a magnetic field. Experiments in this connection have been carried out with a thermal cesium plasma [1, 2]. However, the coefficients describing diffusion in a fully ionized plasma can be measured with plasmas in which the degree of ionization is small, provided the conditions are such that the Coulomb collisions predominate in the diffusion flux across the magnetic field. These conditions can be produced in an afterglow because in an electron gas at low temperatures the cross section for electron-ion collisions is many orders of magnitude greater than the cross section for electron-neutral atom collisions [3, 4].

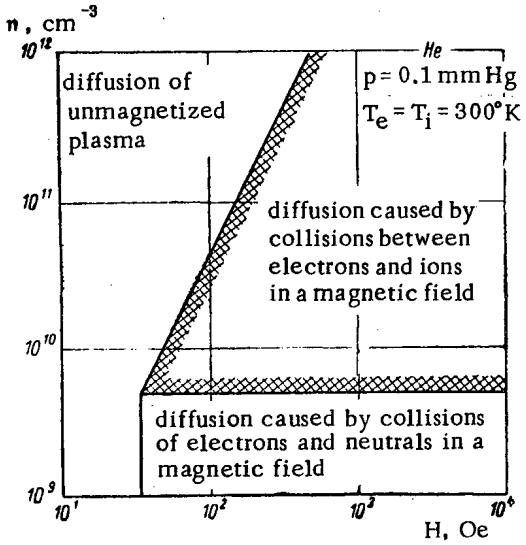

Fig. 1. Diagram of diffusion modes in a three-component plasma.

The region of diffusion due to Coulomb collisions in a three-component plasma as a function of electron density n and magnetic field is shown in Fig. 1. We consider here the typical case of decay of a helium plasma produced by a pulsed microwave discharge. The lower value of the density is that for which the electron-ion collision frequency is equal to the electron-neutral collision frequency. The upper limit is the border between the region of Coulomb diffusion and the region of diffusion due to ion-neutral collisions. This transition occurs when the coefficient of Coulomb diffusion across the magnetic field $D_{ei}^{\perp}$ increases with increasing electron density to such a great extent that it becomes comparable to the diffusion coefficient in the absence of a magnetic field, D_{ia}^{n}. It is evident from Fig. 1 that a rather large region of diffusion corresponding to Coulomb collisions is available for experiments.

Theory of the Experiment

The variation in the density of charged particles in a plasma in which there are no volume processes (ionization, recombination, etc) is described by the usual diffusion equation

$$\frac{\partial n}{\partial t} = \nabla (D \nabla n). \qquad (1)$$

The investigation of plasma decay is carried out in a long thin tube ($L \gg R$) in a fixed longitudinal magnetic field. If $\frac{D_{ei}^{\perp}}{R^2} \gg \frac{D_{ia}^{\parallel}}{L^2}$, a condition that is satisfied in the present experiment, the flux along the axis can be neglected and the diffusion equation for cylindrical geometry becomes

$$\frac{\partial n}{\partial t} = \frac{1}{r}\frac{\partial}{\partial r}\left(D_{ei}^{\perp} r \frac{\partial n}{\partial r} \right). \tag{2}$$

The coefficient of ambipolar diffusion across a magnetic field due to Coulomb collisions is given by [5, 6]

$$D_{ei}^{\perp} = \alpha n, \tag{3}$$

where

$$\alpha = \frac{8\pi}{3}\left(\frac{ce}{H}\right)^2 \left(\frac{m}{kT}\right)^{1/2} \ln \Lambda.$$

Here e and m are the charge and mass of the electron; k is the Boltzmann constant; H is the magnetic field; T is the equilibrium temperature of the plasma (it is assumed that the plasma components reach thermal equilibrium); $\ln \Lambda$ is the Coulomb logarithm, which is defined as follows [6]:

$$\ln \Lambda = \ln \left[\frac{3}{2}\frac{1}{e^3}\left(\frac{k^3 T^3}{\pi n}\right)^{1/2} \right]. \tag{4}$$

In the present case the quantity α can be taken to be independent of coordinates and time.

Converting to the dimensionless variables

$$y = \frac{n}{N_0};\ x = \frac{r}{R};\ \tau = \frac{t}{\tau_0};\ \tau_0 = \frac{R^2}{\alpha N_0};\ N_0 = n|_{r=0,\ t=0}, \tag{5}$$

we write Eq. (2) in the form

$$\frac{\partial y}{\partial \tau} = \frac{1}{x}\frac{\partial}{\partial x}\left(xy \frac{\partial y}{\partial x} \right). \tag{6}$$

The following boundary conditions apply for Eq. (6):

$$\left.\frac{\partial y}{\partial x}\right|_{x=0} = 0;\ y|_{x=1} = 0. \tag{7}$$

The solution of Eq. (6) is written as a series in even powers of x:

$$y = y_0 + y_1 x^2 + \ldots + y_k x^{2k} + \ldots \tag{8}$$

(it is evident that the coefficients of the odd powers must vanish because $\left.\frac{\partial y}{\partial x}\right|_{x=0} = 0$).

We obtain the following system of equations for the functions $y(\tau)$:

$$\left.\begin{aligned} \frac{\partial y_0}{\partial \tau} &= 4 y_0 y_1; \\ \frac{\partial y_1}{\partial \tau} &= 8\,(2 y_0 y_2 + y_1^2); \\ &\cdots\cdots\cdots\cdots \\ \frac{\partial y_k}{\partial \tau} &= 2\,(k+1)^2 \sum_{i=0}^{k+1} y_i y_{k+1-i}. \end{aligned}\right\} \tag{9}$$

Now, if $y_0(\tau)$ is given arbitrarily we can obtain all the $y_k(\tau)$. We investigate possible asymptotic forms of the function $y_0(\tau)$.

If $y_0(\tau) \sim e^{-\gamma\tau}$, then $y_k(\tau)$, starting with k = 2, becomes negative and increases exponentially at large τ. Consequently, for certain values of x, $y_0(x, \tau)$ increases as $\tau \to \infty$; this is not physically reasonable.

Let $y_0(\tau) = a\tau^q$. Then it can be shown by mathematical induction that $y_k(\tau) = \beta_k \tau^{-k(1+q)+q} a^{1-k}$, where β_k is independent of a. In this case the series in Eq. (8) can be reduced to the form of a function:

$$y(x, \tau) = a\tau^q G\left(\frac{x^2}{a\tau^{q+1}}\right), \tag{10}$$

where G is some unknown function.

If $q \neq -1$, solutions of the type given in (10) can not satisfy the boundary conditions. We find

$$y|_{x=1} = a\tau^q G\left(\frac{1}{a\tau^{q+1}}\right) = 0 \text{ for all } \tau, \text{ i.e., } y \equiv 0.$$

If $q = -1$

$$y(x, \tau) = \frac{a}{\tau} F\left(\frac{x^2}{a}\right). \tag{11}$$

The function F can be found from Eqs.(9) in the form of a series:

$$F = 1 - \frac{\lambda^2}{4} - \frac{\lambda^4}{64} - \frac{\lambda^6}{288} - \frac{\lambda^8}{1024} - \ldots, \tag{12}$$

where

$$\lambda^2 = \frac{x^2}{a}.$$

This function is positive at small values of λ and vanishes when $\lambda = \lambda_0$.

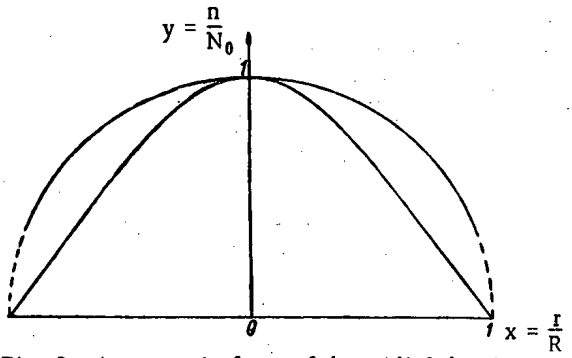

Fig. 2. Aysmptotic form of the radial density distribution in a plasma diffusion across a magnetic field: for the upper curve $D_\perp = \alpha n$, for the lower curve $D_\perp$ = const.

When F = 0 the series in (12) converges very slowly so that λ_0 can not be found directly from it. In order to find λ_0 we substitute $y = (1/\tau) F(x^2)$ in Eq. (6). The equation for F is then

$$-F = \frac{1}{2x} \frac{d}{dx}\left(x \frac{d}{dx} F^2\right). \tag{13}$$

We multiply this equation by 2x, integrate between the limits of 0 and x, divide by x, and integrate over the limits $(0, \lambda_0)$. We find

$$-2 \int_0^{\lambda_0} \frac{dx}{x} \int_0^x xF\, dx = F^2 |_0^{\lambda_0} = -1.$$

Substituting F in the form of the series in (12) we obtain an equation for λ_0:

$$-1 + \frac{\lambda_0^2}{2} - \frac{\lambda_0^4}{32} - \frac{\lambda_0^6}{1152} - \frac{\lambda_0^8}{9216} - \ldots = 0. \tag{14}$$

This series converges rapidly. Retaining the first three terms we find $\lambda_0^2 = 2.4$. The higher terms give a correction of approximately 1%.

To satisfy the boundary conditions we write $a = 1/\lambda_0^2$. Finally,

$$y(x, \tau) = \frac{1}{\lambda_0^2 \tau} F(\lambda_0^2 x^2). \tag{15}$$

Investigation of the function F (x) shows that near the points x = 1 it is of the form $F \simeq \text{const}\sqrt{1-x}$ so that $\left.\frac{\partial F}{\partial x}\right|_{x=1} = \infty$. This relation has a simple physical meaning.

Near x = 1 the density vanishes and for a nonvanishing flux the density gradient must become infinite.

Evidently, a wide class of physically reasonable solutions of the boundary value problem (7) for Eq. (6) will have the same asymptotic behavior. This follows from the fact that in regions of space where n is large there is a rapid equalization of the density whereas at the walls there is an infinite gradient.

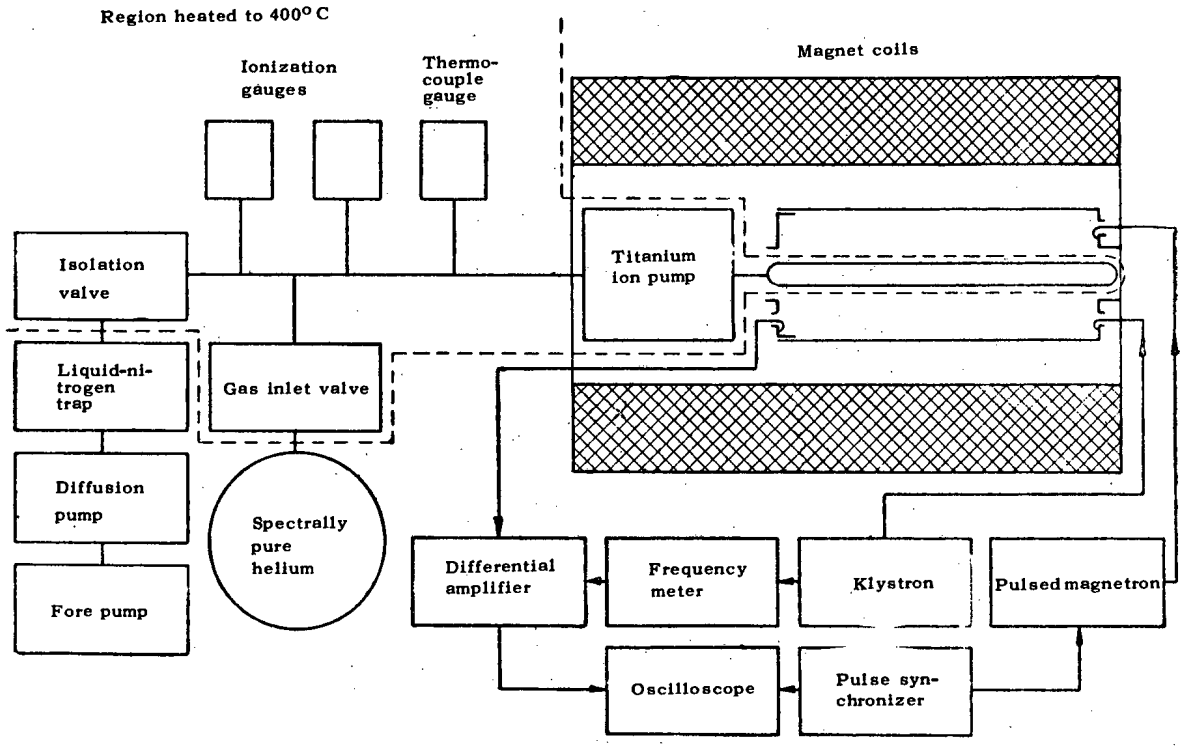

Fig. 3. Block diagram of the apparatus.

We note that the function

$$y(x, \tau) = \frac{1}{\lambda_0^2 \tau + C} F(\lambda_0^2 x^2),$$

where C is an arbitrary constant, is an exact solution of Eq. (6) with the boundary conditions given in (7) and the initial condition

$$y(x, \tau)|_{\tau=0} = \frac{1}{C} F(\lambda_0^2 x^2).$$

In particular, if C = 1 we obtain a function that describes the diffusion process when the initial density at the axis of the tube is N_0. In this case the change in density at the axis of the tube $n_0(t)$ is given by

$$\frac{1}{n_0(t)} - \frac{1}{N_0} = \frac{at}{\Lambda^2}, \tag{16}$$

where $\Lambda^2 = R^2/2.4$ is the square of the diffusion length.

In Fig. 2 we show the asymptotic form of the radial density distribution computed from Eq. (12) for the case of diffusion across a magnetic field caused by Coulomb collisions. For purposes of comparison, in the same figure we show the density distribution when the diffusion coefficient is independent of density [the lower curve $y = J_0(\varkappa_{01} x)$].

Experimental Method

In contrast with measurements of the diffusion coefficient (caused by collisions of charged particles and neutrals), for the determination of which it is sufficient to know the relative plasma density, in the present case the accuracy in the measurement of the diffusion coefficient depends on the accuracy of the determination of the absolute density. To determine the mean density in the present experiment the discharge tube is placed in a long cylindrical resonator in which the TH_{019} mode is excited. The resonator simultaneously serves for producing the plasma by means of a microwave pulse.

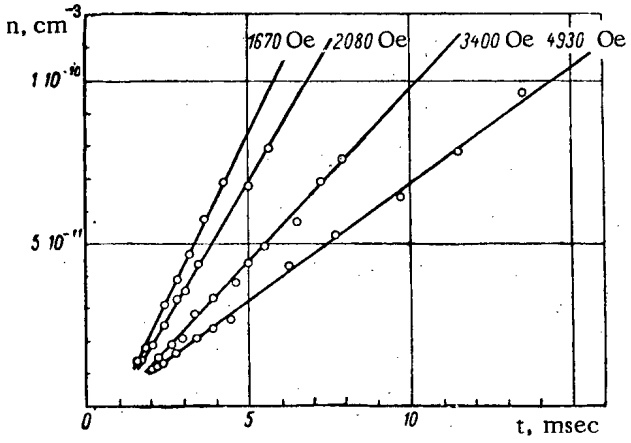

Fig. 4. Typical experimental curves.

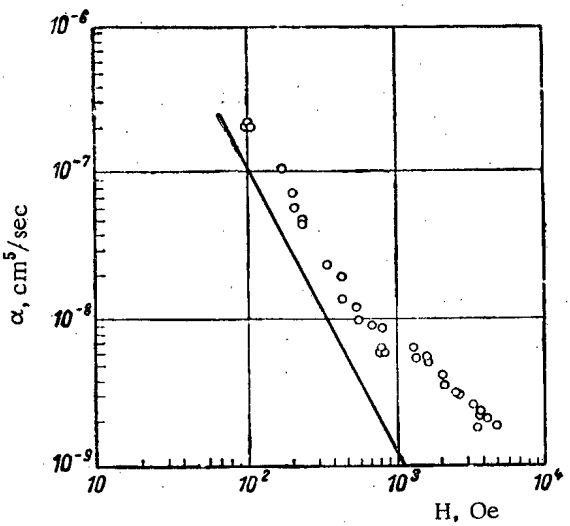

Fig. 5. Variation of diffusion coefficient with magnetic field; the circles denote the experimental points while the solid line is predicted by the Spitzer-Braginskii theory [5, 6].

The long resonator length allows us to neglect end effects in analyzing the interaction of the microwave with the plasma column and also yields the possibility of obtaining a uniform plasma over the length of the tube. A diagram of the apparatus is shown in Fig. 3 and a detailed description has been given in [7].

The determination of the transfer coefficient from the shift of the resonant frequency of the cavity as a function of plasma density requires analytic investigation of the interaction of the TH_{01l} mode with a plasma in a magnetic field.

However, because the plasma radius in the present experiments is small compared with the cavity radius, the transverse components of the electric field can be neglected. This procedure is valid when $k_{\parallel} < k_{\perp}$ and $\omega \neq \omega_{ce}$, where $k_{\parallel} = l\pi/L_0$; $k_{\perp} = \varkappa_{01}/R_0$ (L_0 and R_0 are the length and radius of the cavity; $\varkappa_{01}$ is the first root of the zero-order Bessel function); ω is the resonance frequency of the cavity; ω_{ce} is the electron cyclotron frequency.

In this case the shift of the resonant frequency of the cavity in the presence of plasma is given by the usual perturbation-theory expression [8]:

$$\Delta\omega = -\frac{1}{2\omega}\frac{\int_{\text{plasma}} \omega_0^2 E^2\, dV}{\int_{\text{cavity}} E^2\, dV}, \qquad (17)$$

where ω_0 is the plasma frequency.

Substituting in Eq. (17) the expressions for the density distribution (12) and the electric field distribution in the TH_{01l} mode, we have

$$\Delta\omega = -\frac{4e^2 n_0}{m\omega}\frac{k_\perp^2}{k_\perp^2+k_\parallel^2}\frac{\int_0^R\int_0^{2\pi}\int_0^{L_0} J_0^2(k_\perp r)\cos^2(k_\parallel z)\left[1-\frac{3}{5}\frac{r^2}{R^2}-\frac{3}{80}\frac{r^4}{R^4}-\ldots\right] r\,dr\,d\varphi\,dz}{L_0 R_0^2 J_1(x_{01})}. \quad (18)$$

Integrating with the experimental parameters R_0 = 4.25 cm, L_0 = 75 cm, R = 0.8 cm and $\omega = 2\pi \cdot 3.24 \cdot 10^9$ sec^{-1} we find

$$n_0 = 2.1 \cdot 10^2 \Delta\omega. \quad (19)$$

Discussion of Experimental Results

The measurements of density in the afterglow were carried out in the range 10^{10}-10^{11} cm^{-3}. The lower limit of the measured densities is determined by the lower limit for Coulomb diffusion (cf. Fig. 1) while the upper limit is determined by the time required for the electron gas to cool and the capabilities of the experimental apparatus. The experiments were carried out in a glass tube filled with spectrally pure helium at pressures $5 \cdot 10^{-2} - 2 \cdot 10^{-1}$ mm Hg. The system was first outgassed at a temperature of 400°C for a long period of time after which the residual vacuum was of order 10^{-9} mm Hg. In addition, the walls were processed by a microwave discharge operating at the electron cyclotron resonance.

Several experimental curves from which the diffusion coefficients were determined are shown in Fig. 4. Inasmuch as the experimentally observed time dependence of the density is in good agreement with Eq. (16) it is evident that the process responsible for the removal of charged particles has a quadratic dependence on density.

The deviation from Eq. (16) at the beginning of decay (extrapolation of the curves kt = 0 gives $N_0 < 0$) is due to the fact that in the initial stage of decay in the plasma caused by microwave breakdown there are other mechanisms in operation which have an important effect on the density distribution; these include cooling of the electron gas and other factors which are not taken into account in Eq. (16).

In Fig. 5 the points show the measured values of the coefficients α as a function of the magnetic field. The solid line in the same figure corresponds to Eq. (3) for the coefficient of diffusion in a fully ionized gas. It follows from an analysis of the experimental results that up to the field values of 700-800 Oe we have a $D_{ei}^{\perp} \sim 1/H^2$ dependence. The deviation in the absolute value of the diffusion coefficient from the theoretical value is possibly due to systematic errors in the determination of density. An estimate of the errors in the experimental method gives a value of ± 30%, which is somewhat smaller than the observed discrepancy.

In the region from 1000 to 5000 Oe the dependence approaches 1/H. The coefficient for volume recombination of electrons and ions as well as the coefficient for Coulomb diffusion are directly proportional to the density of charged particles. Hence, the experimentally observed coefficient for the removal of particles is actually the sum $\alpha = \alpha_{rec} + \alpha_{dif}/\Lambda^2$. Starting from these considerations, the deviation in the coefficient α at H > 1000 Oe from the theoretical dependence ($\alpha_{dif} \sim 1/H^2$) can be easily attributed to volume recombination (for example of the form $He_2^+ + e$) if it were not so close to the 1/H dependence on magnetic field. Under these conditions one must make some artifical assumptions as to the dependence of α_{rec} on magnetic field.

In conclusion the authors wish to thank I. F. Kvartskhava for his interest, R. Z. Sagdeev for valuable discussions of the theory, and G. G. Podlesnov for help in the experiments.

LITERATURE CITED

1. N. D'Angelo and N. Rynn, Phys. Fluids, 4, 275 (1961).
2. R. Knechtli and J. Wada, Phys. Rev. Lett., 6, 215 (1961).
3. A. Dougal and L. Goldstein, Phys. Rev., 109, 615 (1958).
4. V. E. Golant and A. P. Zhilinskii, "Zh. tekhn. fiz.", 30, 745 (1960).
5. S. I. Braginskii, "Plasma Physics and the Problem of a Controlled Thermonuclear Reaction" [in Russian]. Moscow, Izd. AN SSSR, p. 178 (1958).
6. L. Spitzer, Physics of Fully Ionized Gases [Russian translation]. Moscow, Izd. inostr. lit. (1957).
7. S. G. Alikhanov et al., "Zh. tekhn. fiz.", 32, 1205 (1962).
8. G. Suhl and L. Walker, Problems of Waveguide Transmission in Gyrotropic Media [Russian translation]. Moscow, Izd. inostr. lit. (1955).

THE EXPERIMENTAL PLASMA DEVICE S-1 WITH HELICAL MAGNETIC FIELDS (STELLARATOR)

I. P. Afonin, B. I. Gavrilov, E. K. Zavoiskii, F. V. Karmanov, G. P. Maksimov, A. G. Plakhov, P. A. Cheremnykh, and V. V. Shapkin

Translated from Atomnaya Énergiya, Vol. 14, No. 2, pp. 143-150, February, 1963
Original article submitted April 17, 1962

We give a brief description of the construction and operation of a stellarator in the form of a racetrack with helical magnetic fields which has been built by the I. V. Kurchatov Order of Lenin Atomic Institute, Academy of Sciences, USSR. Certain results characterizing the operation of this apparatus are described.

The idea of using a system with helical fields (stellarator) was first suggested by Spitzer [1, 2]. In systems of this kind the magnetic force lines undergo a rotational transform about the magnetic axis. The magnetic axis is that line of force which closes on itself after one circuit around the machine. Spitzer and his colleagues have proposed methods of obtaining closed helical fields both by means of topological variation of the toroidal configuration (figure-eight configuration) and by means of special helical windings. Devices with special helical windings are of great interest as compared with figure-eight devices because in addition to the rotational transform of the magnetic force lines they exhibit a number of other interesting properties. In these devices the number of helical windings and the current in the helical windings can be used to change the region of closed magnetic surfaces and the rotational transform angle at different radii. Soviet scientists have also made a large contribution to the theory of the complicated helical field configurations produced by helical windings [3-7].

Theory predicts that the plasma must be stable in the magnetohydrodynamic sense in devices with helical fields in the absence of strong longitudinal currents; for this reason it was decided to build such a device in the I. V. Kurchatov Institute of Atomic Energy. It should be noted, however, that the experimental data on plasma containment have shown a more rapid loss of charged particles from the discharge than that predicted by theory. This might be due to inadequate accuracy in realizing the required magnetic field configurations or might be due to some other processes, as yet unknown, which operate in the plasma. For this reason, in the construction of the device special attention was given to the accuracy of the required magnetic field configurations.

Construction of the Apparatus

The apparatus is in the shape of a racetrack. A general view is shown in Fig. 1. The basic machine parameters are as follows: inner diameter of the vacuum chamber 10 cm; length of the straight sections 120 cm; mean radius of curvature 60 cm; perimeter 617 cm. The longitudinal magnetic field can be raised to 25 kilooersteds; the quantity $H_\perp/H_0$, which characterizes the helical field and has been introduced in [4], can be varied from 0.2 to 0.6. The maximum loop voltage is 400 V. The condenser bank used to produce the longitudinal magnetic field has an energy storage of 1700 kilojoules ($C = 3.45 \cdot 10^{-2}$ farads, v = 10 kV). The energy storage of the condenser bank that supplies the ohmic heating transformers is 45 kilojoules ($C = 3.6 \cdot 10^{-3}$ farads, v = 5 kV).

The longitudinal magnetic field is produced by a magnetic system consisting of coils and solenoids. The solenoids are located on the curved portions of the vacuum chamber while the coils are located on the straight sections. The mean diameter of the coils is 34 cm. Each coil is wound of six turns of rectangular copper tubing 10 × 10 mm^2 with an aperture 5 × 5 mm^2. Between turns there is an insulating gap of 1 mm. After impregnation with an epoxy compound the coils are secured between side walls of nonmagnetic stainless steel. The coil construction is shown in Fig. 2. The distance between coils is 85 mm. To provide "shimming" of the magnetic field between the solenoids and coils in the region of the transition to the curved section, the straight section is provided with four coils having twelve turns with a mean diameter of 200 mm. These are made of copper tubing with diameter 6 × 1 mm, also protected by an epoxy compound, and secured between side walls of stainless teel.

The solenoids are made of copper rings. The basic solenoid is a semi-torus made of textolite. The mean diameter of the rings is 203 mm. They are connected in series by shaped cross sections along which the current flows, forming the semi-torus. In parallel with the cross sections are the compensating conductors in which the current flows in the opposite direction. To the rings are soldered copper tubing 6 × 1 mm in diameter used for water cooling. The solenoid is protected by an epoxy compound. The construction of the solenoid is shown in Fig. 3.

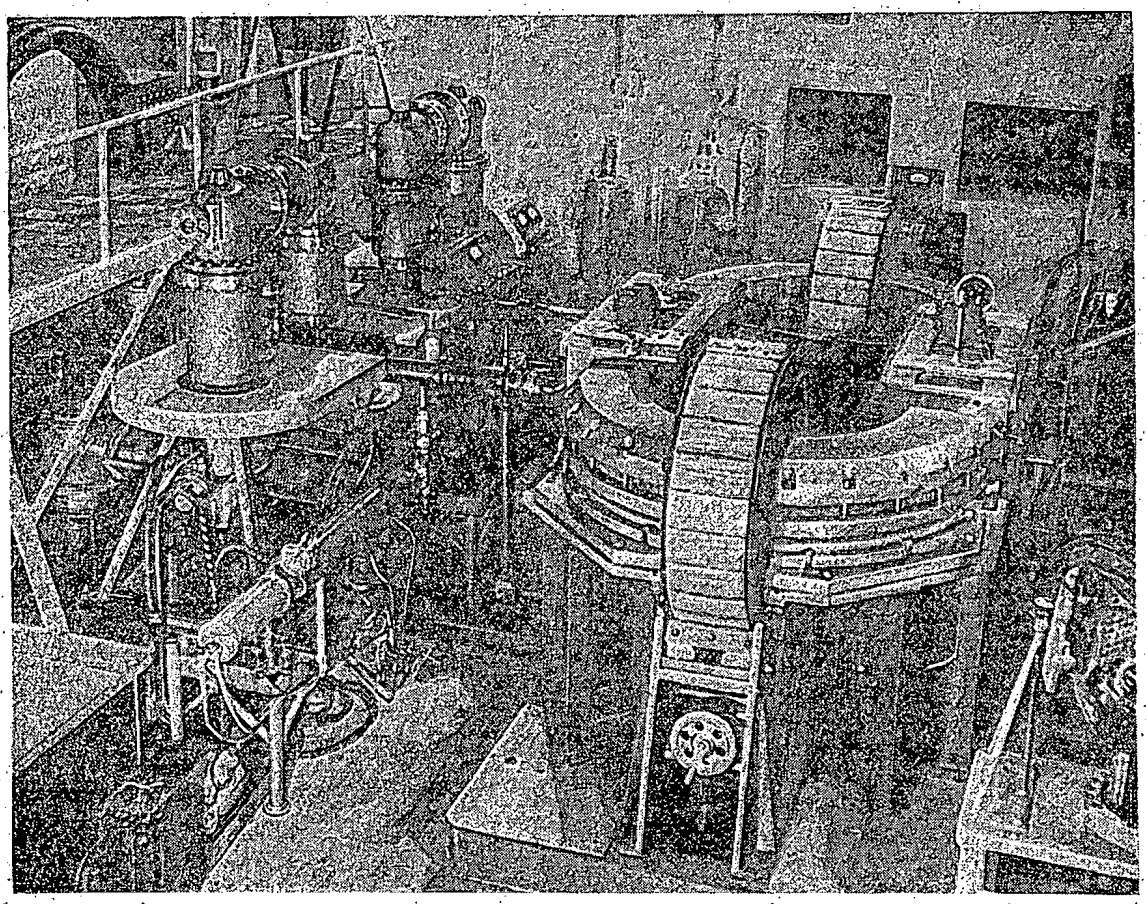

Fig. 1. General view of the S-1 device.

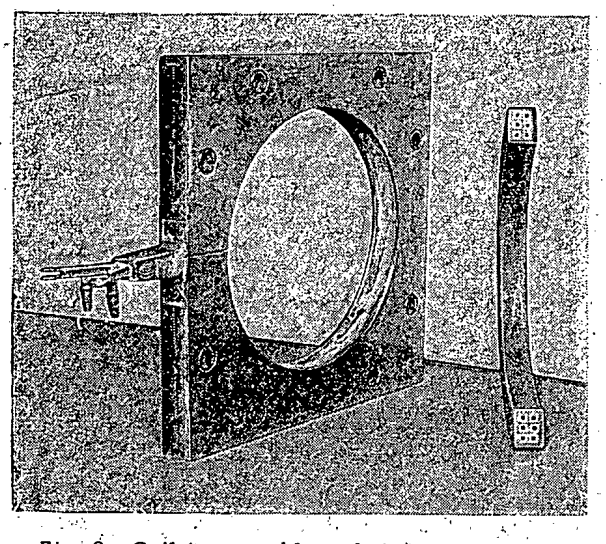

Fig. 2. Coil in assembly and in section.

The main helical windings are frames in the form of a semi-torus assembled from specially shaped rings pressed of AG-4 plastic. The rings have slots at an angle of 12 degrees with respect to the direction of the semi-torus for installation of the helical windings fabricated in the form of a 3-strand winding of copper tubing 8 × 1.5 mm in diameter and consisting of 6 sections. In neighboring sections, each of which consists of four conductors, the current flows in opposite directions. The conductors in the helical winding are connected in series and after installation in the slits the rings are impregnated with an epoxy compound. The helical windings make one turn over the curve; consequently the angle of curvature is 0.0333 rad/cm. In Fig. 4 we show the helical windings before impregnation with the epoxy compound. The semi-torus with the helical windings is located inside the solenoids and is centered in the latter.

The solenoids, coils and helical windings are connected in series. In parallel with the helical winding there is a shunt by means of which the current can be controlled.

The vacuum system of the machine consists of a vacuum chamber, the pumping system, and the gas inlet system. In Fig. 5 we show a sketch of the vacuum chamber, which consists of two semi-tori, two straight sections, and four connection sections, which join the semi-tori to the straight sections.

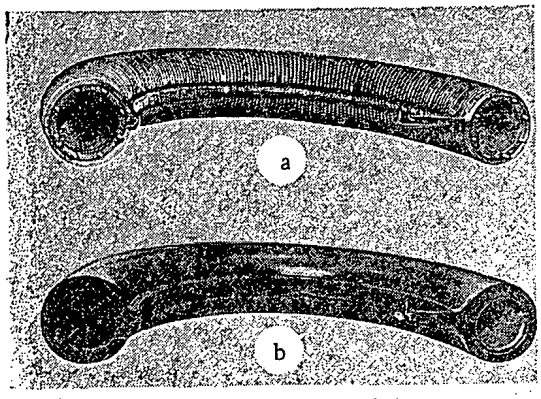

Fig. 3. Solenoid in assembly (a) and protected by epoxy compound (b).

The mean radius of the semi-tori is 60 cm, the inner diameter 10 cm, and the wall thickness 0.2 cm. These are made from 1Kh18N9T stainless steel stamped from sheets of half-sections welded to the generators of the semi-torus. The proper shape of the semi-torus is then achieved by expansion. At the ends of the semi-tori are soldered straight sections 5 cm in length with clamp flanges for joining to the connection sections.

The straight portions of the chamber consist of glass sections, made of 3S-5 glass with inner diameter of 10 cm and a wall thickness of 0.5 cm, and connection joints. The glass-metal transition is made through kovar rings which are soldered to sylphon bellows to protect the glass from stress in installation and outgassing. To the sylphon bellows are soldered flanges for connection to the connection sections.

The connection sections are made from stainless steel. Each connection section has four ports which are used for experimental purposes, for pumping the chamber, and for admission of gas. A heated palladium valve is used for admission of hydrogen while helium is admitted through a needle valve.

To two connection sections through appropriate ports are connected in parallel two oil vapor high-vacuum type VA-0.5-2R vacuum units. These have two traps in series cooled by liquid nitrogen. The maximum pumping rate of the units is 100 liters/sec and can be changed by the DU-100 valves. The fore vacuum is produced by VN-1 pumps.

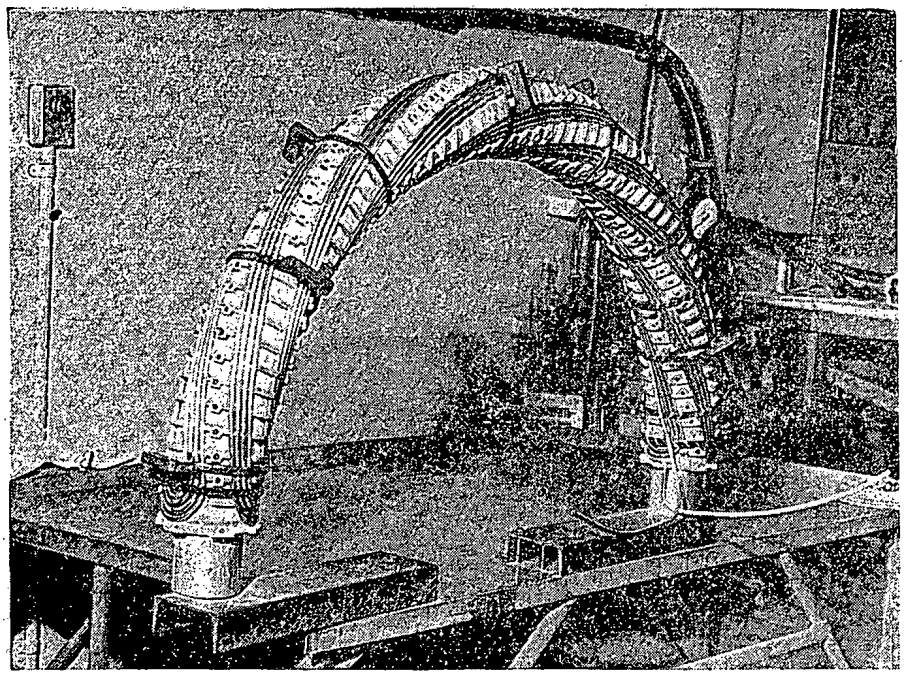

Fig. 4. Helical winding.

All units of the vacuum system up to the fore vacuum use copper gaskets. In principle the assembled vacuum system can be heated to 450°C. However, up to the present, the vacuum system has not been heated completely in assembled form; rather, the individual units of the vacuum system have been outgassed before assembly in a special vacuum unit. The assembled vacuum system can be cleaned by discharge cleaning. The vacuum achieved in the system is $0.8 \cdot 10^{-8}$ mm Hg.

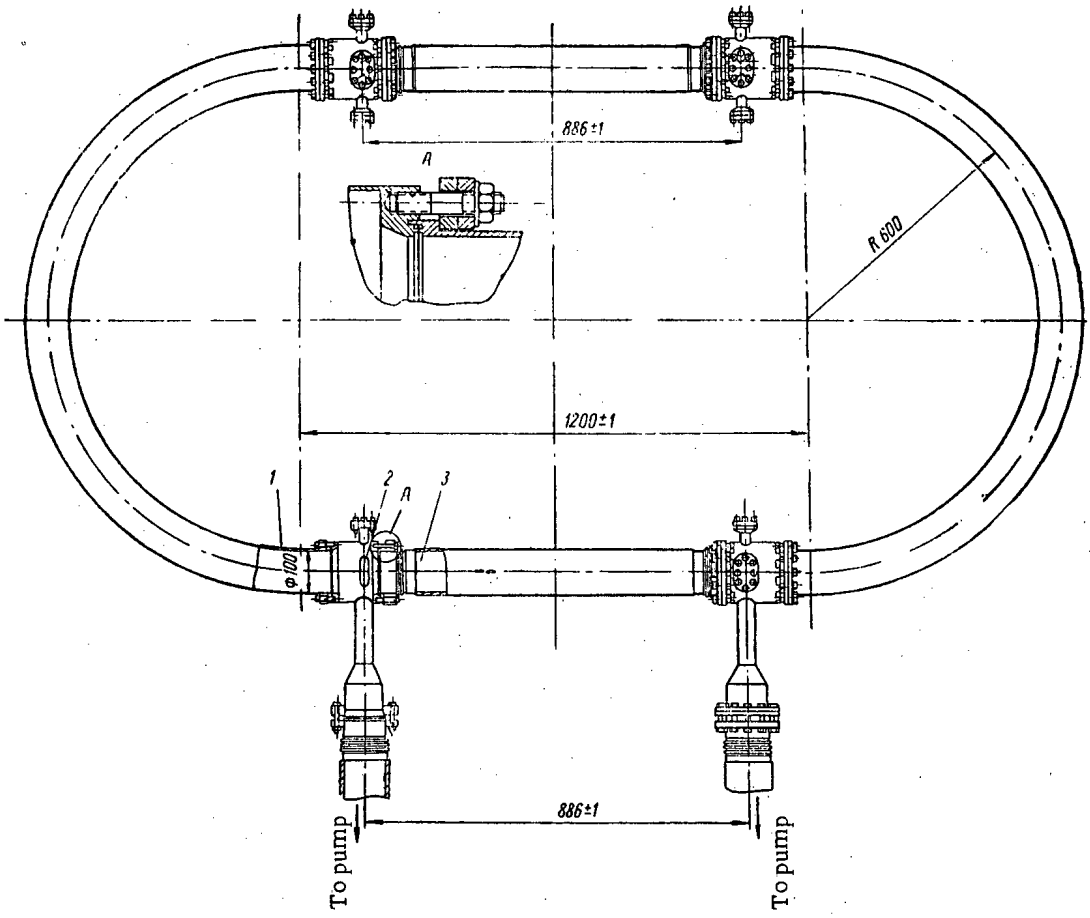

Fig. 5. Vacuum chamber. 1) Semi-torus; 2) connection section; 3) straight section. A) Gasket location.

On the curved sections of the machine are located two transformers for producing the highly ionized hot plasma in the ohmic heating mode. The toroidal cores of the transformers are wound in the form of helices of sheet steel (É-300). The cross section of the core is 600 cm^2. The primary winding of the transformer consists of 25 turns wound uniformly along the core of copper bus with a cross section 15 mm^2. The secondary winding of the transformers is the plasma in the vacuum chamber; this plasma is produced by weak ionization of the operating gas by a radio-frequency field from a special generator.

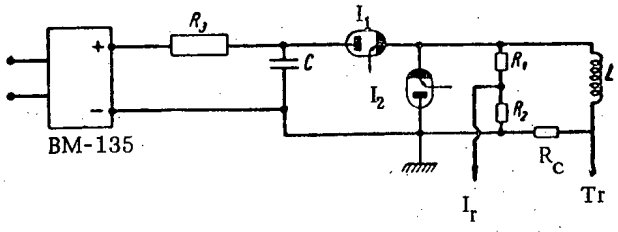

Fig. 6. Diagram showing the power supply for the S-1 device.

On the straight glass sections are located high-frequency circuits for studying the effect of the high-frequency field on the plasma. For these investigations we use a generator with a power of 1 megawatt with a pulse length of 1.5 msec operating at a frequency of 20 Mc. The circuits are located in vacuum shields in which a vacuum of 10^{-6} mm Hg can be produced; the circuits can also be filled with nitrogen or elegas to a pressure of 10 atm to increase the electrical breakdown properties of the circuit.

The machine is mounted on a special support of nonmagnetic material. All supporting details of the magnetic system are also made of nonmagnetic material.

Power Supply

The magnetic system and the transformers are driven from energy stored in condenser banks. The condenser bank that supplies the magnetic system consists of two groups of type IM-150/5 condensers with 458 condensers in each group. The condensers in a group are connected in parallel while the groups are connected in series. Each condenser is protected against overload in the event of breakdown by being connected to the bank through a protective device. A diagram of the supply for the magnetic system is shown in Fig. 6. The bank is charged from a BM-135 supply through a resistance R_3, which is approximately 2 kΩ, made of nichrome wire 1 mm in diameter, and is discharged through the ignitron I_1, which is a type IVS-100/15. A second ignitron I_2 of the same kind is connected in parallel with the load. This ignitron is triggered by a small feedback voltage from the bank. It is used to crowbar the current pulse. In series with the load is connected a calibration resistance R_c, the voltage pulse from which is fed to an oscilloscope used for observing the magnitude and shape of the current pulse in the magnetic system. The pulse from resistance R_2 in the high resistance divider is connected in parallel with the load and serves for observation of the magnitude and shape of the total voltage pulse applied to the magnetic system.

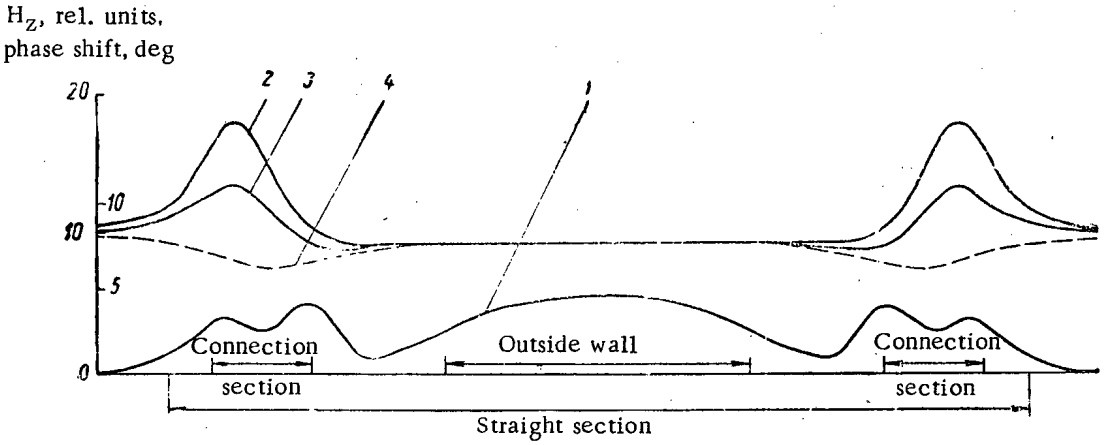

Fig. 7. Graphs showing the phase shift and amplitude of the magnetic field in the region of the straight section: 1) phase shift of the alternating magnetic field; 2-4) amplitude of H_z in relative units (in the region of the connection section the coils have: 2) 20 turns; 3) 12 turns; 4) 6 turns).

The condenser bank which supplies the transformers consists of 24 IM-150/5 condensers connected in parallel. The power supply circuit for the transformers differs from the circuit shown in Fig. 6 only in that the second ignitron I_2 can be fired with the same polarity of the voltage across the load as is used to trigger the first. This makes it possible to obtain a rectangular voltage pulse. The pulse length can be changed by changing the firing time of the second ignitron. To obtain an aperiodic discharge in the circuit a resistance is connected in series with the transformers. Pulses from the divider connected in parallel with the load and from the calibration resistance connected in series with it make it possible to observe the shape and magnitude of the current and voltage pulses in the primary winding of the transformer.

The radio-frequency generator is supplied from a high power modulator. The machine is controlled from a console to which are connected the controls for the power supplies, modulator, generator, vacuum system, charging for both condenser banks, and interlock system. The console also contains a device for programming the cycle of operation of the machine. The apparatus can be controlled manually or automatically.

Startup of the Apparatus and Preliminary Results

Starting up the apparatus means basically the adjustment of the magnetic system. A compensation method was used to measure the longitudinal component along the magnetic field at the axis H_z and at various radii and also to determine the effect of metal parts of the vacuum system. A curve of H_z along the axis of the vacuum chamber is shown in Fig. 7. Curves 2 and 3 are for the case in which the coils with 20 and 12 turns are located in the region of the connection section. The dashed line shows the drop in field when the coils with 6 turns are used. In the same figure we show a curve of the phase shift of an alternating magnetic field at different parts of the apparatus caused by the effect of metal details in the chamber. It is evident from the curve that the maximum phase shift is less than 5% in the region of the connection sections and the jackets.

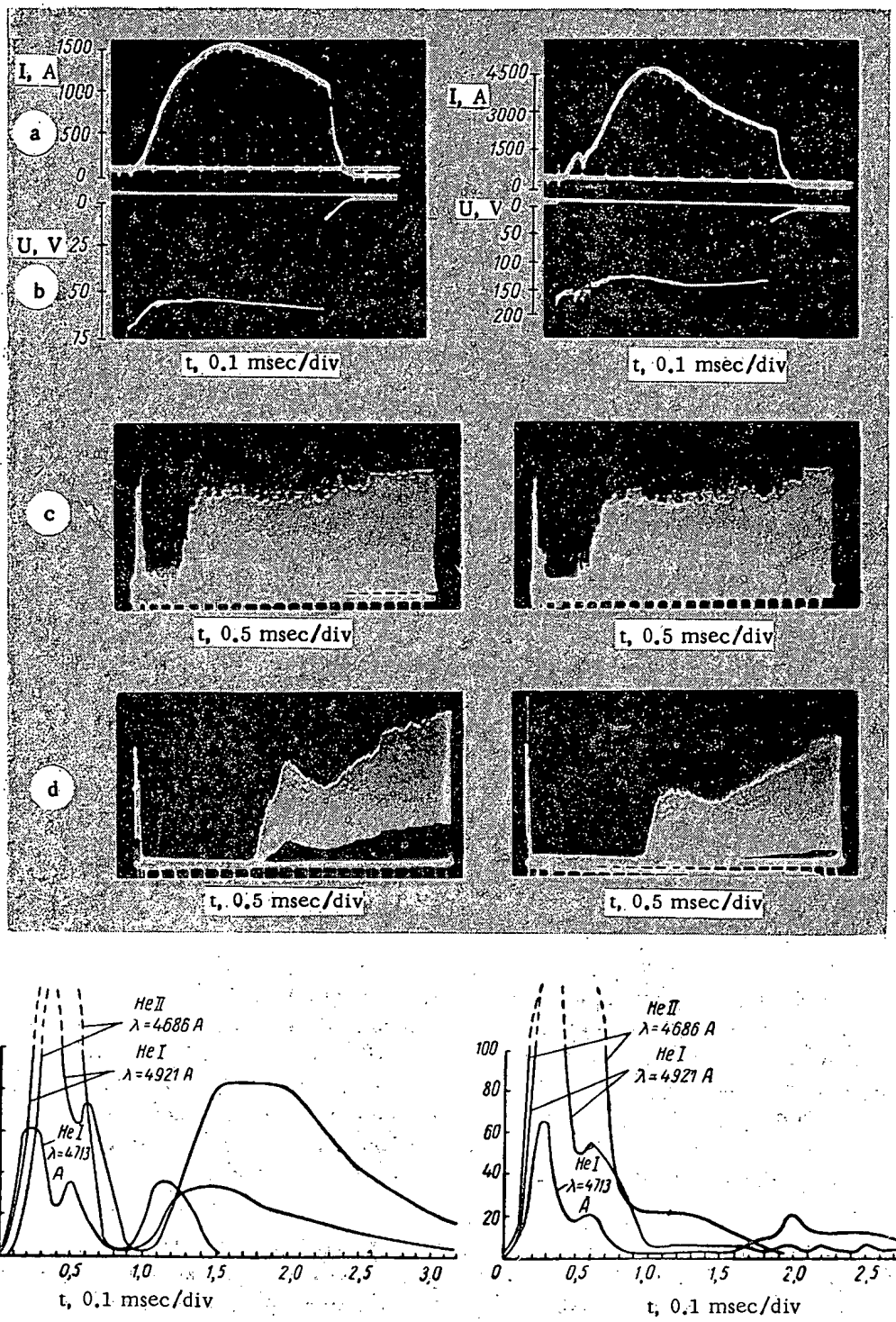

Fig. 8. Ohmic heating of a helium plasma for two values of the circuit voltage (the longitudinal magnetic field is 9.6 kilooersteds, the helium pressure in the chamber before breakdown is $4.5 \cdot 10^{-4}$ mm Hg). In the left column reading from the top down for E = 0.125 V/cm we have a) plasma current; b) loop voltage; c) microwave cutoff at λ = 0.8 cm; d) microwave cutoff at λ = 3 cm; e) emission of the helium line as a function of time. The right column is the same for E = 0.32 V/cm.

To observe complicated magnetic field configurations we have developed earlier the so-called rotating electron-beam method. The assembled magnetic system of the machine was checked with electron beams and the axis of the magnetic system was aligned with the axis of the vacuum chamber by the proper choice of position of the compensating windings. The inner region of the separating magnetic surfaces was determined in the cross section of the vacuum chamber by varying the current in the helical windings. In this case the quantity $H_\perp/H_0$ was 0.55. The magnetic field reaches a peak value some 10 msec after initiation of the discharge and decays in 15 msec.

Various methods are presently in use for investigation of the plasma. The shape and magnitude of the loop voltage pulse around the chamber and the current in the plasma are determined. A microwave transmission technique at 3 cm and 0.8 cm is used to determine the electron density. Optical and spectroscopic measurements using electron optical converters are used to determine the geometry of the plasma emission in time (in total and monochromatic light) by sweeping portions of the spectra in time. Mass spectrometers are used to determine the composition of the gas in the chamber before and after the discharge.

The first experiments on ohmic heating of a helium plasma have been carried out with the apparatus. In Fig. 8, for a pressure of $4.5 \cdot 10^{-4}$ mm Hg and two values of the condenser bank voltage, we show the plasma current, loop voltage, cutoff of the microwave signals at 3 cm and 0.8 cm and emission from the neutral and ionized helium. In both cases the characteristic feature is the relatively high electron density ($1.75 \cdot 10^{13}$ cm^{-3}) after the termination of plasma current. The curves showing the emission of helium lines are obtained by means of an electron-optical light amplifier using a time-resolved spectrum and photometric analysis of the pictures.

Two stages are clearly evident in the emission of all helium lines, including the line HeII (λ = 4686 A). The first stage of intense emission is concluded when the plasma current vanishes. Then there appears a rather intense and long emission pulse. This is especially clear in the experiments with the loop voltage of 0.125 V/cm. When the loop voltage is increased to 0.32 V/cm the general features of the pattern remain the same the only difference being that an important contribution to the plasma emission comes from the ionized helium during the time in which the current flows as well as after it is terminated (the line for the neutral helium is reduced appreciably). This indicates that the electron temperature is increased when the loop voltage is increased.

It if is assumed that the plasma conductivity is uniform over the cross section, its value is of order $6 \cdot 10^{14}$ esu. The electron temperature estimated from the conductivity is 14 eV while the temperature determined from the density ratios of the emission lines of helium is 40 eV.

If we assume that the plasma density falls off exponentially, the mean time constant for decay is 0.5 msec.

Preliminary measurements at different helium pressures show that when the pressure is reduced the effect of the helical windings on the development of the discharge is increased.

The authors wish to thank L. V. Korablev, A. I. Morozov, and L. S. Solov'ev for valuable discussions in the construction of the apparatus and are indebted to A. V. Titov and V. A. Filatov for help in the construction.

LITERATURE CITED

1. L. Spitzer, Proceedings of the International Conference on the Peaceful Uses of Atomic Energy, Geneva (1958). Selected reports of foreign scientists, Vol. 1, Moscow, Atomizdat, p. 505 (1959).
2. Johnson et al., Proceedings of the International Conference on the Peaceful Uses of Atomic Energy, Geneva (1958). Selected reports of foreign scientists, Vol. 1, Moscow, Atomizdat, p. 505 (1959)
3. A. I. Morozov and L. S. Solov'ev, "Dokl. AN SSSR", 128, No. 3, 506 (1959).
4. A. I. Morozov and L. S. Solov'ev, "Zh. tekhn. fiz.", 30, 271 (1960).
5. L. V. Korablev, A. I. Morozov, and L. S. Solov'ev, "Zh. tekhn. fiz.", 31, 1153 (1961).
6. I. M. Gel'fand et al., "Zh. tekhn. fiz.", 31, 1164 (1961).
7. V. F. Aleksin, "Zh. tekhn. fiz.", 31, 1284 (1961).

TO THE MEMORY OF NATAN ARONOVICH YAVLINSKII

Translated from Atomnaya Énergiya, Vol. 14, No. 2,
pp. 151-152, February, 1963

On July 28, 1962 N. A. Yavlinskii was killed in a road accident. The time which has passed has not softened the bitterness of the blow; we are still aware of the finality of our loss. He was a versatile, profound scientist; a manly, simple, and sympathetic person. His whole life was devoted to his creative and inspiring work.

N. A. Yavlinskii was born on February 13, 1912 in Khar'kov, the son of a doctor. He started his working life as a 16-year-old coil winder in the Khar'kov electromechanical plant. At the same time he studied in the Institute to become an engineer. His unusual ability and outstanding talent as an engineer were quickly recognized and in 1939 he was made head of the design bureau of the plant.

N. A. Yavlinskii spent the first years of the war at the front. He took part in the battles near Khar'kov and in the heroic action on the Volga. He went to the front without any special military training and returned as an artillery major with combat decorations. He gained his combat experience during the difficult first years of the war, where he invariably exhibited manliness, persistence and unusual coolness. Even during the worst days he was always confident, giving all he had to the common good.

After the war Natan Aronovich worked in Moscow as head of the design bureau of the All-Union Electrotechnical Institute (VÉI) and from 1948 he headed one of the laboratories in the Institute of Atomic Energy.

His scientific activity covered three regions of modern science. He wrote a number of excellent papers on the theory and planning of electric machines and systems of electroautomatics. Under his leadership one of the first Soviet digital computers was developed and built. He received international acclaim for his work on the investigation of plasma in connection with the controlled thermonuclear reaction.

We will try to cover the main results which he achieved in these directions.

Working before the war at the plant and after the war in VÉI, N. A. Yavlinskii designed and built several new types of electric machines which have found extensive application in industry. As the chief designer of these machines, in 1948 N. A. Yavlinskii was awarded a state prize.

Natan Aronovich also worked successfully on problems in the theory of electric motors; he developed the theory of action of armature reactions in dc motors under iterative transient conditions. He showed that the torque developed on the shaft of the motor depends to a large extent on the reaction of the armature current to the excitation circuit. This theory made it possible to introduce considerable corrections to design methods, for example in rolling mill drives.

Natan Aronovich shared his knowledge and tremendous experience of electrical engineering and automatics with the young workers. For several years he lectured at the All-Union Energy Correspondence Institute. Two of his courses of lectures, "Electric Motors for Automatic Control Systems" and "A Course on Electric Motors for Special Drives," were published in 1956-1957. These works filled a gap which had existed in modern electrotechnical literature.

In the Institute of Atomic Energy he worked on the development of control and supply systems for equipment used in the electromagnetic separation of isotopes.

In recent years the scientific interests of Natan Aronovich have been more and more concerned with very real problems. Because of his sharp penetrative mind and wide erudition in regions of science and technology which were quite different from his usual work, he soon grasped the exceptional importance of electronic computers. Natan

Aronovich was the type of person for whom understanding means acting. He applied his ebullient energy, his talent as an engineer, scientist, and organizer to the construction of computers in the Institute of Atomic Energy. In the opinion of leading specialists these machines are of very high quality and are reliable in operation. Calculations performed with them have been extremely useful not only for the Institute of Atomic Energy, but also for a number of other organizations.

It should be mentioned that these modern computers were developed and built under the direction of N. A. Yavlinskii in an Institute which is not equipped for the solution of such problems, in a very short period and without any special preparation.

In 1951 Natan Aronovich was one of a small group of scientists to commence investigations into the problem of controlled thermonuclear reactions. The engineer had become a physicist. For him this was a new field of science, with new methods of investigation, and a new field of ideas. He soon became a leading experimenter in one of the main aspects of the investigation into the problem of controlled synthesis.

In 1958 N. A. Yavlinskii and a group of physicists were awarded a Lenin prize for investigating the possibilities of producing a high-temperature plasma in powerful gaseous pulse discharges. In the further development of this problem Natan Aronovich headed a group of experimenters dealing with the study of quasi-stationary systems, in which the plasma is created and heated by a ring current stabilized by a strong magnetic field.

With the accumulation of experimental information it was clearly necessary to extend the range of methods for the investigation and to build new apparatus. Various methods were used to study the plasma: microwave probing, high-speed photography, numerous electrotechnical and spectrum methods of measurement – all these were quickly adopted and used to obtain information on the most complex physical processes occurring in a hot plasma.

To obtain a hot pure plasma it was essential to build an all-metal system, ensuring a low content of impurities. Naturally, to achieve the purest vacuum conditions it was essential not only to develop new designs but also to develop the complex technology of vacuum and heat treatment of components. The electrotechnical difficulties arising in the development of this equipment become clear if we bear in mind that magnetic fields with intensities of up to 40000 Oe must be set up in a space measuring many hundreds of liters. The mechanical forces in the windings reach hundreds of kg/cm^2 under these conditions.

Special pulse-action electric motors were used to feed the windings. The complex problems on the building of new equipment and systems for feeding them owed their solution to the engineering talent and outstanding organizational abilities of N. A. Yavlinskii.

It is obviously beyond the scope of the present article to describe the tremendous assistance, energy and willpower needed to overcome those enumerable difficulties, drawbacks and doubts which arose at each step.

The physical results made an important contribution to plasma science. A large step forward had been taken in one of the main directions of investigations into the problem of controlled synthesis.

In the laboratory headed by Natan Aronovich a completely ionized plasma, existing for several milliseconds, was obtained for the first time in the Soviet Union. It was shown that with large stabilizing magnetic fields the plasma is not destroyed by magnetohydrodynamic instabilities and reacts comparatively weakly with the walls of the chamber. A considerable fraction of the energy liberated in a discharge under these conditions goes to heat the plasma and not to the radiation of impurities. The electron temperature reaches a million degrees, and the ion temperature, at least at the initial stage of the discharge, is close to the electron temperature.

It is now clear that the work of N. A. Yavlinskii and his co-workers is not only an essential part of our knowledge on plasma physics, but will influence further investigations in this direction over the next few years.

Throughout his life Natan Aronovich was always a leader in his field, serving as an example for his comrades.

In all aspects of his varied activity he made an important contribution. At the front he was awarded the Order of the Red Star and medals. The scientific and technical achievements of Natan Aronovich won him Lenin and State prizes and the order of the Red Banner of Labor.

His scientific and technical interests were unlimited. He devoted much of his energy to social activities. In 1927 he became a Young Communist and in 1932 he became a party member; he led an active social life. During the years of collectivization, with the permission of the Young Communist League he worked on a farm; in 1934 he became editor of a large-circulation industrial newspaper. As a propagandist he ran discussion groups and seminars. He was repeatedly elected to the party organs of the Institute.

N. A. Yavlinskii was always surrounded by young people. He tried to instill in them an interest in the important problems which he was working on. In the All-Union Energy Institute the specialty "Mathematical and Computer Instruments" was introduced on his initiative in 1956 and Natan Aronovich was the first lecturer in this course. The students enjoyed his lectures because of their content, the liveliness and clarity of the presentation. He spared neither time nor effort and was always ready to help students both in the Institute and at home.

His kind and sensitive attitude to people showed itself most clearly in his dealings with his colleagues.

The door of his study was always open and people could come to him when in trouble. Everyone found a lively welcome; they received kind and wise advice and help. From morning to late evening it was always possible to turn to him with work problems and with problems of a personal nature. Igor' Vasil'evich Kurchatov rightly called him "Natan the wise." His wisdom was combined with a rare modesty and considerable self-criticism.

We have lost a genuine person, a man of considerable talent, and rare humanitarian qualities. He led a good life which was tragically broken off at the height of his powers. Those who had the pleasure of knowing N. A. Yavlinskii closely, for whom he was a comrade and friend, will always remember this brilliant man.

A Group of Comrades

USE OF INDUCTION ELECTRODES TO FORM A BEAM OF ACCELERATED PARTICLES IN THE SYNCHROPHASOTRON

G. S. Kazanskii, A. B. Kuznetsov, A. I. Mikhailov,
N. B. Rubin, and A. P. Tsarenkov

Translated from Atomnaya Énergiya, Vol. 14, No. 2,
pp. 153-158, February, 1963
Original article submitted April 4, 1962

This paper gives some results of a study made on using signal electrodes to form a beam of accelerated particles in the first stage of acceleration in the synchrophasotron. A short description is given of the method of investigation along with the theoretical basis of the experimental results. Analysis is made of the oscillational processes resulting from the behavior of the particle beam in the initial stage of acceleration. In particular, a discussion is given of the azimuthal variation of the density of particles in the accelerated burst, as well as the oscillations of the center of charge in the burst in the radial direction. Recommendations are made which it is useful to follow when adjusting for optimum particle acceleration in the synchrophasotron.

1. The beam of accelerated particles in the synchrophasotron of the United Institute of Nuclear Studies (OIYaI) in Dubna is detected by means of a set of electrostatic signal electrodes [1, 2]. The electrodes consist of broad copper plates placed on both sides of the particle beam. There are two systems of signal electrodes. One set has plane symmetry, coinciding with the median plane of the accelerator magnet, and we shall call these the vertical electrodes. The second set of electrodes (radial) is orthogonal to the first. A schematic representation of the electrodes is shown in Fig. 1.

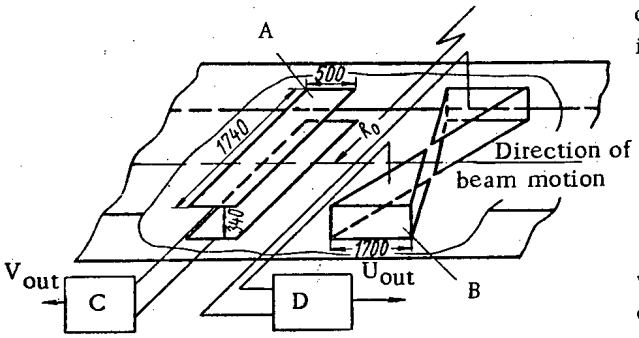

Fig. 1. Induction electrode system: A) vertical electrode; B) radial electrode; C) amplifier of beam-intensity measuring system; D) radial beam-position detector.

The signal $V(\varphi)$, proportional to the varying azimuthal density $q(\varphi)$ of charge on the particles in the moving burst, is induced in the vertical electrodes:

$$V(\varphi) = \frac{1}{C} \int_{\varphi - \frac{l\pi}{\Pi}}^{\varphi + \frac{l\pi}{\Pi}} q(\varphi')\, d\varphi' \simeq \frac{q(\varphi)}{C} \frac{l}{\Pi} 2\pi, \qquad (1)$$

where l is the electrical length of the electrodes, C is the capacity of the plates to ground, including the capacity of the mounting, and Π is the perimeter of the equilibrium orbit.

The signal $V(\varphi)$ may be fed to an integrating circuit which makes it possible to find the potential

$$V_m = \frac{1}{2\pi} \int_0^{2\pi} V(\varphi)\, d\varphi$$

$$= \frac{l}{\Pi C} \int_0^{2\pi} q(\varphi)\, d\varphi = \frac{l}{\Pi} \frac{Q}{C}, \qquad (2)$$

which is proportional to the total charge Q in the accelerated burst. Since the effect of the autophasing mechanism is such that the accelerated burst occupies only a part of the ring orbit, the integration in (2) is in fact performed in the stability region – dividing line – and not over the whole orbit.

The sensitivity of the vertical electrode system (shown in Fig. 1 by the letter A) is

$$\alpha = \frac{N}{V_m} = \frac{Q}{eV_m} = \frac{\Pi C}{el}, \tag{3}$$

where N is the number of protons in the accelerated burst, and e is the charge on a proton.

For the OIYaI synchrophasotron, Π = 208 m, l = 0.5 m, C = 400 pF and so $\alpha = 1 \cdot 10^{12}$ protons/V.

By measuring the voltage V_{out} on the amplifier output of the system, and knowing the amplification factor K, the number of protons in the burst may be found from the formula

$$N = \frac{V_{out}\,\alpha}{K}. \tag{4}$$

The radial electrodes (see Fig. 1,B) detect the beam deviation in a horizontal plane. They give a signal U (φ) proportional to the deviation of the center of charge of the burst element [$q(\varphi)(l/\Pi)2\pi$] from the equilibrium radius, the signal being normalized in such a way that its magnitude is independent of the number of particles in the burst. In general, the radial position of the center of charge of the individual elements in the burst may be different, i.e., the signal from the radial electrodes is, in the general case, dependent on φ. Such cases can occur under definite conditions during radial phase motion.

The sensitivity of the apparatus in the radial system is 2 V/cm*.

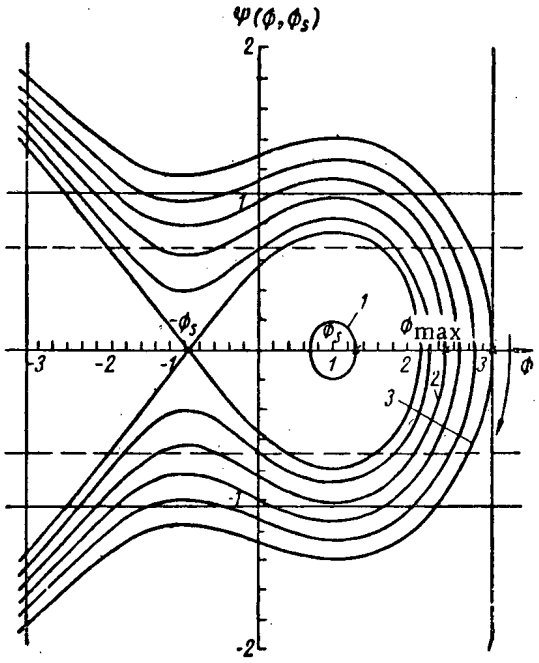

Fig. 2. Dividing line and radial phase trajectories for cos φ_s = 0.5. The solid horizontal lines represent the walls located 65 cm from each side of r_s, and the dotted horizontal lines show the beam boundaries (for the instantaneous orbits), corresponding with a relative energy spread of ± 1%.

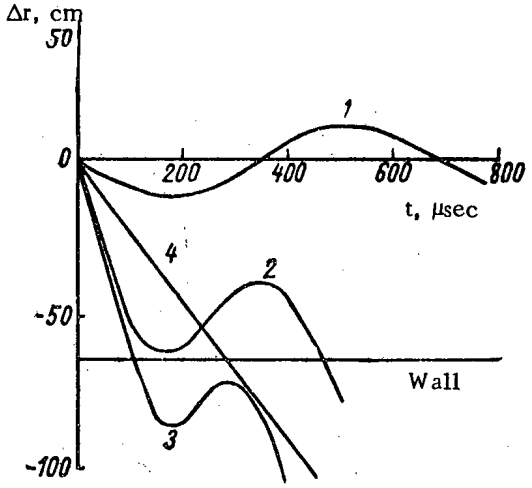

Fig. 3. Radial position of particles as a function of time for the radial phase trajectories 1, 2, and 3 of Fig. 2 (the corresponding initial positions of the particles are shown by asterisks in Fig. 2. A graph of the displacement of the beam when the accelerating field is turned off (curve 4) is given for comparison.

The vertical and horizontal electrode equipment has a frequency passband from 0.1 to 3 Mc, which makes possible distortionless detection of both the form [$V(\varphi)$] of the particle burst after each revolution in the azimuthal

*At the present time, the sensitivity is a factor of 10 greater than that given in [1, 2].

direction and the position of the center of charge in the radial direction [U(φ)]. Further, there is the possibility of observing any amplitude modulation of the signals produced by radial phase motion of the particles in the accelerated burst, which, as we shall see, gives very important information on the behavior of the accelerated burst.

2. When the accelerating voltage is turned on, as we know, a region of stable motion is formed, bounded by a dividing line [3].

Figure 2 shows the phase trajectories of the particles for the OIYaI synchrophasotron ($\cos \varphi_s = 0.5$), which are described by the familiar first integral of the phase equation [4]:

$$\Psi = \pm \sqrt{(\sin \varphi - \varphi \cos \varphi_s) - (\sin \varphi_{in} - \varphi_{in} \cos \varphi_s) + \psi_{in}^2}, \qquad (5)$$

where $\Psi = \frac{\dot{\varphi}}{\Omega} \sqrt{\frac{2}{\sin \varphi_s}}$; φ is the phase of the accelerating voltage at the instant the particles pass through the accelerating space, φ_s is the equilibrium phase, and Ω is the angular frequency of the radial phase oscillations.

A consideration of the motion of the particles on the phase trajectories (Fig. 3) including free oscillations has shown that:

a) The flux of particles lost at the external wall of the chamber lasts approximately a half-period of the small phase oscillations, i.e., in the present case 350 μsec, although some particles may also be somewhat retarded (those which pass through in the region of the point $\varphi = -\varphi_s$, $\Psi = 0$).

b) The greater part of the flux of particles lost at the internal wall also passes through during a time of the order of a half period of the small phase oscillations, but an appreciable fraction of the flux can still be retarded by a time of the order of one or two periods of the small phase oscillations. The particles very quickly get out of the range of phases in the vicinity of $\varphi = \pi$ (in 200-300 μsec), and, accordingly, the "dive" in azimuthal particle density in this region shows up in as little as 100-150 μsec (Fig. 4).

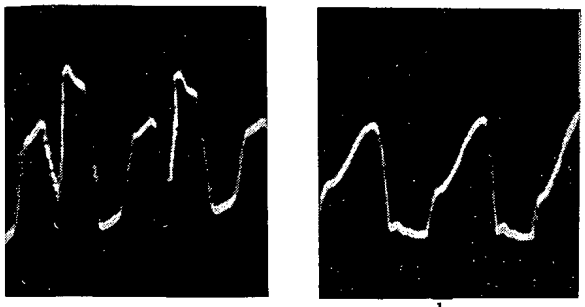

Fig. 4. Azimuthal structure of accelerated particle beam V(φ): a) 100 μsec from the start of acceleration; b) after phase oscillation.

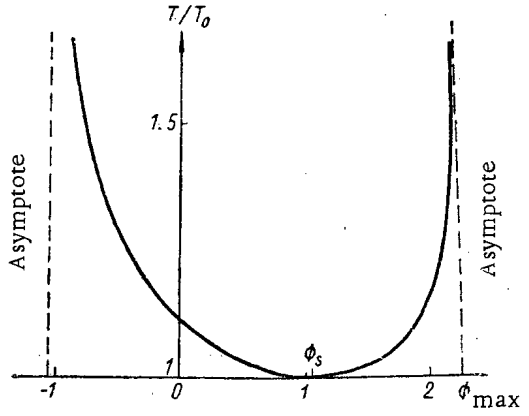

Fig. 5. Period of radial phase oscillations as a function of the amplitude $\alpha = \varphi_s - \varphi_{in}$ for $\cos \varphi_s = 0.5$.

Thus, the azimuthal structure of the beam will be observed starting 100-150 μsec after the accelerating voltage is turned on, and beam formation lasts up to 1-1.5 msec or more, depending on the capture conditions and the distribution of the particles in the free oscillations during betatron operation.

3. Let us now consider the behavior of a formed burst in the first stage of acceleration in the light of the information obtained from the signal electrodes. For simplicity we shall assume at the start that the beam undergoing capture is quite monoenergetic, i.e., the initial spread in the instantaneous orbits, $2\Delta M$, is much less than the radial dimension of the dividing line 2b, and that at the instant the accelerating voltage is applied the beam is in an equilibrium orbit. Since the period of the radial phase oscillations of the majority of the particles (excluding the particles moving in the vicinity of the dividing line) is approximately the same (Fig. 5), in this case the behavior of the beam

inside the dividing line may be thought of as the rotation of a rod with respect to an equilibrium phase φ_s at the frequency Ω. Because of the asymmetry of the dividing line with respect to the equilibrium phase, the center of charge does not coincide with the center of rotation of the rod, with the result that the center of charge executes radial phase oscillations at the frequency Ω. The azimuthal density distribution in the accelerated beam will be of the form shown in Fig. 6. The increase in density at the instants $t = T_0/4$ and $t = 3T_0/4$ comes from the fact that at these instants the beam under discussion is grouped in phase around φ_s, while at the instants $t = 0$ and $t = T_0$ the beam is extended in phase, with a minimum energy spread. Obviously, the ratio of densities is given by the formula

$$\frac{q_{T_0}}{q_{T_0/4}} = \frac{\Delta M}{b}. \qquad (6)$$

The step-function distribution of the density at the instant $t = T_0/2$ comes from the asymmetry of the dividing line with respect to φ_s.

The particles, distributed at the start of the phase range from $-\varphi_s$ to $+\varphi_s$, are, after a half-period, grouped in the phase range from $+\varphi_s$ to φ_{max}, and since $\varphi_{max} - \varphi_s \simeq \varphi_s$, the density in this phase range increases by approximately a factor of two. On the other hand, the particles from the phase range from $+\varphi_s$ to φ_{max} pass during this time to the phase range from $-\varphi_s$ to $+\varphi_s$, which at this point leads to a reduction in density also of approximately a factor of two.

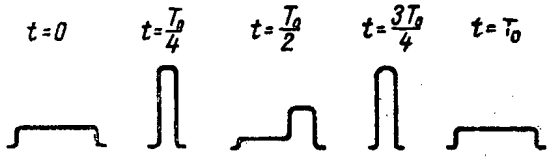

Fig. 6. Change in form of the azimuthal density distribution in the accelerated beam as a result of radial phase motion. It is assumed that $\Delta M/b \ll 1$ and that the beam is initially on an equilibrium radius.

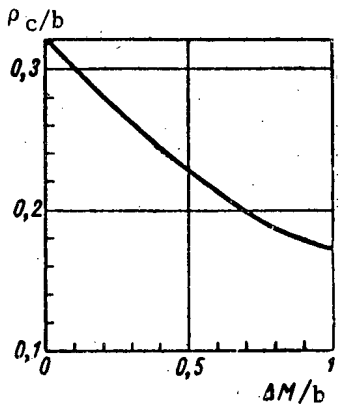

Fig. 7. Initial amplitude (ρ_c) of the radial oscillations at the center of charge as a function of the initial energy spread ΔM. The values are expressed in units of the radial half-dimension b of the dividing line.

Thus, the radial phase oscillations of the beam are accompanied by oscillations in the azimuthal density with frequencies of 2Ω and Ω. The oscillations at frequency 2Ω, as may be seen from (6), is related essentially to the extent to which the beam is initially monoenergetic and disappear if the dividing line is initially completely filled ($\Delta M/b = 1$). The oscillations in density at frequency Ω, just as the oscillations of the center of charge, are determined by the asymmetry of the dividing line. For a monoenergetic beam these oscillations are considerably weaker than the oscillations of frequency 2Ω, but their amplitude is only very weakly dependent on the ratio $\Delta M/b$.

Figure 7 shows how the amplitude of the radial oscillations of the center of charge varies with the ratio $\Delta M/b$ if the energy center of the beam coincides with the equilibrium radius at the instant the accelerating voltage is applied.

The phenomena described above are well supported by the oscillograms taken with the aid of the signal electrodes (Figs. 8-10). Since the period of the phase oscillations depends on their amplitude as a result of nonlinearity (see Fig. 5), the phenomena described above will be gradually smoothed out. The length of time required to damp out the oscillations in density at frequency 2Ω depends on the ratio $\Delta M/b$. For $\Delta M/b \ll 1$, the damping can last 30-50 periods of the phase oscillations, but if the beam of particles is far from being monoenergetic, the damping will occur considerably more rapidly. Here, as has already been noted, the initial amplitude of the oscillations will be small.

If at the instant of capture the position of the beam fails considerably to coincide with an equilibrium radius (incorrect application of accelerating voltage), the oscillations in density at frequency 2Ω will also be rapidly damped. However, the initial amplitude of the oscillations will now depend not only on the energy spread but also on the error in the instant at which the frequency of the accelerating voltage is applied.

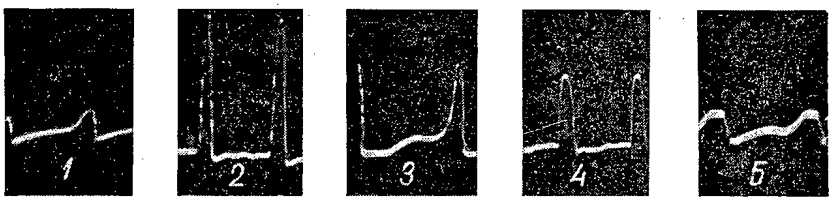

Fig. 8. Pulse shapes V (φ) at instants of time corresponding with those shown in Fig. 6.

The damping of the oscillations of the center of charge depends on $\Delta M/b$ in a similar way: the damping will be greater, the greater the value of $\Delta M/b$. Incorrect application of the accelerating voltage will here further increase the damping.

The following must be emphasized. For the same value of $\Delta M/b$, but with incorrect application of the high frequency, the amplitude of the oscillations in density at frequency 2Ω is decreased, while the amplitude of the oscillations of the center of charge is increased. The relations pointed out here are easily observable experimentally.

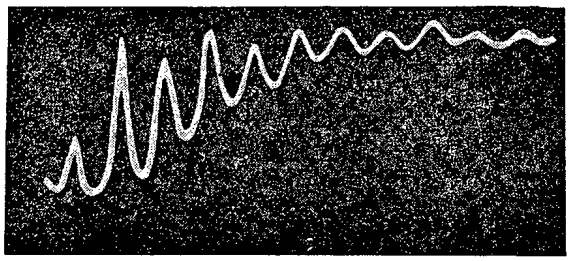

Fig. 9. Envelope of the signals V(φ) detected by the vertical signal electrodes. The fundamental frequency of the oscillations is 2Ω (weak oscillations of frequency Ω are also visible).

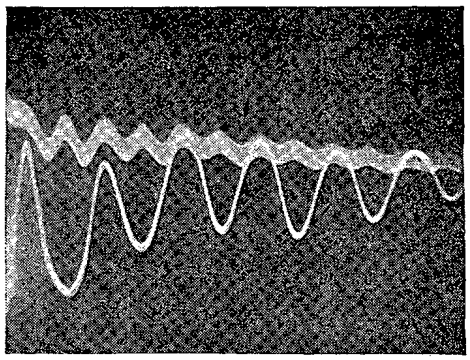

Fig. 10. Envelope of the signals U (φ) detected by the radial electrodes (lower trace). In the upper trace, the envelope of the signals from the vertical electrodes is given for comparison.

4. Considering everything that has been said, the following conclusion may be drawn: the envelopes of the signals taken from the signal electrodes will, with correct application of the accelerating voltage, have modulation: on the vertical electrodes at frequencies 2Ω and Ω, and on the radial electrodes at frequency Ω. The depth of modulation of the oscillations at frequency 2Ω is determined with correct adjustment by the width of the energy spread in the beam being injected. In particular, the modulation to a depth of 40-50% observed experimentally in the OIYaI synchrophasotron corresponds with a total initial energy spread of $\sim 1.5\%$ (this is somewhat less than the value found by direct measurement [5]).

On the basis of what has been presented, some recommendations can be made for controlling the instant the accelerating field is applied from the pulsations in the signals given by the signal electrodes. For constant injection conditions, the correct instant for applying the accelerating voltage corresponds with the minimum radial oscillations in the center of charge and the maximum modulation of the density, as well as the largest damping time for the pulsations of the signals given by both the radial and the vertical signal electrodes. If the instant for applying the accelerating voltage has been correctly chosen from the signal electrodes, it is possible to adjust the energy spectrum of the beam taken from the linear accelerator. The smaller the energy spread, the greater the pulsations in the signals given by the vertical electrodes.

The oscillations in the center of charge and the oscillations in density described above can also occur further on in the accelerating process. The reasons for this may be, in particular, discontinuous changes in frequency and amplitude of the accelerating voltage, as well as jumps in the value of dH/dt, where H is the magnetic field.

LITERATURE CITED

1. F. Vodop'yanov, A. Kuzmin et al., Proc. Inter. Conf. High-Energy Accelerators and Instrumention. CERN, Geneva, p. 470, 477 (1959).
2. G. S. Kazanskii, A. I. Mikhailov, and A. P. Tsarenkov, OIYaI Preprint B-50-819. Dubna (1961).
3. V. I. Kotov, A. B Kuznetsov, and N. B. Rubin "Usp. fiz. nauk", 64, 197 (1958).
4. M. S. Rabinovich, "Tr. FIAN", 10, 23 (1958).
5. S. K. Esin et al., OIYaI Preprint R-555. Dubna (1960).

All abbreviations of periodicals in the above bibliography are letter-by-letter transliterations of the abbreviations as given in the original Russian journal. *Some or all of this periodical literature may well be available in English translation.* A complete list of the cover-to-cover English translations appears at the back of this issue.

STUDY OF NUCLEAR REACTIONS ON THE CYCLOTRON OF THE INSTITUTE OF PHYSICS, ACADEMY OF SCIENCES, UkrSSR

O. F. Nemets, M. V. Pasechnik, and N. N. Pucherov

Translated from Atomnaya Énergiya, Vol. 14, No. 2,
pp. 159-170, February, 1963
Original article submitted July 19, 1962

This paper gives a short review of the work done on the cyclotron of the Institute of Physics, Academy of Sciences, UkrSSR from 1957 to 1961. Results are given of the studies made on elastic and inelastic scattering of 6.8 MeV protons, both by targets with the natural isotopic composition (aluminum, iron, cobalt, nickel, copper, zinc, silver, cadmium, tin, lead, and bismuth) and by separated isotopes ($Ni^{58,60,62,64}$, $Cu^{63,65}$, $Zn^{64,68,70}$, $Zr^{90,91,92,96}$, $Sn^{116,117,119,124}$). A study of the angular and energy distributions ofprotons in deuteron stripping by the nuclei Be^{9}, C^{12}, $Si^{28,29}$, Ca^{40}, $Ti^{46,47,48}$, $Ni^{58,60,62,64}$, Sr^{88}, $Zr^{90,91}$, $Mo^{91,92,95,96}$, $Cd^{111,113}$, and $Sn^{117,119}$ has made it possible to find the spins and parities of the fundamental and excited states. In addition to stripping, a study was made of capture, as well as of elastic and inelastic deuteron scattering.

Introduction

The cyclotron of the Institute of Physics, Academy of Sciences, UkrSSR was put into operation in the middle of 1957, and the results of the first physics experiments were obtained at the end of the same year. The cyclotron makes it possible to extract a beam of 6.8 MeV protons and a beam of 13.6 MeV deuterons.

Some substantial changes were made in the original design of the cyclotron to improve stability and reliability of operation. Equipment was developed and built for remote control and monitoring of the position of the source, the dee's, and the external shims; changes were made in the construction of the insulators for the deflecting plates and in the master oscillator circuit; current and voltage stabilization was provided, etc. All this produced a great reduction in the time required to adjust the cyclotron and brought the useful operating time of the cyclotron with a beam up to 90-95% of the total operating time.

Continuous operation of the cyclotron has made it possible to carry out a large number of investigations, the results of which have been published as scientific communications in various journals and conference reports.

The present paper gives a review of what has been done by a large group of workers at the Institute [1-39].

The physics investigations were carried out along the following basic lines: 1) verifying the basic ideas of the optical model of the nucleus,and refining and determining the parameters involved; 2) finding the quantum characteristics of the nuclear levels; 3) investigating the mechanism of nuclear reactions.

Investigation of Proton Interaction with Atomic Nuclei

Nucleon scattering by nuclei is one of the most important sources of information on the nuclear potential. The development of the optical model of the nucleus has provided the stimulus for setting up a program of work on the angular distribution of elastically scattered 6.8 MeV protons.

Figure 1 gives a schematic diagram of the arrangement of the basic equipment which was used in all the measurements made on the cyclotron. The angular distributions of the elastically scattered protons were investigated in a scattering chamber 1.6 m in diameter. The proton detector was a scintillation spectrometer using a thin cesium iodide crystal. The amplitude spectrum of the spectrometer pulses was recorded on a 50-channel amplitude analyzer. Studies were made on the angular distributions of protons elastically scattered from the nuclei of aluminum, iron, cobalt, nickel, copper, silver, zinc, cadmium, tin, lead, and bismuth [1-4]. The targets used had the natural mixture of isotopes.

The angular distributions found may be divided into three groups. For heavy nuclei, the differential cross sections are less than Rutherford at large angles. Nuclei of moderate atomic weight show clearly defined maxima and minima in the angular distributions, which change in a regular way with change in mass number of the scattering nucleus. As the mass number of the target nuclei increases, extrema in the angular distributions move toward smaller angles. The position of the extrema is quite well described by the expression $A^{1/3} \sin(\theta_m/2) = \text{const}$, where θ_m is the angle at which a particular extremum occurs. Finally, with light nuclei, the regularity in the change in angular distribution with change in mass number no longer holds. These nuclei show a large amount of back scattering.

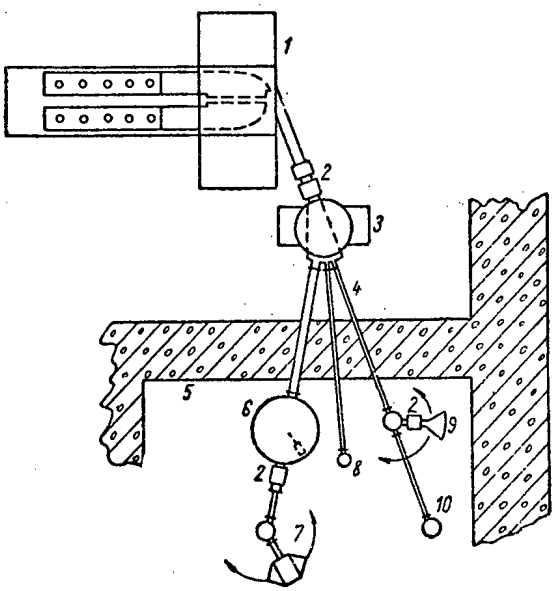

Fig. 1. Diagram of over-all location of experimental equipment: 1) cyclotron; 2) focusing lenses; 3) rotating magnet; 4) ion conductors; 5) protective wall; 6) scattering chamber; 7) magnetic spectrograph; 8) scattering chamber; 9) polarization measuring equipment; 10) (d, p, γ)-correlation measuring equipment.

Since the angular distributions changed quite smoothly with change in mass number of the scattering nucleus, we were encouraged in the hope of being able to describe the scattering by means of the optical model of the nucleus. However, when investigating the group of nuclei with Z = 22-30, it turned out that the gradual monotonic change in the angular distributions on going from element to element no longer held [5]. In particular, the differential cross sections of nickel and iron turned out to be considerably greater at large scattering angles than those of the neighboring elements cobalt, copper, and zinc. A satisfactory explanation of these facts could not be found until after some experiments had been made with separated isotopes.

In cooperation with A. K. Val'ter, A. P. Klyucharev, I. I. Zalyubovskii, and V. I. Lutski, workers of the Physico-technical Institute, Academy of Sciences, UkrSSR, experiments were made in our laboratories on the elastic scattering of protons by the series of separated isotopes (Cr^{50}, Cr^{52}, Cr^{53}, Cr^{54}; Ni^{58}, Ni^{60}, Ni^{62}, Ni^{64}; Cu^{63}, Cu^{65}; Zn^{64}, Zn^{68}, Zn^{70}; Zr^{90}, Zr^{91}, Zr^{92}, Zr^{96}; Sn^{116}, Sn^{117}, Sn^{119}, Sn^{124}) [6-9]. The enriched targets in the form of free films were made up in A. P. Klyucharev's laboratory.

It may be seen from Fig. 2 that the angular distributions for different isotopes differ appreciably from one another even for a small difference in mass number. Above all, in a number of cases a difference is observed in the value of the differential cross section at large scattering angles. Examples are provided by Cr^{52}, Cr^{53}, Ni^{58}, and Ni^{62}.

One of the possible reasons for this difference is that there is a difference in the cross sections for the (p, n) reaction, which is in competition with the elastic scattering. However, any such interpretation, in spite of appearing obvious, requires further verification.

A second peculiarity of the angular distributions is the shift in the extrema with change in mass number. The extrema shift much more than is to be expected from the optical model of the nucleus, assuming that the nuclear radius changes as $R = r_0 \cdot A^{1/3} \cdot 10^{-13}$ cm. Accordingly, in analyzing the angular distributions from the standpoint of the optical model, agreement with experiment can only be achieved if there is a change in the real part of the complex potential or a change in the parameter r_0 on passing from isotope to isotope.

Inelastic proton scattering by a number of nuclei was investigated in addition to elastic scattering. In particular, the angular distributions of inelastically scattered protons were found, coming from the first excited levels of the nuclei Mg^{24}, Cr^{52}, and Ni^{58} [10, 11]. The angular distributions are isotropic for nuclei of moderate atomic weight, which shows that the inelastic scattering occurs by a mechanism in which a compound nucleus is formed. The nucleus Mg^{24} shows appreciable asymmetry with respect to 90°; in this case one of the possible direct processes is to be expected.

It has been shown in recent years that an important role is played by spin-orbit interaction in elastic scattering of nucleons. The double scattering method (the second scatterer being carbon) was used to investigate the angular dependence of the polarization when protons were elastically scattered by carbon, aluminum, nickel, copper, and iron [12, 13]. In spite of the comparatively low proton energy used in the experiment, it was shown that the

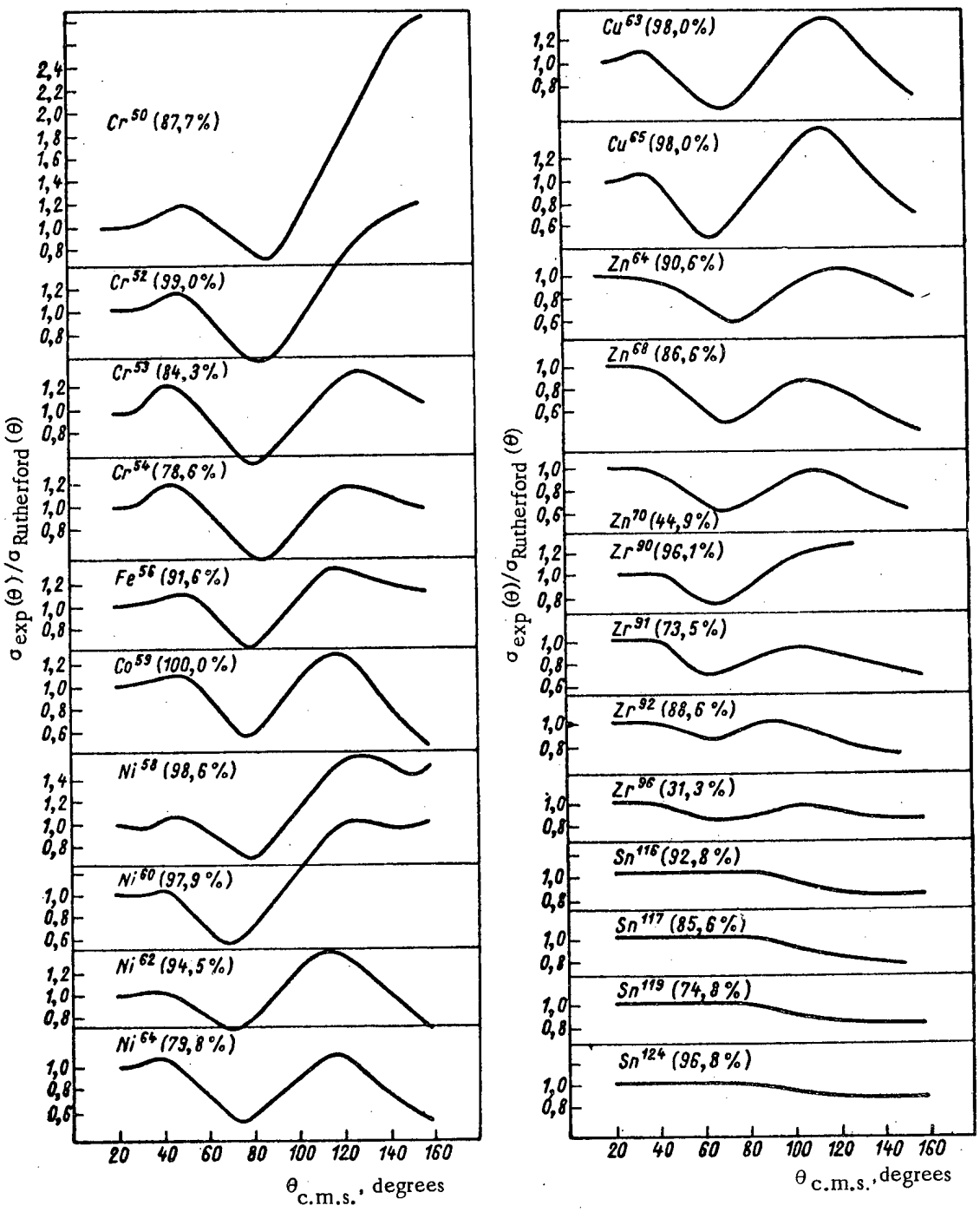

Fig. 2. Angular distributions of 6.8 MeV protons elastically scattered by separated isotopes. (The percent enrichment of the target is shown for each nucleus.)

polarization reaches a value of the order of 30% even for nuclei of moderate atomic weight. This testifies to the importance of spin-orbit interaction in the energy range investigated. The angular dependence of the polarization exhibits a number of maxima and minima.

Nuclear Reactions Produced by Deuterons

As a result of the specific properties of the deuteron (small binding energy, large radius, and large asymmetry) its behavior in nuclear reactions is appreciably different from the behavior of other particles and, in the majority of cases, it has a direct reaction mechanism. Accordingly, reactions produced by deuterons are of great interest in the development of both nuclear reaction theory and nuclear spectroscopy.

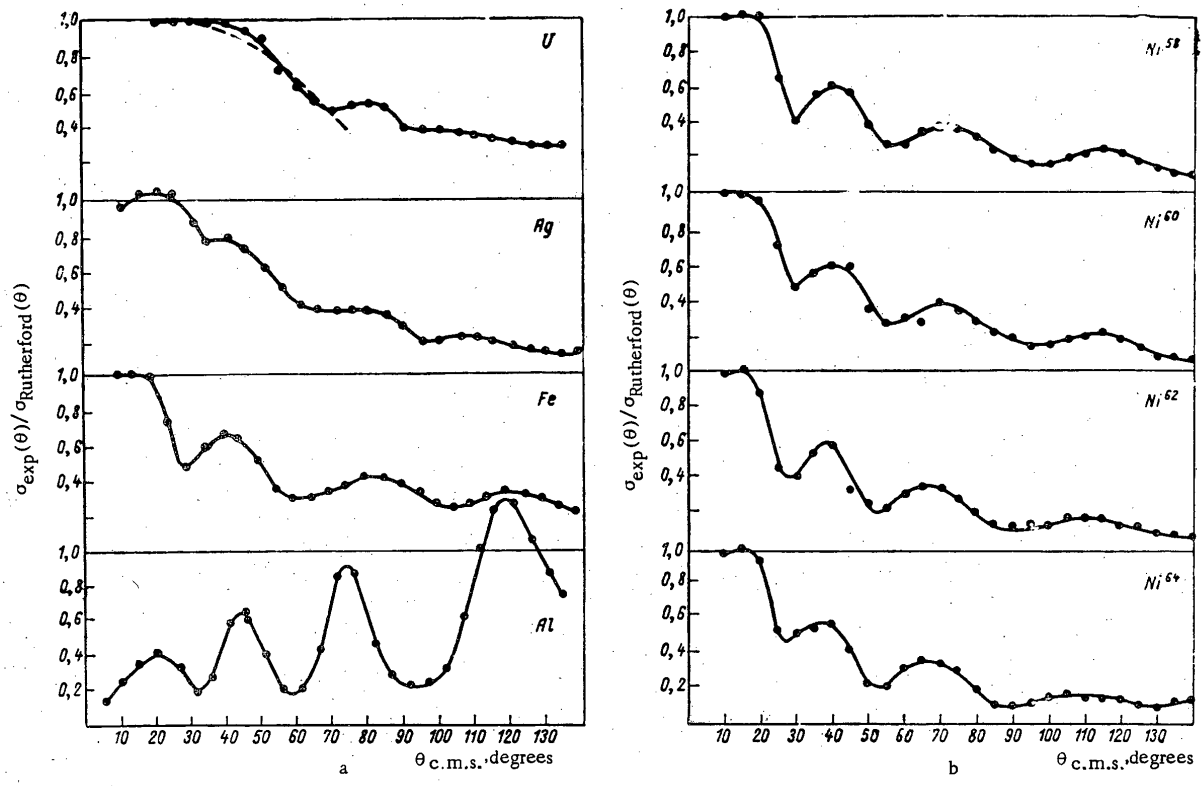

Fig. 3. Angular distributions of elastically scattered 13.6 MeV deuterons.

Elastic scattering of deuterons. A substantial departure from Rutherford scattering was observed in the first experiments on the angular distributions of elastically scattered deuterons. This departure could have been caused either by the specific properties of the deuteron or by nuclear interaction playing a role. In order to obtain additional information on the mechanism of the elastic scattering of deuterons, the angular distributions were found from scattering by the nuclei of 18 elements [14, 15]. The measurements were made with an ionization chamber [16].

Figure 3a gives angular distributions typical of deuteron scattering by heavy, medium, and light nuclei. Not one of the theories existing at the present time is able to provide an interpretation of the angular distributions over the whole range of atomic masses. For heavy nuclei, the way the cross section varies in the range of angles ~ 40-70° could be accounted for by assuming that the only thing taking place here was electrical splitting of the deuteron. Since even for platinum we have the ratio $Ze^2/\hbar u \simeq 5$, it is possible for us to use the quasiclassical approximation[40]. In this case, there is a unique relation between the collision parameter and the scattering angle:

$$\sin\frac{\theta}{2} = \frac{Ze^2}{2M_p u^2 q - Ze^2}.$$

If we take $q_{cr} = R_n + R_d + \lambda$, where $R_n = 1.35 \cdot A^{1/3}$ F and $R_d = 4.31$ F, the values of θ_{cr} for nuclei from platinum to uranium will lie in the range 60-75°. At the same time, departures from Rutherford scattering are observed at angles ~ 40°, for which the values of q are approximately 6-8 F greater than q_{cr}. It is perfectly obvious that at these distances from the nucleus the nuclear forces cannot exert any appreciable effect on the scattering, and the only process that can possibly be responsible for the departure from Rutherford scattering is electrical splitting of the deuteron. This conclusion was subsequently confirmed by the work of other authors [41, 42].

TABLE 1. Quantum Characteristics of Nuclear Levels Found from Inelastic Deuteron Scattering

Nucleus	J^π_H	E^*, MeV	l	J^π_k	$d\sigma(0°)/d\omega$, mbarn per steradian	a, F	R, F
Be^9	$3/2^-$	2,43	1	$5/2^+$	—	4	4,24
Mg^{24}	0^+	1,37	2	2^+	—	15,8	5,34
Si^{28}	0^+	1,78	2	2^+	18	7,2	5,40
Ti^{48}	0^+	0,99	2	2^+	74	6,2	6,15
Fe^{56}	0^+	0,85	2	2^+	80	7,0	6,37
Ni^{58}	0^+	1,45	2	2^+	70	7,0	6,43
Ni^{60}	0^+	1,33	2	2^+	49	7,0	6,50
Ni^{62}	0^+	1,17	2	2^+	36	6,9	6,54
Ni^{64}	0^+	1,34	2	2^+	100	7,0	6,58

Note: Here J^π_H and J^π_k are the spin and parity of the nucleus in the initial and final state respectively. E^* is the energy of the excited level. l is the orbital momentum given to the nucleus. $d\sigma(0°)/d\omega$ is the differential cross section extrapolated to 0°. a and R are the radii used in the theory of electrical and nuclear interaction.

It is interesting that a diffraction pattern is observed in the angular distributions of all nuclei for $\theta > \theta_{cr}$ (i.e., $q < q_{cr}$). Since the diffractional character of the angular distributions is associated with nuclear interaction, the assumption is once more confirmed that the quasiclassical treatment is a good approximation in our case.

In order to find out to what extent the isotopic effects observed in proton scattering [6] show up in the scattering of other particles, measurements were made of deuteron scattering by nickel isotopes [17]. It may be seen from the results, shown in Fig. 3b, that no such isotopic effect is observed in deuteron scattering. This permits us to assume that one of the probable causes of the difference in proton scattering cross sections between neighboring isotopes is the difference in cross sections for the competing (p,n) reaction and not the "loosening up" of the nuclear surface when the number of neutrons is increased above that required for a closed shell. It is true however that as a result of the "looseness" of the deuteron itself, it may be less sensitive to changes in the nuclear surface than the proton is.

Inelastic scattering of deuterons. The mechanisms of inelastic deuteron scattering may be of extremely different types. The fundamental mechanisms include: stripping, in which the deuteron undergoes virtual dissociation and only one of the nucleons interacts with the nucleus, direct deuteron knock out, heavy particle stripping (a process of charge redistribution type), diffractional scattering, Coulomb excitation, and, finally, formation of a compound nucleus. It is possible to tell what role is being played by what reaction mechanism from the form of the differential cross sections. The numerous papers in existence are as a rule lacking in information on the behavior of the differential cross sections in inelastic scattering at small angles, so that in making the measurements it was important to give serious attention to the small angle range.

The measurements were made both with the ionization chamber mentioned above [16] and with the ionization chamber described in [18], as well as with the scintillation spectrometer of [19]. In order to discriminate between particles of different kinds, use was made of the difference between the values of the products of the specific and total ionization losses [(dE/dx)E].

TABLE 2. Spectroscopic Data Found in (d,p) Reaction Studies

Target nucleus	Spin and parity of target nucleus	Energy of nucleus in final state, MeV	Angular momentum transferred	Parity and possible spins of final states	Most probable values for spin of final states	Interaction radius in Butler's theory (10^{-13} cm)	Absolute values of differential cross sections at maximum, mbarn per steradian	Normalized transition probabilities $(2J_k+1)\theta^2$	Normalized level widths, θ^2	Values of Q, MeV
Be^9	$3/2^-$	0	1	0^+, 1^+, 2^+, 3^+	0^+	4,8	2,15 (10°)	0,041	0,041	4,6
Be^9	$3/2^-$	3,37	1	0^+, 1^+, 2^+, 3^+	2^+	4,8	4,8 (10°)	0,050	0,01	1,22
C^{12}	0^+	0	1	$1/2^-$, $3/2^-$	$1/2^+$	4,6	13 (15°)	0,048	0,024	2,73
C^{12}	0^+	3,09	0	$1/2^+$	$1/2^+$	4,6	39,6 (10°)	0,34	0,17	−0,36
C^{12}	0^+	3,68	1	$1/2^-$, $3/2^-$	$3/2^-$	4,6	—	—	—	−0,95
C^{12}	0^+	3,86	2	$3/2^+$, $5/2^+$	$5/2^+$	4,6	—	—	—	−1,13
Si^{28}	0^+	0	0	$1/2^+$	$1/2^+$	5,4	24,4 (5°)	0,0516	0,026	6,25
Si^{28}	0^+	1,28	2	$3/2^+$, $5/2^+$	$3/2^+$	5,4	6,2 (25°)	0,081	0,020	4,97
Si^{28}	0^+	2,03	2	$3/2^+$, $5/2^+$	$5/2^+$	5,4	2,56 (25°)	0,033	0,0055	4,22
Si^{28}	0^+	3,07	2	$3/2^+$, $5/2^+$	—	5,4	1,4 (25°)	0,0158	—	3,18
Si^{28}	0^+	3,62	3	$5/2^-$, $7/2^-$	$7/2^-$	5,4	6,5 (30°)	0,19	0,0238	2,63
Si^{28}	0^+	4,86 4,90 4,93	1	$1/2^-$, $3/2^-$	$3/2^-$	5,4	57 (5°)	0,143	0,0358	1,32
Si^{29}	$1/2^+$	0	0	0^+, 1^+	0^+	5,45	5,4 (0°)	0,15	0,0152	8,39
Si^{29}	$1/2^+$	2,24	2	1^+, 2^+, 3^+	2^+	5,45	2,4 (25°)	0,014	0,0732	6,15
Ca^{40}	0^+	0	3	$5/2^-$, $7/2^-$	$7/2^-$	6,0	7,8 (30°)	0,0328	0,262	6,14
Ca^{40}	0^+	1,95	1	$1/2^-$, $3/2^-$	$3/2^-$	6,0	36,5 (10°)	0,0344	0,137	4,19
Ca^{40}	0^+	2,42	1	$1/2^-$, $3/2^-$	—	6,0	16,9 (10°)	—	0,061	3,72
Ti^{46}	0^+	0,160	3	$5/2^-$, $7/2^-$	$5/2^-$, $7/2^-$	6,07	2,6 (30°)	—	0,0906	6,45
Ti^{47}	$5/2^-$	0	3	0^{+-}, 6^+	0^+	6,1	0,33 (30°)	0,0745	0,0745	8,14
Ti^{47}	$5/2^-$	1,33	1	1^+, 2^+, 3^+, 4^+	2^+	6,1	0,78 (10°)	0,00523	0,0262	6,81
Ti^{47}	$5/2^-$	2,31	1	1^+, 2^+, 3^+, 4^+	—	6,1	3,2 (10°)	—	0,097	5,83
Ti^{48}	0^+	0	3	$5/2^-$, $7/2^-$	$7/2^-$	6,13	1,9 (30°)	0,0074	0,060	5.81
Ti^{48}	0^+	1,35	1	$1/2^-$, $3/2^-$	$3/2^-$	6,13	30 (10°)	0,03	0,12	4,46
Ti^{48}	0^+	1,7	1	$1/2^-$, $3/2^-$	—	6,13	14 (10°)	—	0,054	4,11
Ti^{48}	0^+	2,4	1^+ (3)	$1/2^-$, $3/2^-$	—	6,13	4,08 (50°)	—	0,0246	3,4
Ti^{49}	$7/2^-$	0	1^+ (3)	0^+, -7^+	0^+	6,16	—	—	—	8,62
Ti^{49}	$7/2^-$	1,58	1	2^+, 3^+, 4^+, 5^+	2^+	6,16	—	—	—	7,04
Ti^{49}	$7/2^-$	2,8	0	3^-, 4^-	—	6,16	—	—	—	5,82
Ni^{58}	0^+	0,0 0,34 0,88	1	$1/2^-$, $3/2^-$	$3/2^-$	5,5	26,2 (12,5°)	0,142	0,0355	6,7
Ni^{58}	0^+	3,05 3,42 3,46	1^+ (4)	$1/2^-$, $3/2^-$	—	6,4	6,3(10°)	0,019	—	3,5
Ni^{58}	0^+	4,6	2	$3/2^+$, $5/2^+$	—	6,0	17,8(20°)	0,140	—	2,1

TABLE 2. (continued)

Target nucleus	Spin and parity of target nucleus	Energy of nucleus in final state, MeV	Angular momentum transferred	Parity and possible spins of final states	Most probable values for spin of final states	Interaction radius in Butler's theory (10^{-13} cm)	Absolute values of differential cross sections at maximum, mbarn per steradian	Normalized transition probabilities $(2J_k+1)\theta^2$	Normalized level widths, θ^2	Values of Q, MeV
Ni^{60}	0^+	0,0 0,061 0,280 0,67	1	$1/2^-$, $3/2^-$	$3/2^-$	5,5	17,1 (12,5°)	0,084	0,021	5,6
Ni^{60}	0^+	1,1	1	$1/2^-$, $3/2^-$	—	6,47	4,2 (10°)	0,016	—	4,5
Ni^{60}	0^+	2,17	1^+ (4)	$1/2^-$, $3/2^-$	—	6,47	5,6 (10°)	0,018	—	3,6
Ni^{60}	0^+	2,75 3,10	0^+ (2)	$1/2^+$	$1/2^+$	6,47	8,2 (5°)	0,016	0,008	2,9
Ni^{60}	0^+	3,54 3,77	2	$3/2^+$, $5/2^+$	—	6,00	10,2 (20°)	0,085	—	2,2
Ni^{62}	0^+	0	1	$1/2^-$, $3/2^-$	$3/2^-$	5,5	16,4 (10°)	0,066	0,0165	4,4
Ni^{62}	0^+	1,2	1^+ (4)	$1/2^-$, $3/2^-$	—	6,0	5,5 (10°)	0,0165	—	3,2
Ni^{62}	0^+	2,3	2	$3/2^+$, $3/2^+$	—	6,0	13,8 (15°)	0,108	—	2,1
Ni^{64}	0^+	0	1	$1/2^-$, $3/2^-$	$3/2^-$	5,5	20,5 (10°)	0,077	0,0192	3,9
Ni^{64}	0^+	1,1	1^+ (4)	$1/2^-$, $3/2^-$	—	6,0	13,3 (10°)	0,044	—	2,8
Ni^{64}	0^+	2,2	2	$3/2^+$, $5/2^+$	—	6,0	20,3 (15°)	0,150	—	1,7
Sr^{88}	0^+	0	2	$3/2^+$, $5/2^+$	$5/2^+$	6,2	16,2 (20°)	0,03	0,175	4,32
Sr^{88}	0^+	1,05	0	$1/2^+$	$1/2^+$	7,1	25,5 (5°)	0,06	0,127	3,25
Zr^{90}	0^+	0	2	$3/2^+$, $5/2^+$	$5/2^+$	6,15	20 (20°)	0,225	0,0376	5,0
Zr^{90}	0^+	1,21	0	$1/2^+$	$1/2^+$	7,16	50 (5°)	0,252	0,126	3,79
Zr^{91}	$5/2^+$	0	2	0^+, 1^+,...5^+	0^+	7,19	0,8 (17,5°)	0,059	0,059	6,5
Zr^{91}	$5/2^+$	0,93	2	0^+, 1^+,...5^+	2^+	7,19	6 (17,5°)	0,412	0,0824	5,57
Mo^{92}	0^+	0	2	$3/2^+$, $5/2^+$	$5/2^+$	6,0	—	—	—	5,8
Mo^{92}	0^+	0,91	0	$1/2^+$	$1/2^+$	6,0	—	—	—	4,89
Mo^{94}	0^+	0 0,16	2	$3/2^+$, $5/2^+$	$5/2^+$	6,2	—	—	—	5,0
Mo^{94}	0^+	0,76—1,0	0	$1/2^+$	$1/2^+$	6,2	—	—	—	4,84
Mo^{95}	$5/2^+$	0	2	0^+, 1^+,...5^+	0^+	6,6	—	—	—	6,83
Mo^{95}	$5/2^+$	0,77	0^+ (2)	0^+, 1^+,...5^+	2^+	6,6	—	—	—	6,06
Mo^{96}	0^+	0	2	$3/2^+$, $5/2^+$	$5/2^+$	5,8	—	—	—	4,5
Mo^{96}	0^+	0,66	0	$1/2^+$	$1/2^+$	5,8	—	—	—	3,84
Cd^{111}	$1/2^+$	0	0	0^+, 1^+	0^+	7,57	0,9 (5°)	0,00469	0,00469	7,28
Cd^{111}	$1/2^+$	0,618	2	1^+, 2^+, 3^+	2^+	6,6	0,15 (20°)	0,00470	0,00094	6,66
Cd^{113}	$1/2^+$	0	0	0^+, 1^+	0^+	7,6	1,6 (5°)	0,00674	0,00674	6,7
Cd^{113}	$1/2^+$	0,56	2	1^+, 2^+, 3^+	2^+	6,0	0,56 (20°)	0,0157	0,00314	6,19
Sn^{117}	$1/2^+$	0	0	0^+, 1^+	0^+	7,67	2,4 (5°)	0,011	0,011	6,97
Sn^{117}	$1/2^+$	1,210	2	1^+, 2^+, 3^+	2^+	6,36	0,33 (20°)	0,0095	0,0019	5,77
Sn^{119}	$1/2^+$	0	0	0^+, 1^+	0^+	7 7	2,0 (5°)	0.0124	0,0124	7,02
Sn^{119}	$1/2^+$	1,180	2	1^+, 2^+, 3^+	2^+	6,65	0,26 (28°)	0,00795	0,00159	5,84

The angular distributions were found for the nuclei given in Table 1[11, 20-22]. A diffraction pattern is observed in all cases, and the maximum in the angular distribution occurs at 0°. A typical angular distribution is shown in Fig. 4. The broken curve gives the results of a calculation based on stripping theory [43], while the solid curve is based on electrical interaction theory [44]. It may be seen from the figure that the differential cross sections at small angles are satisfactorily described by electrical interaction theory but cannot be accounted for by nuclear interaction theory, which only begins to hold at angles of 20-25°. The maximum differential cross section at 0° for $l = 2$ is also predicted by the theory of diffractional scattering [45], but the results of a calculation based on this theory (as well as the calculations for the other reaction mechanisms) do not agree with the experimental data.

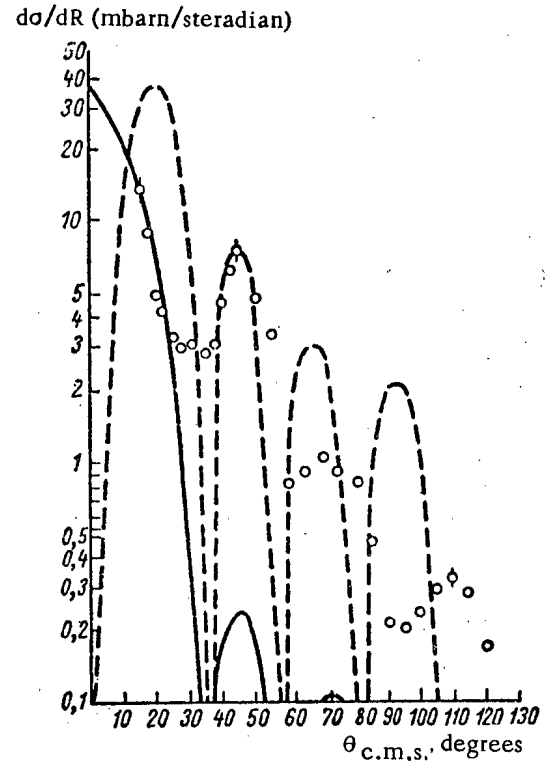

Fig. 4. Angular distribution of deuterons inelastically scattered by Ni^{62} with level excitation 1.17 MeV (E_d^0 = 13.6 MeV); O) experimental points; —) calculated from electrical interaction theory (l = 2, $r_0 = 6.9 \cdot 10^{-13}$ cm); – –) calculated from nuclear interaction theory (l = 2; $d = 8.66 \cdot 10^{-13}$ cm).

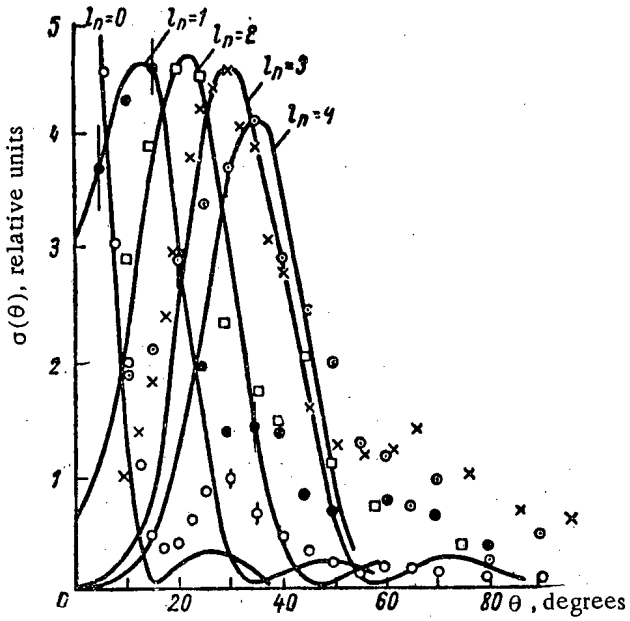

Fig. 5. Typical angular distributions of protons from (d,p) reactions with E_d^0 = 13.6 MeV: O) Zr^{90}; ●) Ti^{49}; □) Sn^{119}; ×) Ca^{40}; ⊙) selenium; —) results of calculation from Butler's theory [46].

The large contribution to the cross section from electrical interaction (at $\theta < 25°$) may, in our opinion, be accounted for qualitatively by the structural peculiarities of the deuteron, which lead to large cross sections for the competing (d,p) and (d,n) stripping reactions. The data obtained are given in Table 1.

The (d,p) stripping reaction. After Butler [46] had developed the theory of stripping reactions, they began to be widely used in nuclear spectroscopy. It is sufficient to say that the number of papers devoted to this question exceeds 500. However, the nuclei investigated have been principally those with $A \leq 40$. The reason for this is that going to heavier nuclei entails an increase in deuteron energy, since the angular distributions are greatly distorted if the deuteron energy is below the Coulomb barrier. On the other hand, using deuterons with energies above 23-25 MeV is also undesirable, since in this case the maxima in the angular distributions for different orbital momenta transferred are at 0°, and determining the momenta becomes unreliable.

At our deuteron energy (13.6 MeV) the orbital momenta transferred can be determined uniquely for $A \leq 130$ and l = 0-4. Figure 5 shows typical angular distributions for the nuclei Zr^{90}, Ti^{49}, Sn^{119}, Ca^{40} and selenium in order of increasing l from 0 to 4. Table 2 gives all of our spectroscopic results [23-33].

In addition to the nuclear spectroscopic data, some results were obtained during the study of stripping reactions which seemed to us to be of interest from the point of view of nuclear reaction theory. Thus, for carbon, where the measurements were made at 4.65, 7.15, 12.1, and 13.3 MeV, it turned out that Butler's theory with a radius of 4.6 F gives a description of the transition to the ground state for all energies except the lowest one. At 4.65 MeV the radius had to be taken equal to 5.5 F. The radius has to be increased as a result of the dynamic peculiarities of stripping reactions, as was pointed out by Wilkinson [47].

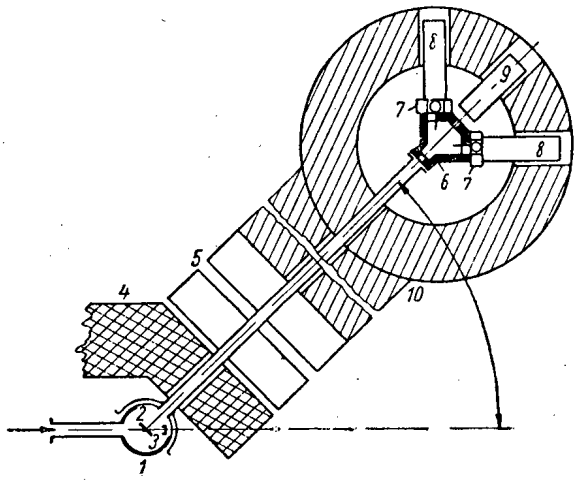

Fig. 6. Diagram of apparatus for investigating the polarization of protons formed in (d,p) reactions: 1) reaction chamber; 2) target; 3) Faraday cylinder; 4) lead shield; 5) magnetic lenses; 6) helium scattering chamber; 7) proportional counters; 8) scintillation spectrometers; 9) monitor; 10) paraffin shield.

The first excited state of Zr^{92} has spin 2^+. Since the spin of Zr^{91} is equal to $5/2^+$, the transition to this state in the stripping reaction can entail transfer of the angular momenta 0, 2, and 4, and the most intense will be the transition with the minimum orbital momentum transfer. At the same time no increase in cross section is observed in the small angle range, i.e., the term with $l = 0$ is absent. Since filling of the neutron state $d_{5/2}$ occurs in zirconium, which requires capturing a neutron with orbital momentum equal to two, we are here encountering a case where the selection rules of the shell model forbid a transition with minimum orbital momentum transfer, which is allowed in the theory of stripping reactions. The possibility of situations of this sort has been pointed out in the paper by Bethe and Butler [48]. Similar phenomena have been observed before this for transitions to the ground states of the final nuclei. This is the only example that we have heard so far of a transition to an excited state of the final nucleus. It is interesting that transitions with $l = 0$ and $l = 2$ are observed in the reaction Mo^{95} (d,p)Mo^{96} with excitation of the first level. Here the intensity of the transition with $l = 2$ (including the kinetic factor) is ~ 70%. The reduction in forbiddenness of j–j-coupling as compared with Zr^{92} may be due to the Zr^{92} having two neutrons beyond a closed shell, while Mo^{96} has four.

TABLE 3. Data on Proton Polarization in Stripping Reactions (E_d^0 = 13.6 MeV)

Target nucleus	Excitation energy of final nucleus, MeV	Angle of measurement, deg.	Momentum transferred	Final spin	No. of counts on the right	No. of counts on the left	Polarization (P ± ΔP), %
Be^9	0	10	1	3/2	1457	1046	+33±6
		17			1657	1436	+14±5
		25			1732	1479	+16±5
		35			602	449	+29±10
		45			374	391	−4±10
		55			385	345	+11±11
		70			285	273	+4±10
B^{10}	0	10	1	3/2	1105	914	+19±5
		20			1055	952	+10±5
		25			353	314	+11±8,5
		30			680	556	+17±6,5
		40			360	360	0±8,5
		50			966	916	+5±9
		60			268	221	+19±10
		70			190	159	+18±11
Ca^{40}	0	10	3	7/2	677	500	+30±8
		20			379	374	+1,3±8
		30			613	554	+10±6,5
		40			273	267	+2±9
		45			480	462	+4±7,5
		50			256	269	−5±9
		55			205	239	−15±9
		60			351	310	+12±9
		65			385	401	−4±8
		70			408	410	−0,5±8
Ni^{58}	0	10	1	3/2	769	631	+20±8
		20			418	407	+3±7
		30			1217	1122	+9±5
		50			119	98	+19,5±11
Si^{28}	0	10	0	1/2	539	514	+5±6,5
	1,28	20	2	3/2	1007	1000	+0,7±6
		30	2	3/2	475	540	−13±7
Ni^{60}	0	10	1	3/2	464	314	+39±7

Satchler has shown theoretically that the probabilities of reactions accompanied by excitation of successive levels of the same vibrational or rotational band will differ by approximately an order of magnitude [49]. In order to check Satchler's conclusions, some measurements were made on the nuclei Cd^{111}, Cd^{113}, Sn^{117} and Sn^{119}. The ratios of the normalized widths for transitions to the ground and first excited states turned out to be equal to 4.4, 2.2, 4.8, and 5.7 for Cd^{112}, Cd^{114}, Sn^{118}, and Sn^{120} respectively. With the exception of the ratio for Cd^{114} they are close to the values predicted by Satchler.

In order to get some information on the origin of the "gross structure", the proton spectra were measured at an angle of 40° in the (d,p) reactions occurring during deuteron bombardment of the nuclei of iron, Cu^{63}, Cu^{65}, selenium, zirconium, Nb^{93}, Ag^{107}, Ag^{109}, Cd^{116}, Sn^{116}, Sn^{118}, Sn^{120}, Sn^{124}, platinum, gold, Pb^{208}, and Bi^{209} ; we also measured the angular distributions of the protons from (d, p) reactions with the nuclei Cu^{63}, Cu^{65}, selenium, niobium, Cd^{115}, Sn^{116}, Sn^{118}, and Sn^{124} [34]. A comparison of the data of measurements made with high resolution shows that the maxima of the "gross structure" contain several isolated levels. Each of the maxima may be referred to a corresponding nuclear shell. Such a comparison may be made from the Q values and the orbital momenta of the states forming a "gross peak". It follows from this analysis that the gross peaks for the (d,p) reactions may be brought into correspondence with the neutron shells of the nucleus. Thus, in selenium, transition to the ground state is accompanied by the angular momentum transfer $l = 4$, corresponding with the state of the last neutron $g_{7/2}$, while transition to an excited state is accompanied by the angular momentum transfer $l = 0$, corresponding with the minimum orbital momentum of the stages in the next shell. If the reaction were associated with excitation of a proton shell, the angular momenta transferred would be 1 and 3, and the observed transition to the ground state with $l = 4$ would be suppressed by the transition with $l = 1$. A similar picture is found for other nuclei.

On passing from platinum and gold to lead and bismuth a discontinuous change is observed in the value of Q, which may be due to the fact that the neutron shell with 126 neutrons is filled between gold and lead. Here, in platinum, gold, and lead, the last protons are in the same states ($h_{11/2}$), while the neutron states belong to different shells.

In addition to the angular distributions and stripping reactions, a study was made of the proton polarization [35, 36] and the angular (d,p,γ)-correlations [37]. A general view of the equipment used to measure the polarization is shown in Fig. 6. The protons from the target 2 were focused by the quadrupole lenses 5, and after slowing down to an energy of ~ 11.5 MeV were incident on an He^4 scatterer. The right-left scattering asymmetry was recorded by the scintillation counters 8, connected for coincidence with the proportional counters7. Using quadrupole lenses made it possible to introduce the heavy shielding 4, 10 between the first and second scattering, which made the experiment substantially easier. The angular dependence of the polarization was measured for the nuclei Be^9, B^{10}, Si^{28}, Ca^{40}, Ni^{58}, and Ni^{60}. The results of the measurements are shown in Table 3. In all cases, the sign of the polarization was positive for $j = l + s$ and negative for $j = l - s$.

The angular (d,p,γ)-correlation was investigated in the Be^9 (d,p) Be^{10} reaction for the transition to the first excited state. The measurements were made in the plane of the reaction. The proton counter was in the position corresponding with the maximum of the angular distribution. The measuring equipment consisted of a special reaction chamber which made it possible to take measurements both in the plane of the reaction and in a plane perpendicular to the axis of emission, two scintillation spectrometers, and a fast-slow coincidence circuit with a resolution of $3 \cdot 10^{-9}$ sec. The resulting angular correlation may be expressed analytically by the function $W(\theta) = 1 - (0.39 \pm 0.06) \times \cos^2\theta$.

Other types of reactions. Among the other types of reactions studied were Be^9 (d, t)Be^8, Be^9 (p,d) Be^8, and Be^9 (d,α) Li^7 [38-39]. In all cases, the angular distributions have a clearly defined forward direction, indicating a direct mechanism for the reaction. Since the (p,d) and (d,t) reactions were investigated in the Be^9 nucleus for the same transition, the ratio of the differential cross sections for these reactions can be used to find the probability of representing the triton wave function as the wave function of the ground state of the deuteron plus one neutron [50]. The value calculated for the probability turned out to be less than 0.07 in our case.

SUMMARY

Investigating the interactions of protons and deuterons with separated isotopes has made it possible to do the following:

1. Observe and study the isotope effect in elastic scattering of protons by the nuclei of chromium, nickel, copper, and zinc, the effect consisting in a considerable difference in the differential scattering cross sections at large angles by isotopes differing from one another by one or two neutrons.

2. Use the energy and angular distributions of the products of stripping reactions to find the quantum characteristics of both the ground and the lowest excited states of a large number of nuclei.

3. Verify the ability of the optical model of the nucleus to describe elastic and inelastic proton scattering, and find the parameters of the model including the polarization associated with spin-orbital interaction of the nucleons in the nuclei. The angular dependence in elastic deuteron scattering may be accounted for by ideas based on electrical splitting of deuterons.

LITERATURE CITED

1. V. A. Kovtun, M. V. Pasechnik, and N. N. Pucherov, in collection "Nuclear Reactions at Small and Medium Energies" [in Russian] Moscow , Academy of Sciences Press, USSR, p. 301 (1958).
2. M. Pasetchnik, N. Poutcherov, and I. Totsky, Comptes rendus du Congress International de Physique Nucleaire. Paris, p. 598 (1958).
3. N. N. Pucherov, "Ukr. fiz. zh." 4, 313 (1959).
4. M. Pasetchnik et al., Proceedings of the International Conference on Nuclear Structure. Canada, Kingston, p. 176 (1960).
5. N. N. Pucherov, "Ukr. fiz. zh." 4, 318 (1959).
6. A. K. Val'ter et al., "Zh. éksperim. i teor. fiz." 38, 1419 (1960); "Ukr. fiz. zh." 5, 270 (1960).
7. A Valter et al., Proceedings of the International Conference on Nuclear Structure. Canada, Kingston, p. 173 (1960).
8. M. V. Pasechnik et al., "Ukr. fiz. zh." 6, 425 (1961).
9. A. K. Val'ter et al., "Zh. éksperim. i teor. fiz." 41, 71 (1961).
10. M. V. Pasechnik, N. N. Pucherov, and V. I. Chirko, "Izv. AN SSSR. Ser. fiz." 24, 874 (1960).
11. O. F. Nemets and G. A. Prokopets, "Zh. éksperim. i teor. fiz." 38, 693 (1960).
12. M. V. Pasechnik et al., ibid, 39, 915 (1960).
13. M. V. Pasechnik et al., Transactions of the Meeting of the Academy of Sciences, UKrSSR, on the Peaceful Uses of Atomic Energy [in Russian], Kiev, Academy of Sciences Press, UkrSSR (1961).
14. Yu. V. Gofman and O. F. Nemets, "Zh. éksperim. i teor. fiz." 39, 1489 (1960).
15. Yu. V. Gofman and O. F. Nemets, ibid, 40, 477 (1961).
16. O. F. Nemets, Transactions of the Session of the Academy of Sciences, UkrSSR, on the Peaceful Uses of Atomic Energy [in Russian], Kiev, Academy of Sciences Press, UkrSSR, p. 146 (1958).
17. Yu. V. Gofman and O. F. Nemets, "Zh. éksperim. i teor. fiz." 42, 657 (1962).
18. Yu. V. Gofman et al., "Izv. AN SSSR Ser. fiz." 25, 1305 (1961).
19. O. F. Nemets, Yu. I. Struzhko, and V. V. Tokarevskii, "Pribory i tekhnika éksperimenta" (in press).
20. O. F. Nemets et al., "Izv. AN SSSR. Ser. fiz." 24, 858 (1960).
21. Yu. V. Gofman, O. F. Nemets, and Yu. S. Stryuk, "Zh. éksperim. i teor. fiz." 42, 653 (1962).
22. Yu. V. Gofman and O. F. Nemets, ibid., 1013 (1962).
23. N. I. Zaika and O. F. Nemets "Izv. AN SSSR Ser. fiz." 23, 1460 (1959).
24. N. I. Zaika and O. F. Nemets, "Ukr. fiz. zh." 4, 519 (1959).
25. N. I. Zaika, O. F. Nemets, and V. S. Prokopenko, "Zh. éksperim. i teor. fiz." 38, 287 (1960).
26. N. I. Zaika, O. F. Nemets, and M. Tserineo, ibid., 39, 3 (1960).
27. N. I. Zaika and O. F. Nemets, "Izv. AN SSSR Ser. fiz." 24, 865 (1960).
28. N. I. Zaika, O. F. Nemets, and V. S. Prokopenko, ibid., 872 (1960).
29. N. I Zaika and O. F. Nemets, "Zh. éksperim. i teor. fiz." 40, 1019 (1961).
30. O. F. Nemets and V. V. Tokarevskii, "Izv. AN SSSR Ser. fiz." 25, 1138 (1961).
31. N I. Zaika and O. F. Nemets, ibid. 25, 1308 (1961).
32. M. V. Pasechnik and P. G. Ivanitskii, "Ukr. fiz. zh." 6, 603 (1961).
33. N. I. Zaika, O. F. Nemets, and V. V. Tokarevskii, "Zh. éksperim. i teor. fiz." (in press).
34. O. F. Nemets and V. Tokarevskii, ibid, 42, 1481 (1962).
35. D. I. Tambovtsev, ibid (in press).
36. M. V. Pasechnik and D. I. Tambovtsev, "Ukr. fiz. zh." fiz." 7, 12 (1962).
37. G. Kosinov and O. F. Nemets, "Izv. AN SSSR Ser. fiz." 26, No. 12 (1962).
38. O. F. Nemets, L. S. Saltykov, and M. V. Sokolov, "Zh. éksperim. i teor. fiz." 38, 1663 (1960).
39. P. G. Ivanitskii, ibid (in press).
40. J. French and M. Goldberger, Phys. Rev. 87, 899 (1952).
41. P. Gugelot et al., Proceedings of the International Conference on Nuclear Structure. Canada, Kingston (1960).

42. D. Hoffman, Nucl. Sci. Abstrs. 15, 2604 (1961).
43. R. Huby and H. Newns, Philos. Mag. 42, 1442 (1951).
44. C. Mullin and E. Guth, Phys. Rev. 82, 141 (1951).
45. S I. Drozdov," Zh. éksperim. i teor. fiz." 28, 734 (1955); E. V. Inopin, ibid., 31, 901 (1956); J. Blair, Phys. Rev. 115, 928 (1959).
46. S. Butler, Proc. Roy. Soc. A208, 559 (1951).
47. D. Wilkinson, Philos. Mag. 3, 1185 (1958).
48. H. Bethe and S. Butler, Phys. Rev. 85, 1045 (1952).
49. G. Satchler, Ann. phys. 3, 275 (1958).
50. S. Butler and E. Salpeter, Phys. Rev. 88, 133 (1952).

POSSIBILITY OF THE STUDY OF FISSION AT A FIXED COMPOUND-NUCLEUS EXCITATION ENERGY

V. M. Pankratov and V M. Strutinskii

Translated from Atomnaya Énergiya, Vol. 14, No. 2,
pp. 171-176, February, 1963
Original article submitted May 4, 1962

A "subtraction" method is proposed for the study of fission (the fragment mass distribution, the kinetic energy distribution) for a fixed compound-nucleus excitation energy. By way of illustration, the experimental data obtained with the time-of-flight method for the fission of U^{233} and Th^{232} induced by α particles are analyzed.

It is shown that for a nuclear excitation energy of the fissioning nucleus equal to ~ 25 Mev the fission is asymmetric, while the dip in the kinetic energy for symmetric fission is also preserved.

Recently a considerable amount of experimental data has become available on fission induced by charged particles and neutrons with energies of the order of several tens of million electron-volts. The study of fission in this energy region is of interest for the explanation of the fission mechanism since the range of studied nuclei is considerably broadened and, moreover, it is possible to study the influence of the nuclear excitation energy on the fission process. The interpretation of the experimental data for this energy region is made difficult by the fact that there is usually a contribution from fission accompanied by the emission of one or several neutrons (emission fission) and the fact that what is observed experimentally is in most cases the result of some very indefinite averaging over different fissioning nuclei and a broad interval of excitation energies. The only exceptions appear to be such cases in which the compound nucleus is characterized either by very high or very small fissility. In the latter case the contribution from emission fission is small, owing to the sharp decrease in the fissility with decreasing excitation energy for a large difference in energy between the fission threshold and the binding energy of the neutron.

The difficulty arising in connection with the presence of emission fission is bypassed relatively simply in those cases in which it can be assumed that the observed distribution does not depend on the compound-nucleus production mechanism, but is determined only by the nucleon composition and the excitation energy of the compound nucleus. For this, it is necessary to compare the observed distributions for two initial fissioning nuclei which differ by one neutron and have initial excitation energies differing by the mean energy carried away from the initial nucleus by the neutron:

$$\overline{\Delta U} = B_n + \bar{\varepsilon}, \tag{1}$$

where B_n is the binding energy of the neutron and $\bar{\varepsilon}$ is the mean kinetic energy of the neutron. In fact, the partial cross section for fission of a given type ν of a compound nucleus with N neutrons* induced by a bombarding particle of energy E_1 can be represented as

$$\sigma_{f\nu}^{(N)}(E_1) = \sigma_c^{(N)}(E_1)\left[\gamma_f^{(1)}\hat{Q}_{U_1}^{(N)}(\nu) + (1-\gamma_f^{(1)})P_{U_2}^{(N-1)}(\nu)\right], \tag{2}$$

where $\sigma_c^{(N)}(E_1)$ is the cross section for compound nucleus formation; $\gamma_f^{(1)}$ is the relative probability for the direct fission of an initial compound nucleus of excitation energy U_1:

$$\gamma_f^{(1)} = \frac{\Gamma_f^{(1)}}{\Gamma_f^{(1)} + \Gamma_n^{(1)}};$$

*The emission of charged particles here is neglected and the charge of the nucleus is assumed to be unchanged.

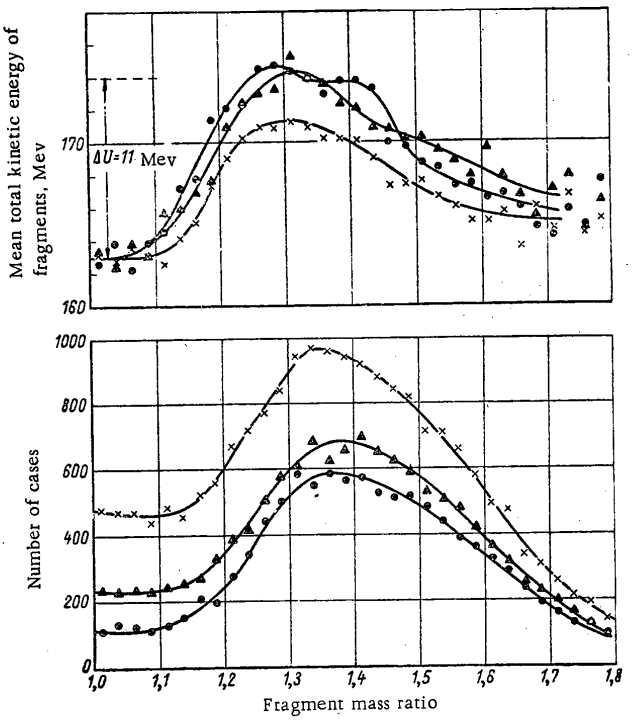

Fig. 1. Fragment mass distribution (bottom) and fragment total kinetic energy distribution (top) as a function of the mass ratio for the fission of Th^{232} induced by α particles of energy 21.8 Mev (●), 25.5 Mev (▲), and 29.2 Mev (×).

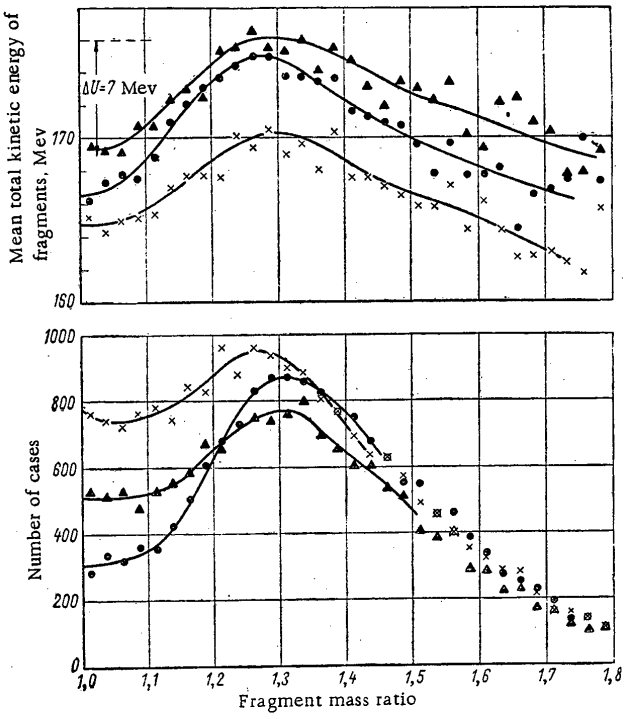

Fig. 2. Fragment mass distribution (bottom) and fragment total kinetic energy distribution (top) as a function of the mass ratio for the fission of U^{233} induced by α particles of energy 21.8 Mev (●), 25.5 Mev (▲), and 29.2 Mev (×).

$\hat{Q}_U^{(N)}(\nu)$ is the relative probability for fission of a given type ν directly from a compound nucleus with N neutrons and excitation energy U and is normalized to unity:

$$\int d\nu \hat{Q}_U^{(N)}(\nu) = 1. \tag{3}$$

In expression (2), the quantity $P_U^{(N)}(\nu)$ is the probability for the fission of a type ν of a nucleus (Z, N, U) summed over all cascades of emission fission. It is assumed that this probability is normalized to one compound nucleus. It is obvious that the ratio of the cross sections entering into the left- and right-hand parts of formula (2) is the

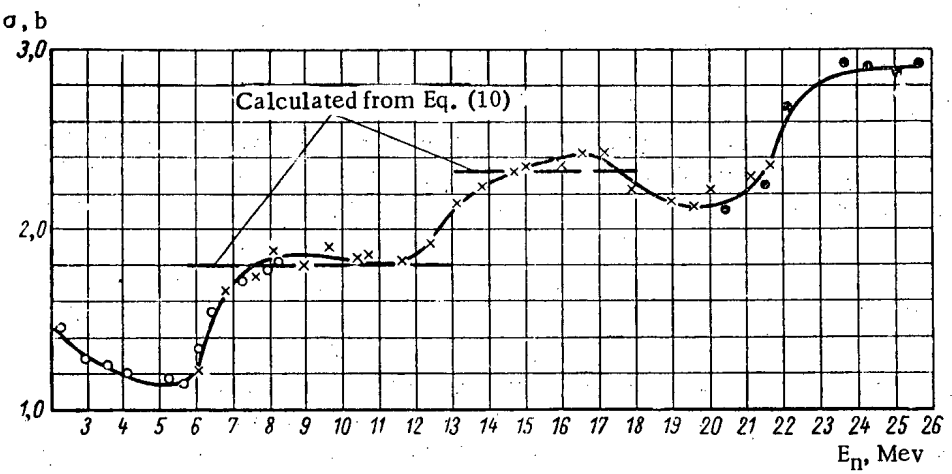

Fig. 3. Comparison of the experimental value of the fission cross section of U^{235} induced by neutrons from the reactions: ○) $T(p,n)He^3$; ×) $D(d,n)He^3$; ●) $T(d,n)He^4$ with the value calculated from Eq. (10) on the basis of data on the fission probability at excitation energies of 8-10 Mev. The experimental data are taken from [3]. The fission probability is taken from [1].

analogous probability for the fission of the initial compound nucleus, while $P_{U_2}^{(N-1)}(\nu)$ can also be expressed through a similar ratio of the fission cross section to the cross section for production of the compound nucleus (Z, N-1, U_2). For what follows it will be convenient to introduce the total fission cross section

$$\sigma_f^{(N)} = \int d\nu \sigma_{f\nu}^N,$$

and to normalize the probability $P_U^{(N)}(\nu)$ to unity:

$$P_U^{(N)}(\nu) = \frac{\sigma_f^{(N)}}{\sigma_c^{(N)}} \hat{P}_U^{(N)}(\nu), \tag{4}$$

where $\int \hat{P}^{(N)}(\nu)\, d\nu = 1$.

It is important to note that within the framework of the compound-nucleus model we can take for the quantities $\sigma_f^{(N)}$ and $\sigma_c^{(N)}$ in formula (4) the fission cross section and the compound-nucleus production cross section for any process leading to the formation of the compound nucleus (Z, N, U)*.

*It is assumed that the value of the angular momentum is not important. A similar analysis is also possible in the more general case, but it is much more complicated.

In formula (2)

$$U_2 = U_1 - \overline{\Delta U} \simeq U_1 - B_n - \bar{\varepsilon} = U_1 - B_n - 2T, \tag{5}$$

where T is the nuclear temperature. Here it is assumed that the neutron energy spread is not important, which usually proves to be the case.

From expressions (2) and (4) we can obtain the distribution $Q_U^{(N)}(v)$, which is of physical interest:

$$Q_{U_1}^{(N)}(v) = \hat{P}_{U_1}(v) - \left(1 - \gamma_f^{(1)}\right) \frac{\sigma_f^{(N-1)}(U_2)}{\sigma_c^{(N-1)}(U_2)} \frac{\sigma_c^{(N)}(U_1)}{\sigma_f^{(N)}(U_1)} \hat{P}_{U_2}^{(N-1)} \tag{6}$$

(an unessential normalizing factor is omitted).

In principle, all quantities in the right-hand part of equality (6) can be directly measured experimentally with a suitable choice of the target, incident particle, and incident energy. Various methods [1] can be used to determine the quantity $\gamma_f^{(1)}$. In some cases the quantity $\gamma_f^{(1)}$ can be determined by formula (2), from which it follows that

$$\frac{\sigma_f^{(N)}(U_1)}{\sigma_c^{(N)}(U_1)} = \gamma_f^{(1)} + \left(1 - \gamma_f^{(1)}\right) \frac{\sigma_f^{(N-1)}(U_2)}{\sigma_c^{(N-1)}(U_2)} \tag{7}$$

(in this formula the excitation energy of the corresponding compound nucleus appears in place of the particle energy). For the determination of $\gamma_f^{(1)}$ it is more convenient to use the cross sections for fission induced by neutrons, which have been measured quite accurately for a large number of targets and over a broad energy interval [2, 3]. The cross sections

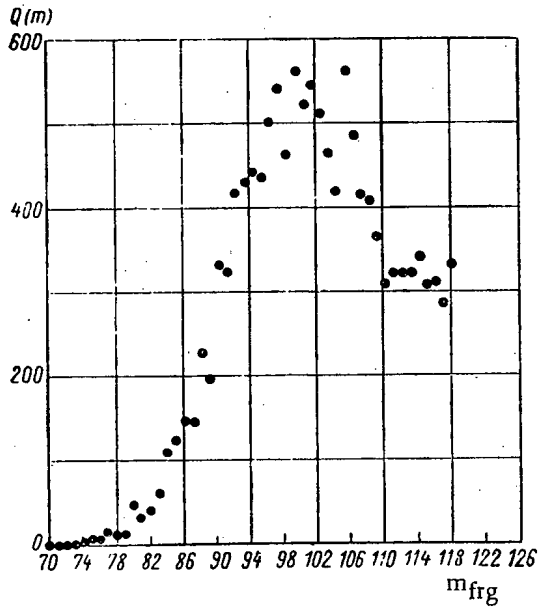

Fig. 4. Fragment mass distribution for the U^{236} fission directly from a state with excitation energy 24.6 Mev.

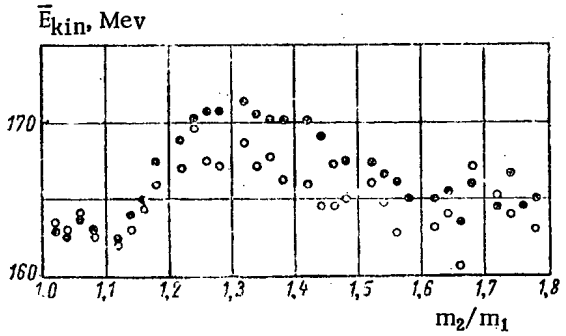

Fig. 5. Mean total kinetic energy of fragments for U^{236} fission directly from a state with excitation energy 24.6 Mev (●) and values calculated for $\gamma_f^{(1)} = 0.4$ and $\sigma_f^{234}/\sigma_f^{235} = 0.8$ (○).

σ_c weakly depend on the energy and can be taken equal to the geometric cross section of the nucleus. Formula (7) permits one to find the value of $\gamma_f^{(1)}$ with sufficient accuracy if it is not too small or close to unity and if σ_f differs appreciably from σ_c.

The case of very high or very low fissility does not, in general, present difficulties, since for the aforementioned reasons it can be assumed that it is the initial nucleus that undergoes fission. If as a result of the high

excitation energy of the nucleus we have $\sigma_f = \sigma_c$ (which, of course, can occur even for nuclei with an average fission probability), then all cross sections drop out of the formulas and other methods (for example, the use of the probability of deep splitting) must be used to determine $\gamma_f^{(1)}$.

Apart from the mass distribution, the dependence of the mean total kinetic energy of the fragments on the fragment mass ratio for direct fission of a given compound nucleus at a given excitation energy is also of interest. This distribution can be found in a similar way.

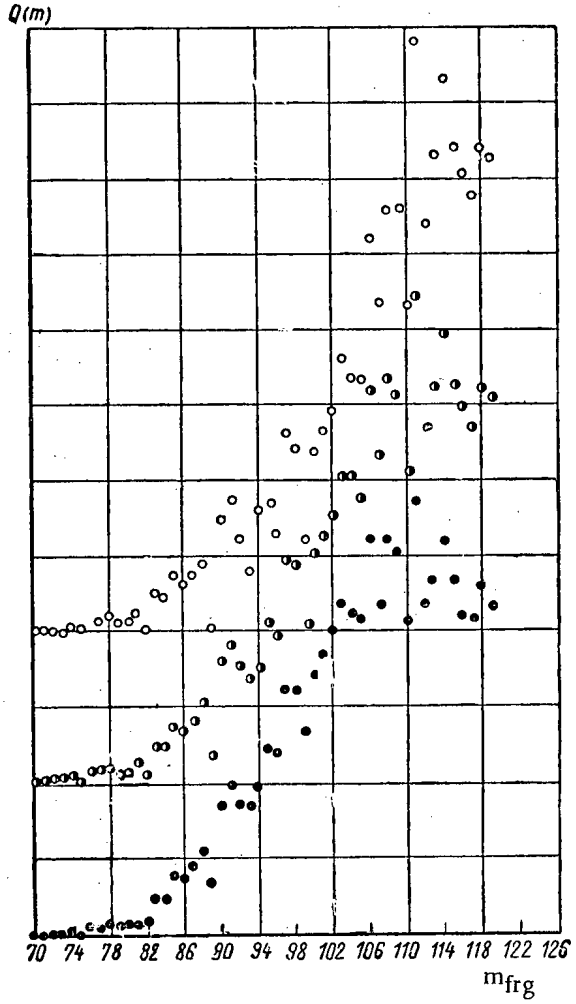

Fig. 6. Fragment mass distribution for fission of Pu^{237} directly from a state with excitation energy 23.5 Mev for different values of the parameter $\gamma_f^{(1)}$: ●) 0.65; ◑) 0.55; ○) 0.45. The distributions have been normalized to unity. For convenience, the points corresponding to the last two values of the parameter have ordinates displaced by two and four scale units.

We introduce quantity $q(\mu)$ (where μ is the fragment mass ratio), equal to the relative probability of direct fission from the initial compound nucleus. It is obvious that $q(\mu)$ differs from the corresponding distribution $Q_{U_1}^{(N)}(\nu)$ only in the normalization factor.

From expression (2) we find

$$q(\mu) = 1 - (1 - \gamma_f^{(1)}) \frac{\sigma_f^{(N-1)}(U_2)}{\sigma_c^{(N-1)}(U_2)} \frac{\sigma_c^{(N)}(U_1)}{\sigma_f^{(N)}(U_1)} \frac{\hat{P}_{U_2}^{(N-1)}(\mu)}{\hat{P}_{U_1}^{(N)}(\mu)}. \quad (8)$$

With the aid of formula (8) we find that the mean total kinetic energy of the fragments for a given mass ratio in the case of direct fission of the initial compound nucleus (Z, N, U) is equal to

$$E_{\text{kin}\,U_1}^{(N)}(\mu) = \frac{\overline{\{E_{\text{kin}\,U_1}^{(N)}(\mu) - [1 - q(\mu)]\, E_{\text{kin}\,U_2}^{(N-1)}(\mu)\}}}{q(\mu)}. \quad (9)$$

Here $\overline{E_{\text{kin}\,U_1}^{(N)}}(\mu)$ is the total kinetic energy of the fragments for a given mass ratio μ averaged over all forms of emission fission, i.e., the experimentally observed quantity; $\overline{E_{\text{kin}\,U_2}^{(N-1)}}$ is the similar quantity for the chain of emission fission, where the initial nucleus is (Z, N-1, U_2).

The most complete and most accurate data on the fission fragment distribution and the quantity $\overline{E_{\text{kin}}}$ as a function of μ were obtained in [4] by the time-of-flight method (Figs. 1 and 2). Using these data, we can determine the distributions $Q_{U_1}^{(N)}(\mu)$ and $E_{U_1}^{(N)}(\mu)$ if we compare the corresponding distributions for the α-particle energies, which differ approximately by the value $\overline{\Delta U}$. A difference of one neutron can be neglected here. Strictly speaking, to determine the distribution at smaller energy we should take as a target an isotope with one less neutron and choose the α-particle energy correspondingly.

We first consider the case of the fission of thorium. Here we can use the value $\gamma_f^{(1)}$ determined from the cross section for the fission of U^{235} induced by 3-Mev neutrons, since the probability of fission of a U^{236} compound nucleus appears to change little with the energy. This statement follows from the comparison of the experimental value of the neutron-induced fission cross section for U^{235} with the value calculated on the basis of the known data on fissionability. Figure 3 shows the results of a similar comparison. Here the fission cross section for each plateau was calculated from the formulas

$$\left.\begin{aligned}\sigma_f^2 &= \sigma_c^2[\gamma_f^{233} + (1-\gamma_f^{236})\gamma_f^{235}];\\ \sigma_f^3 &= \sigma_c^3[\gamma_f^{236} + (1-\gamma_f^{236})\gamma_f^{235})\\ &+ (1-\gamma_f^{236})(1-\gamma_f^{235})\gamma_f^{234}],\ \text{etc.},\end{aligned}\right\} \quad (10)$$

where σ_f^2, σ_c^2, σ_f^3, σ_c^3, etc. are the cross sections for fission and production of a compound nucleus corresponding to the 2nd, 3rd, etc., plateau, and γ_f is the relative fission probability for the succession of isotopes in emission fission.

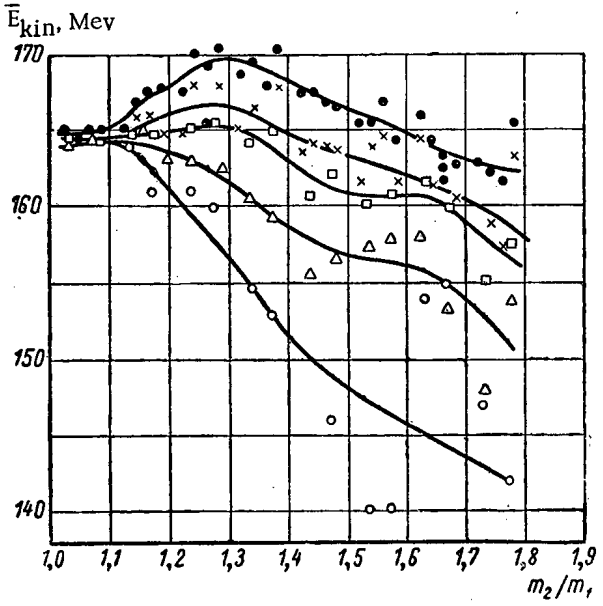

Fig. 7. Mean total kinetic energy distribution for fragments from the fission of Pu^{237} directly from the state with excitation energy 23.5 Mev for different values of the parameter $\gamma_f^{(1)}$: ×) 0.65; □) 0.55; △) 0.45; ○) 0.35; ●) based on experimental data for E_α = 29.2 Mev.

The ratio $\sigma_f^{(N-1)}(U_2)/\sigma_f^{(N)}(U_1)$ is also most easily estimated on the basis of cross section data for fission induced by 11- and 18-Mev neutrons. The cross section for the fission of U^{235} induced by 18-Mev neutrons is 2.2 b. Similar data on the cross sections for the fission of U^{234} at 11 Mev are lacking. However, comparison of the data on the cross sections for the fission of U^{233} and U^{235} in this region and also data on the fissility indicate that the U^{234} fission cross section is close to 2b, while $\frac{\sigma_f^{234}(11\,\text{Mev})}{\sigma_f^{235}(18\,\text{Mev})}$ is equal to 0.8-0.9.

Figure 4 shows the obtained fragment mass distribution for the fission of U^{236} directly from a state with excitation energy 24.6 Mev and Fig. 5 shows the corresponding function $E_{kin}(\mu)$. Both distributions are qualitatively similar to the distributions observed in fission with small energy, although the depth of the dips in both cases is considerably less. For symmetric fission of U^{236} the dip in the mass distribution corresponds to about 600 (see [5]) while the dip in the kinetic energy is approximately equal to 40 Mev [6]. We note that despite the use of the subtraction of the two distributions, they are quite distinct, and the possible uncertainty in the experimental data employed cannot lead to any essential change.

In the case of the $U^{233}(\alpha,f)$ reaction the Pu^{237} compound nucleus that is formed is characterized by a high fissility, and the corresponding ratio of the fission cross section to the total cross section is close to unity at both higher and lower excitation energies. The value of $\gamma_f^{(1)}$ is not known here with sufficient accuracy. In Figs. 6 and 7 the mass distribution and the function $\bar{E}_{kin}(\mu)$ for the fission of the Pu^{237} compound nucleus directly from a state with excitation energy 23.5 Mev is shown for different values of the parameter $\gamma_f^{(1)}$. The value $\gamma_f^{(1)} = 0.65$ is the most probable. The distribution corresponding to this value of the parameter is qualitatively similar to the distributions shown in Figs. 4 and 5. In particular, the mass distribution has a dip in the region of symmetric fission.

The fact that, even at an excitation energy of ~ 25 Mev for the fissioning nucleus, the qualitative features characteristic of fission at low energy are preserved is difficult to reconcile with the views on the influence of the quantum structure of the fissioning nucleus (or fragments) on the basic properties of fission. It can be hoped that more accurate and more complete experiments will permit clarification of this question, which is important for the theory of fission. It would appear that the accuracy of the analysis of the results by the method described here can be improved in more elaborate experiments.

LITERATURE CITED

1. R. Vandenbosh, Proceedings Second Intern. Conf. on the Peaceful Use of Atomic Energy, Geneva, 1958 [Russian edition] (Moscow, Atomic Press, 1959), Vol. 2, p. 336.
2. D. Hughes and R. Schwartz, Neutron Cross Sections [Russian translation] (Moscow, Atomic Press, 1959).
3. V. M. Pankratov, Atomnaya Énergiya, Vol. 14, No. 2 (1963), p. 177.
4. S. Whetstone Jr., and R. Leachman, Bull. Amer. Phys. Soc. II, 6, 376 (1961).
5. A. Hemmendinger, Proceedings Second Intern. Conf. on the Peaceful Uses of Atomic Energy, Geneva, 1958 [Russian edition] (Moscow, Atomic Press, 1959), Vol. 2, p. 89.
6. J. Milton and J. Fraser, Phys. Rev. Lett., 7, 67 (1961).

FISSION CROSS SECTIONS OF Th^{232}, U^{233}, U^{235}, Np^{237}, U^{238}, FOR 5-37 MeV NEUTRONS*

V. M. Pankratov

Translated from Atomnaya Énergiya, Vol. 14, No. 2,
pp. 177-184, February, 1963
Original article submitted May 4, 1962

Results are reported for measurements of the fission cross sections of Th^{232}, U^{233}, U^{235}, Np^{237}, U^{238} with 5-37 MeV neutrons. The measurements were made with the 1.5-meter cyclotron of the I. V. Kurchatov Order of Lenin Institute of Atomic Energy. The reactions $D(d,n)He^3$ and $T(d,n)He^4$ were used to obtain the neutrons. Energy selection of the neutrons was accomplished by the time-of-flight method. Gas-filled scintillation fission counters were used as detectors.

In [1, 2], results were given for measurements of the fission cross sections of Th^{232}, U^{233}, U^{235}, Np^{237}, U^{238}, and Pu^{239} with neutrons in the energy ranges 3-10 and 10-22 MeV. In the first of these, the measurements were done in the usual way with ionization fission chambers, while in the second, they were made with gas-filled scintillation fission counters and a time-of-flight fast neutron spectrometer.

In this paper, results are reported for measurements of Th^{232} and U^{238} fission cross sections with 22-37 MeV neutrons, of U^{235} and Np^{237} cross sections with 22-27 MeV neutrons, and of the U^{233} cross section with 10-22 MeV neutrons. In addition, results are presented for measurements in the 5-10.5 MeV neutron energy range which were made for the purpose of clarifying the cross section curve, as well as results of measurements of the absolute values of the cross section in the 10-22 MeV range where, previously, only a relative curve had been obtained which was normalized to absolute values given in the literature, in the main for measurements with 14 MeV neutrons.

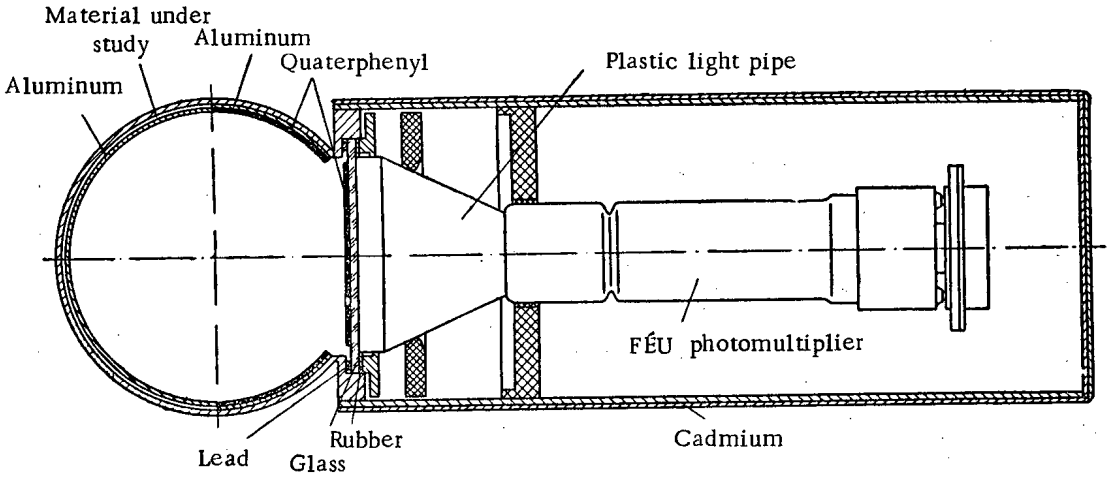

Fig. 1. Diagram of the gas-filled scintillation fission counter.

The reactions $D(d,n)He^3$ and $T(d,n)He^4$ were used to produce the neutrons. The measurements were carried out on the 1.5-meter cyclotron of the I. V. Kurchatov Order of Lenin Institute of Atomic Energy. Two types of accelerator operation were employed. In the first type, where E_d = 9.9 MeV, measurements were carried out in the 22-27 MeV neutron energy range ($T(d,n)He^4$ reaction) and the 5-10.5 MeV range ($D(d,n)He^3$ reaction). The second type of accelerator operation, where E_d = 19.5 MeV, was used for measurements in the 27-37 MeV range ($T(d,n)He^4$ reaction) and the 10-22 MeV range ($D(d,n)He^3$ reaction).

*See V. M. Pankratov, Reports of the meeting on the physics of nuclear fission (April 18-24, 1961). Moscow-Leningrad., Izd-vo AN SSSR (1961), p. 38.

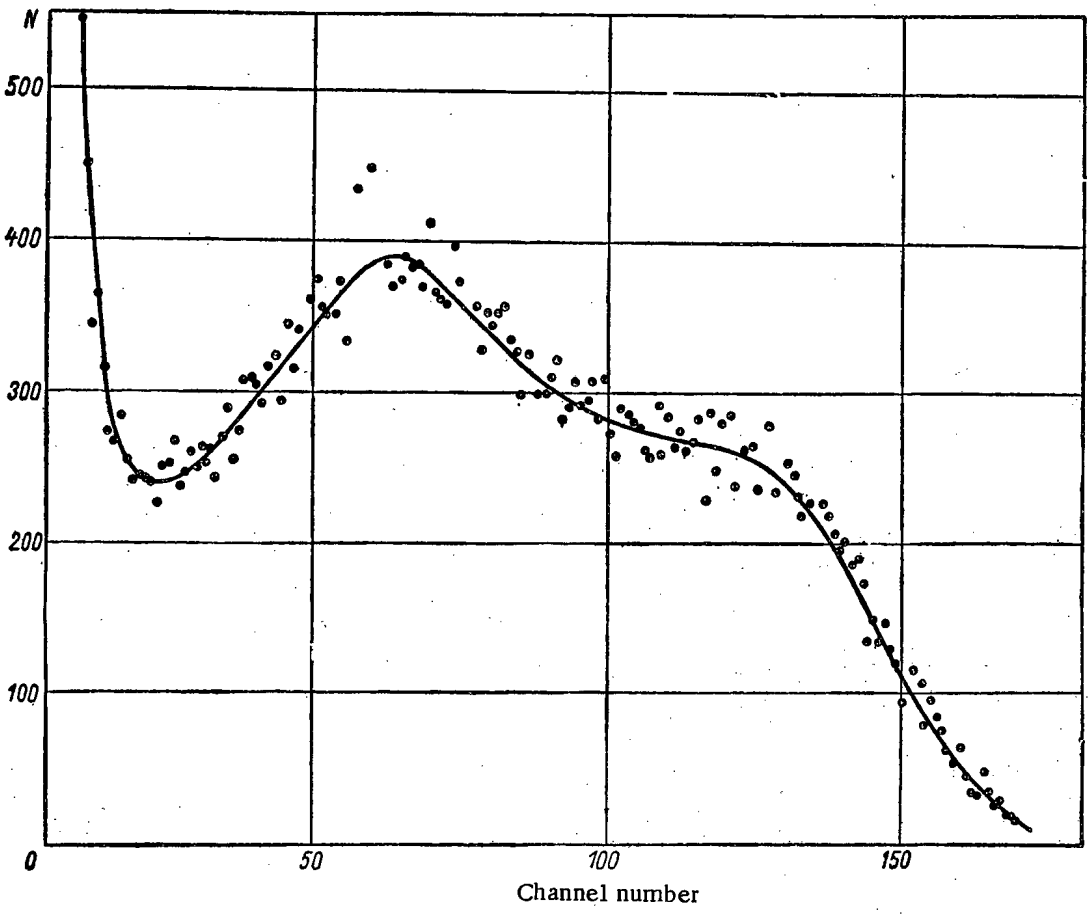

Fig. 2. Pulse height spectrum of Th^{232} fission fragments.

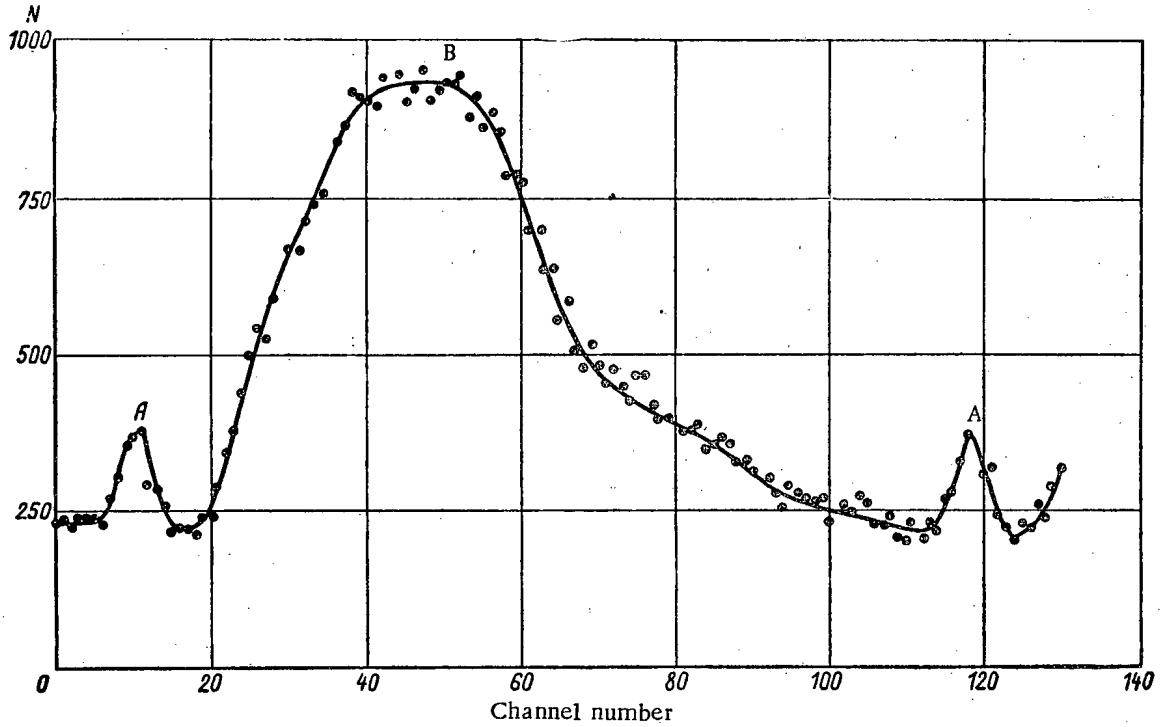

Fig. 3. Time spectrum of the pulses from fragments of U^{233} fissioned by neutrons from the $D(d,n)He^3$ reaction. Deuteron energy, 19.5 MeV; flight path, 2.7 m; A) fission by neutrons from the $D(d,n)He^3$ reaction; B) fission by neutrons from deuteron breakup.

The variation of neutron energies within the indicated ranges was accomplished by slowing down the deuterons with calibrated platinum foils which were placed in front of the target. All the measurements were made at an angle of 0° with respect to the beam of bombarding particles. In measurements with neutrons from the d-T reaction, a tritium-zirconium target was used, and a gaseous deuterium target was used in the measurements with neutrons from the d-d reaction.

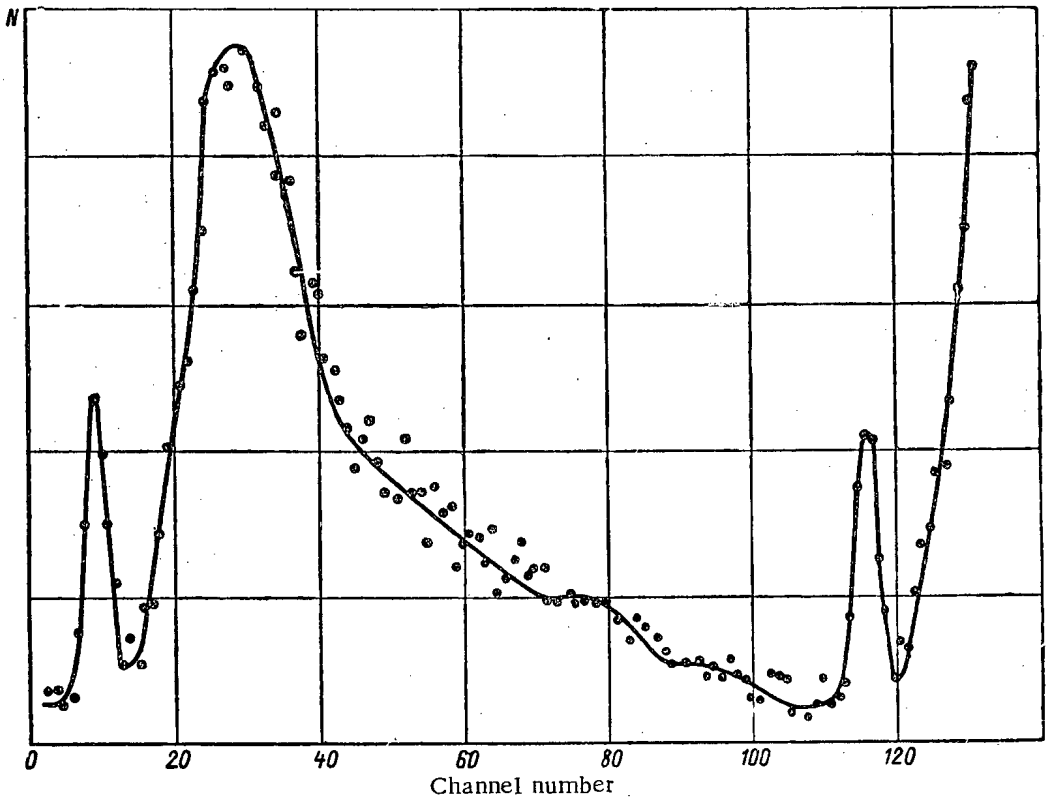

Fig. 4. Time spectrum of the pulses from fragments of Np^{237} fissioned by neutrons from the $T(d,n)He^4$ reaction. Deuteron energy, 9.9 MeV; flight path, 1.5 m.

Over a large part of the energy range investigated, a great number of neutrons arising from D(d,pn), T(d,pn), and other reactions were produced together with the neutrons from the $D(d,n)He^3$ and $T(d,n)He^4$ reactions. A multichannel, fast neutron time-of-flight spectrometer [3] was employed to separate monoenergetic neutrons. The time resolution of the spectrometer was 3 mμsec. In order to satisfactorily separate the effects associated with monochromatic neutrons with the resolution indicated, a fast fission fragment detector was required which had a relatively high efficiency, allowing measurements to be made over a 2.5-3 m base. The usual ionization fission chambers and proportional counters were unsuitable since the pulse rise time in them was not less than 10^{-7} sec. The use of solid scintillators was also ruled out because of the reduction in specific light yield with increasing ionization density produced by the detected particles. The effect mentioned made it practically impossible to differentiate fragments from α particles.

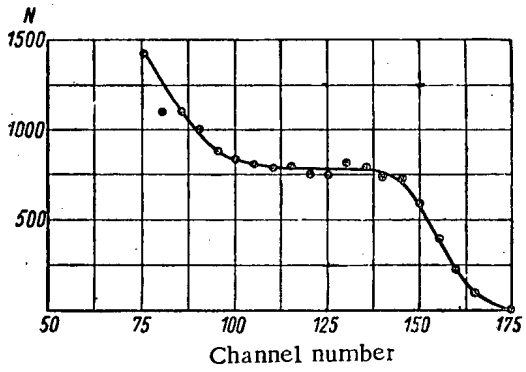

Fig. 5. Pulse height spectrum of recoil pulses in a stilbene crystal.

Gas-filled scintillation counters were used as fission detectors in our measurements. A schematic representation of a counter is shown in Fig. 1. It is in the form of a spherical chamber 10 cm in diameter with a circular glass window to which a photomultiplier is connected by means of a light pipe. On the internal surface of the hemisphere opposite the window, there was deposited by vacuum vaporization a layer of fissile material 1-1.5 mg/cm² thick so that the total weight of the layer amounted to 150-180 mg. An aluminum

layer of the order of 20 $\mu g/cm^2$ was deposited by vacuum vaporization on top of the fissile material layer. An aluminum layer several mg/cm^2 thick was deposited on the all the remaining surfaces of the sphere. A layer of quaterphenyl $30\mu g/cm^2$ thick was deposited over the aluminum on the inside surface of the chamber (the right hemisphere in the figure). Quaterphenyl was also deposited on the inside surface of the window (~ 10 $\mu g/cm^2$). The counter chamber was filled with xenon to a pressure somewhat greater than 1 atm. A type FÉU-33 photomultiplier, operated in the usual pulse mode, was used as a scintillation detector with the counter. However, in view of the heavy loading by α particles, the voltage to several of the lower multiplier dynodes was supplied from a low-resistance divider.

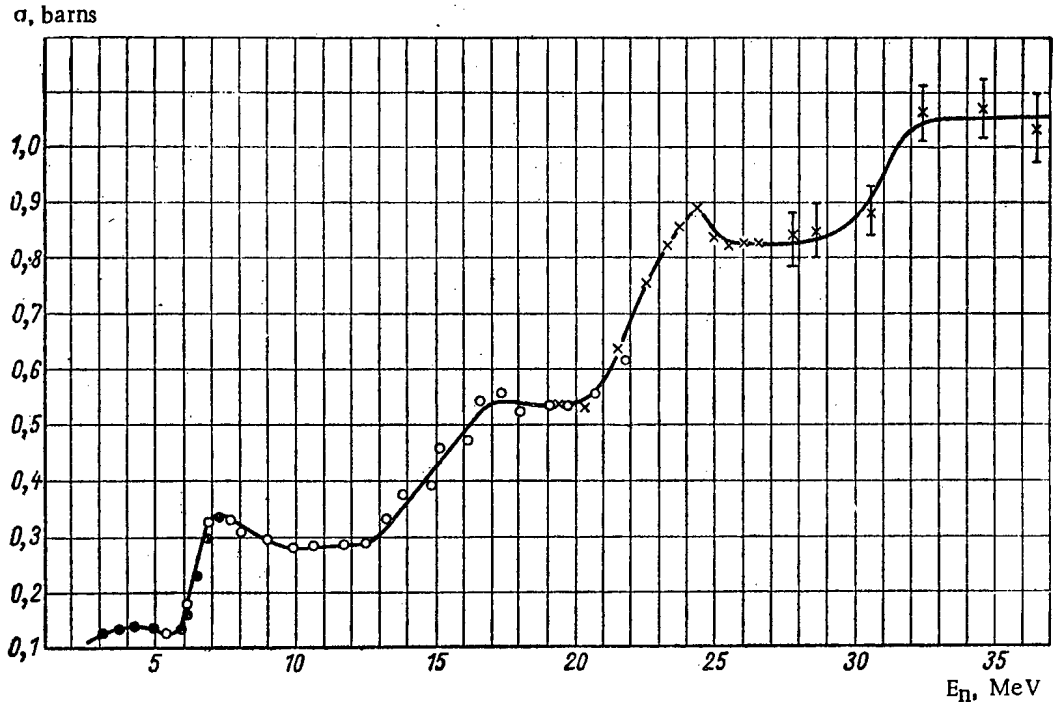

Fig. 6. Th^{232} fission cross sections for 3-37 MeV neutrons: ●) $T(p,n)He^3$ neutrons [1]; ○)$D(d,n)He^3$ neutrons; ×)$T(d,n)He^4$ neutrons.

The differential pulse height spectrum of the fission fragments from Th^{232} is shown in Fig. 2. For the measurements about 150 mg of thorium were placed in the counter. In Figs. 3 and 4, the time spectra of the pulses from the fission fragments of U^{233} and Np^{237} are shown. The sharp peak represents the effect of the monoenergetic neutron groups from the d-T and d-d reactions. The broad, continuous distribution corresponds to fission by neutrons arising from

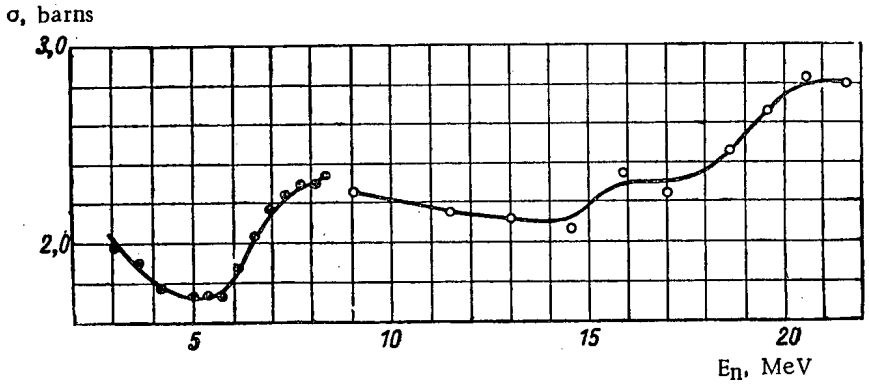

Fig. 7. U^{233} fission cross sections for 3-22 MeV neutrons: ●) $T(p,n)He^3$ neutrons; ○) $D(d,n)He^3$ neutrons.

deuteron breakup, and the base of the peak corresponds to the effect of scattered and moderated neutrons. Similar distributions are obtained for all the isotopes studied within the energy range mentioned. The area under the peak corresponds to the total number of fissions produced in the layer by neutrons of the monoenergetic group.

The neutron flux intensity from the $D(d,n)He^3$ and $T(d,n)He^4$ reactions at various deuteron energies was measured by a scintillation counter with a stilbene crystal which was connected into the time-of-flight spectrometer circuit. Simultaneously with the measurement of the neutron time spectra, the pulse height distribution of recoil protons in the crystal was recorded, picking out only those events connected with the detection of monochromatic neutrons from

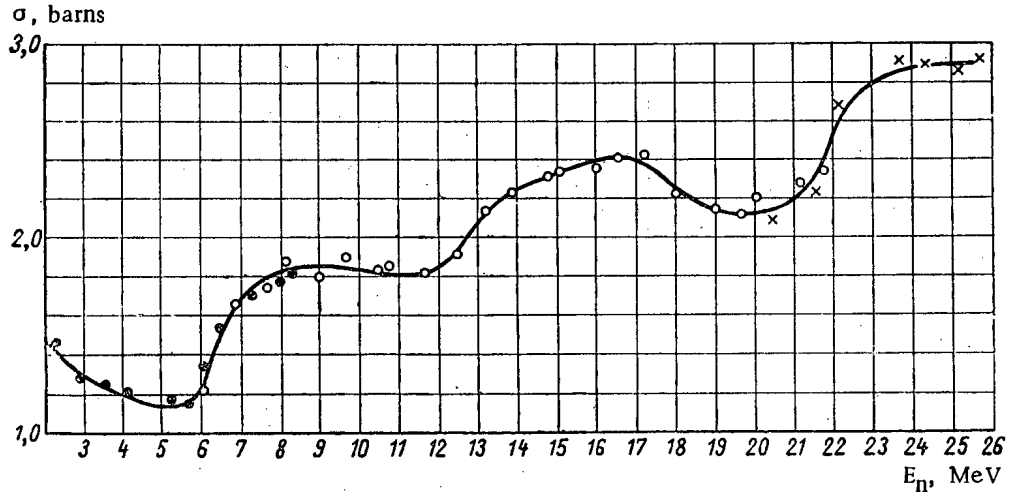

Fig. 8. U^{235} fission cross sections for 3-27 MeV neutrons: ●) $T(p,n)He^3$ neutrons [1]; ○) $D(d,n)He^3$ neutrons; ×) $T(d,n)He^4$ neutrons.

the d-T and d-d reactions by means of an auxiliary single-channel time analyzer which controlled the pulse height analysis circuit. As an example, the pulse height spectrum of recoil pulses in the stilbene crystal for E_n = 36.5 MeV is shown in Fig. 5. The plateau in the curve corresponds to recoil protons; the sharp rise in the soft portion of the spectrum is the result of pulses from recoil carbon nuclei and the products of other reactions. The determination of neutron fluxes from this data was made in accordance with procedures described in detail elsewhere [3].

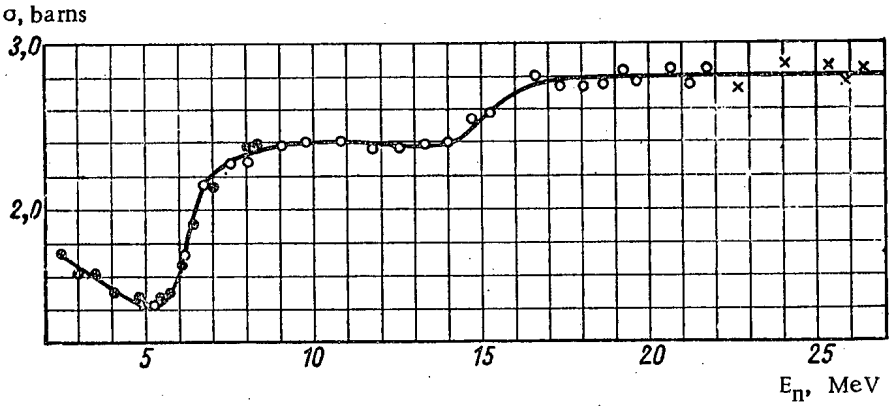

Fig. 9. Np^{237} fission cross sections for 2.5-27 MeV neutrons: ⊛) $T(p,n)He^3$ neutrons [1]; ○) $D(d,n)He^3$ neutrons; ×) $T(d,n)He^4$ neutrons.

In order to determine absolute cross section values, the counter layers were "weighed" in the monoenergetic 3.4 MeV neutron flux from the $T(p,n)He^3$ reaction for which the fission cross sections were well known for the isotopes mentioned. All the measurements for weighing were done under conditions exactly like those for the basic measurements. The fission cross sections at E_n = 3.4 MeV were taken to be 0.135 [4], 1.23 [2], 1.62 [2], and 0.55 [2] barns for Th^{232}, U^{235}, Np^{237}, and U^{238} respectively. The chamber containing U^{233} was not weighed and normalization was done with data for 10 MeV neutrons [5].

The results of fission cross section measurements are shown in Figs. 6-10. The over-all precision of the measurements was no worse than 5% in the 5-27 MeV range. Measurement precision was no worse than 10% in the 27-37 MeV range. The increase in error was connected with an increase in background and with some indeterminacy in the method of its measurement. Energy resolution was determined mainly by target thickness, and it was from 300 to 500 keV in the 5-10.5 MeV neutron energy range, from 250 to 700 keV in the 10-22 MeV range, and from 300 keV to 1 MeV in the 22-37 MeV range. In Fig. 11, and also in the 3-8.5 MeV range in Figs. 6-10, results are given for previously published measurements [1]. Corrections which were made to the curves in [1] were based on more accurate knowledge of the efficiency of the long counter with which the neutron flux measurements were made.

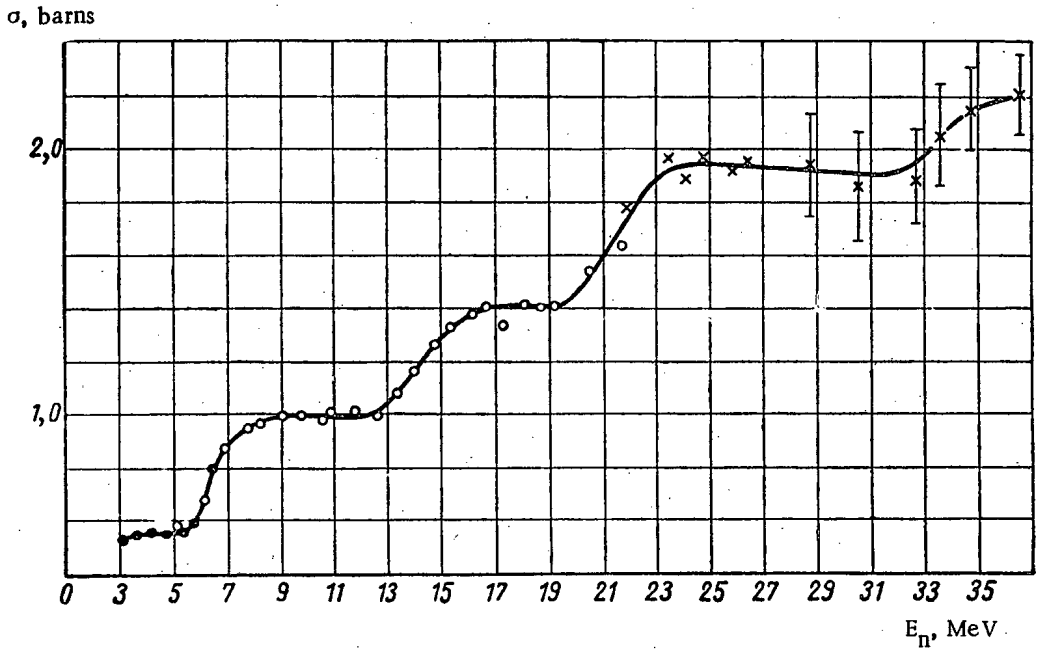

Fig. 10. U^{238} fission cross sections for 3-37 MeV neutrons: ●) $T(p,n)He^3$ neutrons [1]; ○) $D(d,n)He^3$ neutrons; × $T(d,n)He^4$ neutrons.

Common to all isotopes in the energy range investigated was a stepwise increase in fission cross section with increasing energy. On this general background, irregularities were noticed which were characterized by comparatively sharp increases in the cross section and subsequent slow decreases. Such an irregularity was first noticed in the Th^{232} cross section at neutron energies of 7-8 MeV. We also detected such "jumps" in the U^{235} cross section at 15-17 MeV, in the Th^{232} cross section in that same energy range, and apparently in the U^{238} cross section at a neutron energy of the order of 25 MeV. Jumps were observed only at places where a step was formed by the contribution from fission of even-even isotopes, which are characterized by high neutron binding energy and reduced fission threshold. The jumps depend on the fact that, at the beginning of the step, the emission of the next neutron is forbidden with respect to energy.

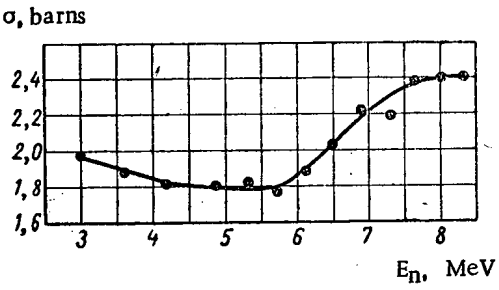

Fig. 11. Pu^{239} fission cross sections for 3-8.5 MeV neutrons.

The course of the U^{233} fission cross section curve in the 12-17 MeV region is extremely interesting. The rise, which results from the contribution of U^{232} to the cross section, is only slightly apparent here. This is all the more unexpected because the fission threshold for U^{232} is more than 2 MeV less than the neutron binding energy, and it indicates either a small fission probability for U^{232}, which completely disagrees with accepted ideas about fission probability dependence, on Z^2/A, for example, or it indicates a rapid reduction of U^{233} fission probability with energy.

In all the energy ranges under study, the steps have a clearly defined character, and it is therefore possible to determine with a precision of about 10% the contribution to the cross section from one or another isotope, and to determine the fission probability of that isotope. Data on fissility are given in the table and in Fig. 12 where the fission probabilities from data in [6, 7] are also shown.

Fission Probabilities for Isotopes of Thorium, Uranium, Neptunium and Plutonium

Isotope	E_n, MeV	$\frac{\Gamma f}{\Gamma f + \Gamma n}$ from our measurements	$\frac{\Gamma f}{\Gamma f + \Gamma n}$ from other measurements
Th^{233}	3	—	0,04 [6]
Th^{232}	10	0,060	—
Th^{231}	17	0,10	0,12 [7]
Th^{230}	26	0,13	—
Th^{229}	34	>0,16	—
U^{239}	3	0,17	0,17 [6]
U^{238}	10	0,21	—
U^{237}	17	0,24	0,25 [6]
U^{236}	26	0,37	—
U^{235}	34	~0,40	—
U^{236}	3	0,39	0,38 [6]
U^{235}	10	0,45	—
U^{234}	17	0,55	0,52 [6]
U^{234}	3	0,55	0,52 [6]
U^{233}	10	0,50	—
Np^{238}	3	0,50	0,43 [6]
Np^{237}	10	0,68	—
Pu^{240}	3	0,59	0,59 [6]
Pu^{239}	10	0,58	—

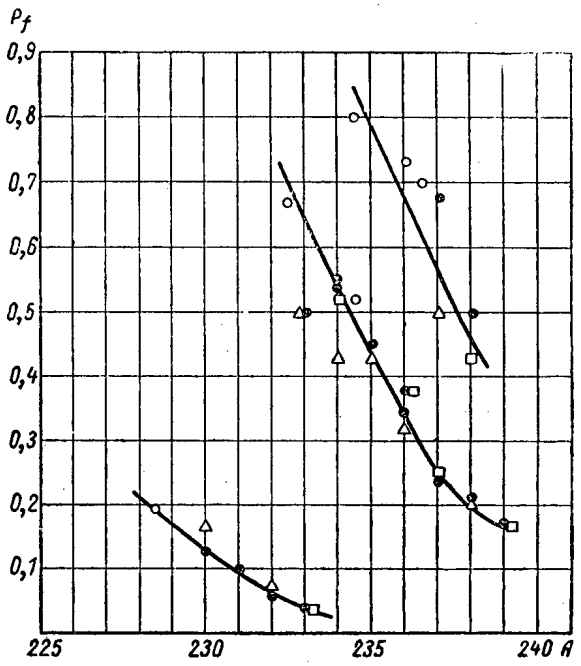

Fig. 12. Fission probabilities for isotopes of thorium, uranium, and neptunium: ●) from the present work; □) with 3 MeV neutrons; △) from photofission and photoneutrons; ○) from spallation reactions.

In order to calculate the fissility, the following values of the cross section for compound nucleus formation were used, the same values being used for all the isotopes studied:

E_n, MeV	3	10	18	25	35
σ, barns	3,3	2,9	2,8	2,8	<2,8

It should be pointed out that all the fissilities presented in the table correspond to the excitation energy of intermediate nuclei, 8-10 MeV. However, their close agreement with fissilities obtained from measurements with 3 MeV neutrons is not trivial, since at neutron energies of the order of 20 MeV, they are captured by nuclei with orbital momenta of the order of 10.

Comparison of the measured cross sections with estimates of these same cross sections obtained by adding fissilities seemingly indicates that the fission probabilities are constant in the energy range investigated (except for the case of U^{233}, discussed above).

In conclusion, the authors consider it their pleasant task to thank A. V. Antonov, R. A. Ariskin, N. A Vlasov, N. I. Venikov, Yu. A. Glukhov, S. P. Kalinin, A. A. Kurashov, N. V. Kartashov, V. P. Rudakov, and B. V. Rybakov for participating or assisting in carrying out various stages of the work.

LITERATURE CITED

1. S. P. Kalinin and V. M. Pankratov, Transactions of the Second International Conference on the Peaceful Uses of Atomic Energy (Geneva, 1958) [in Russian], Dokl. sovetskikh uchenykh. V. 1. Moscow, Atomizdat (1959), p. 387.
2. V. M. Pankratov, N. A Vlasov, and B. V. Rybakov, "Atomnaya Énergiya" 9, No. 5, 399 (1960).
3. B. V. Rybakov and V. A. Sidorov, Fast Neutron Spectrometry [in Russian], Moscow, Atomizdat (1958).
4. D. Hughes and R. Schwartz, Neutron Cross Section Atlas [in Russian], Moscow, Atomizdat (1959).

5. A. Hemmendinger, Transactions of the Second International Conference on the Peaceful Uses of Atomic Energy (Geneva, 1958) [in Russian],Izbr. dokl. inostrannykh uchenykh. V. 2, Moscow, Atomizdat (1959), p. 89.
6. R. Vandenbach and J. Huisenga, Transactions of the Second International Conference on the Peaceful Uses
7. of Atomic Energy (Geneva, 1958) [in Russian], Izbr. dokl. inostrannykh uchenykh. V. 2, Moscow, Atomizdat (1959), p. 366.

THE EFFECT OF AN EVEN NUCLEON NUMBER ON THE MAGNITUDE OF THE RADIATION CAPTURE CROSS SECTION

T. S. Belanova and O. D. Kazachkovskii

Translated from Atomnaya Énergiya, Vol. 14, No. 2,
pp. 185-192, February, 1963
Original article submitted May 27, 1961

The effect of an even number of nucleons in the nucleus on the magnitude of the capture cross section was investigated.

From existing data for isotopic mixtures and individual isotopes, the fast neutron (below 1 MeV) capture cross sections were determined with acceptable precision for a number of isotopes with odd neutron numbers. The values obtained, on the average, were several times larger than the values of the capture cross sections for nuclei with even neutron numbers (both for odd and even Z).

The results contradict existing ideas about the characteristic level.

Much data has been accomulated in recent years on the capture cross sections for monochromatic neutrons in the 0.010-1 MeV energy range. An analysis of the results obtained for various types of nuclei can lead to the discovery of individual mechanisms having important significance from the standpoint of nuclear theory. One of the interesting problems in this field is the study of the effect of even nucleon number on the size of the cross section. Presently known experimental values are related to practically only two types of nuclei: the even-even and odd-even (here, and in what follows, the first term of the pair refers to evenness or oddness of protons; the second refers to neutron evenness or oddness), which, naturally enough, limits the possibilities for investigation in this direction. The capture cross sections for even-odd isotopes, which are not activated by neutron capture and which are found in very small

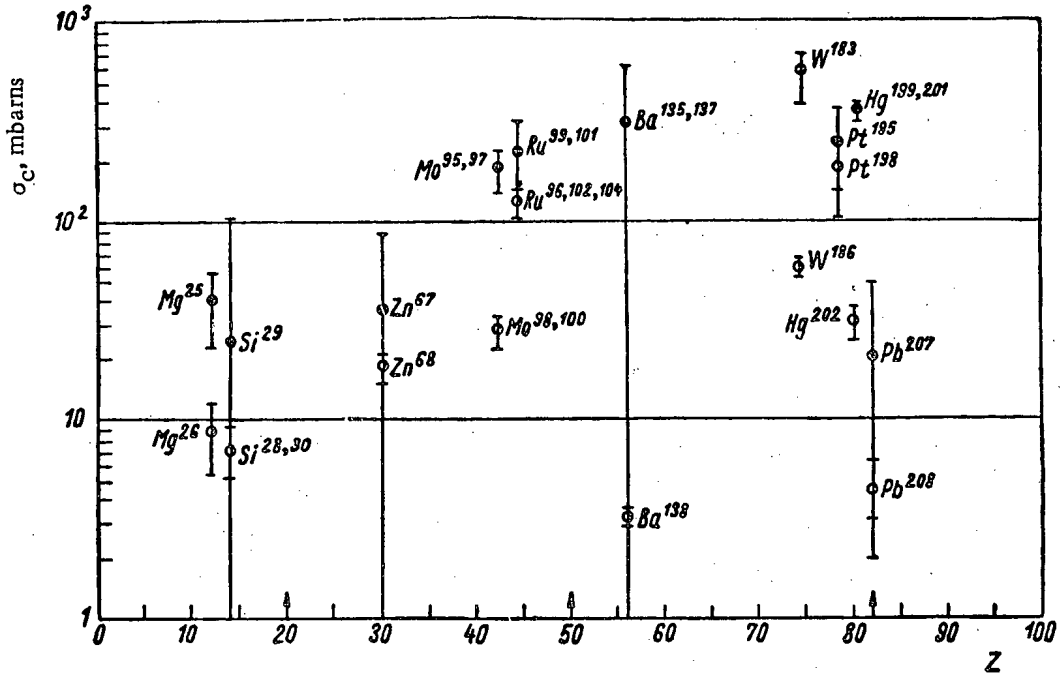

Fig. 1. Dependence of σ_c (e-o) and σ_c (e-e) on Z for 220 keV neutrons: ⊛) values of σ_c (e-o); ◑) σ_c (e-e); arrows indicate proton magic numbers.

TABLE 1. Capture Cross Sections for 24 keV Neutrons

Isotope	σ_c (e-o)$_{exp}$, mb	σ_c (e-o)$_{theor}$, mb	Isotope	σ_c (e-e), mb	σ_a, mb
Mg^{25}	15	55	Mg^{26}	14 [10]	18 [1]
Si^{29}	110±50	7	Si^{28} Si^{30}	5,1 ** 2,1 [11]	10 [1]
$Ti^{47, 49}$ *	140±50	40	Ti^{50}	5 [10]	23 [1]
Zn^{67}	160±60	170	Zn^{68}	24 [11]	29 [1]
Zr^{91}	700±180	960	Zr^{94} Zr^{96}	24 [9] 22 [10]	100 [1]
$Mo^{95, 97}$	500±50	380	Mo^{98} Mo^{100}	210 [10] 110 [11]	262 [1]
Pd^{105}	1530±380	4000	Pd^{108}	290 [9]	570 [8]
$Ba^{135, 137}$	260±300	280	Ba^{138}	8,4 [11]	53 [1]
$Sm^{147, 149}$	2750±640	4300	Sm^{152} Sm^{154}	670 530 } [10]	1225 [8]
$Gd^{155, 157}$	2150±570	6700	Cd^{158}	710 [10]	1150 [8]
$Dy^{161, 163}$	1630∓310	3100	Dy^{164}	330 [12]	900 [8]
Er^{167}	2920±590	4100	Er^{170}	300 [10]	900 [8]
W^{183}	1060±430	2570	W^{184} W^{186}	350 270 } [12]	419 [1]
Pt^{195}	1120±240	1930	Pt^{196} Pt^{198}	210 240 } [12]	520 [8]
$Hg^{199, 201}$	630±30	80	Hg^{202}	57 [10]	229 [1]

* Titanium has two odd isotopes. The symbol $Ti^{47 49}$ indicates the capture cross sections σ_c (e-o) which were obtained are quantities averaged over the titanium isotopes Ti^{47} and Ti^{49} (taking their respective concentrations into account). Similar symbols are also used in this table (and in those that follow) for other elements which contain more than one odd isotope.

** σ_c (e-e) was found by calculation for Si^{28}.

TABLE 2. Capture Cross Sections for 220 keV Neutrons

Isotope	σ_c (e-o)$_{exp}$, mb	σ_c (e-o)$_{theor}$, mb	Isotope	σ_c (e-e), mb	σ_a, mb
Mg^{25}	40±15	30	Mg^{26}	8,9*	12 [1]
Si^{29}	25±80	10	Si^{28} Si^{30}	7,3** 3,0***	8 [1]
Zn^{67}	40±50	140	Zn^{68}	19,1 [2]	20 [1]
$Mo^{95, 97}$	200±25	240	Mo^{98} Mo^{100}	30 27 } [9]	70 [1]
$Ru^{99, 101}$	200±100	560	Ru^{96} Ru^{102} Ru^{104}	140 190 28 } [9]	155 [5]
$Ba^{135, 137}$	300±320	100	Ba^{138}	3,2 [9]	57 [1]

TABLE 2. Capture Cross Sections for 220 keV Neutrons (Continued)

Isotope	σ_c (e-o)$_{exp}$, mb	σ_c (e-o)$_{theor}$, mb	Isotope	σ_c (e-e), mb	σ_a, mb
W^{183}	550±150	900	W^{186}	62 [11]	132 [1]
Pt^{195}	220±120	700	Pt^{198}	190 [10]	202 [5]
$Hg^{199, 201}$	350±20	50	Hg^{202}	32 [9]	126 [1]
Pb^{207}	20±20	30	Pb^{208}	4,13 [2]	8 [1]

* The values of σ_c (e-e) are for 150 keV neutrons [2], which corresponds to the mean neutron energy at which σ_a was measured.
** σ_c (e-e) was found by calculation for Si^{30}
*** The data indicated [2] was recalculated in accordance with the presently accepted cross section for radiation capture in iodine, σ_c = 250 mb [15].

TABLE 3. Capture Cross Sections for 830 keV Neutrons

Isotope	σ_c (e-o)$_{exp}$, mb	σ_c (e-o)$_{theor}$, mb	Isotope	σ_c (e-e), mb	σ_a, mb
Mg^{25}	<100	3	Mg^{24} Mg^{26}	1,04* 0,6 [10]	<10 [1]
Si^{29}	180±150	3	Si^{28} Si^{30}	2,6* 1,1 [13]	11 [1]
$Ti^{47, 49}$	70±150	15	Ti^{50}	1,9 [13]	11 [1]
Zn^{67}	250±70	50	Zn^{68}	8,0 [13]	18 [1]
Sr^{87}	1470±170	10	Sr^{88}	2,1 [13]	105 [1]
Zr^{91}	60±20	40	Zr^{96}	6,6 [2]	13 [5]
$Mo^{95, 97}$	330±40	130	Mo^{98} Mo^{100}	10 [13] 16 [11]	93 [1]
$Ru^{99, 101}$	120±40	220	Ru^{102} Ru^{104}	30 31 [13]	56 [5]
$Sn^{115, 117, 119}$	140±40	130	Sn^{120} Sn^{122} Sn^{124}	14 12 [13] 15	35 [1]
$Ba^{135, 137}$	300±300	60	Ba^{138}	2,3 [13]	53 [1]
W^{183}	350±240	400	W^{186}	48 [11]	91 [1]
Pt^{195}	150±50	220	Pt^{198}	64 [10]	91 [5]
$Hg^{199, 201}$	120±70	930	Hg^{204}	102 [13]	105 [1]
Pb^{207}	30±40	7	Pb^{208}	2 [13]	9 [1]

* σ_c (e-e) was found by calculation for Mg^{24} and Si^{28}.

amounts in natural isotopic mixtures, have not been measured separately by anyone thus far. However, the magnitude of these cross sections can be determined with sufficient precision from the measured cross sections for natural isotopic mixtures and for the corresponding even-even nuclei. The purpose of this paper is to determine the capture cross sections for even-odd nuclei, to compare them with the capture cross sections for other types of nuclei, and to discuss the regularities found.

TABLE 4. Capture Cross Sections for 150 and 175 keV Neutrons

Isotope	σ_c (e-o)$_{exp}$, mb	σ_c (e-o)$_{theor}$, mb	Isotope	σ_c (e-e), mb		σ_a, mb	
			150 keV				
$Dy^{161, 163}$	250±70	1370	Dy^{164}	150	[14]	195	[8]
$Sm^{147, 149}$	850±160	890	Sm^{154}	93	[14]	310	[8]
			175 keV				
$Mo^{95, 97}$	150±40	240	Mo^{98} Mo^{100}	30 27	[9]	60	[5]
$Ru^{99, 101}$	290±90	1050	Ru^{96} Ru^{102} Ru^{104}	140 190 28	[9]	177	[5]
$Sm^{147, 149}$	900±180	760	Sm^{152} Sm^{154}	150 75	[9] [4]	340	[8]
W^{183}	430±120	940	W^{186}	79	[11]	130	[5]

The even-odd capture cross sections, σ_c (e-o), were determined by subtracting the known capture (activation) cross sections for even-even isotopes, σ_c (e-e), from the total absorption cross sections for natural isotopic mixtures, σ_a.

Since the content of even-odd isotopes in natural mixtures is very small (of the order of a few per cent), it might seem at first glance that the values of σ_c (e-o) found must be assigned excessively large errors. However, this is not so since, as will be seen in the following, the cross section σ_c (e-o) is itself very large. Therefore, the contribution of the even-odd isotopes to the cross section which is measured for the natural mixture turns out to be of the same order as, and in some cases even larger than, the corresponding contribution of the even-even isotopes, and the statistical accuracy of the values obtained for σ_c (e-o) is completely acceptable in the majority of cases.

When, in addition to isotopes with known cross sections, other even-even isotopes with unknown cross sections entered into the composition of a mixture, it became necessary to make estimates of the capture cross sections for those isotopes. Usually, the concentrations of isotopes with known cross section were sufficiently great so that it was possible to consider the cross sections for individual even-even isotopes as being alike, and, in this way, large errors did not arise in the calculations. However, in a few cases, where the concentration of an isotope with known capture cross section was small and the binding energy released by neutron capture in various even-even isotopes was noticeably different, it became necessary to make a preliminary estimate of the corresponding cross sections from approximate formulas.

In our calculations, data on absorption cross sections for natural mixtures of isotopes were used which were given in papers [1-8]. Values for activation cross sections were taken from [9-14]. The values found for σ_c (e-o), together with their computed statistical errors, are given in Tables 1-4 (they are designated as σ_c (e-o)$_{exp}$). For example, the capture cross sections of even-odd isotopes are shown in Fig. 1 as a function of the number of protons in the nucleus for 220 keV neutrons. Also shown are the activation cross sections σ_c (e-e) which were taken as starting points in the computations which were made.

From a comparison of the data obtained, it follows that the values of the capture cross sections for even-odd isotopes are quite large. The differences between the cross sections for the two types of nuclei are rather considerable in the majority of cases, and their relative magnitude changes from element to element.

In order to obtain the dependence of σ_c (e-o) on neutron energy for $Mo^{95, 97}$, Pd^{105}, W^{183}, and Pt^{195}, total absorption cross sections from [5, 7, 8] and activation capture cross sections from [10-12] were used. Calculations showed that

the capture cross sections of the even-odd isotopes were higher than the capture cross sections of the even-even isotopes for all these elements. As an illustration, the neutron energy dependence of σ_c (e-o) and σ_c (e-e) for molybdenum is shown in Fig. 2.

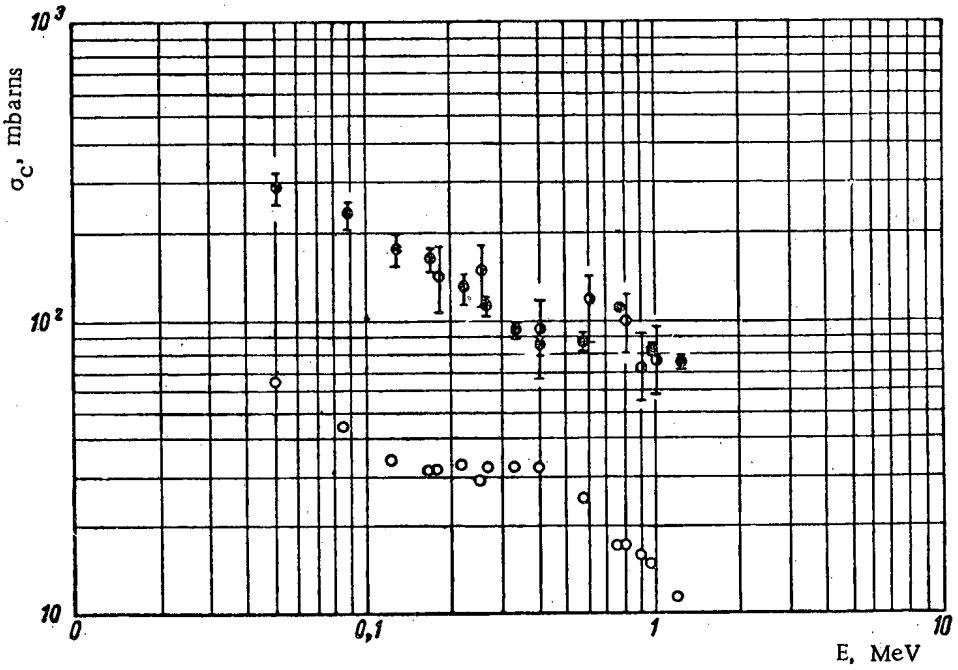

Fig. 2. σ_c as a function of neutron energy: ○) σ_c (e-e) [11] (Mo^{100}); ◑) values of σ_c (e-o) obtained from [5] and [11] ($Mo^{95,97}$); ●) values of σ_c (e-o) obtained from [7] and [11] ($Mo^{95,97}$).

It should be noted that the effect of an even number of neutrons on the magnitude of the capture cross section also appears in measurements with continuous neutron spectra. In that sense, the results obtained by Rose [16] with reactor neutrons were of interest. The cross sections obtained by Rose were the so-called perturbation cross sections, which were essentially a function of the inelastic scattering within the samples. Thus, in that experiment the effect of an even number of neutrons on capture cross section magnitude was masked partly because the perturbation cross sections were not purely capture cross sections and partly because the energy dependence of the capture cross sections generally was different for different isotopes. However, it turned out that the effect of evenness itself was so great that it appeared even in Rose's results; in them, σ_c (e-o) was much larger than σ_c (e-e).

It is of interest to include the odd-even nuclei in the comparison as well. An analysis was made of the activation cross sections given in [2, 9, 11-14, 16] for the neutron energy region studied. Of 130 neighboring pairs of even-even and odd-even nuclei investigated, σ_c (o-e) was larger than σ_c (e-e) in 60% of the cases; the two were comparable in 22% of the cases, and in 18% of the cases σ_c (o-e) was less than σ_c (e-e). An evaluation of the cross sections for both types of nuclei by energy (nuclei with A > 20 were investigated) showed that σ_c (o-e) was 1.7 times greater than σ_c (e-e), on the average, for 24 and 830 keV neutrons, and 2.7 times greater for 220 keV neutrons. A similar cross section evaluation was made by Hughes [13] for the fission neutron spectrum. He found that the capture cross section for odd-even nuclei, on the average, was approximately 35% greater than the capture cross section for even-even nuclei.

There now remains the investigation of the ratio of the capture cross sections of even-odd and odd-even nuclei. In 56 out of the 60 neighboring pairs studied, it turned out that the capture cross sections for even-odd nuclei were greater than the capture cross sections for odd-even nuclei over the entire neutron energy range studied.

As an example, the capture cross sections for odd-even and even-odd nuclei as a function of the number of protons in the nucleus are shown in Fig. 3 for 220 keV neutrons.

An evaluation of the cross sections for both types of nuclei showed that σ_c (e-o), on the average, was three to four times larger than σ_c (o-e) for 24 and 220 keV neutrons, and was six to seven times larger for 830 keV neutrons.

Thus, an analysis of the data made the following conclusions possible:

1) σ_c (e-o) greatly exceeds σ_c (e-e);

2) σ_c (o-e), on the average, is larger than σ_c (e-e);

3) σ_c (e-o) is noticeably larger than σ_c (o-e).

The considerable amount by which the absorption cross sections for even-odd nuclei exceed all the others is a new and, to a certain extent, an unexpected result. Naturally, one can have doubts as to the accuracy of the individual values of σ_c (e-o) (only satistical errors are given in the tables). Since the values of σ_c (e-o) were determined from

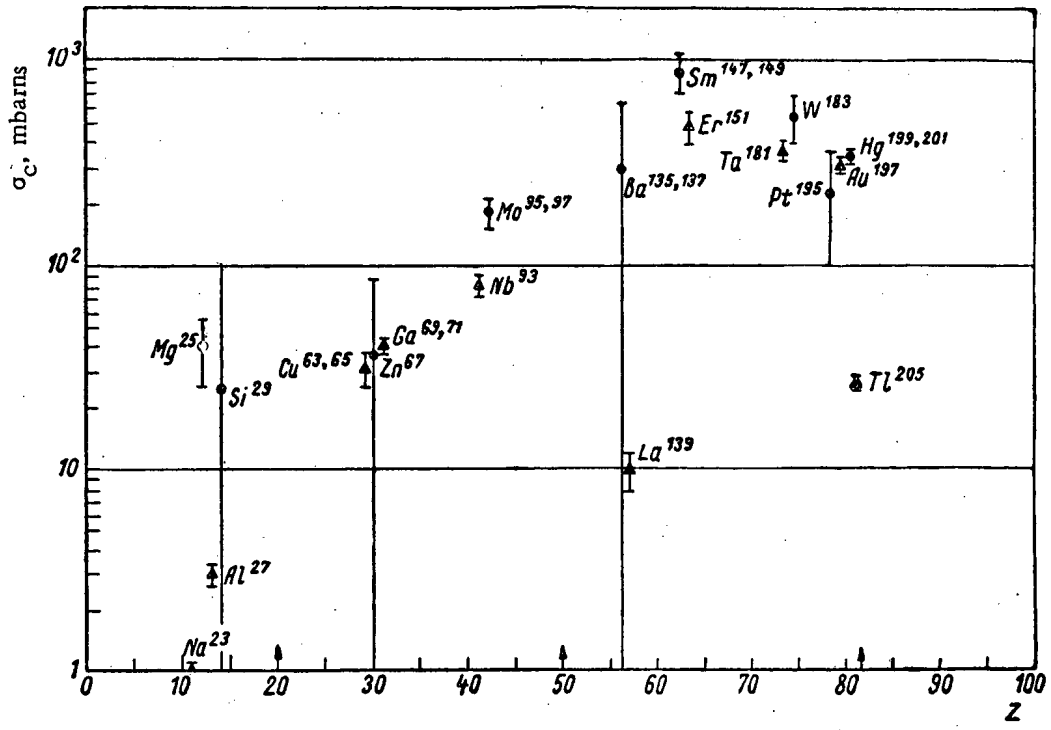

Fig. 3. Dependence of σ_c on Z for 220 keV neutrons: ● σ_c (e-o); ▲ σ_c (o-e); arrows indicate proton magic numbers.

experimental values which were obtained by various methods and various authors, it might be expected that some of these values would vary noticeably from the actual values because of some sort of undiscovered systematic error. However, in spite of the possibility of error in the individual values, the considerable excess of the cross sections for the even-odd nuclei over all the rest is clearly revealed. Entirely without exception, the 45 experimental points for even-odd nuclei lie above the corresponding values for neighboring even-even nuclei.

Let us enumerate the basic processes which can have an effect, in various ways, on the magnitude of σ_c for different types of nuclei.

One of the main factors in this regard is the amount of nuclear excitation energy from neutron capture, this determining the level density ρ. Two possibilities must be considered. If it is considered that ρ is determined by the actual excitation energy of the compound nucleus (equal to the sum of the neutron binding energy E_b and the kinetic energy of the neutron E_k, then the contribution to the capture cross sections, which depends on ρ, should be much larger for even-odd nuclei than for even-even or odd-even nuclei. It is also possible [17] to measure excitation energy not from the ground state but from the characteristic level of Bethe and Hurwitz, E_c, the location of which is supposed to compensate for variations in the total binding energy for different nuclei resulting from an even proton or neutron number or from the presence of magic numbers of protons or neutrons. In this situation, the effect of level density will be approximately the same both for even-odd and for odd-even nuclei. It will be considerably less for even-even nuclei.

A difference in compound nucleus spins I can give rise to a systematic difference in σ_c for nuclei with differing even numbers of nucleons. If it is assumed that $\rho \sim (2I + 1)$, then this quantity ought to be approximately the same for even-odd and odd-even nuclei and much larger than for even-even nuclei because of the participation of neutron waves with small momenta in the process. A certain, relatively small, difference will also be observed in the spin factor for different types of nuclei. It will be approximately the same for even-odd and odd-even nuclei and somewhat less than for even-even nuclei.

TABLE 5. Basic Factors Influencing the Size of σ_c

Factor	Type of nucleus		
	(e-e)	(o-e)	(e-o)
1a. Difference in excitation energy ($\rho = \rho\ (E_b + E_k)$)	−	−	+
1b. Difference in excitation energy ($\rho = \rho\ (E_b + E_k - E_c)$)	−	+	+
2. Spin ($\rho \simeq (2I + 1)$)	−	+	+
3. Spin factor	+	−	−
4. Nuclear dimensions	−	+	+
5. Competition from inelastic scattering	−	+	+

A systematic difference in the dimensions of nuclei with even and odd numbers of nucleons can also give rise to a difference in σ_c. The contribution from neutron waves of various momenta to the capture cross section is increased for nuclei with an odd number of nucleons which have rather large dimensions.

Finally, it is necessary to consider the competition from inelastic scattering. This competition will be approximately the same for even-odd and odd-even nuclei. For even-even nuclei, inelastic scattering turns out to be practically negligible in the energy region under consideration.

All the effects considered above are collected together in Table 5. The effect of each factor on the magnitude of the cross section is qualitatively indicated in the table by plus or minus signs (the plus sign indicates a relatively greater effect than the minus sign). Identical signs in each row correspond to an approximately equal effect.

As can be seen from Table 5, the effect of all the factors except for 1a is the same for even-odd and odd-even nuclei. Thus, it is absolutely necessary to consider factor 1a in order to explain the noticeable excess of σ_c (e-o) over σ_c (o-e). Hence, if a certain characteristic level does exist, then it cannot completely compensate for the differences in binding energy for different nuclei as Bethe and Hurwitz assumed. From the point of view of the effects considered here, it is possible and generally necessary to give up the idea of characteristic level, since the observed relatively small difference between the cross sections for even-even and odd-even nuclei can be explained, in principle, entirely by the effects of factors 2-5. Of course, such qualitative reasoning is insufficient for a final conclusion. However, it should be noted that Gugelot[18] also arrived at a conclusion concerning the absence of the characteristic level in the concept of Bethe and Hurwitz. That conclusion was reached on the basis of data from an entirely different area of research – the analysis of proton inelastic scattering spectra.

It appears that level density, which depends on excitation energy, has a most important effect on the magnitude of σ_c. As an illustration (starting from level densities only), the magnitudes of the cross sections for even-odd nuclei were evaluated and compared with the magnitudes of the cross sections for neighboring even-even nuclei. The usual exponential dependence of level density on excitation energy was assumed. The capture cross section values that were obtained for even-odd nuclei are presented in Tables 1-4 from which it can be seen that, on the average, the theoretical and experimental values are sufficiently close, although there is not total agreement between them. It is also significant that the theoretical values of σ_c (e-o) considerably exceed the experimental values for σ_c (e-e) and this excess approximately corresponds to that found experimentally. It is impossible to expect more from so crude an evaluation. Therefore it is impossible to consider the greater values for capture cross sections of even-odd nuclei as unexpected from the theoretical point of view as might have seemed at first glance.

In conclusion, we emphasize the basic results of this paper.

1. From existing experimental data for total absorption cross sections for natural mixtures of isotopes and from existing data for capture cross sections in even-even nuclei, it is possible in many cases to determine the capture cross section for even-odd isotopes with acceptable statistical precision.

2. The values found for σ_c (e-o) considerably exceed the magnitudes of σ_c (e-e), and also of σ_c (o-e), for neighboring nuclei.

3. The data obtained contradict the idea of Bethe and Hurwitz about the characteristic level, the location of which should completely eliminate variations in binding energy resulting from even numbers of nucleons in the nucleus.

The authors thank A. I. Leipunskii and their associates V. S. Stavinskii and A. V. Malyshev for valuable discussions and comments.

LITERATURE CITED

1. T. S. Belanova, Dissertation (1960).
2. A. I. Leipunskii et al., Transactions of the Second International Conference on the Peaceful Uses of Atomic Energy (Geneva, 1958) [In Russian], Dokl. sovetskikh uchenykh. V. 1, Moscow, Atomizdat (1959), p. 316.
3. T. S. Belanova, "Atomnaya énergiya", 8, No. 6, 549 (1960).
4. T. S. Belanova, "Zh. éksperim. i teor. fiz.", 34, No. 3, 574 (1958).
5. B. Diven, J. Terrell, and A. Hemmerdinger, Phys. Rev., 120, 556 (1960).
6. H. Schmitt and C. Cook, Nucl. Phys., 20, 202 (1960).
7. A. V. Shapar', and Yu. Ya. Stavisskii, Collection "Neutron Physics" [In Russian], Moscow, Gosatomizdat (1961), p. 310.
8. D. Hughes, B. Magurno, and M. Brussel, "Neutron cross sections". New York (1960).
9. W. Lyon and R. Macklin, Phys. Rev., 114, 1619 (1959).
10. D. Hughes and R. Schwartz, "Neutron cross sections". New York (1958).
11. V. A. Tolstikov, Dissertation (1960).
12. R. Booth et al., Phys. Rev., 112, 226 (1958).
13. D. Hughes, et al., Phys. Rev., 91, 1423 (1953).
14. A. Johnsrud et al., Phys. Rev., 116, 927 (1959).
15. S. Barne and R. Cubitt, Phys. Rev., 113, 256 (1956).
16. H. Rose, J. Nucl. Energy, 5, 4 (1957).
17. H. Hurwitz and H. Bethe, Phys. Rev., 81, 898 (1951).
18. P. Gugelot, Phys. Rev., 93, 425 (1954).

A STUDY OF NEUTRON DIFFUSION IN SINTERED BERYLLIUM OXIDE BY A PULSE METHOD

I. F. Zhezherun

Translated from Atomnaya Énergiya, Vol. 14, No. 2,
pp. 193-199, February, 1963
Original article submitted March 1, 1962

The pulsating source method was used to study neutron diffusion in sintered beryllium oxide, the neutron-physical properties of which have not been studied sufficiently well. Diffusion and nuclear constants of the thermal neutrons were obtained (diffusion coefficient, diffusion length, transfer length, effective transfer cross section and absorption cross section, diffusion time, and also certain characteristics in the last stage of neutron moderation).

Beryllium oxide is known to be one of the best moderators for nuclear reactors. Because of its good moderating properties, its high thermal stability, the low absorption and additional multiplication of the fission neutrons in the $Be^9(n, 2n)$ reaction it can find extensive application in high-temperature power reactors. However, the diffusion parameters of neutrons in sintered beryllium oxide are not known sufficiently well. The literature data are very contradictory [1-8] (see the table, which gives all published data converted to a BeO density of 2.79 g/cm^3). This is particularly true of the transfer length λ_t, since the scatter in the values for the diffusion length L can be explained by the varying purity of the material.

Diffusion Parameters of Neutrons in Sintered Beryllium Oxide

Diffusion length L, cm	Transfer length λ_t, cm	Diffusion coefficient D, cm^2/sec × 10^{-5}	Source	Remarks
30	1.65	—	[1]	—
28 ± 2	0.87	—	[2]	λ_t calculated from original work SR-3647, 1946
34.1 ± 0.5	2.5 ± 0.2	—	[3]	λ_t determined from experimental measurements of effective addition
31.1	—	—	[4]	—
31.6	1.50 ± 0.024	1.25 ± 0.02	[5]	—
28.6	—	—	[6]	—
—	1.68	1.40	[7]	Theoretical calculated values
—	1.80	—	—	From data of [7], the value of λ_t was taken from a private communication of Raevskii
34.1	1.85	—	[8]	According to [8], λ_t was measured by Laccour

Only one paper has been published on the study of diffusion parameters in sintered beryllium oxide by the pulse method [5]. The authors conducted measurements with blocks of various sizes, the geometrical parameter B^2 of which varied within the range 0.02-0.06 cm^{-2}. In addition to the parameters shown in the table (L and D) they also obtained (converted to a density of 2.79 g/cm^3) the neutron diffusion time (T = 8.05 ± 0.16 msec) and coefficient of diffusion cooling (C = 4.1 × 10^5 cm^4/sec). Their data for the diffusion coefficient B is much less than the theoretical value obtained by other authors [7], and on conversion according to the formula

$$\lambda_t = \frac{3D}{\bar{v}}, \tag{1}$$

where $\bar{v}$ is the mean velocity of neutrons in equilibrium with the medium at T = 293° K, it gives λ_t = 1.50 cm.

Considering the existing data to be insufficient, we undertook measurements to obtain more accurate values for the diffusion parameters of thermal neutrons in BeO. The measurements were made by a pulse method in the same beryllium oxide for which moderation lengths were measured in [9].

Experimental Arrangement

The measurement of diffusion parameters involves determining the constant of time decay λ of the main harmonics of the thermal neutron density in a moderator block of certain dimensions after the injection of a neutron pulse into it: λ^{-1} is evidently the neutron lifetime in the block.

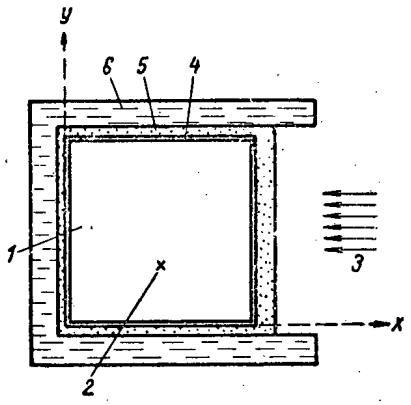

Fig. 1. BeO block and its arrangement during experiment: 1) Moderator block; 2) neutron detector; 3) direction of neutron beam; 4) sheet cadmium; 5) boron carbide layer; 6) paraffin layer.

If a fast neutron pulse is injected into a moderator block having the form of a parallelepiped with effective dimensions a, b, and c at the point x', y', z', then the neutron density ρ at the point x, y, z, in the age approximation, is expressed by the following function of time t passing after injection:

$$\varrho(x, y, z, t) = s_0 \sum_{lmn} A_{lmn}(x', y', z') \times \Phi_{lmn}(x, y, z)\, l^{-B^2_{lmn}\tau} l^{-\lambda_{lmn} t}. \tag{2}$$

Here

$$A_{lmn}(x', y', z') = \frac{8}{abc} \sin\frac{l\pi x'}{a} \sin\frac{m\pi y'}{b} \sin\frac{n\pi z'}{c};$$

$$\Phi_{lmn}(x, y, z) = \sin\frac{l\pi x}{a} \sin\frac{m\pi y}{b} \sin\frac{n\pi z}{c};$$

$$B^2_{lmn} = \pi^2 \left[\frac{l^2}{a^2} + \frac{m^2}{b^2} + \frac{n^2}{c^2}\right];$$

$$\lambda_{lmn} = \Sigma_c \bar{v} + DB^2_{lmn} - CB^4_{lmn}$$

(Σ_c is the macroscopic absorption cross section, $\bar{v}$ is the neutron velocity); s_0 is the source strength, τ is the Fermi age. The origin then coincides with one of the corners of the parallelepiped.

After damping of the highest harmonics only the fundamental harmonic remains:

$$\varrho(x, y, z, t) = s_0 A(x', y', z')\, \Phi(x, y, z)\, l^{-B^2\tau} l^{-\lambda t} \tag{2'}$$

with a constant of time decay λ which is suitable for determination.

We had bricks of sintered beryllium oxide measuring 100 × 100 × 50, 100 × 50 × 50, 100 × 50 × 15 and 50 × 50 × 50 mm with density between 2.75 and 2.90 g/cm^3; these could be built up into blocks of any required sizes. The mean density of BeO in the blocks was 2.79-2.80 g/cm^3.

The block was placed in one of the beams (Fig. 1) of the linear accelerator of the I. V. Kurchatov Institute of Atomic Energy. The neutron pulse lasted about 1 μsec, the frequency of repetition was 50 or 100 cps. In order to eliminate the effect of neutrons scattered in the room, the block was surrounded on all sides except the front (through

which neutrons entered) by 0.5-1.0 mm thick sheet cadmium, a 2.5-5.0 g/cm^2 layer of boron carbide and a 10 g/cm^2 layer of paraffin. The front side of the block was covered with 2 mm thick cadmium and a 5 g/cm^2 layer of boron carbide. The latter made it possible to conduct measurements of λ simultaneously with the performance of other work with the accelerator (for which the target of the accelerator was usually surrounded by a small layer of water), since only neutrons whose transit times did not exceed 300-400 μsec could penetrate into the block.

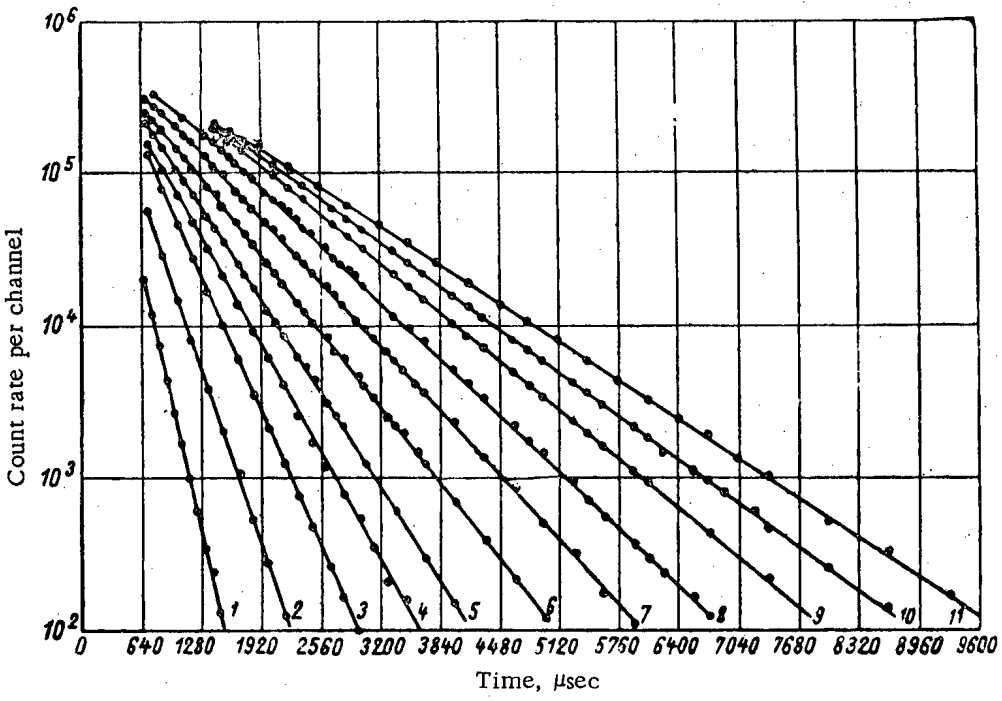

Fig. 2. Typical graphs for the decay of neutron density with time for blocks measuring: 1) 20 × 30 × 23 cm; 2) 30 × 30 × 30 cm; 3) 35 × 35 × 35 cm; 4) 40 × 40 × 40 cm; 5) 45 × 45 × 45 cm; 6) 50 × 50 × 50 cm; 7) 55 × 55 × 55 cm; 8) 60 × 60 × 60 cm; 9) 65 × 65 × 65 cm; 10) 75 × 75 × 75 cm; 11) 80 × 70× 75 cm.

BF_3 proportional counters with enriched boron were used to detect the neutrons. In most of the measurements two counters were used, 10 cm in length and 20 mm in diameter, connected in parallel. The counters were placed above the block at the point $x = a/2$, $y = b/3$, $z \approx c$, which was favorable for separating the fundamental harmonic.

The decay in neutron density with time was analyzed with the 20-channel time analyzer developed by A. A. Osochnikov. The channel width and the time of the start of analysis could be varied over wide limits (from 10 μsec to 2 sec). There were scaling circuits at the channel exits with scaling factors between 2 and 16.

We paid special attention to the suppression of a powerful flux of γ quanta, incident on the detector at the start of the neutron pulse and leading to overloading of the radio apparatus. In the measurements we therefore used the nonoverloading UIS-2 amplifier with a specially designed nonoverloading preamplifier. The "dead" inlet time of the counter channels was determined by scaling circuits and was 2 μsec, the "dead" exit time (~ 20 msec) was determined by mechanical indicators. The presence of scaling circuits and the pulse detector of the source made it possible, however, to operate at fairly high count rates, with practically no counting losses connected with the "dead" exit time, counting losses not exceeding 1-2% in the first channels, connected with the "dead" inlet time [10].

We measured the decay constant λ for 26 blocks with a geometrical parameter B^2 within the limits 0.005-0.095 cm^{-2}. Since the preparation of the sintered beryllium oxide included pressing, a BeO brick could have anisotropy in the neutron scattering [11]. To eliminate the effect of possible anisotropy on the measurement data, the bricks were placed on the blocks in such a way that the direction of pressing coincided with the c edge of the block and the blocks themselves were in the shape of a cube or a shape equivalent to it (in accordance with the condition $1/a^2 + 1/b^2 = 2/c^2$). Furthermore, to determine the anisotropy of the diffusion coefficient D we measured λ for "plane" and "long" blocks.

Processing of Measurement Data and Their Discussion

Under the actual measurement conditions the neutron density in a BeO block consisted of two components: a time-dependent term determined by formula (2) and a small constant background caused by the delayed neutrons of the uranium target of the accelerator. The background was determined from the count in the analyzer channels at those instants of time after the injection of the pulse when the time-dependent term had completely decayed.

Figure 2 shows typical graphs for the decay of neutron density with time for certain blocks with corrections for the counting losses and background. The origin for the time reading coincides with the injection of the pulse. As can be seen from the graphs, a certain time after the pulse only the fundamental harmonic remains, although for the largest block (graph 11) the decay time of the highest harmonics reaches 3 msec.

The logarithm of the ratio of number of counts in neighboring channels will evidently be proportional to the decay constant λ, i.e.,

$$\lambda_i = \frac{1}{\Delta t} \ln \frac{N_i}{N_{i+1}}, \tag{3}$$

where Δt is the channel width.

The values of λ and the mean-square errors $\Delta\lambda$ for each block were calculated with an electronic computer using the method of least squares; we found the weighed-mean λ_i with weights determined by the statistical errors of the number of counts N_i and N_{i+1} in neighboring channels. The values of λ calculated in this way coincided with those determined by the Peierls' method [12], but the errors in $\Delta\lambda$ exceeded those for the Peierls' values. This is evidently due to the small apparatus fluctuation in the number of counts in the channel N_i in addition to the statistical fluctuation. In some cases, when the background was not determined sufficiently accurately, control calculations of λ were also made by the Cornell method, which is mentioned in the paper by Beckurst [13]. The decay constants λ for blocks of the following dimensions (cm) were determined in this way:

80×70×75	55×55×55	35×35×35	20×20×20
70×70×70	50×50×50	30×35×33	15×20×18
65×70×68	40×40×100	30×30×30	15×15×15
80×80×50	45×45×45	30×25×28	20×20×25
65×65×65	45×40×43	25×25×25	15×20×20
65×60×61,5	40×40×40	20×30×23	15×20×15
60×60×60	40×35×38	20×25×23	

The mean-square errors $\Delta\lambda$ were within the limits 0.5-1.5% for blocks with $B^2 < 0.05$ cm^{-2} and reached a few per cent for small blocks.

The measured values of λ are shown in Fig. 3 by points; the vertical lines through these points represent the errors in the measurements. The continuous curve corresponds to the parabola

$$\lambda = \Sigma_c \bar{v} + DB^2 - CB^4, \tag{4}$$

the parameters $\Sigma_c \bar{v}$, D and C of which were obtained by matching to the experimental points by the method of least squares with an electronic computer and were 174, 155, 760 and 411, 700 respectively. Since B^2 depends on D through an extrapolated addition, the calculations were performed by the method of successive approximations. The addition was determined according to [14], the dependence of λ_t on the mean velocity of the neutron spectrum in the block being neglected. For BeO this does not introduce any appreciable error (for example, see [15]).

Several variants were used to calculate the parameters, in which the values of λ were taken to be equal weights and the weights determined by the errors in the measurements of $\Delta\lambda$. In particular, bearing the mind that the three-term formula (4) is valid for values of B^2 which are not very large [16-17], when $B^2 < M_2/\lambda_t$, where M_2 is the mean-square loss in energy of a neutron per unit length, in one variant of the calculation measurements of λ were used only for blocks with $B^2 \leq 0.043$ cm^{-2}. This variant gave a value $C = (3.888 \pm 0.436) \cdot 10^5$ cm^4/sec somewhat less when all measurements of λ are used, when $C = (4.117 \pm 0.270) \cdot 10^5$ cm^4/sec. For $\Sigma_c \bar{v}$ and D all variants gave practically coinciding values, from which, using known relationships, we obtain the remaining diffusion and nuclear parameters: diffusion length $L = 29.9 \pm 1.0$ cm; transfer length $\lambda_t = 1.88 \pm 0.02$ cm; neutron diffusion time $T = 5750 \pm 200$ μsec; effective absorption cross section for one BeO molecule, averaged over the Maxwell spectrum, $\bar{\sigma}_c = 10.4 \pm 0.4$ mb; the effective cross section for a velocity of 2200 m/sec, $\sigma_c = 11.8 \pm 0.4$ mb.

The values for L, T and σ_c are in agreement with our previous measurements [9] and the data of other authors. The value for λ_t coincides with the recent data of Laccour [8]. As regards the diffusion coefficient D, it is much greater than the data of [5], the different crystal structure being unable to explain such a difference [11]. Our value for the coefficient of diffusion cooling C agrees with the value of [5]. As mentioned above, to check the anistropy of the diffusion coefficient D measurements were made for "plane" and "long" blocks, for which the ratio of geometrical parameters $B_\perp^2 : B_\parallel^2$ determining the neutron diffusion in the directions of supposed anisotropy D, differed considerably from the ratio $B_\perp^2 : B_\parallel^2$ for a cubic block. For a "plane" block measuring 80 × 80 × 50 cm the ratio $B_\perp^2 : B_\parallel^2$ was 0.81, and the sum $B_\perp^2 + B_\parallel^2$, i.e., $B^2 = 0.643 \cdot 10^{-2}$ cm^{-2}, and for a "long" block (40 × 40 × 100 cm) – 11.5 and $1.172 \cdot 10^{-2}$ cm^{-2}; for a cube the ratio $B_\perp^2 : B_\parallel^2$ was 2. Large block dimensions were taken so that the possible anisotropy in C could be neglected. The decay constants λ in this case were measured for two positions of the neutron detector (x = a/2, y = b/3, z ≈ c and x = a/2, y ≈ b, z = c/3) and were somewhat different: for a "plane" block – 1152 ± 6 and 1129 ± 8 sec^{-1}, for a "long" block they were 1886 ± 13 and 1931 ± 15 sec^{-1} respectively. The difference somewhat exceeds the error in measurements, its character being as if the neutron leakage occurs more rapidly in the direction of the least transverse dimension of the block. This can serve as an indication of the possible incomplete separation of the variables for blocks of this shape.

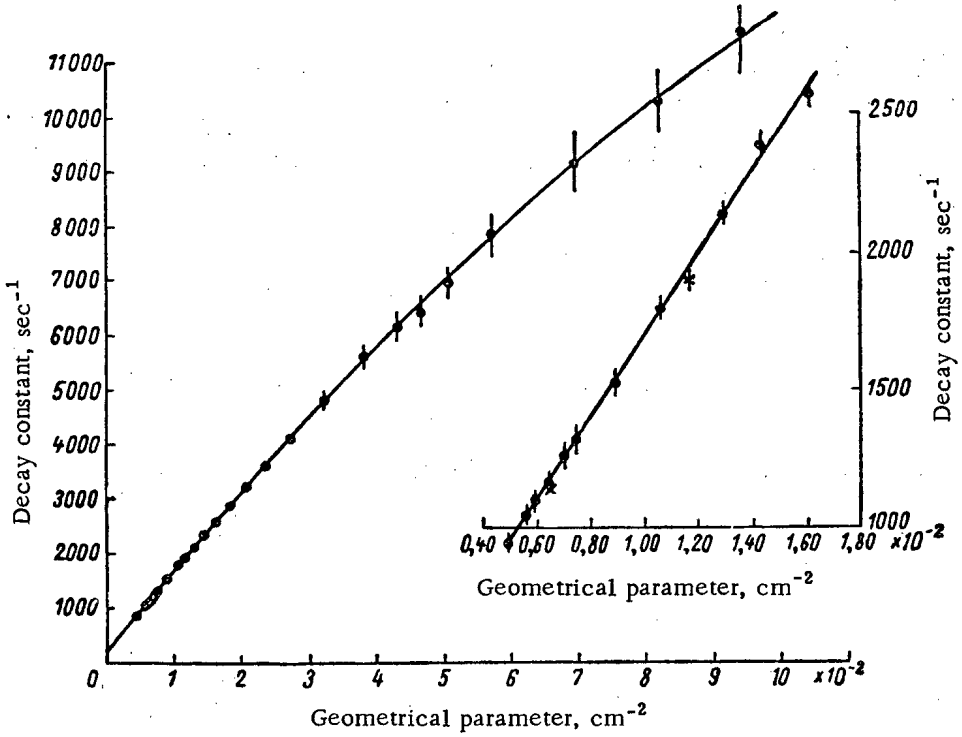

Fig. 3. Dependence of the decay constant on the geometrical parameter (× represents "plane" and "long" blocks).

When determining the anisotropy we took the averages of two measured values of λ for each block, with errors equal to a half of their difference. The calculations showed that if there is a difference between $D_\perp$ and $D_\parallel$ in directions perpendicular and parallel to the direction of pressing of the BeO bricks, then it does not exceed 1.5-2%.

The coefficient of diffusion cooling C in a certain sense is a measure of the effectiveness of energy exchange between neutrons and the moderator medium. It is related to the mean-square energy losses of a neutron per unit length M_2, sometimes called the thermalization parameter, by the well-known relationship [15]:

$$C = \left(\alpha + \frac{1}{2}\right)^2 \frac{\sqrt{\pi} D^2}{v_0 M_2}, \qquad (5)$$

where $v_0 = \sqrt{2kT_0/m}$ (T_0 is the temperature of the moderator, °K), and M_2 is determined by the formula

$$M_2 = \frac{1}{(kT_0)^2} \int_0^\infty \int_0^\infty \Sigma_s (E' \to E) \times (E - E')^2 M(E)\, dE\, dE'. \tag{6}$$

For a free atom $M_2 = 4\xi\Sigma_s$, where ξ is the mean logarithmic loss in energy for one collision.

Relationship (5) was obtained with the assumptions that, in the first place, the equilibrium energy distribution of neutrons in the block remains Maxwellian, corresponding to the characteristic temperature T_n, which can differ from the temperature T_0 of the moderator and, in the second place, the dependence of λ_t on the energy has the form $\lambda_t \sim E^\alpha$ where α is a free parameter.

For BeO, λ_t averaged over the neutron spectrum can be assumed to be approximately independent of the energy, i.e., we can set $\alpha = 0$. Then, (5) gives

$$M_2 = \frac{\sqrt{\pi}}{4} \frac{D^2}{v_0 C}. \tag{7}$$

Before calculating M_2 from this formula we will introduce corrections to C, connected with the above-mentioned assumptions and the approximate nature of formula (4). The main corrections [17] are corrections for the deviation of the neutron spectrum from Maxwellian (about + 25%), for the nondiffusion character (about + 5%) and for neglecting of a term containing B^6 in formula (4) (approximately − 10 and − 5% for two variants in the calculation of the parameters). When these corrections are taken into account both the above values of C give the same value $C = 4.9 \cdot 10^5$ cm^4/sec, hence

$$\frac{M_2}{4\xi\Sigma_s} = \frac{0,10}{0,48} = 0,21.$$

The last result shows that the energy loss of a neutron for one collision near equilibrium with the medium is reduced, due to the chemical bond, to about 20% of the loss on collision with a free atom.

We can obtain certain other information on the character of the moderation process at the last stage. From measurements of D and $C = 4.9 \cdot 10^5$ cm^4/sec the mean velocity $\bar{v}$ of the neutrons in a block of a given size is equal to

$$\bar{v} = \sqrt{\frac{8kT_0}{\pi m}} (1 - 3,1B^2), \tag{8}$$

where B^2 is the geometrical parameter of the block and the coefficient for B^2 is equal to the ratio C : D. On the other hand, from the numerical calculations of [18]

$$\bar{v} \approx \sqrt{\frac{8kT_0}{\pi m}} \left(1 - \frac{\Gamma}{25}\right), \tag{9}$$

where $\Gamma = 2A\lambda_t B^2/3\Sigma_s$. A comparison of the formulas gives an average effective mass A per molecule of moderator equal to 41.

The thermalization time τ can be estimated from the relationship of [15]:

$$\tau = \frac{6C}{D^2} = 120 \ \mu\text{sec}, \tag{10}$$

which is much less than the value given in [5, 16, 19]. However, bearing in mind the approximate nature of relationship (10) and the large error in C connected with the approximate nature of the introduced corrections, the value of τ should be refined by other methods.

In conclusion the author would like to thank N. Ya. Lyashchenko, V. V. Mel'gunova, A. A. Rodionova, and M. P. Shustova for the numerous computer calculations, A. A. Osochnikov for developing the time analyzer and for helping with its servicing, and the whole of the operating personnel of the linear accelerator who made this work possible.

LITERATURE CITED

1. R. Stephenson, An Introduction to Nuclear Engineering [Russian translation]. Moscow , Gosudarstvennoe izdatel'stvo tekhnikoteoreticheskoi literatury, p. 526 (1959).
2. Reports of the US Atomic Energy Commission. Nuclear Reactors. Reactor Physics. Moscow , Izd. inostr. lit., p. 200 (1956).
3. Koechlin, Martelli, and Daggal. Reports of the International Conference on the Peaceful Uses of Atomic Energy (Geneva, 1955), Vol. 5, Moscow , Izd. AN SSSR, p. 31 (1958).
4. Gamba, Santalo, and Alsina, Reports of the International Conference on the Peaceful Uses of Atomic Energy (Geneva, 1955), Vol. 5, Moscow , Izd. AN SSSR, p. 578 (1958).
5. S. Iyenger et al., Proc. Ind. Acad. Sci., XLV s. A, No. 4, 215 (1957).
6. Nuclear Engineering Handbook. N. Y., McGraw Hill Book Company Inc.(1958).
7. K. Singwi and L. Kothari, Transactions of the Second International Conference on the Peaceful Uses of Atomic Energy (Geneva, 1958). Selected reports of non-Soviet scientists. Vol. 2, Moscow , Atomizdat, p. 675 (1959).
8. P. Benoist et al., Second United Nations Int. Conf. on Peaceful Uses of Atomic Energy, Vol. 12, p. 585, P/1192.
9. I. F. Zhezherun et al., "Atomnaya énergiya", 13, No. 3, 258 (1962).
10. I. F. Zhezherun, Counting Losses in Work with Pulse Sources of Particles [in Russian] (in preparation).
11. I. F. Zhezherun, I. P. Sadikov, and A. A. Chernyshov, "Atomnaya énergiya", 13, No. 3, 250 (1962).
12. R. Peierls, Proc. Roy. Soc. London, 149, 467 (1935).
13. K. Beckurst, Nucl. Instr. and Methods, 11, 144 (1961).
14. N. Sjöstrend, Arkiv för Fysik, 15, No.12, 147 (1959).
15. M. Nelkin, J. Nucl. Energy, 8, 48 (1958).
16. K. Singwi and L. Kothary, J. Nucl. Energy, 8, 59 (1958).
17. K. Singwi, Arkiv för Fysik, 16, No. 36, 385 (1960).
18. K. Beckurst, Z. Naturforsch. 12, H. 12, 956 (1957).
19. R. Rammann, Transactions of the Second International Conference on the Peaceful Uses of Atomic Energy (Geneva, 1958). Selected reports of non-Soviet scientists. Vol. 2, Moscow , Atomizdat, p. 741 (1959).

CERTAIN ASPECTS OF THE APPLICATION OF THE DIFFUSION TWO-DIMENSIONAL TWO-GROUP PROGRAM

Ya. V. Shevelev and V. K. Saul'ev

Translated from Atomnaya Énergiya, Vol. 14, No. 2,
pp. 200-205, February, 1963
Original article submitted March 17, 1962

The basic properties of the program for calculating reactors with a two-dimensional geometry by using the diffusion two-group approximation are given. The methods which make it possible to enlarge the scope of this program are described.

Introduction

In 1957-1958, a program was composed at the Order of Lenin Institute of Atomic Energy, Academy of Sciences, USSR, for the numerical solution of reactor equations that are given by

$$-\operatorname{div}(D_1 \operatorname{grad}\Phi_1) + \Sigma_1\Phi_1 = \frac{1}{k_e}\Sigma_{2\to 1}\Phi_2; \quad (1)$$

$$-\operatorname{div}(D_2 \operatorname{grad}\Phi_2) + \Sigma_2\Phi_2 = \Sigma_{1\to 2}\Phi_1 \quad (2)$$

under the following assumptions (i = 1, 2):

1) The integration region R is a rectangle given by $0 \le r \le a_M$, $0 \le z \le b_N$;

2) the symmetry condition $\partial\Phi_i/\partial_r = 0$ is satisfied at the cylinder axis ($r = 0$, $0 \le z \le b_N$); the condition $\Phi_i \equiv 0$ is satisfied over a portion of the external boundary ($0 \le r \le a_M$, $z = b_N$ and $r = a_M$, $0 \le z \le b_N$); finally, for $0 \le r \le a_M$, $z = 0$, either the symmetry condition $\partial\Phi_i/\partial_z = 0$ or the condition $\Phi_i \equiv 0$ is satisfied;

3) $D_i(r, z)$, $\Sigma_i(r, z)$ $\Sigma_{2\to 1}(r, z)$ and $\Sigma_{1\to 2}(r, z)$ are sectionally constant in R; in this, the lines of the discontinuity of coefficients are parallel to the coordinate axes;

4) $D_i(r, z) > 0$, $\Sigma_i(r, z) \ge 0$ in R;

5) $\Phi_i(r, z)$ and $D_i(r, z)$ grad $\Phi_i(r, z)$ are continuous in $\overline{R}$.

The quantities which have to be determined are the effective neutron-multiplication factor k_e, i.e., the smallest intrinsic parameter of the problem, and the fluxes of thermal and fast neutrons, i.e., the eigenfunctions Φ_1 and Φ_2, which are normalized by using the max $\Phi_1 = 1$ relationship. The other quantities are assumed to be given. The program also presupposes the possibility of solving the inhomogeneous equation

$$-\operatorname{div}(D \operatorname{grad}\Phi) + \Sigma\Phi = F \quad (3)$$

for similar assumptions concerning the R region, the boundary conditions, and the D, Σ, and F coefficients.

The aim of the present article is to draw the reader's attention to the possibility of using this comparatively simple program for solving a large class of reactor problems without any changes in the code. Before considering this problem, we shall briefly discuss the program treated in this article.

Numerical Method

For solving Eqs. (1)-(3), we used the method of grids with the subsequent iterative solution of the corresponding systems of grid equations. For this purpose, the R region was covered with a rectangular grid in such a manner that the lines along which the constancy of the coefficients D_i, Σ_i (i = 1, 2), $\Sigma_{2\to 1}$ and $\Sigma_{1\to 2}$ is disturbed coincided with the lines of this grid. Then, at the points (r, z) of discontinuity of the coefficients, Eq. (3) was approximated by the

following five-point grid equation:

$$\frac{h_2D^{(\mathrm{I})}+h_4D^{(\mathrm{IV})}}{2h_1}\left(1+\frac{\gamma h_1}{2r}\right)\Phi^{(1)}+\frac{h_1D^{(\mathrm{I})}+h_3D^{(\mathrm{II})}}{2h_2}\Phi^{(2)}$$

$$+\frac{h_2D^{(\mathrm{II})}+h_4D^{(\mathrm{III})}}{2h_3}\left(1-\frac{\gamma h_3}{2r}\right)\Phi^{(3)}+\frac{h_3D^{(\mathrm{III})}+h_1D^{(\mathrm{IV})}}{2h_4}\Phi^{(4)}$$

$$-\left[s+\frac{1}{4}\left(h_1h_2\Sigma^{(\mathrm{I})}+h_2h_3\Sigma^{(\mathrm{II})}+h_3h_4\Sigma^{(\mathrm{III})}+h_4h_1\Sigma^{(\mathrm{IV})}\right)\right]\Phi^{(0)}$$

$$=\frac{1}{4}\left(h_1h_2F^{(\mathrm{I})}+h_2h_3F^{(\mathrm{II})}+h_3h_4F^{(\mathrm{III})}+h_4h_1F^{(\mathrm{IV})}\right), \qquad (4)$$

where $\Phi^{(0)}$, $\Phi^{(1)}$, $\Phi^{(2)}$, $\Phi^{(3)}$, $\Phi^{(4)}$ are the values of the Φ function at the point (r, z) and the four neighboring points $(r+h_1,\ z)$, $(r,\ z+h_2)$, $(r-h_3, z)$, $(r, z-h_4)$ respectively; $D^{(\mathrm{I})}$, $D^{(\mathrm{II})}$, $D^{(\mathrm{III})}$, $D^{(\mathrm{IV})}$ are the limiting values of the coefficient D at the point (r, z) from the sides of the $(r,\ z)$, $(r+h_1,\ z)$, $(r+h_1,\ z+h_2)$, $(r,\ z+h_2)$; $(r,\ z)$, $(r,\ z+h_2)$, $(r-h_3,\ z+h_2)$, $(r-h_3,\ z)$; $(r,\ z)$, $(r-h_3,\ z)$, $(r-h_3,\ z-h_2)$, $(r,\ z-h_4)$; $(r,\ z)$, $(r,\ z-h_4)$, $(r+h_1,\ z-h_4)$, $(r+h_1,\ z)$ rectangles, respectively. The quantities $\Sigma^{(i)}$, $F^{(i)}$ $(i=\mathrm{I},\ \mathrm{II},\ \mathrm{III},\mathrm{IV})$ constitute a similar notation for the Σ and F coefficients; $\gamma = 0$ for the Cartesian geometry, and $\gamma = 1$ for the cylindrical geometry; s is the sum of the coefficients for $\Phi^{(i)}$(i = 1,2,3,4).

For the main group of points, we used the ordinary five-point grid equation

$$\frac{l^2}{h^2}\left[\left(1+\frac{\gamma h}{2r}\right)\Phi^{(1)}+\left(1-\frac{\gamma h}{2r}\right)\Phi^{(3)}\right]+\Phi^{(2)}+\Phi^{(4)}-\left[2\left(1+\frac{l^2}{h^2}\right)+l^2\frac{\Sigma}{D}\right]\times\Phi^{(0)}=l^2\frac{F}{D}, \qquad (5)$$

which was obtained from (4) for $h_1=h_3=h$, $h_2=h_4=l$, $D^{(i)}\equiv D$, $\Sigma^{(i)}\equiv\Sigma$, $F^{(i)}\equiv F$.

Together with the equations that correspond to the boundary conditions at the boundary S of rectangle R, the totality of the grid equations (4) and (5) forms a system of linear algebraic equations, which can be solved by using the iteration method of sequential upper relaxation with the automatic choice of the optimum relaxation factor. In the case of Eqs. (1) and (2), the intrinsic vector $\{\Phi_1, \Phi_2\}$ is found by using the simple iteration method (internal iterations). In this, for the zero approximation, we can assign either a function which is identically equal to unity [this is compulsory in the case of Eq. (3)] or a two-dimensional parabola or, finally, the solution of the previous variant of the problem with the same grid.

Principle of Program Composition

The method for composing the program is based on a regular (cyclic) presentation of the given region R in the form of the sum MN of "elementary" rectangles $\Pi^{(pq)}$(p = 1, 2,..., M; q = 1, 2,..., N). The regular presentation is provided as a result of extending the lines of discontinuity of the coefficients with straight lines until they intersect the boundary S of rectangle R. The general grid equation (4) is used at the points located on $M-1$ vertical sections with the abscissas $a_1, a_2,..., a_{M-1}$ and on $N-1$ horizontal sections with the ordinates $b_1, b_2,..., b_{N-1}$, by means of which the above presentation of the R region is realized. The simpler grid equation (5) was used for the points inside $\Pi^{(pq)}$.

All of the initial information is assigned in the form of the following sequence of MN + 2M + 3N + 6t + 10 codes:

$$\left.\begin{array}{l} \varepsilon_1,\ \varepsilon_2,\ \varepsilon_3,\ \varepsilon_4,\ \varepsilon_5;\ \pi_1;\ \pi_2;\ \pi_3; \\ \qquad \pi^{(11)},\ \pi^{(21)},\ \ldots,\ \pi^{(M1)},\ 1; \\ \pi^{(12)},\ \pi^{(22)},\ \ldots,\ \pi^{(M2)},\ 1;\ \ldots;\ \pi^{(1N)}, \\ \qquad \pi^{(2N)},\ \ldots,\ \pi^{(MN)},\ 1; \\ 0,\ a_1,\ a_2,\ \ldots,\ a_M;\ 0,\ b_1,\ b_2,\ \ldots,\ b_N; \\ m_1,\ m_2,\ \ldots,\ m_M;\ n_1,\ n_2,\ \ldots,\ n_N; \\ \qquad D_1^{(1)},\ \Sigma_1^{(1)},\ \Sigma_{2\to1}^{(1)}; \\ D_2^{(1)},\ \Sigma_2^{(1)},\ \Sigma_{1\to2}^{(1)},\ \ldots;\ D_1^{(t)},\ \Sigma_1^{(t)},\ \Sigma_{2\to1}^{(t)}; \\ D_2^{(t)},\ \Sigma_2^{(t)},\ \Sigma_{1\to2}^{(t)}, \end{array}\right\} \qquad (6)$$

where ε_i ($\varepsilon_1 > \varepsilon_2 > \varepsilon_3 > \varepsilon_4 > \varepsilon_5$) is the maximum allowable difference with respect to the modulus between two successive "internal" iterations in the ith ($i \leq 5$) "external" iteration [for $i > 5$, ε_5 is used; in the case of Eq. (3), we can put $\varepsilon_2 = \varepsilon_3 = \varepsilon_4 = \varepsilon_5 = 0$]; $\pi_1 = 0$ in the case of systems (1) and (2), and $\pi_1 = 1$ in the case of Eq. (3); $\pi_2 = 0$ for $\gamma = 1$, and $\pi_2 = 1$ for $\gamma = 0$; π_3 is equal to 0 or 1 in dependence on whether the $z = 0$ axis constitutes the symmetry axis; $\pi^{(pq)}$ is the index which is ascribed to the elementary rectangle $\Pi^{(pq)}$ and which is equal to one of the numbers 3, 4, ..., t (t is the number of different zones); m_p is the number of parts into which the section $a_p - a_{p-1}$ is divided ($p = 1, 2, \ldots, M$); n_q is the number of parts into which the $b_q - b_{q-1}$ ($q = 1, 2, \ldots, N$) segment is divided; the index (j) in the $D_i^{(j)}$, $\Sigma_i^{(j)}$, ... coefficients indicates belonging to the jth zone ($j = 3, 4, \ldots, t$). In this, the elementary rectangles $\Pi^{(pq)}$ are ordered in the following manner: The first is the $\Pi^{(11)}$ rectangle, which is adjacent to the coordinate origin; then follows rectangle $\Pi^{(21)}$, which is next to $\Pi^{(11)}$ and is adjacent to the Or axis, etc., up to rectangle $\Pi^{(M1)}$; then follows rectangle $\Pi^{(12)}$, which is next to $\Pi^{(11)}$, but is adjacent to the Oz axis, then rectangle $\Pi^{(22)}$, which is next to $\Pi^{(12)}$ and $\Pi^{(21)}$, etc. The index 1 after $\Pi^{(Mq)}$ ($q = 1, 2, \ldots, N$) and the index 0 in front of a_1 and b_1 are used for separation; they are intended to enable the computer to decipher the mutual position of individual zones. In the case of Eq. (3), D, Σ, and F are used instead of D_1, Σ_1, and $\Sigma_{2\to1}$ in sequence (6), while D_2, Σ_2 $\Sigma_{1\to2}$ are considered to be equal to zero.

Besides the code sequence (6), the maximum allowable difference with respect to the modulus between two consecutive k_e values must be assigned at the control panel in the case of the problem (1), (2) for the intrinsic parameter.

The program consists of three units. Unit 3 is auxiliary; it is intended for shaping commands in units 1 and 2, which depend on the shape and the dimensions of the grid. Unit 2, which also is an auxiliary unit, serves for calculating (according to the Gauss-Seidel method) the optimum relaxation factors for the fast and the thermal groups. Simultaneously with the first iteration, the coefficients of the grid equations (4) and (5) are calculated; 27 of these coefficients for each $\Pi^{(pq)}$ are recorded on the magnetic drum (later, as they are needed, these coefficients are read off the magnetic drum in groups of 27 M numbers). Unit 1 constitutes the main "working" unit.

The auxiliary units 2 and 3 are used only at the initial stage of computer operation, after which the control is transferred to the basic unit 1, while units 2 and 3 are cancelled. The basic operative field – the values of the function to be iterated at the grid points – is put in the freed space in the computer's fast memory.

In the latter variant, the program was fulfilled without reference to the file of subprograms, so that the program utilized the entire fast memory and all the magnetic drums. Magnetic tapes were not used.

In order to use this program, concrete contents must be assigned to the mathematical scheme presented in the introduction. This is not always easy to achieve. The description of a reactor in the first approximation often fits the scheme, but contains elements that contradict it. We shall give such examples below and indicate the methods to be used for eliminating these difficulties. Many of these methods can also be used in other programs (one-dimensional and multigroup programs).

Nondiffusion Effects

1. Assume that a plate whose thickness is Δ, which is black with respect to thermal neutrons, is located in the core. At the boundaries of this plate, the diffusion equation for the flux Φ_2 of thermal neutrons must be supplemented by the effective boundary condition

$$\frac{1}{\frac{\partial \ln \Phi_2}{\partial x}} = 0{,}7103\lambda^{tr} \quad \text{or} \quad D_2 \frac{\partial \Phi_2}{\partial x} = \frac{\Phi_2}{2{,}131} \quad (2{,}131 = 3 \cdot 0{,}7103). \tag{7}$$

For the realization of condition (7), we shall consider that the diffusion equation with the specially selected constants D_2^*, Σ_2^* and $\Sigma_{1\to 2}^*$ is valid inside the plate. If we assume that

$$\Sigma_2^* = \frac{k}{2{,}131\Delta}, \quad D_2^* = \frac{\Delta}{2{,}131k}, \quad \Sigma_{1\to 2}^* = 0, \tag{8}$$

where k is a certain constant ($k \simeq 3$-4), condition (7) will be satisfied. Actually, the fictitious diffusion length is $L_2^* = \Delta/k$ and $L_2^*/D_2^* = 2.131$. Since Δ is much larger than L_2^* while there are no sources ($\Sigma_{1\to 2}^* = 0$), the flux inside the plate will be exponentially attenuated from the boundaries toward the center, and

$$D_2 \frac{\partial \Phi_2}{\partial x} = D_2^* \frac{\partial \Phi_2^*}{\partial x} = \frac{D_2^*}{L_2^*} \Phi_2^* = \frac{\Phi_2^*}{2{,}131} = \frac{\Phi_2}{2{,}131}.$$

This method can also be used in calculating small reactors with basically different values of the transport path length λ^{tr} for different energy groups. Beyond the external surface of the reactor, it is sufficient to place a fictitious layer with the thickness Δ^* and with constants that are equal for all groups, which are determined by relationships (8).

2. Assume that a tube whose diameter d is large in comparison with λ^{tr} is placed in the reactor. For exact calculations pertaining to the tube surface, integral-type boundary conditions should be written. Since they are not included in the program, diffusion equations must be written for the region inside the tube. It is obvious that $\Sigma_1 = \Sigma_2 = 0$, $\Sigma_{1\to 2} = \Sigma_{2\to 1} = 0$, while the diffusion coefficients can be determined by analogy with the Knudsen flow, i.e., by substituting the tube diameter for the transport path length:

$$D_1 = D_2 = \frac{d}{3}. \tag{9}$$

This yields the correct value for the neutron flux through the transverse cross section of the tube if the flux changes sufficiently smoothly along its axis. The neutron flux across the tube cannot be accurately taken into account, since Eqs. (1) and (2) do not provide for the anisotropy of the diffusion coefficient. If the shape of the cavity is noncylindrical, its effect can be estimated following the same approach and using the hydraulic diameter as the characteristic dimension.

Inadequacy of the Two-Dimensional Geometry

1. Assume that there are n absorbing rods in the reactor, which are arranged along a ring at the distance r_{ro} from the reactor axis and which pass through the end-face reflector. If the two-dimensional program is to be used, the rods must be replaced by an annular layer with different properties in the core and in the reflectors. The properties of the layer must be such that the flux in the actual reactor that is averaged with respect to the azimuth angle coincides at least asymptotically with the flux in the reactor with an equivalent layer (at a distance from the layer that exceeds the migration length).

The asymptotic flux is proportional to

$$\psi(\mathbf{r}) = \psi_0 + C \sum_{k=0}^{n-1} Y_0(|\mathbf{r} - \mathbf{r}_k| \varkappa_r), \quad \varkappa_r^2 = \varkappa^2 - \varkappa_z^2, \tag{10}$$

where ψ_0 is a function without singularities at $\overline{r_k}$, i.e., on the axes of the rods; $\overline{r}$ is a vector which is normal to the axes of the rods. The derivative of the flux $\overline{\psi(r)}$ which is averaged with respect to the azimuth angle will have a discontinuity at the radius r_{ro}. The discontinuity can be simulated by creating an artificial narrow annular layer with the thickness Δ and with specially selected constants. The diffusion coefficients may coincide with their actual values, while the cross sections should be determined in the following manner:

$$\Sigma_{i\to j}=0, \quad \Sigma_i = D_i\left(\varkappa^2+\frac{\delta Z_{r0}}{\Delta}\right), \quad \Delta \ll \frac{2}{\delta Z_{r0}}. \tag{11}$$

Here,

$$\delta Z_{r\sigma}=\left.\frac{\partial \ln \bar{\psi}}{\partial r}\right|_{r_{r0}+0}-\left.\frac{\partial \ln \bar{\psi}}{\partial r}\right|_{r_{r\sigma}-0}$$

$$=\frac{\frac{2}{\pi}\,n/r_{r0}}{\frac{\bar{\psi}_{0\,r0}}{C}+nY_0(\varkappa_r\varrho_{r0})\,J_0(\varkappa_r r_{r0})}; \tag{12}$$

$$\frac{\bar{\psi}_{0r0}}{C}\simeq\frac{1}{f}-S(\varkappa_r r_{r0};n); \tag{13}$$

$$S(a,\,n)=\sum_{k=1}^{n-1}Y_0\left(2a\sin\frac{\pi k}{n}\right); \tag{14}$$

$$\frac{1}{f}\simeq\frac{2}{\pi}\left(\frac{1}{\varrho Z_{r0}}+\ln\frac{1}{\varkappa_r\varrho}+0{,}11\right); \tag{15}$$

$$Z_{r\sigma}=\left.\frac{\partial \ln \psi}{\partial r}\right|_{r=\varrho} \tag{16}$$

The last quantity can be calculated by using multigroup equations for a single rod that is located in a symmetric neutron field.

Similarly, in the reflector,

$$\delta Z_{r\sigma}=\frac{-\frac{n}{r_{r0}}}{\frac{1}{f}-T(\alpha_r r_{r0},n)+nK_0(\alpha_r r_{r\sigma})\,I_0(\alpha_r r_{r0})}; \tag{17}$$

$$T(a,\,n)=\sum_{k=1}^{n-1}K_0\left(2a\sin\frac{\pi k}{n}\right);$$

$$\alpha_r^2=\frac{1}{L^2}-\frac{1}{\psi}\frac{\partial^2\psi}{\partial z^2}. \tag{18}$$

The term $\frac{1}{\psi}\frac{\partial^2\psi}{\partial z^2}$ is estimated in correspondence with the actual conditions of the problem; its effect is slight. For a rod which absorbs only thermal neutrons, we have

$$\frac{1}{f}\simeq\gamma\frac{\lambda^{tr}}{\varrho}+\ln\frac{1}{\alpha_r\varrho}+0{,}11; \quad \frac{1}{\gamma}=\lambda^{tr}\left.\frac{\partial \ln \Phi}{\partial r}\right|_{r=\varrho}. \tag{19}$$

2. As another example, consider an annular band of absorbers which are arranged in rows at distances that are small in comparison with the L and $\sqrt{\tau}$ lengths. If the flux is averaged in such a band in the direction of its length, not only the derivative, but also the function itself will vary in jumps. By means of special calculations, a homogeneous absorbing band can be selected, beyond which the flux will coincide with the actual averaged flux.

Inadequacy of Two-Group Equations

1. If its influence is slight, the fission in the epithermal region can be taken into account, for instance, by determining the constants in the following manner:

$$\left.\begin{aligned} \Sigma_1 &= \frac{D_1}{\tau}\left[1-(1-\varphi)\,K_{\infty\,\mathrm{res}}\,e^{-\varkappa^2\tau}\right];\\ \Sigma_{2\to1} &= \frac{D_2}{L^2}\,K_{\infty\ \mathrm{ther}};\\ \Sigma_2 &= \frac{D^2}{L^2}, \quad \Sigma_{1\to2} = \frac{D_1}{\tau}\,\varphi, \end{aligned}\right\} \tag{20}$$

where φ is the probability that absorption (including absorption by fissionable nuclei) in the resonance region will be avoided, $K_{\infty res}$ and $K_{\infty ther}$ are the yields of new neutrons per single capture event in the resonance and the thermal regions, respectively, τ is the "age", and L is the diffusion length. There are also other methods for choosing the constants.

2. It is known that, in a homogeneous reactor with a heavy moderator, the probability that leakage will be avoided is equal to

$$e^{-\varkappa^2\tau},$$

while two-group calculations yield the accurate value for this probability:

$$\frac{1}{1+\varkappa^2\tau}.$$

Therefore, a considerable portion of the errors connected with the use of two groups can be eliminated if, instead of K_∞, we introduce the corrected calculated value

$$K_{\infty\mathrm{cal}} = K_\infty\,\frac{1+\varkappa^2\tau}{e^{\varkappa^2\tau}}, \tag{21}$$

where $\varkappa^2$ is the root of the transcendental equation

$$K'_\infty = e^{\varkappa^2\tau}(1+\varkappa^2L^2), \tag{22}$$

which is determined with good accuracy by the expression

$$\varkappa^2 \simeq \frac{\ln K'_\infty}{M^2}\left[1+\frac{\ln K'_\infty}{2}\left(\frac{L^2}{M^2}\right)^2\right]. \tag{23}$$

In expressions (22) and (23), $M^2 = \tau + L^2$; $K'_\infty = K_\infty/k_e$, where k_e is the expected effective value of the neutron-multiplication factor. It is, of course, not necessary to introduce a correction in K_∞; τ can be changed instead.

3. We shall give an example of using the theory of disturbances for introducing the correction in two-group calculations. Assume that in a reactor with a heavy moderator, there is a neutron trap in the form of a screened hydrogenous moderator, for instance, water in a tube which is covered with cadmium. Fast neutrons enter the water, are slowed down in it, and, as they are transformed into thermal neutrons, they cannot leave the trap; their value is equal to zero. However, after losing a certain amount of energy, some of the fast neutrons emerge from the water as a consequence of the fact that the slow-down density of the neutrons around the trap decreases as the lethargy increases (due to leakage).

This effect cannot be taken into account directly within the framework of the two-group theory. The effect reduces the efficiency of the trap; it can be taken into account indirectly by replacing the actual moderating power of water by a certain reduced value:

$$(\zeta\Sigma)_{H_2O\mathrm{eff}} = (\zeta\Sigma)_{H_2O}\left[1-2\,(\mathrm{ch}\,\varkappa^2\tau-1)\right]. \tag{24}$$

Calculation of Temperature Fields

The program can also be used for purposes other than the original one, for instance, for calculating temperature fields in solids with a complex (two-dimensional) geometry and sectionally-constant properties.

1. Nonsteady-state temperature fields without sources and with sectionally-constant initial conditions can be calculated according to the following finite-difference scheme:

$$\left.\begin{aligned} -\operatorname{div}\lambda\operatorname{grad}T^{(n)}+\frac{c}{\Delta t}T^{(n)}&=\frac{c}{\Delta t}T^{(n-1)};\\ -\operatorname{div}\lambda\operatorname{grad}T^{(n+1)}+\frac{c}{\Delta t}T^{n+1}&=\frac{c}{\Delta t}T^{(n)}. \end{aligned}\right\} \quad (25)$$

Here, λ is the coefficient of thermal conductivity, c is the specific heat, Δt is the time "step," and $T^{(n)} = T(n\Delta t)$. For a single external iteration, two steps are left out, i.e., the transition is made from $T^{(n-1)}$ to $T^{(n+1)}$ (the constants for the "thermal and fast neutrons" are the same). It is understood that the operation of the normalizing unit must be stopped. In order to assign the initial values of the temperature $T^{(0)}$, one external iteration must be left out for the following constants:

$$D_1 = D_2 = 0, \quad \Sigma_1 = \Sigma_2 = 1, \quad \Sigma_{2\to 1} = T^{(0)}, \quad \Sigma_{1\to 2} = 1. \quad (26)$$

Then, if we assign $\Phi_2^{(0)} = 1$, we obtain

$$\Phi_2^{(1)} = \Phi_1^{(1)} = T^{(0)}, \quad (27)$$

and this value is used for $\Phi_2^{(0)}$ in the calculations based on Eqs. (25).

2. For calculating a steady-state temperature field, Eq. (3) must be solved, assuming that

$$D = \lambda, \quad \Sigma = 0, \quad F = q, \quad (28)$$

where q is the density of sources. This is equivalent to the use of one-half of the external iteration for $\Phi_2^{(0)} = 1$ and $\Sigma_{2\to 1} = q$.

3. In solving temperature problems, difficulties arise in connection with the special type of boundary conditions.

In order to realize the condition given by

$$-\lambda\frac{\partial T}{\partial x} = \alpha(T - T_{bo}) \quad (29)$$

(λ, α, and T_{bo} are sectionally-constant functions) in a problem concerning a nonsteady-state temperature field, it is necessary to introduce two fictitious layers whose thicknesses are Δ^* and Δ^{**}. In the Δ^* layer, the field must change linearly, while in the Δ^{**} layer, it must exponentially approach the T_{bo} value, for which it is necessary to put

$$\Sigma_{2\to 1}^{**} = \Sigma_1^{**} T_{bo}; \qquad L_1^{**} \ll \Delta^{**}; \qquad \Sigma_{2\to 1}^{*} = \Sigma_1^{*} = 0. \quad (30)$$

Then, if $D_1^* = D_1^{**}$, the slope of T(x) in the Δ^* layer will be

$$\frac{dT^*}{dx} = \frac{T_{bo} - T}{\Delta^* + L_1^{**}}$$

and condition (29) will be satisfied for

$$D_1^* = D_1^{**} = \alpha(\Delta^* + L_1^{**}). \quad (31)$$

However, in (30) it was assumed that $\Phi_2^{**} = 1$. Therefore, in this case, for a single external iteration, it will be possible to make only one time step, since the equation for Φ_2 must be used for the purpose of restoring the properties of the Δ^{**} layer. For this, we can put

$$D_2^* = D_2^{**} = 0; \quad \Sigma_2^* = \Sigma_2^{**} = 1;$$
$$\Sigma_{1\to 2}^* = \Sigma_{1\to 2}^{**} = \frac{1}{T_{bo}}, \tag{32}$$

and, in the actual zones

$$D_2 = 0, \quad \Sigma_2 = 1, \quad \Sigma_{1\to 2} = 1. \tag{33}$$

The actual Δ^{**} is not completely restored, since, instead of $\Phi_2^{**(0)} = 1$, we obtain the function $\Phi_2^{**(1)}$, which deviates from unity:

$$|1 - \Phi_2^{**(1)}| \leqslant \frac{|T_{bo} - T|}{T_{bo}} \frac{L_1^{**}}{\Delta^* + L_1^{**}}. \tag{34}$$

The error connected with this will increase from one step to another. If it is necessary to make $n = t/\Delta t$ steps, L_1^{**}/Δ^* must be determined from the condition

$$n \frac{L_1^{**}}{\Delta^*} \ll 1. \tag{35}$$

If a boundary layer of the type (29) is used in the problem of a steady-state temperature field, the fictitious layer Δ^* is superfluous.

It is understood that, in all cases where D = 0 is written, we must actually use a finite, although very small, constant such that $(D/\Sigma)^{\frac{1}{2}}$ is small in comparison with the size of the grid cells.

DECANTATION PROCESSES IN THE HYDROMETALLURGY OF URANIUM

I. A Yakubovich

Translated from Atomnaya Énergiya, Vol. 14, No. 2,
pp. 206-212, February, 1963
Original article submitted June 6, 1962

Extraction, sorption, and electrochemical methods for the extraction of valuable components can be applied to clarified solutions and directly to commercial suspensions or pulps. To separate pulps and to wash soluble substances from precipitates, increasing use is being made of decantation processes in combination with highly efficient flocculating reagents to speed up sedimentation and obtain clarified solutions. Comparative technical-economical calculations should be made in each actual case to confirm the choice of the technological arrangement with the extraction of valuable components either from clarified solutions or directly from pulps.

The article gives generalized equations for the calculation of technological parameters for the decantation washing of soluble substances from precipitates.

The uranium industry has developed over the last two decades and characterizes the general state of hydrometallurgy. The development of this industry has led to the discovery of new highly efficient methods for the intensification of various hydrometallurgical processes, and new methods for the extraction of valuable components from ores, solutions, and suspensions. The technological and other data characterizing plants for uranium ore processing in capitalist countries are dealt with in a recent book [1], which emphasizes the increasing importance of sorption and extraction processes, not only in the fine purification of uranium-containing solutions, but also in the extraction of uranium from solutions and pulps obtained from ore leaching.

Sorption, extraction, and electrochemical methods in the technology of uranium and the rare metals can be applied to clarified solutions and to various hydrometallurgical pulps. For the various cases there are known advantages and disadvantages of a technological and economic character; the correct method can only be selected on the basis of an objective calculation and a comparison of all the technical and economic indices.

Until recently, difficulties in the separation of pulps, the production of clarified solutions and the washing of precipitates during filtration and thickening have been considered to be insurmountable; they can now be successfully solved by the use of highly efficient flocculating reagents in combination with decantation methods for washing the precipitates [2-4].

Most of the uranium ore processing plants built in recent years in capitalist countries operate with acid leaching and subsequent extraction of the uranium from clarified solutions. In addition to high technical and economic indices, the apparatus is simpler and the continuous technological process is completely automated. A typical example of the use of this system in conjunction with counter-current decantation is the largest US plant – Cermac Nuclear in New Mexico, producing 3,300 t of ore per day.

At plants which process silicate and carbonate ores simultaneously and which produce acid and carbonate solutions using the decantation method, these solutions can be used for the reextraction of uranium from the organic phase which forms during the extraction of uranium from acid solutions. This process, used in the plant of the "Susquehanna" company in Wyoming, has permitted a considerable reduction in the consumption of soda; a high uranium content has been achieved in solutions arriving for precipitation of the chemical concentrates.

Complex ores with differing combinations of valuable components can be very important in the hydrometallurgy of uranium. The separation of the pulp after leaching and processing of the clarified solution eliminates a number of difficulties which arise in the selective extraction of valuable components directly from the pulp.

Numerous investigations are now being conducted and equipment is being developed to eliminate difficulties connected with the extraction of valuable components from pulps after leaching [1, 5, 6]. However, in some cases the separation of pulps after leaching with subsequent extraction of the valuable components from clarified solutions by various methods can be economically more desirable.

The separation of the pulp into liquid and solid phases and the washing of soluble substances from the precipitates is conducted in various units of the settling or filtering type under the action of the force of gravity, centrifugal force or pressure difference [7, 8].

If the precipitates are washed in spiral or rake classifiers and hydrocyclones, then the wash solutions circulating throughout the system contain a large amount of solid slurry particles; in the case of decantation washing in separation concentrators clarified solutions are obtained at each stage of the process.

The concentrators can be arranged so that the solutions flow through the system by gravity. Diaphragm, centrifugal or jet pumps, and also air lifts and other devices are used to move the concentrated products. If the level of filling of the coagulators is the same, then both the clarified solutions and coagulated product are transferred by the pumps. The necessity of using pumps is a serious difficulty in the industrial use of counter-current decantation washing of flocculated precipitates.

If the solid phase of the pulp is crystalline or a fairly coarse-grain product, then the washing of these precipitates can be performed with filtering equipment by drawing the washed liquid through a layer of precipitate or by multistage filtering with intermediate repulping of the precipitates.

Work is now being conducted to simplify the apparatus for the separating and wash processes by using multistage concentrators, suspension filters and equipment based on the properties of a fluidized bed.

The most complete separation of soluble substances from the precipitate can be achieved by successive washing of the precipitate with separate portions of the wash liquid [9].

In order to reduce its total amount and maintain sufficiently high efficiency and continuity in the process, extensive use is made of continuous counter-current washing of precipitates. The reduction in the consumption of wash liquid is an important problem in hydrometallurgical practice since this not only reduces the amount of processed suspensions and solutions but there is also an increase in the concentration of soluble salts in the wash solutions. The process of continuous counter-current washing is set up to produce pure solutions containing no suspended solid particles, and to produce pulps in which the solid particles are less than a given size. Uranium plants are described [1, 7] which use a combined system of counter-current washing of the sand and slurry fractions of the ore material. The sand fraction is washed counter-current in a system of spiral classifiers or hydrocyclones, and the slurry fraction (discharge from the classifiers) is washed in a system of settling concentrators with the addition of flocculating reagents to increase the productivity of the concentrating process and to produce a clarified commercial solution. In these arrangements the same wash solution passes successively through all separation units.

The technological indices characterizing counter-current washing of soluble substances are calculated by compiling and solving a system of equations representing the material balance of the steady process [10-14].

In hydrometallurgical practice the given values are usually the ratio $L:S = R$ in the initial pulp, the concentration of the washed material C in the liquid phase of the initial pulp and the ratio $L:S = R_{pr}$ in the concentrated pulp (or in the cake) at each stage of washing. It is usually necessary to determine the change in concentration of the washed substance in the liquid phase of the waste pulp and the efficiency of the process as a function of the number of stages of washing. It is also very important to compare the theoretically calculated concentrations of the washed substance in the solutions circulating in the system with those actually obtained. From this comparison we can draw important practical conclusions on the properties of the precipitate and on the equipment needed to mix the precipitates with the solutions.

An important technological index characterizing the washing of soluble substances from a precipitate is the efficiency of washing, determined as the ratio of the amount of soluble substances in commercial solutions obtained from the process to the amount of these substances entering together with the precipitates (in the liquid phase of the pulp or cake) for washing.

The efficiency of washing is determined from the expression

$$\varepsilon = \frac{L_{de} C_{de}}{RC} 100 = \left[1 - \frac{R_n C_n}{RC} \right] 100\%, \quad (1)$$

where ε is the efficiency of washing, %; C, C_{de}, C_n are the concentrations of the washed substance in the liquid phase of the initial pulp, in the commercial solution, and in the liquid phase of the pulp at the last stage of washing, kg/t; R, $R_{n_{pr}}$ are the amounts of liquid related to 1 t of solid insoluble substance in the initial pulp or cake arriving for washing, and in the concentrated pulp or cake at the last stage of washing respectively, t/t; L_{de} is the amount of liquid derived from the process as a commercial solution, per 1 t of solid substance, t/t. The efficiency of the washing depends on the number of stages of washing, the consumption of wash liquid, the content of liquid in the precipitate removed from the process by washing, sorption properties of the solid phase of the pulp with respect to the washed substance and some other factors.

When calculating the technological indices of the washing processes we assumed that the solid phase of the pulp does not sorb the washed substance, which is uniformly distributed throughout the whole volume of the liquid phase of the pulp at all stages of washing; the clarified solutions derived from the process do not contain solid suspended particles; the weight of the precipitate is not reduced during washing.

If the pulp with an L:S ratio equal to R arrives for successive decantation washing of the soluble substances from the precipitate, and at each stage of the washing the thickened pulp after settling has an L:S ratio equal to R_{pr}, then from 1 t of solid material L_{de} t of solution will be decanted, where $L_{de} = R - R_{pr}$.

We will assume that at all stages of the decantation washing the L:S ratio in the thickened pulp gradually becomes equal to R_{pr}, and the dilution by fresh wash liquid is conducted in such a way that the pulp always has an L:S ratio equal to R. By solving the system material balance equations we can then obtain an expression for the concentration of washed substance in the liquid phase of the pulp C_x at a given stage of washing:

$$C_x = \left(\frac{R_{pr}}{R} \right)^x C. \quad (2)$$

If we use M to represent the modulus of washing, i.e., the ratio of the amount of liquid separated at each stage of washing in the form of a solution to its amount remaining with the precipitate, based on 1 t of solid substance then, after introducing the quantity M into equation (2), we obtain

$$M = \frac{L_{de}}{R_{pr}} = \frac{R - R_{de}}{R_{pr}}; \quad (3)$$

$$C_x = \frac{C}{(M+1)^x} \quad \text{or} \quad \frac{C}{C_x} = (M+1)^x. \quad (4)$$

The dimensionless quantity C/C_x, or the index of reduction in concentration, is the ratio of the concentration of the washed substance in the liquid phase of the initial pulp to the concentration of this substance in the liquid phase of the washed precipitate.

The general expression for the efficiency of successive decantation washing after small conversions of equations (1) and (4) will have the form

$$\varepsilon = \frac{(M+1)^{n+1} - 1}{(M+1)^{(n+1)}}. \quad (5)$$

The technological indices obtained in the actual process may differ from the calculated indices. From the difference in the indices we can decide on the sorption properties of the solid phase of the pulp relative to the washed solute and on the uniformity of its distribution throughout the whole volume of the liquid phase. We should mention that the addition of flocculating reagents to the pulps to speed up the thickening and filtration causes aggregation of the particles and may lead to an increase in the concentration of washed substance in the solution enclosed within the separate floccules, compared with its concentration in the whole liquid. However, with sufficient, but not intensive mixing of the flocculated particles with the wash solution these concentrations even out in a comparatively short space of time.

For example, in the six-stage successive washing of an insoluble residue after carbonate leaching of ore with the addition of the necessary amount of polyacrylamide flocculant the following results were obtained: C = 0.79 g/liter; C_1 = 0.260 g/liter; C_2 = 0.090 g/liter; C_3 = 0.030 g/liter; C_4 = 0.014 g/liter; C_5 = 0.006 g/liter; C_6 = 0.003 g/liter. The calculated concentrations for this experiment at M = 2 were C_1 = 0.263 g/liter; C_2 = 0.088 g/liter; C_3 = 0.029 g/liter; C_4 = 0.010 g/liter; C_5 = 0.003 g/liter; C_6 = 0.001 g/liter. The experiments were conducted in glass cylinders; the thickened residue and the wash solution were mixed by twice inverting the cylinder with the residue and added solution.

This agreement between the actual and calculated results was obtained in numerous laboratories and large-scale experiments, and also under industrial conditions.

The effect of individual factors on the continuous counter-current washing of soluble substances can be established by compiling material balance equations for each separate stage of the process under steady conditions and by simultaneously solving the obtained system of equations.

We will assume that in a certain period of time the system of continuous counter-current washing receives an amount of initial pulp which contains 1 t of solid suspended particles and R t of solution with concentration of washed substance C kg/t. During this period of time L_0 t of wash liquid is fed to the last stage of washing and the amounts removed from each stage are $L_{1_{de}}$, $L_{2_{de}}$, ..., $L_{n_{de}}$ t of solutions respectively. The amount of liquid transferred from 1 t of precipitate throughout the system of thickeners or other separating equipment will be $R_{1_{pr}}$, $R_{2_{pr}}$, ..., $R_{n_{pr}}$ t respectively.

We will compile material balance equations for each separate stage of continuous counter-current washing:

$$\left.\begin{array}{l}\text{First stage}\\ RC + L_{2_{de}} C_2 = (R_{1_{pr}} + L_{1_{de}}) C_1;\\ \text{second stage}\\ R_{1_{pr}} C_1 + L_{3_{de}} C_3 = (R_{2_{pr}} + L_{2_{de}}) C_2.\end{array}\right\} \quad (6)$$

For the last stage n with the condition that wash water which does not contain washed substance arrives for the washing of the precipitates, we obtain the following equation:

$$R_{(n-1)} C_{(n-1)} + L_0 0 = (R_{n_{pr}} + L_{n_{de}}) C_n. \quad (6')$$

The material balance of the steady process of counter-current washing can also be represented by the following equations:

$$\left.\begin{array}{l}\text{for the first stage}\\ RC = L_{1_{de}} C_1 + R_{n_{pr}} C_n;\\ \text{for the second stage}\\ R_{1_{pr}} C_1 = L_{2_{de}} C_2 + R_{n_{pr}} C_n;\\ \text{for the last stage}\\ R_{(n-1)_{pr}} C_{(n-1)} = L_{n_{de}} C_n + R_{n_{pr}} C_n.\end{array}\right\} \quad (7)$$

In the most general case, by simultaneously solving equations (6) and (7), we can calculate the concentrations of the washed substance in the wash apparatus of a multistage process and determine the number of stages needed to ensure a given efficiency of washing.

In most practical cases in a steady process of counter-current washing the following conditions are observed:

1) The L : S ratio in the pulp arriving for the counter-current washing in the first wash apparatus of the system is equal to the L : S ratio in the precipitates (cake, thickened pulp), obtained at each of the washing stages:

$$R = R_{1_{pr}} = R_{2_{pr}} = \ldots = R_{n_{pr}};$$

2) The amount of wash liquid introduced to the last stage of washing based on 1 t of solid insoluble substance is equal to the amount of clarified solution derived from 1 t of solid substance at each stage of washing:

$$L_0 = L_{1\,de} = L_{2\,de} = \ldots = L_{n\,de}.$$

By rewriting equations (6) and (7), we therefore obtain

$$\left.\begin{aligned} C_1 &= \frac{1}{M}(C - C_n);\\ C_2 &= \frac{1}{M}(C_1 - C_n);\\ &\cdots\cdots\cdots\\ C_n &= \frac{1}{M+1}\cdot C_{(n-1)}, \end{aligned}\right\} \tag{8}$$

hence

$$C_n = \frac{M-1}{M^{(n+1)}-1}C. \tag{9}$$

By solving equations (8) and (9) we can find the concentration of the washed substance in the solutions in all stages of counter-current washing.

One of the main indices of the quality of a commercial solution obtained during counter-current washing is the concentration of the washed substance in it. In this connection it is of interest to calculate the index of reduction in concentration of the commercial solution K, which is determined by the ratio of the concentration of washed substance in the liquid phase of the initial pulp C to the concentration of this substance in the commercial solution C_1:

$$K = \frac{C}{C_1} = \frac{M^{(n+1)}-1}{M^n-1}. \tag{10}$$

To calculate the efficiency of continuous counter-current washing from equations (1) and (7) we obtain

$$\varepsilon = \frac{M^{(n+1)}-M}{M^{(n+1)}-1}\,100\%. \tag{11}$$

When the conditions of continuous counter-current washing are such that M = 1, then to calculate the efficiency of the washing we must use a transformed expression, which is obtained from (11) by the l'Hôpital rule:

$$\varepsilon = \frac{n}{n+1}\,100\%.$$

After the simultaneous solution of equations (8)-(11) it can be seen that for a multistage process of counter-current washing the concentration of washed substance in the liquid phase of the pulp at any intermediate stage C_x will be determined by the following expression:

$$C_x = \frac{M^{(n+1-x)}-1}{M^{(n+1)}-1}C. \tag{12}$$

In counter-current washing under industrial conditions the ratio L : S = R in the initial pulp arriving for the washing can differ considerably from the ratio L : S = R_{pr} in the thickened products (cakes) unloaded from the apparatus at each stage of washing:

$$R \gtrless R_{1\,pr} = R_{2\,pr} = \ldots = R_{n\,pr}.$$

This process can be considered as consisting of two separate operations:

1) The mixing of the initial pulp with a ratio L : S = R and a concentration of washed substance in the liquid phase equal to C kg/t, with decantation (by clarified solution) of a second stage of washing, containing C_2 kg/t of washed substance and obtained in an amount of L_{2de} t per 1 t of solid substance in the initial pulp;

2) Counter-current washing of the thickened product (cake), obtained at the first stage of washing with the ratio L : S = R_{1pr} and concentration of the washed substance in the liquid phase C_1 kg/t in the system from (n-1) stages of washing.

During a steady process from the first leading apparatus a commercial clarified solution will be obtained in amounts of L_{1de} t per 1 t of solid substance; it is then quite obvious that

$$L_{1de} = R + L_{2de} - R_{1pr}. \tag{13}$$

If we use M_1 to represent the modulus of washing in the first leading apparatus, i.e.,

$$M_1 = \frac{L_{1de}}{R_{pr}}, \tag{14}$$

then, using previously derived equations, we obtain for this case

$$\varepsilon = \frac{M^n - 1}{(M^n - 1) + \frac{M-1}{M_1}} 100\%; \tag{15}$$

$$C_x = \frac{M^{(n+1-x)} - 1}{M^n - 1} \frac{M_1 + 1 - M}{M_1 + \frac{M-1}{M^n - 1}} C. \tag{16}$$

In hydrometallurgical plants dissolved substances are frequently washed from precipitates by solutions obtained in the recovery of clarified liquid from the tailings storage tank, during the precipitation of chemical concentrates from commercial solutions, in the washing of ion-exchange resins and at other stages of the technological process.

If the wash liquid fed to the last stage of washing in amounts of L_0 t per 1 t of solid substance in the initial pulp contains C_0 kg/t of washed substance, then, by solving a system of equations representing the material balance of the process under steady conditions and with the condition $L_0 = L_{de}$, we obtain

$$C_x = \frac{M^{(n+1-x)} - 1}{M^{(n+1)} - 1} C + \frac{M^{(n+1)} - M^{(n+1-x)}}{M^{(n+1)} - 1} C_0. \tag{17}$$

It is quite apparent that the use of recovered solutions containing a certain amount of dissolved washed substance leads to an over-all increase in the concentration of this substance in the solutions at all stages of washing. Equation (17) permits a quantitative determination of the effect of the content of a washed substance in the wash solution on the change in concentration of solutions at each separate stage of washing.

In industrial practice the dissolved substances can be washed from the precipitate by a wash liquid containing a solute and, furthermore, the ratio L : S = R in the initial pulp may differ from the ratio L : S = $R_{1pr} = R_{2pr} = \ldots = R_{npr}$ in the thickened products (cakes), obtained in the separation apparatus at each of the washing stages.

We will give calculation equations which we have derived for the technological parameters of the washing process for this case:

$$C_x = \frac{M^{(n+1-x)} - 1}{M^n - 1} \frac{M_1 + 1 - M}{M_1 + \frac{M-1}{M^n - 1}} C + \left[\frac{M^{(n+1-x)} - 1}{M^n - 1} \frac{M^{(n+1)} - M^n}{M_1 (M^n - 1) + M - 1} + \frac{M^n - M^{(n+1-x)}}{M^n - 1} \right] C_0; \tag{18}$$

$$\varepsilon = \frac{(M^{(n+1)} - M) C + M (M^{(n+1)} - M) C_0}{(M^{(n+1)} - 1)(C + MC_0)} 100\%. \tag{19}$$

When calculating the number of stages of counter-current washing (n) needed to achieve a given efficiency in the process or concentration of washed substance in the liquid phase of the pulp at the last stage of washing C_n, we use equation (18) or simpler equations, depending on the set conditions.

For example, for the case where the modulus of the process M remains constant at all stages and the wash liquid fed to the last stage of washing does not contain the washed substance, i.e., $M = M_1$ and $C_0 = 0$, from equation (15), after taking the logarithm and simple transformations, we obtain

$$n = \frac{\lg \frac{M - \varepsilon}{1 - \varepsilon} - \lg M}{\lg M}.$$

In this equation ε is expressed in fractions.

Similarly, we can obtain a calculation equation for the required number of stages of counter-current washing in more complex cases, i.e., when $M_1 \gtrless M$ and $C_0 \neq 0$.

These equations enable us to solve all problems which can arise in the investigation, planning and industrial realization of the counter-current washing of dissolved substances from precipitates.

A more complex problem is the determination of the amount of wash liquid to ensure the required efficiency of the process and the concentration of commercial solution for given values of n and C_n. In this case we must solve the exponential equations by a graphical or analytical method, leading to difficult calculations. The solution of all calculation problems is considerably simplified by the use of nomograms, which can be plotted from the obtained generalized equations.

LITERATURE CITED

1. A. P. Zefirov, B. V. Nevskii, and G. F. Ivanov, Uranium Ore Processing Plants in Capitalist Countries [in Russian]. Moscow, Gosatomizdat (1962).
2. A. P. Zefirov, B. N. Laskorin, and B. V. Nevskii, "Atomnaya énergiya", 11, No. 2, 153 (1961).
3. I. A. Yakubovich, "Tsvetnye metally", No. 12, 9 (1957).
4. I. A. Yakubovich, "Atomnaya énergiya", 8, No. 6, 525 (1960).
5. G. E. Kaplan, B. N. Laskorin, and B. V. Nevskii, "Atomnaya énergiya", 6, No. 2, 113 (1959).
6. B. V. Nevskii, "Atomnaya énergiya", 6, No. 1, 5 (1959).
7. V. B. Shevchenko and B. P. Sudarikov, Uranium Technology [in Russian], Moscow, Atomizdat (1961).
8. N. P. Galkin and V. A. Tikhomirov, Processes and Equipment in Uranium Technology [in Russian]. Moscow, Atomizdat (1961).
9. L. M. Batuner and K. S. Fedorov, Methods for the Calculation of the Washing of Precipitates [in Russian]. Moscow, Oborongiz (1939).
10. M. Cahlan, Mining Mag., 46, No. 4, 201 (1957).
11. R. Woody, Mining Engng. 10, No. 7, 786 (1958).
12. T. Girby, Chem. Engng. 66, No. 8, 169 (1958).
13. R. Emmet and D. Dahlstrom, Canad. I. Chem. Engng. 37, No. 1, 3 (1959).
14. O. L. Bruk, "Khimicheskaya promyshlennost", No. 8, 660 (1960); No. 8, 596 (1962).

COMPARISON OF CASCADE GENERATOR CIRCUITS

G. I. Kitaev

Translated from Atomnaya Énergiya, Vol. 14, No. 2,
pp. 213-215, February, 1963
Original article submitted February 24, 1962

Comparing a symmetric circuit (essentially a two-phase circuit) and a three-phase circuit with a Cockroft-Walton circuit (more accurately, a single-phase half-wave circuit) [1-4], we find that multiphase circuits have decided advantages when they are used in high-voltage sources with comparatively high power. The comparison was made for equal capacitances C in the stages. It was found [1, 3] that the pulsation value δU (the maximum value) in a symmetric circuit is n + 1 times as large, while the voltage drop ΔU (the average value) is one-quarter as large, as in an ordinary circuit. The optimum number of stages n_{opt} in a symmetric circuit is twice as large. The three-phase circuit was not subjected to such a detailed analysis; however, it was shown in a concrete example [2-4] that the values of δU and ΔU are only one-third as large in this circuit for equal n values and for the same load. In this example, there were given the ratios of ΔU of an ordinary circuit to ΔU of other circuits: circuits with decreasing capacitances, and symmetric and three-phase circuits for the same total capacitance of all the capacitors.

The method of comparing the circuits for the same ΣC value seems to be the best, since the properties of the circuits are in this case most clearly revealed and the economic side of the comparison is taken into account. In connection with this, the present article provides a comparison between the efficiencies of the most promising circuits with respect to ΔU, δU, and n_{opt} for the same total capacitance. Since ΔU and δU depend on n, the circuits must be compared for equal n values, or the dependence of the efficiency on n must be determined. The comparison must be made for the same load (it is more convenient when $Q_l = i_l T = i_l / f = 1$). The load value, especially in the case of multiphase circuits, must be smaller than that for which mutual overlapping arises in the operation of the rectifiers. Failure to observe this condition may lead to errors in estimating the circuits with respect to the experimental results, which was the case, for instance, in [1] in evaluating a three-phase circuit.

While the ΣC value is the same for all circuits, the capacitances of the capacitors in the stages of various circuits are different, since the number N of capacitors in the circuits is not the same, i.e.,

$$C = \frac{\Sigma C}{N} .$$

Then, the efficiency factors with respect to ΔU and δU for the circuits which are being compared can be expressed by the following relationships:

$$K_{\Delta U} = \frac{\Delta U_{or}}{\Delta U_{ci}} = \frac{\frac{i_l}{f}\frac{F(n)_{or}N_{or}}{\Sigma C}}{\frac{i_l}{f}\frac{F(n)_{ci}N_{ci}}{\Sigma C}} = \frac{F(n)_{or}N_{or}}{F(n)_{ci}N_{ci}} \; ; \quad K_{\delta U} = \frac{\delta U_{or}}{\delta U_{ci}} = \frac{\frac{i_l}{f}\frac{G(n)_{or}N_{or}}{\Sigma C}}{\frac{i_l}{f}\frac{G(n)_{ci}N_{ci}}{\Sigma C}} = \frac{G(n)_{or}N_{or}}{G(n)_{ci}N_{ci}} ,$$

where the "or" and "ci" indices denote the ordinary circuit and the circuit which is being compared, respectively.

The circuit's efficiency with respect to the optimum number of stages can be expressed as the ratio

$$K_{n_{opt}} \simeq \frac{n_{opt\,ci}}{n_{opt\,or}} .$$

The following equations hold for an ordinary n-stage half-wave single-phase circuit (Cockroft-Walton) in the case where the capacitances of the capacitors, the number of which is equal to $N_{or} = 2n$, are the same [5, 6]:

$$\Delta U=\frac{i_l}{fC}\frac{8n^3+9n^2+n}{12};\quad F(n)_{or}=\frac{8n^3+9n^2+n}{12};\ \delta U=\frac{i_l}{fC}\frac{n^2+n}{2};\quad G(n_{or}=\frac{n^2+n}{2};\ n_{opt\,or}\simeq\sqrt{\frac{U_m fC}{i_l}}$$

For a single-phase full-wave circuit (Fig. 1), the following equations hold in the case of equal capacitances of the capacitors, whose number is equal to N = 3n − 2 [7]:

$$\Delta U=\frac{i_l}{fC}\frac{2n^3-3n^2+4n}{12};\quad F(n)=\frac{2n^3-3n^2+4n}{12};\ \delta U=\frac{i_l}{fC}\frac{n}{2};\ G(n)=\frac{n}{2};\ n_{opt}\simeq\sqrt{\frac{2U_m fC}{i_l}}.$$

The results obtained in comparing the circuits indicate that

$$K_{\Delta U}=\frac{(8n^3+9n^2+n)\,2n}{(2n^3-3n^2+4n)\,(3n-2)}\to\frac{8}{3}\ \text{for}\ n\to\infty;\ K_{\delta U}=\frac{2(n^2+n)\,2n}{2n\,(3n-2)}=\frac{2\,(n^2+n)}{3n-2};\ K_{n\,opt}\simeq\sqrt[3]{\frac{4n}{3n-2}}\simeq 1{,}1.$$

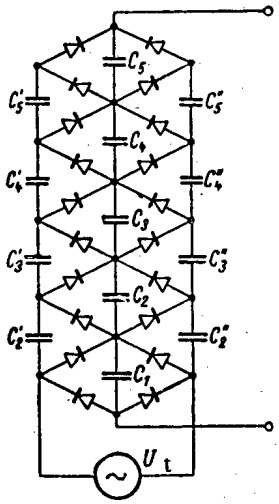

Fig. 1. Single-phase full-wave circuit.

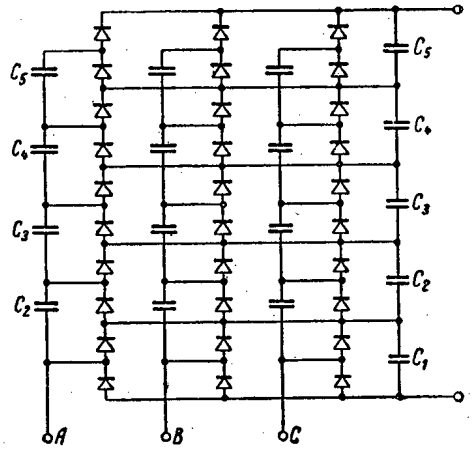

Fig. 2. Three-phase full-wave circuit (A, B, and C denote the supply phases).

If the capacitances in the steps of the end (boost charge) columns are proportional to the degree of discharge of the capacitors in this circuit, i.e., $C'_k = C''_k = [n-(k-1)]\,C_n$, while all the capacitances in the middle (discharge) column are equal to $C_k = C_n = C$, then $N = n^2 + 2n - 2$, and the equations for ΔU and δU have the following form:

$$\Delta U=\frac{i_l}{fC}\frac{n^2}{4};\quad F(n)=\frac{n^2}{4};\quad \delta U=\frac{i\,l}{fC}\frac{n}{2};\quad G(n)=\frac{n}{2}.$$

Then, such a circuit is characterized by the coefficients

$$K_{\Delta U}=\frac{4(8n^3+9n^2+n)\,2n}{12n^2\,(n^2+2n-2)}=\frac{2\,(8n^2+9n+1)}{3\,(n^2+2n-2)}\to\frac{16}{3}\ (\text{for}\ n\to\infty);$$

$$K_{\delta U}=\frac{2(n^2+n)\,2n}{2n\,(n^2+2n-2)}=\frac{2\,(n^2+n)}{n^2+2n-2}\to 2\ (\text{for}\ n\to\infty).$$

For a two-phase (symmetric) circuit, we obtain:

1) for equal capacitances in the stages ($C'_k = C''_k = C_k = C$; N = 3n [1, 2, 6])

$$\Delta U=\frac{i_l}{fC}\frac{2n^3+3n^2+4n}{12};\quad F(n)=\frac{2n^3+3n^2+4n}{12};$$

$$\delta U = \frac{i_l}{fC}\,\frac{n}{2};\quad G(n) = \frac{n}{2};$$

$$n_{opt} \simeq 2\sqrt{\frac{U_m fC}{i_l}};$$

$$K_{\Delta U} = \frac{(8n^3+9n^2+n)\,2n}{(2n^3+3n^2+4n)\,3n} \longrightarrow \frac{8}{3}\ (\text{for } n \longrightarrow \infty);$$

$$K_{\delta U} = \frac{2(n^2+n)\,2n}{2n3n} = \frac{2(n+1)}{3}$$

$$K_{n_{opt}} \simeq \sqrt[3]{\frac{8}{3}} \simeq 1{,}39;$$

2) if $C'_k = C''_k = [n-(k-1)]\,C_n$ in the end columns, while $C_k = C_n = C$ and $N = n^2 + 2n$ [6] in the middle column, we have

$$\Delta U = \frac{i_l}{fC}\,\frac{n^2+2n}{4};\quad F(n) = \frac{n^2+2n}{4};\quad \delta U = \frac{i_l}{fC}\,\frac{n}{2};\quad G(n) = \frac{n}{2};$$

$$K_{\Delta U} = \frac{4(8n^3+9n^2+n)\,2n}{12(n^2+n)\,(n^2+2n)} \longrightarrow \frac{16}{3}\ (\text{for } n \longrightarrow \infty);\quad K_{\delta U} = \frac{2(n^2+n)\,2n}{2n\,(n^2+2n)} \longrightarrow 2\ (\text{for } n \longrightarrow \infty).$$

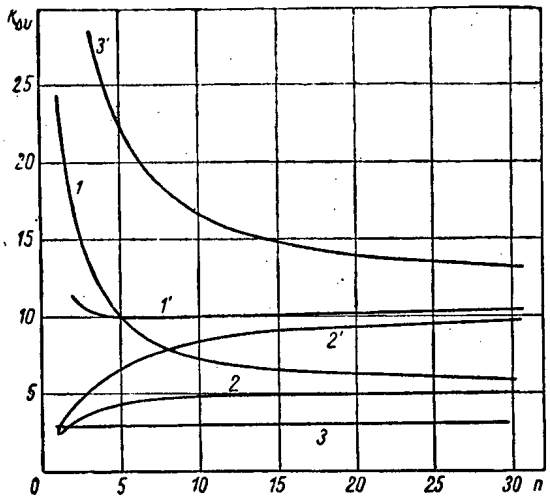

Fig. 3. Efficiency of the circuits with respect to ΔU [$K_{\Delta U} = F(n)$]: 1) circuit of Fig. 1 with equal C values; 1') the same circuit with $C'_k = C''_k = [n-(k-1)]C_n$ and $C_k = C_n = C$; 2) two-phase (symmetric) circuit with equal C values; 2') the same circuit with $C'_k = C''_k = [n-(k-1)]C_n$ and $C_k = C_n = C$; 3) ordinary three-phase circuit with equal C values; 3') three-phase full-wave circuit with equal C values (see Fig. 2).

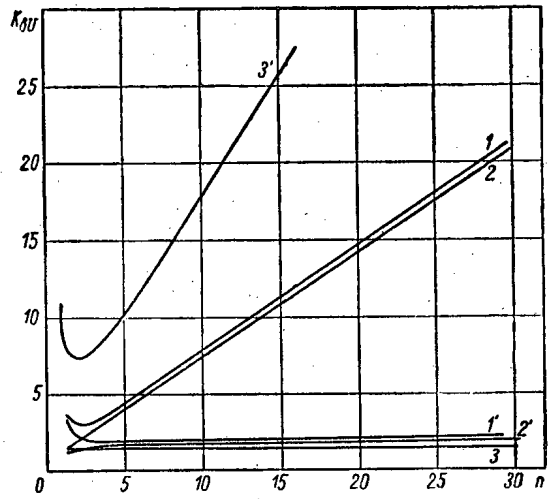

Fig. 4. Efficiencies of the circuits with respect to δU($K_{\delta U} = G(n)$). The notation is the same as in Fig. 3.

Comparison with an ordinary three-phase circuit [1, 6] indicates that

$$\Delta U = \frac{i_l}{fC}\,\frac{8n^3+9n^2+n}{36};\quad F(n) = \frac{8n^3+9n^2+n}{36};\quad \delta U = \frac{i_l}{fC}\,\frac{n^2+n}{6};\quad G(n) = \frac{n^2+n}{6};\quad n_{opt} \simeq \sqrt[3]{\frac{3U_m fC}{i_l}}.$$

For N = 4n, we have $K_{\Delta U} = K_{\delta U} = 1.5$, $K_{n_{opt}} \simeq \sqrt[3]{\frac{3}{2}} \simeq 1{,}15$.

The new three-phase full-wave circuit (Fig. 2), where N = 4n − 3 for equal capacitances, is characterized by the following formulas [8]:

$$\Delta U=\frac{i_l}{fC}\,\frac{2n^3-3n^2+4n}{36};\quad F(n)=\frac{2n^3-3n^2+4n}{36};\quad \delta U=\frac{i_l}{fC}\,\frac{n}{6};\quad G(n)=\frac{n}{6};$$

$$n_{opt}\simeq\sqrt{\frac{6U_m fC}{i_l}};\quad K_{\Delta U}=\frac{3(8n^3+9n^2+n)2n}{(2n^3-3n^2+4n)(4n-3)}\longrightarrow 6\ (\text{for } n\longrightarrow\infty);$$

$$K_{\delta U}=\frac{6(n^2+n)2n}{2n(4n-3)}=\frac{6(n^2+n)}{4n-3};\quad K_{n_{opt}}\simeq\sqrt[3]{\frac{12n}{4n-3}}\simeq 1{,}45.$$

For a clear presentation of the dependences of $K_{\Delta U}$ and $K_{\delta U}$ on n (up to n = 30) for the circuits considered in this article, Figs. 3 and 4 show the graphs of the functions.

The following conclusions can be drawn on the basis of the results obtained in comparing the most promising cascade generator circuits:

1. The efficiency of circuits must be estimated for the same total capacitance of all the capacitors.

2. From among the circuits considered, the most efficient one is the three-phase full-wave circuit, which can be recommended for high-power cascade generators. The ordinary three-phase circuit is the least efficient one.

3. For a large n value, the two-phase (symmetric) and the single-phase full-wave circuits are approximately equivalent; however, for n < 20, the new circuit is much more efficient.

LITERATURE CITED

1. B. S. Novikovskii, Atomnaya Énergiya, 4, No. 2, 175 (1958).
2. A. A. Vorob'ev et al., High-Voltage Test Equipment and Measurements [in Russian], Moscow, Gosénergoizdat (1960).
3. E. M. Balabanov and Yu. S. Smirnov, Pribory i Tekhnika Éksperimenta, 5, 23 (1960).
4. A. A. Vorob'ev and S. F. Pokrovskii, Atomnaya Énergiya, 9, No. 4, 305 (1960).
5. A. Boumers and A. Kuntke, Z. techn. Phys., 18, 209 (1937).
6. G. I. Kitaev, Izv. Vyssh. Uchebn. Zavedenii. Énergetika, 11, 32 (1962).
7. G. I. Kitaev, Author's certificate No. 143897 (1962).
8. G. I. Kitaev, Author's certificate No. 146858 (1962).

SPACE DISTRIBUTION OF NEUTRON RESONANCE ABSORPTION IN A BLOCK

V. A. Kremnev and A. A. Luk'yanov

Translated from Atomnaya Énergiya, Vol. 14, No. 2,
pp. 216-217, February, 1963
Original article submitted May 21, 1962

The determination of the space distribution of resonance neutron absorption in a block placed in a moderator is of interest both for the theory of heterogeneous reactors and for a number of practical cases (for example, distribution of plutonium in a uranium fuel element). The ratio of the number of neutrons of resonance energy absorbed in a volume dv to the number of nuclei of the absorber can be regarded as a characteristic of resonance absorption in an elementary volume dv surrounding a point in the block with the coordinate $\mathbf{r}$. We call this ratio the effective resonance integral of absorption:

$$J(\mathbf{r}) = \frac{1}{\rho\, dv} \int_u \Sigma_c(u)\, \varphi(u, \mathbf{r})\, du\, dv = \int_u \sigma_c(u)\, \varphi(u, \mathbf{r})\, du, \tag{1}$$

where $\varphi(u, \mathbf{r})$ is the neutron flux at the point $\mathbf{r}$ at the energy (lethargy) u; ρ is the absorber nucleus concentration in the block; $\sigma_0(u)$ is the absorption cross section at the energy u. In the energy region in which the resonances can be regarded as isolated, the resonance integral (1) is calculated in the form of a sum over the individual levels:

$$J(\mathbf{r}) = \sum_i J^i(\mathbf{r}) = \sum_i \int_u \sigma_c^i(u)\, \varphi(u, \mathbf{r})\, du, \tag{1a}$$

and since the behavior of the cross section in the neighborhood of the i-th resonance is usually known, the problem of investigating the space distribution of the resonance absorption is limited to a problem of finding the neutron flux in the blocks $\varphi(u, \mathbf{r})$.

Orlov [1] and Wagner [2] found the distribution of neutron resonance absorption in a block by means of the Gurevich-Pomeranchuk approximation. In this approximation the resonances are assumed to be strong ($\Sigma_0 d \gg 1$), and the effect of neutron moderation in the block is considered unimportant ($\Sigma_{sp} d \ll 1$). In a number of practical cases, however, the resonance absorption of the moderated neutrons cannot be neglected. For example, in a block consisting of UO_2 of diameter 1 cm, the moderated neutrons contribute about 15% to J(r) (see [3]). A method proposed for the calculation of the space-energy distribution of the resonant neutron flux takes into account the effect of neutron moderation in the block within the framework of the "narrow resonance" approximation (the mean energy loss in collisions between neutrons and nuclei of the absorber is considerably greater than the resonance width) and is based on the use of the corresponding functions determined in monoenergetic transport theory [4] for the space distribution of neutrons in a block after the first collision.

For a block placed in an infinite moderator, the neutron flux of energy sufficiently removed from the energy of the isolated resonance E_i is the same at all points of the block and is equal to the neutron flux in the moderator. Using this fact and the general integral equation for the neutron flux at a point [4], we can obtain an expression for the neutron flux of resonant energy:

$$\varphi(u, \mathbf{r}) = \Sigma_{sp} \int_v K(\mathbf{r}' \to \mathbf{r})\, dv + \int_s K(\mathbf{r}_s' \to \mathbf{r})\, dS\, |\Omega_n|, \tag{2}$$

where

$$K(\mathbf{r}' \to \mathbf{r}) = \frac{1}{4\pi} \frac{e^{-\Sigma |\mathbf{r}-\mathbf{r}'|}}{|\mathbf{r}-\mathbf{r}'|^2};$$

$|\Omega_n|$ is the cosine of the angle between the direction $\mathbf{r}'_s - \mathbf{r}$ and the external normal to the surface of the block at the point $\mathbf{r}'_s$; dS is an element of the surface of the block in the neighborhood of the point $\mathbf{r}'_s$; Σ is the total cross section in the block and is equal to $\Sigma_{sp} + \Sigma_r = \rho(\sigma_{sp} + \sigma_r)$. Here σ_{sp} is the cross section for potential scattering relative to one nucleus of the absorber, σ_r is the total resonance cross section. Using the properties of the function $K(\mathbf{r}' - \mathbf{r})$ (see [5]) relation (2) can be reduced to the form

$$\varphi(u, \mathbf{r}) = \frac{\sigma_{sp}}{\sigma} + \frac{\sigma_r}{\sigma} \int_s K\left(\mathbf{r}'_s - \mathbf{r}\right) |\Omega_n| \, dS = \frac{\sigma_{sp}}{\sigma} + \frac{\sigma_r}{\sigma} \varphi^*(u, \mathbf{r}), \tag{2a}$$

where $\varphi^*(u, \mathbf{r})$ is the neutron flux distribution function in the block after the first collision, under the condition that a uniformly distributed isotropic source of unit strength is located at the surface of the block [6]. Inserting formula (2a) into (1a) and replacing the variable u by E, we obtain

$$J^i(\mathbf{r}) = \int_{(E)} \frac{\sigma_c^i \sigma_{sp}}{\sigma} \frac{dE}{E} + \int_E \frac{\sigma_c^i \sigma_r^i}{\sigma} \varphi^*[\Sigma(E), \mathbf{r}] \frac{dE}{E}. \tag{3}$$

Here the first term represents the resonance absorption integral for the i-th level in an infinite homogeneous medium [4]. With the aid of formula (3), which was used for the calculation of the resonance absorption by an individual level with values of the function $\varphi^*(\Sigma, \mathbf{r})$ given by Stuart [6], we determined the space distribution of resonance absorption in a cylindrical block composed of UO_2 with a radius R = 0.5 cm (Fig. 1) for temperatures of 300 and 0°K. The absolute value of J(r) in an element of the volume was determined by summation over the known allowed levels of U^{238} [7]; in the calculations for higher energies, we used the mean resonance parameters. The results of the calculation are in good agreement with the experimental data [3].

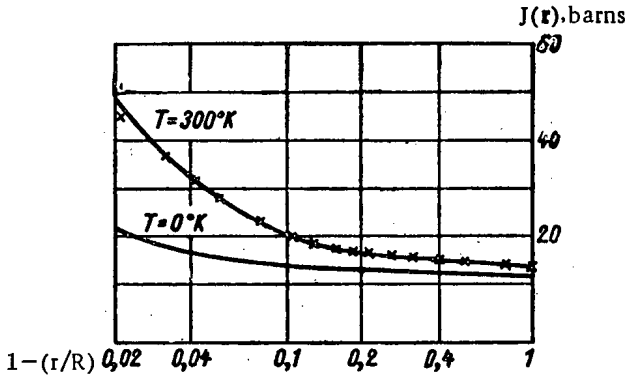

Fig. 1. Distribution of neutron resonance absorption in a cylindrical block of radius R = 0.5 cm: —) calculated; X) experimental data [3].

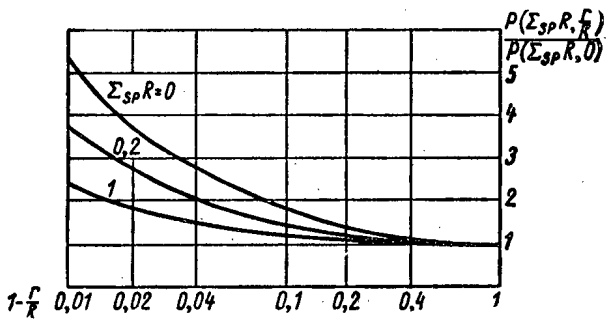

Fig. 2. Relative values of the coefficient P for cylindrical blocks for different values of the parameter $\Sigma_{sp}R$.

In those cases in which the Doppler-effect broadening of the resonances is not important we can separate, for all strong levels, a general coefficient dependent only on the coordinates of the point under consideration in the block and the absorber concentration. For this, we put formula (3) in the form

$$J^i(\mathbf{r}) = \int_{(E)} \frac{\sigma_c^i \sigma_{sp}}{\sigma} \frac{dE}{E} + \frac{1}{4\pi} \int_s \left[F(|\mathbf{r} - \mathbf{r}'_s|) - \Sigma_{sp} \int_{|\mathbf{r}-\mathbf{r}'_s|}^{\infty} F(x)\, dx \right] \frac{|\Omega_n| \, dS}{|\mathbf{r} - \mathbf{r}'_s|^2}, \tag{4}$$

where

$$F(x) = \int_{(E)} \sigma_c^i e^{-\Sigma x} \frac{dE}{E}. \tag{5}$$

If for the description of the energy dependence of the cross section in the vicinity of the resonance we use the Breit-Wigner formula, then, for large values of the parameter $\Sigma_0^i|\mathbf{r}-\mathbf{r}_s'|$ (here Σ_0^i is the cross section at resonance), we can use for F (x) the asymptotic expression [8]

$$F\left(|\mathbf{r}-\mathbf{r}_s'|\right) \simeq J_v^i \frac{e^{-\Sigma_{sp}|\mathbf{r}-\mathbf{r}_s'|}}{\sqrt{\pi\Sigma_{sp}|\mathbf{r}-\mathbf{r}_s'|}}, \tag{5a}$$

where $J_v^i = \int\limits_{(E)} \frac{\sigma_c^i \sigma_{sp}}{\sigma} \frac{dE}{E}$. Inserting (5a) into (4) we obtain

$$J^i(\mathbf{r}) = J_v^i P(\Sigma_{sp}, \mathbf{r}).$$

where

$$P(\Sigma_{sp}, \mathbf{r}) = \frac{1}{4\pi} \int\limits_s \frac{dS|\Omega_n|}{|\mathbf{r}-\mathbf{r}_s'|^2} \left[\frac{e^{-\Sigma_{sp}|\mathbf{r}-\mathbf{r}_s'|}}{\sqrt{\pi\Sigma_{sp}|\mathbf{r}-\mathbf{r}_s'|}} + \Phi\left(\sqrt{\Sigma_{sp}|\mathbf{r}-\mathbf{r}_s'|}\right)\right] \tag{6}$$

(here Φ is the error integral).

The function $P(\Sigma_{sp}, \mathbf{r})$ represents the screening coefficients which depend on the block geometry, distance from the center of the block, and absorber concentration. Figure 2 shows the ratio of the coefficient P at the point r of a cylindrical block to the corresponding value of P at the center of the block. The ratio of the distance from the surface of the block to the radius is given along the abscissa axis on a logarithmic scale. In the case of $\Sigma_{sp}R = 0$, corresponding to the Gurevich-Pomeranchuk approximation, the quantity $P(0, r/R)/P(0, 0)$ agrees with the values obtained in [2]. The moderation in the block leads to an equalizing of the space dstribution of resonance absorption. At the surface of the block the function P goes to infinity, which is connected with the use of the asymptotic formula (5a).

LITERATURE CITED

1. V. V. Orlov, Atomnaya Énergiya, 4, 6, 531 (1958).
2. M. Wagner, J. Nucl. Sci. and Engng. 8, 278 (1960).
3. G. Smith, D. Klein, and J. Mitchell, J. Nucl. Sci. and Engng. 9, 421 (1961).
4. B. Davison, Neutron Transport Theory [Russian translation] (Moscow, State Atomic Press, 1960), p. 30.
5. G. I. Marchuk, Methods of Calculating Nuclear Reactors [in Russian] (Moscow, State Atomic Press, 1961), p. 30.
6. G. Stuart, J. Nucl. Sci. and Engng. 2, 617 (1957).
7. J. Rosen, J. Rainwater, and W. Havens, Phys. Rev., 118, 687 (1960).
8. A. A. Luk'yanov and V. V. Orlov, Collection: Theory and Methods of Calculating Reactors [in Russian](Moscow, State Atomic Press, 1962), p. 179.

NEUTRON DIFFUSION IN A MOVING MEDIUM

A. A. Kostritsa

Translated from Atomnaya Énergiya, Vol. 14, No. 2,
p. 218, February, 1963
Original article submitted May 16, 1962

The entrainment of neutrons by a moving medium can be considerable at comparatively low rates of flow, despite the high neutron diffusion coefficient D and the scattering length l_s. Reactors are known [1, 2] whose operation is accompanied by intensive movement of the moderator. Reactors with still more intensive movement of the moderator in the active zone will evidently be used to an increasing extent in the future. In this connection it is desirable to consider the entrainment of monoenergy (primarily thermal) neutrons by a moving medium.

We will consider the convective transfer of neutrons by a medium moving with velocity **u** in a single-velocity kinetic equation of neutron transfer, connecting the change in neutron density $N(\mathbf{r}, \mathbf{n})$ with diffusion, absorption, scattering of neutrons and their sources*:

$$\frac{\partial N(\mathbf{r}, \mathbf{n})}{\partial t} + \mathbf{u}\nabla N(\mathbf{r}, \mathbf{n}) = -v\nabla N(\mathbf{r}, \mathbf{n}) - \frac{v}{l} N(\mathbf{r}, \mathbf{n}) + \frac{v}{4\pi l_s} \int \mu(\Phi) N(\mathbf{r}, \mathbf{n}') d\Omega' + \frac{1}{4\pi} S(\mathbf{r}). \quad (1)$$

In the simplest case of a plane single-dimensional problem of diffusion in a uniform stream moving in the direction of the x axis, equation (1) can be solved by known methods [3] and we can obtain the following expression for the diffusion length L:

$$\frac{L}{2l_s} \ln \frac{1 + l(1-\gamma)/L}{1 - l(1+\gamma)/L} = 1, \quad (2)$$

which assumes the usual form when $u/v = \gamma \to 0$ (see formula (32.27) in [3]).

The dependence of L on γ determined by expression (2) is fairly complex. For practical use it is convenient to consider the approximate solution of equation (1) in the region outside the sources.

In the P_1 approximation for a neutron density N_0 the following equation holds:

$$\frac{3D}{v^2} \frac{\partial^2 N_0}{\partial t^2} + \frac{6uD}{v^2} \frac{\partial^2 N_0}{\partial x \partial t} + \left(1 + \frac{3D}{v^2 T}\right) \frac{\partial N_0}{\partial t} = D(1 - 3\gamma^2) \frac{\partial^2 N_0}{\partial x^2} - u\left(1 + \frac{3D}{v^2 T}\right) \frac{\partial N_0}{\partial x} - \frac{N_0}{T}. \quad (3)$$

Equation (3) is of the hyperbolic type: When u = 0 it changes to the known relationship{ see equation (9.18) in monograph [4]}. According to [4], in a nonstationary diffusion equation we can never neglect the front of the wave and it is shown that the velocity of the wave front is $v/\sqrt{3}$ and not v. We notice that when $u = v/\sqrt{3}$ in equation (3) the term determining the neutron diffusion disappears.

In the diffusion approximation from equation (3) under stationary conditions and $\gamma^2 \ll 1$ we can obtain an equation for the neutron density:

$$D \frac{d^2 N_0}{dx^2} - u \frac{dN_0}{dx} - \frac{N_0}{T} = 0, \quad (4)$$

* The usual notations are used [3].

from which in a single-dimensional case it follows that the neutron density falls according to the law

$$N_0 \sim \exp\left[-\frac{x}{L}\left(1-\frac{uL}{2D}\right)\right]=\exp\left[-\frac{x}{L^*}\right]. \quad (5)$$

The diffusion length L^* in a stream with velocity $\underline{u}$ will therefore be greater than the diffusion length L in a stationary medium.

The difference between L^* and L can be considered acceptable for the experimental determination if it is 10%. This will be the case when u = 3-3.5 m/sec in D_2O and when u = 20-25 m/sec in H_2O. Consequently, by comparing the results or measurements of the diffusion length in a stationary medium and in a stream we can observe the entrainment of neutrons by a moving medium experimentally.

LITERATURE CITED

1. T. N. Zubarev, "Atomnaya Énergiya", 5, No. 6, 605 (1958); 7, No. 5, 421 (1959).
2. S. A. Colgate and R. L. Aamodt, "Atomnaya tekhnika za rubezhom", No. 4, 3 (1957).
3. A. D. Galanin, Thermal Reactor Theory [in Russian]. Moscow., Atomizdat (1959).
4. A. Weinberg and E. Wigner, The Physical Theory of Nuclear Reactors [Russian translation]. Moscow., Izd. inostr. lit. (1961).

SIMULATION OF EXTENDED γ-RAY SOURCES

V. I. Popov

Translated from Atomnaya Énergiya, Vol. 14, No. 2,
pp. 219-220, February, 1963
Original article submitted March 10, 1962

The possibility of the experimental study of extended γ-ray sources by the simulation technique has been discussed earlier [1] and results of the simulation of sources in which absorption and multiple scattering are absent have been presented.

This technique was applied to the study of self-absorption and multiple scattering effects on the γ-ray yield. A cylindrical Plexiglas sector with angular opening 2.5° was filled with an aqueous solution of a sulphate of Co^{60} and placed in a cylindrical vessel of suitable size filled with water. The vessel was placed on the rotating disc of the simulating arrangement. The dose rate of the γ radiation was measured by an ionization chamber of volume 200 cm^3 with air-equivalent walls.

Figure 1 shows the measured values of the dose rate from real and simulated cylindrical sources. As the units in both cases we took the dose rate at a distance of 100 cm from the cylinder surface in the base plane. It is seen from Fig. 1 that the agreement between the results is quite satisfactory.

We studied the experimental distribution of the dose rate in the base plane of the cylindrical sources with self-absorption and multiple scattering (vessel filled with water) and in the absence of self-absorption and multiple scattering (the vessel with the sector rotated without water). The ratio of the measured dose rate in the first and second cases gives the experimental values of the attenuation factor in the source and characterizes the effect of self-absorption and multiple scattering on the γ-ray yield [2].

For illustration, we give in Fig. 2 the experimental and the calculated curves for the attenuation factors as a function of the distance l to the source surface.

The results of the measurements indicate the character of the dependence of the attenuation factor on the distance for various relative heights (k = h/R) of the cylindrical source. The attenuation factor increases with increasing distance for large relative heights and decreases with increasing distance for small relative heights. This dependence

is similar to the dependence of the self-absorption factor on the distance [3]. The value of the attenuation factor depends on the radius of the cylindrical source; for a fixed height it increases with decreasing radius.

Comparison of the experimental and calculated values shows that the best agreement is obtained when multiple scattering of the γ radiation in the source is taken into account by the γ method [3]. The calculated values of the attenuation factor in this case exceed the experimental values by 10-12%. With the use of an analytic representation of the accumulation factors to take into account multiple Coulomb scattering, the difference is about 30%. This is connected with the error contributed by the analytic representation. In both cases the calculated curves run above the experimental curves, which is due to the neglect of the boundary effect in the calculations [4].

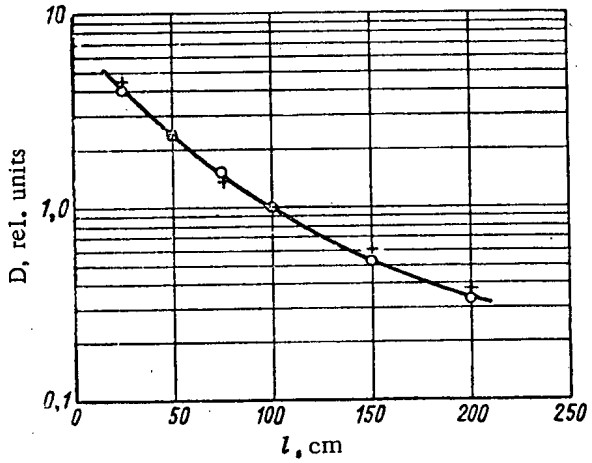

Fig. 1. Measured dose rates from real (O) and simulated (+) cylindrical sources of radius R = 50 cm and height h = 50 cm.

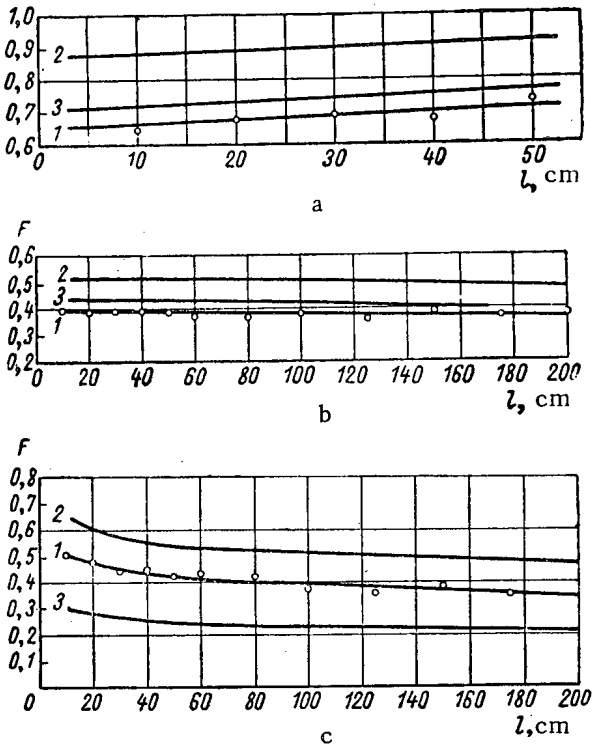

Fig. 2. Dependence of the attenuation factor F on the distance. a) Cylindrical source with R = 12.5 cm, h = 40 cm, k = 3.2; b) source with R = 50 cm, h = 50 cm, k = 1; c) source with R = 50 cm, h = 20 cm, k = 0.4. 1) Experimental curve; 2) curve calculated with allowance for multiple scattering, where an analytic representation of the concentration factors in the form of the sum of two exponents has been used; 3) curve calculated with allowance for multiple scattering by the γ method [3] (a and b), calculated curve for the self-absorption factor (c).

LITERATURE CITED

1. E. E. Kovalev et al., Atomnaya Énergiya, 2, No. 6, 553 (1957).
2. E. E. Kovalev and V. I. Popov, Zh. tekhn. fiz. 27, No. 7, 1621 (1957).
3. N. G. Gusev et al., Protection from Radiation of Extended Sources [in Russian] (Moscow, State Atomic Press, 1961).
4. A. V. Larichev, D. P. Osanov, and V. I. Popov, Atomnaya Énergiya, 13, No. 2, 145 (1962).

SECOND INTERNATIONAL SYMPOSIUM ON INELASTIC SCATTERING OF NEUTRONS BY SOLIDS AND LIQUIDS

N. A. Chernoplekov

Translated from Atomnaya Énergiya, Vol. 14, No. 2,
pp. 221-222, February, 1963

In recent years, the extensive development registered in research on the dynamics of condensed-phase matter by means of inelastic scattering of neutrons has gained prominence. The reasons for this are quite evident, since the study of inelastic scattering of neutrons presents a unique opportunity to study the particular features of the phonon and magnon (spin-wave) branches of crystal excitation, the nature of the collective motion of atoms in liquids, and other problems which are now on the agenda in condensed-state physics. The 2nd international symposium on inelastic scattering of neutrons by solids and liquids, organized by IAEA, was devoted to a discussion of papers and work completed in the last two or three years in this field. The symposium was held at the Canadian Chalk River research center in September, 1962. About 70 scientists participated in the deliberations; 67 papers presented by 15 nations and two international organizations (the Dubna Joint Institute and Euratom) were heard. The Soviet Union presented 6 papers to the symposium.

The following major topics were discussed at the symposium: 1) the theory of neutron interactions with matter; 2) inelastic scattering of neutrons by solids; 3) inelastic scattering of neutrons by liquids and gases; 4) inelastic scattering of neutrons by magnetic materials; 5) techniques in measurements of inelastic neutron scattering.

The most important papers discussing aspects of the theory of inelastic scattering of neutrons by matter and the interpretation of experimental data are, apparently, those dealing with the effects of phonon-phonon and phonon-electron interactions on inelastic coherent scattering of neutrons by single crystals. Two scientists dealt with this topic:: J. Kokkedee (Netherlands), "The theory of the effects of phonon-phonon and phonon-electron interactions on inelastic scattering of neutrons on crystals, " and H. Hahn (West Germany), "The theory of the excitation and the effects of anharmonicity on inelastic scattering of neutrons by crystals." It was shown in these papers that both phonon-phonon and phonon-electron interactions lead to a shift and a broadening of the maxima of coherent inelastic scattering of neutrons. Experimental investigation of these effects renders possible a determination of the degree of anharmonicity in the interatomic interaction forces, and at the same time makes it possible to estimate the cross section for the electron-phonon interaction. In addition to the papers mentioned, several theoretical and empirical papers were presented to the symposium: on the dielectric constants and lattice vibrations of ionic crystals, a report by W. Cochran, R. Cowley (Great Britain), on the practical analysis of neutron scattering data in terms of correlation functions, by P. Egelstaff and co-workers (Great Britain). In addition, an extensive review paper on the use of the Mössbauer effect in studies of the condensed state was presented by K. Singvi (USA).

Twenty-six papers were presented on studies of inelastic scattering of neutrons on solids, and several discussions took place. In his report, A. Woods (Canada) presented a review of results of an investigation into the dynamics of crystals, based on inelastic neutron scattering. Data on the dynamics of Pb, Na, alkali halides, and several semiconductors were considered. The difference between the electron-phonon interaction in Pb and Na, the different extent of the effect of anharmonicity at high temperatures in the materials studied, and the existence of a marked temperature dependence of the width of the inelastic coherent scattering maxima at low temperatures, which defies as yet any satisfactory theoretical explanation, were established. In the wake of this report, the symposium discussed the problem of the correctness of analyzing the constants of the interatomic interaction in conducting crystals on the basis of the dispersion curves for phonons.

B. Brockhouse (Canada) told of work in which the polarization vectors of atom vibrations in Na and Ge lattices are being experimentally determined. It is evident that experiments set up for this purpose provide a gold mine of information on the kinetic properties of phonons.

Several papers were devoted to investigations of the dynamics of some transitional metals and their alloys. M. G. Zemlyanov et al. (USSR), "Investigation of the phonon spectrum and dispersion curves for vanadium," and N. A. Chernoplekov et al. (USSR), "Investigation of the phonon spectrum of nickel," reported quantitative results on the phonon spectra of the elements mentioned, recovered from experimental neutron data, and showed how these data and the elastic constants of the substances concerned may be exploited to yield the necessary information and the kinetic properties of phonons, and consequently, enable investigators to compute all the physical properties dependent on the phonon branch of crystal excitation.

Reports by N. A. Chernoplekov et al. (USSR),"Investigation of the inelastic scattering of neutrons on Ti–Zr alloy," and B. Moser, K. Otness (USA), "Measurement of the spectra of vibratory frequencies of Ni–Pd alloys," based on experimental data on inelastic neutron scattering, discussed various aspects of the dynamics of binary disordered systems and local impurity frequencies. In addition, many papers dealt with studies of dispersion curves for phonons in such elements as Si, Cu, Zn, Mg, Be, etc.,and their chemical compounds (CaF_2, $SrTiO_3$, etc.), and compared the results obtained with various theoretical constructs.

Twenty-three papers were presented on the topic of inelastic scattering of neutrons by liquids and gases. The major brunt of the attention in these papers went to the study of free and hindered rotation of molecules in liquids as a function of the nature of the bond and molecular configurations, and also to the investigation of the nature of diffusion flow of molecules in liquids. One of the outstanding results of an investigation of inelastic scattering of neutrons on liquids was the confirmation of the quasi-crystalline model of the liquid for temperatures not too far removed from the melting point. New results on studies of inelastic scattering of neutrons on water were communicated in reports by D. Cottwitz et al. (USA) and A. Bajorik et al. (Dubna Joint Institute), the first report providing estimates of the settled lifetime of molecules and diffusion coefficients. K. Larsson and W. Dahlborg (Sweden) showed that the determining mechanism in diffusion in the case of glycerine (a substance with a high temperature coefficient of viscosity) is "jump" diffusion.

Some experimental papers dealt with studies of the "generalized frequency function" of liquids (similar to the phonon spectrum in solids, a concept introduced by P. Egelstaff), and, although the quantity of physical information derived from these functions is modest as yet, such measurements are nonetheless valuable since the results may be used directly in practical computations, including reactor physics computations.

The problem of inelastic scattering of neutrons by magnetic materials was the subject of at least four papers. B. Brockhouse and H. Watanabe (Canada), "Spin waves and neutron scattering," told of measurements using the methods of constant variation of momentum and neutron energy in measuring dispersion curves for optical and acoustical spin waves in magnetite. On the basis of these magnetite measurements (magnetite being a ferromagnetic material with an inverted spinel structure), estimates were made of the values of the exchange integrals, leading to results which clashed sharply with those obtained by other methods. It was found that the exchange integral for interaction between iron ions in positions A and B is $J_{AB} = 2.3 \cdot 10^{-3}$ eV, with J_{BB} significantly less, and ferromagnetic, and the results obtained show little sensitivity to the value of J_{AA}.

An investigation of low-angle neutron scattering in Fe and Ni near the Curie point was the subject of a paper by B. Jacquereau et al. (France). These experiments brought confirmation that the critical scattering of neutrons is inelastic. The temperature dependence of regions of spin correlation in the specimens studied was also evaluated. In addition, a report by D. Cribier, B. Jacquereau (France) dealt with measurements of inelastic neutron scattering on $MnFe_2$ in the paramagnetic state, and a report by Z. Krasnicki et al. (Poland) was devoted to inelastic magnetic scattering measurements, on franklinite and chromium oxide.

Eight papers were devoted to experimental research techniques in inelastic scattering of neutrons on solids and liquids. A paper by F. Webb and J. Pearce (Great Britain) reported an automatically operated cold-neutron source set up at the Harwell DIDO reactor, in which liquid hydrogen functions as moderator. A description of a multirotor phased systems of choppers making it possible to effect a considerable improvement in the resolving power of experimental arrangements was discussed in papers by K. Otness, G. Palevsky (USA), and D. Harris et al. (Great Britain). V. V. Golikov et al. (Dubna) devoted their paper to a discussion of the problem of the IBR reactor used as a source of neutrons in studying inelastic scattering of neutrons on solids and liquids. Also of interest was a communication by D. Harris et al., presented as a joint report under British and Canadian auspices, on scintillation detectors using Li^6-enriched lithium compounds.

As one might well conclude from the papers discussed at the Chalk River symposium, the basic experimental research method relied upon in the study of inelastic scattering of neutrons at low-flux reactors is the range of techniques employing cold neutron sources with time-of-flight spectrometers, and at high-flux reactors, three-crystal spectrometers and multirotor chopper systems with time-of-flight neutron spectrometers.

The proceedings of the Chalk River symposium will be published during 1963 IAEA. At the organization session of the symposium, a desire was expressed to schedule a subsequent symposium on inelastic scattering of neutrons by solids and liquids, to be convened in another two to three years.

MOSCOW CONFERENCE ON RADIATION CHEMISTRY APPLICATIONS OF CHARGED-PARTICLE ACCELERATORS

E. V. Egorov and M. Ya. Kaplunov

Translated from Atomnaya Énergiya, Vol. 14, No. 2,
pp. 222 -224, February, 1963

A conference on the application of charged-particle accelerators in radiation chemistry, convoked by the Division of Chemical Sciences of the USSR Academy of Sciences, was held in Moscow in May, 1962.

Over fifteen papers and communications were heard and discussed at the conference.

In a brief introductory speech, Academician N. N. Semenov emphasized the fact that, although research in the field of radiation chemistry has been under way for 15 years, the problem of the practical realization of this new and important trend in chemistry cannot be viewed as near solution since there are not available as yet facilities capable of turning out the variety of products on an industrial and even pilot-plant scale, which would enable us to arrive at an estimate of the costs picture and practical significance of radiation-chemical processes. Taking a brief look at the principal types of available radiation sources, N. N. Semenov noted that there is a great future ahead for electron accelerators in chemistry. The comparative simplicity of design and control, compactness, and the high radiation utilization factor of electron accelerators, tens and even hundreds greater than that offered by γ -sources, render these machines highly suitable for most radiation-chemical processes. N. N. Semenov also took note of the fact that the technology of electron accelerators must be developed further and improved simultaneously with the technology of γ -ray facilities, the one supplementing the other.

In reports presented to the conference, topics concerning the description of the design and engineering specifications of linear accelerators, electrostatic generators, betatrons, and other types of electron accelerators being developed and fabricated in the USSR and in other countries were discussed. Several reports devoted to the engineering requirements imposed on accelerators specially designed to facilitate radiation-chemical processes in laboratory or pilot-plant applications were also heard. For example, pulsed standing-wave linear accelerators (the LUÉ-5-1 and the LUÉ-5-2) of 5 MeV electron energy and average beam current to 1 mA may be of interest as tools for radiation-chemical processes under laboratory conditions with later scale-up to pilot-plant experiments. It should be noted that accelerators of this type lend themselves to use in experimental research on modifying the properties of polymeric materials, radiation-chemical oxidation, sulfuration, and chlorination of hydrocarbons, vulcanization of crude rubbers and rubber mixtures.

B. A. Kononov presented a paper on work in progress at Tomsk Polytechnic Institute (TPI) in the design and fabrication of electron accelerators (betatrons) extensively employed for therapeutic purposes and physics research.

The TPI induction accelerators, of 25 MeV electron energy, make it possible to obtain an average current several orders of magnitude higher than in betatrons, where the average beam current is 10^{-8} A. The bremsstrahlung dose rate at a distance of 1 meter from the target of an accelerator of this type is ~ 5000 r/min. This bremsstrahlung dose rate is already acceptable for carrying out various radiation-chemical processes, whereas most betatrons are unsuitable in that function because of the low bremsstrahlung dose rate (5 to 200 r/min).

The most promising tools for various pilot-plant radiation-chemical processes (graft polymerization, modification of the properties of thin polymeric films, etc.) are several types of direct-acting accelerator tubes of 0.5 MeV electron energy and beam current to 0.13 A, also developed at TPI. It would be highly useful to conduct experiments directed to enhancing electron energy, since success in that endeavor might very well considerably extend the range of application of these accelerators in radiation chemistry.

In his report, S. P. Kapitsa dealt with a microtron developed at the Institute of Physics Problems (IFP) of the Academy of Sciences of the USSR, reported on a study of features of the electron beam and on an investigation of the energy spectrum of the beam. The fairly broad potentialities of this accelerator in radiation-chemistry research applications were stressed.

The report by F. G. Zheleznyakov was devoted to the principal characteristics of direct-action electron accelerators, and to the development of small-size electrostatic generators of 1-2 MeV electron energy, which are of unusual interest for laboratory research in radiation chemistry. A communication on the development of an accelerator known as the kapotron excited some interest; this accelerator is an original variant of the cascade-type accelerator known as the dynamitron and employed outside the USSR in radiation-chemical processes. The speaker also informed the audience that a 2.5 MeV cascade generator of 25 kW beam power will be built in 1963.

O. A. Val'dner's report (Moscow Engineering and Physics Institute) on a line of accelerators being developed and built at the Institute (MIFI) was received with heightened interest. Pulsed traveling-wave linear accelerators of 3, 5, and 10 MeV electron energy and beam power ranging from 500 to 700 W have been designed, built, and put into operation. Experimental work on vulcanization of rubber, searching for new radiation-stable polymers, research on radiation topochemical processes, and on production of highly disperse active catalysts and sorbents is being performed with these accelerators.

A paper presented by V. L. Karpov and L. V. Chepel' (of the L. Ya. Karpov Physical Chemistry Institute of the USSR Academy of Sciences) detailed the principal engineering requirements and specifications of an electron accelerator designed for pilot-plant work on various radiation-chemical processes. Radiation-chemical processes of practical interest have been worked out under laboratory conditions and run through tests (crosslinking of polyethylene and polyvinyl chloride, graft polymerization of vinyl acetate on teflon, etc.).

The requirements imposed on electron accelerators for the vulcanization of crude rubbers and rubber mixtures were the subject of a paper jointly authored by Z. N. Tarasova, V. K. Khozak, E. V. Egorov, M. Ya. Kaplunov, and V. S. Sobolev (Scientific Research Institute of the Rubber Tire Industry, Institute of Chemical Physics of the USSR Academy of Sciences). It was mentioned in the paper that electron accelerators appear to be highly promising radiation sources for the vulcanization of rubber, since the high intensity of the electron beam makes it possible to effect an appreciable suppression of the role of degradative processes in polymers, such as are usually observed to occur in polymers irradiated by γ-ray sources. The exposure time can be reduced to a mere fraction in the bargain. The beam utilization factor may reach as high as 50 to 70% or even higher. The authors state that, to be suitable candidates for radiation-chemical vulcanization of rubber, the electron accelerators must have 5-7 MeV energy, a beam current of 1 mA, a beam spread to 1 meter, and an energy flux in the vicinity of 0.25 W/cm^2.

A. P. Sechenkov dwelt on the design features of a 0.5 MeV electrostatic accelerator with a beam current as high as 250 μA. The outstanding feature of this machine is the technique used to generate a high voltage from the rigid-rotor electrostatic generator.

The audience manifested interest in the report by L. V. Chepel' on foreign accelerator advances and progress registered in that field.

D. N. Margolin (of the L. Ya. Karpov Physical Chemistry Institute) shared the experience of his work on the ÉG-2.5 electrostatic generator. The accelerator is capable of controlling particle energies from 0.3 to 2.0 MeV and controlling current from $5 \cdot 10^{-3}$ μA to 200 μA. The peak beam power is 0.4 kW.

A variety of research efforts are being conducted at the Physical Chemistry Institute, centered on the 2 MeV and 0.8 MeV electron accelerators, and constituted the subject of a paper read by N. Ya. Buben. Experiments on investigations of the nature and properties of free radicals formed in radiolysis are being conducted over a broad temperature range; gaseous radiolytic products of hydrocarbons are being studied; the radiothermoluminescence of irradiated substances in their structural and phase transitions are being investigated; the role of ions in radiation-chemical processes is under study; the electrophysical properties of irradiated organic materials are being measured;

radiation-induced polymerization and vulcanization of rubber mixtures are under study; the effects of radiation on adhesion of polymers is being investigated; a search is being conducted for radiation-resistant polymers; endoergic radiation-chemical processes are under study, etc.

Experience in working with a 1.2 MeV electrostatic accelerator was reported on by P. Ya. Glazunov (Physical Chemistry Institute). The accelerator was employed to investigate such processes as radiation cracking, radiation polymerization and grafting, effects of ionizing radiations on topochemical, catalytic, corrosive processes, the effect of high absorbed dose rates on aqueous solutions, etc.

An expanded resolution was adopted at the conference. The resolution stated that several radiation-chemical processes are presently on the verge of scale-up to pilot-plant tests. These processes are particularly well promoted by the powerful, compact-size, and operationally reliable electron accelerators now coming into the picture. Compact low-power accelerators reliable in performance and designed specifically for radiation-chemistry research are of great significance in the development of this field.

The conference was of the view that the principal role in the utilization of accelerators in carrying out radiation-chemical processes in the coming years will be played by linear accelerators and electrostatic accelerators, which must be used at the stage of pilot-plant testing of radiation-chemical processes.

The main burden of the conference's attention was turned to the improvement and development of accelerators:

a) for work with gaseous and liquid products, vulcanization of rubber stocks, crosslinking of polyethylene, etc., a 2 to 8 MeV linear accelerator (pulsed or continuous-wave) with average beam current of 3 mA, and possibility of scanning the target with the beam;

b) 1.5 Mev electrostatic accelerator of 1.5 MeV energy and 1 to 5 mA current, for various forms of grafting and similar processes;

Compact small electrostatic accelerators hold out excellent promise for laboratory and research applications.

The conference resolution singled out the microtron as a particularly promising accelerator, suited for use in the first stage as a laboratory device, and subsequently as a pilot-plant accelerator.

The conference registered the viewpoint that further development of a number of engineering design and costs problems will have a salutary effect on the expansion of the range of application of the various accelerator types:

1) extraction of beams of 20 to 50 kW power from accelerators;

2) rotation of a beam through 90° and beam scanning;

3) development of filters for equalizing depth doses;

4) introducing the beam into chemical reactors at up to 100 atm reactor pressure and up to 300°C reactor temperature;

5) reducing costs of 1 kWh beam.

The resolution noted the necessity of intensifying work on modification of accelerators for industrial use in radiation-chemical processes.

DEVELOPMENT OF INDUSTRIAL LINEAR ACCELERATORS

O. A. Val'dner and A. A. Glazkov

Translated from Atomnaya Énergiya, Vol. 14, No. 2,
pp. 224-226, February, 1963

Research work in the field of linear electron accelerators has been in progress for several years at the Moscow Engineering and Physics Institute (MIFI). Theoretical work is being advanced in two directions: a) the study of the properties of iris-loaded waveguides by field theory techniques (dispersion, structure of field) and by circuit theory techniques (bandpass characteristics); b) the study of the dynamics of the interaction between particles and a traveling-wave field, in order to find the conditions for optimizing the phase-energy characteristics of the accelerated beam. As a result of experimental and design work, six linear accelerators ranging in particle energy from 2 to 7 MeV have been designed and put into operation. These machines have been used both for research on physical processes at work in linear accelerators and for applied research on the irradiation of dielectrics, semiconductors, etc.

Fig. 1. The U-10 accelerator.

On the basis of the experience accumulated thus far, a program of research projects has been adopted at MIFI on standardized linear accelerators for research and production functions, the latter function acquiring increased importance of late because of the constantly expanding sphere of the national economy which is experiencing a need for high-level sources of ionizing radiations.

The specific requirements imposed on a general-purpose linear accelerator are: operational reliability and operational stability, stability of the characteristics, low cost, and maintenance accessibility, simplicity in control and servicing, with compact size and low energy consumption.

Considerations of simplicity and reliability dictate, as choice for the high-frequency supply generator, an S-band magnetron of 1-2 MW pulse power. It has been shown [1] that this power level makes it possible to produce a beam of electrons with an energy spectrum no wider than 5% and the phase dimensions of the electron bunch kept to within 30°, that is, the bunching capacity of magnetron-powered accelerators is not inferior to that of klystron-powered accelerators of much greater power. The average beam power has to be brought up to 400-800 W, and the high-frequency efficiency is as high as 50% or greater.

The design of an accelerating system for the beam parameters (current, energy, spectrum) specified is carried out according to a specially elaborated procedure [2, 3], which enables designers to predict and minimize accelerator sensitivity to frequency swings and to fluctuations in the power supply. Difficulties attendant upon stabilizing the operation of the magnetron coupled into an iris-loaded waveguide were overcome without resorting to expensive ferrite decoupling devices in the most complete utilization of the magnetron power for acceleration.

Four types of linear accelerators have been developed for mass production. They are designed for rated generator power of about 1.5 MW and are excited by pulses lasting 3 μsec at a modulation frequency of 400 cps. The beam current may be controlled smoothly from zero to rated value in all these accelerators.

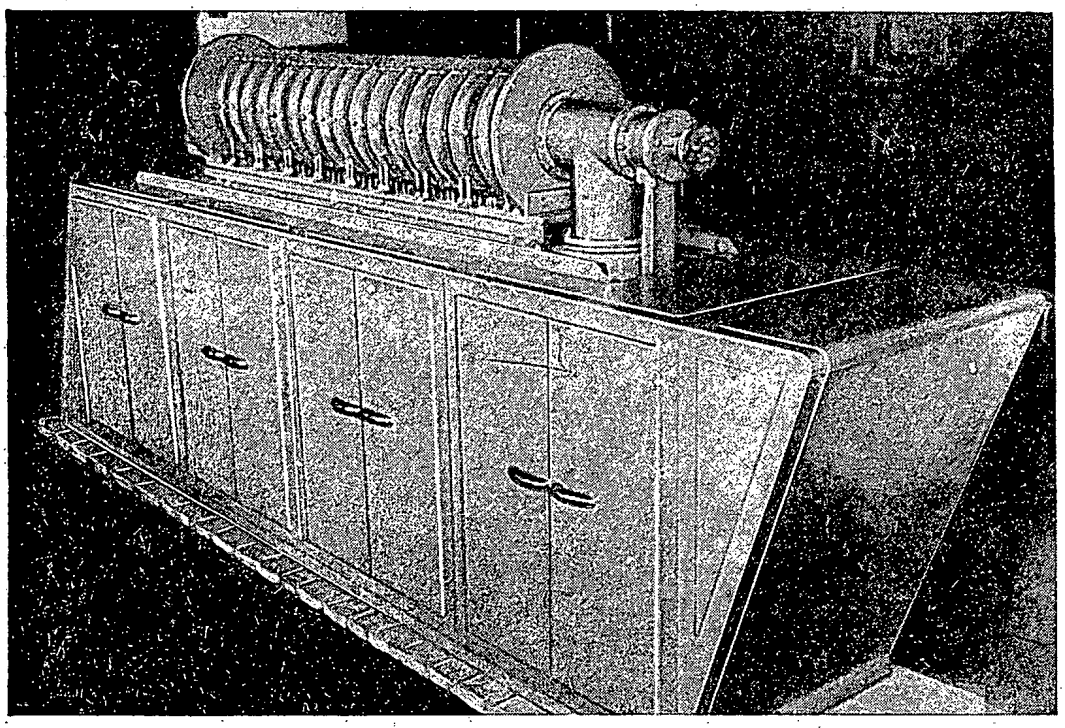

Fig. 2. The U-12 accelerator.

The U-10 accelerator (Fig. 1) has passed its tests successfully. The total electron energy is 3 MeV, the mean beam current 220 μA (and may be elevated to 600 μA), the γ intensity 260 r/min. The accelerator waveguide is 122 cm long (54 cells). The phase velocity β_w of the accelerating wave varies over the range 0.436-0.987, the load factor a/λ averages out at 0.16, and the field amplitude E is 17.4-30.0 kV/cm.

The U-12 accelerator (Fig. 2) has an electron energy of 5 MeV, average beam current to 100μA, γ intensity 600 r/min. The waveguide is 200 cm long (84 cells); it begins as an exact replica of the U-10 accelerator, with the last 78 cm (30 cells) being of constant structure; $\beta_w = 1.00$; $a/\lambda = 0.155$; E declines from 30 to 26 kV/cm. The U-12 machine differs from the U-10 not only in the higher energy, but also in its improved design and enhanced operational reliability. The U-12 accelerator has been tested.

The U-13 accelerator is characterized by10 MeV energy, beam current 70 μA, γ intensity 2500 r/min. The waveguide consists of two sections each 200 cm long; the first is identical to the U-12 waveguide, while the second section has a constant structure over its entire extent. The two sections are excited from two magnetrons coupled in series, which are synchronized by small signals tapped from each magnetron and fed to the input of the other magnetron. The U-13 accelerator is designed for smooth control of the energy of the accelerated electrons over the 5-10 MeV range by retuning a phase inverter placed before the input wave transformer of the second section.

The U-16 accelerator is characterized by a beam current of 200 μA, electron energy controlled over the 1-2 MeV range. The accelerator boasts the special feature of close control of energy with current kept constant and at a low peak energy value. Since particle capture falls off sharply as the input power is reduced, the energy is controlled by readjusting the frequency of the supply source. This requires building an extremely wide band iris-loaded waveguide

to facilitate stable operation of the magnetron over the entire adjustment range. The laws of variation of the parameters β_w and a/λ were found, thus simultaneously making possible smooth energy control and wideband matching. The waveguide is 100 cm long (52 cells); the load factor decreases uniformly over the range 0.18-0.12; E increases from 9.9 to 38.9 kV/cm. Electron energy varies linearly from 2.1 to 1.0 MeV as the frequency increases by 8 Mc from the rated value. The spectrum then experiences a negligible broadening (from 7 to 9.5%) with no beam current losses.

Orders are now in from several organizations for building over 15 accelerators of the types described in specialized variants. Over half of these accelerators have already been built and tested.

LITERATURE CITED

1. E. G. Pyatnov, A. A. Glazkov, and S. P. Lomnev, Symp. proceedings of MIFI. Nekotorye voprosy inzhenernoi fiziki, No. 2, 65 (1957).
2. A. V. Shal'nov, E. G. Pyatnov, and A. A. Glazkov, Proc. MIFI.Lineinye uskoriteli (1959), p. 16.
3. A. G. Tragov, Proc. MIFI, Uskoriteli, No. 3, 148 (1962).

THE ISOTOPES CENTER IN WARSAW*

Translated from Atomnaya Énergiya, Vol. 14, No. 2,
pp. 228-229, February, 1963

An isotope center was organized in late 1960 at the Medical Institute in Warsaw. Applications of radioactive isotopes in treatment of patients are carried out at the Center, diagnostic techniques are worked out, and training of students in a program under the auspices of the therapeutic faculty of the Medical Institute is underway. The Isotopes Center occupies four main rooms. From the standpoint of isotope zone classification, the premises of the Center may be divided into a "hot" zone and a "clean" zone, or, from a functional standpoint, into a clinical and an experimental section. The individual rooms contain an isotope bay with an isotope vault, a room for washing glassware and equipment, and locker rooms (one "clean" and one "dirty"), with a shower room in-between.

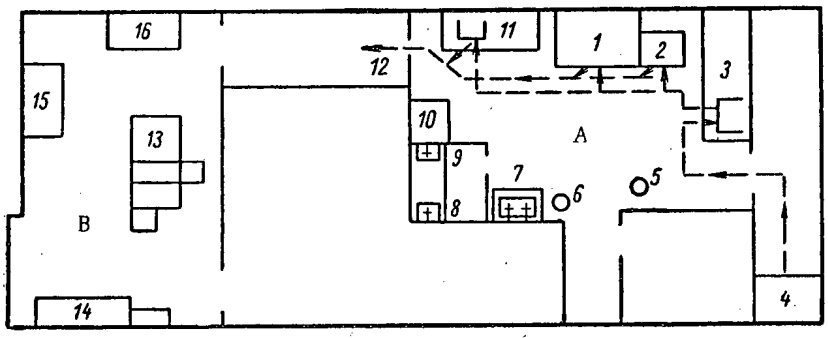

Placement of equipment in isotope laboratory A) "hot" zone; B) "clean" zone): 1) radiochemical hood; 2) glove box; 3) laboratory bench; 4) isotope storage vault; 5) solid wastes receptacle; 6) liquid wastes receptacle; 7) sink and drain for radiochemical wastes; 8) sink draining directly into sewage; 9) sink draining into dilution tank; 10) dilution tank; 11) lab bench; 12) window for distributing preparations; 13) γ-ray scanning machine; 14) scintillation counter rig; 15) same as 14; 16) end-window counter rig.

* Postepy techniki jadrowej 6, No. 3, 205 (1962).

The basic equipment of the laboratory for the preparation of isotope preparations is shown in the accompanying diagram. Manipulators and automatic pipettes, various types of containers equipped with γ - and β-shields, are not shown. The major work carried out in this room is the packing of isotopes, making up preparations for patients, chemical analyses, etc. The most frequently and extensively used isotope is I^{131}, in various compounds; other isotopes, such as Cr^{51}, Fe^{59}, P^{32} are used in lesser amounts. Solid wastes are removed in an intermediate receptacle, and from there are conveyed to a settling tank located off the premises of the Center.

The major measuring instruments in use are a scintillation counter on a movable stand, recording equipment with scintillation counters, a set for measuring beta emissions with an end-window gas discharge counter, and a γ -ray scanning device.

As mentioned above, the isotopes center assumes the tasks of medical service, experimental research, and training program. The medical service consists in diagnostic examination of patients. The most thorough examinations are given to cases of thyroid malfunction, diagnosis and localization of brain tumors with the aid of human serum albumin tagged with I^{131} isotope, functional examinations of the liver, and γ -ray surveys carried out with I^{131}-labeled Bengal Rose dye.

The content of the experimental research concerns diagnosing, problems relating to the pathophysiology of the thyroid gland and iodine metabolism in the organism, some aspects of liver function, and radiobiological problems. Studies bearing on techniques are also attended to, in connection with advancement of clinical research.

The training program of the Center consists in the main of seminars and the organization of practical courses for advanced students. The curriculum covers the fundamentals of the physics of radioactive radiations and the fundamentals of measurements, the most vital information from the field of radiobiology, the use of isotopes in medicine, and radiological shielding. The staff works in collaboration with the students undergoing the radiology courses, familiarizing the latter with the use of isotopes and radiological shielding in practice. Open seminars are conducted weekly at the Center, to spread other specialized features of knowledge of isotope applications among medical practitioners invited to attend.

L. P.

A NEW LINE OF VAKUTRONIK EQUIPMENT (EAST GERMANY)*

W. Hartmann

Translated from Atomnaya Énergiya, Vol. 14, No. 2,
pp. 232-233, February, 1963

The Vakutronik industry was set up in Dresden in 1955, and its original staff had been working for some time in the Soviet Union. It has now grown to a sizable enterprise, manufacturing a large quantity of instruments and facilities which to a large extent answer the needs of the young republic in nucleonics equipment. Radiation detectors, laboratory measuring instruments, industrial measuring devices, and health-physics instruments are being fabricated.

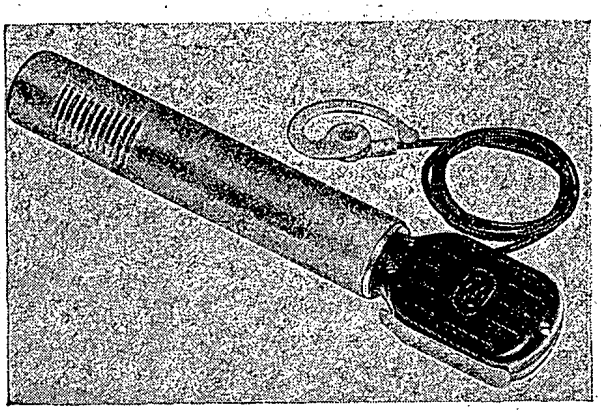

Fig. 1. Aktifon-D VA-J-22 γ-β indicator.

The varied line of equipment includes instruments of some interest to the Soviet reader. Below, we cite the engineering characteristics of some of the most interesting items.

The VA-Z-410 liquid measuring counter boasts a count rate of 3 cpm at a P^{32} concentration of 10^{-9} curie/liter. The counter is deactivated with ease by means of a double-clamp design of the base.

The VA-J-22 γ - β indicator Aktifon-D, dynamo-powered (Fig. 1). A halide Geiger counter serves as the radiation sensor in this portable compact instrument; the device is completely transistorized and is supplied from a hand-operated current generator. Two turns of the generator handle are sufficient to run the instrument continuously for 5 min (at a γ radiation level 10 times greater than natural background). Radiation readings are obtained by a telephone set.

The VA-T-81 air monitor (Fig. 2) may be used as a measuring and recording system for continuous monitoring of the concentration of radioactive aerosols in the air surrounding a reactor, in radiochemical laboratories, in mines, and also has applications in meteorology, etc. The set consists of two portable units: a 15 m^3/h capacity air blower and a measuring instruments cabinet.

α and β activity of aerosols settled on a continuously moving filtering strip are measured immediately and again after a certain time has elapsed (as long as 80 h). The long-lived component of aerosol activity may be singled out in this manner after the short-lived component has decayed, and the radon and thoron concentrations may be measured simultaneously. Concentrations of α- and β-active aerosols can be reliably detected down to $2 \cdot 10^{-15}$ curie/liter (for Pu^{239}) and 10^{-16} curie/liter (for Sr^{90} and Y^{90}). Light and sound alarms operating in the case where the measured concentration of radioactive aerosols exceeds or falls below preset levels are provided. An alarm is also actuated when the strip breaks or stops.

The RICU type VA-J-35 measuring device (Fig. 3) is a high-sensitivity instrument with an electrometer input for measuring resistance, current, capacitance, and voltage. The input resistance of the device is 10^{14} ohms at a capacitance of 25 mμF, zero drift not greater than 10 mV/h. It has a lightproof and moistureproof measuring chamber shielded against magnetic fields, and is capable of reliable measurements under high ambient moisture conditions. The second stage utilizes two electrometer tubes type DC-760 in a bridge circuit.

*This article was written in East Germany.

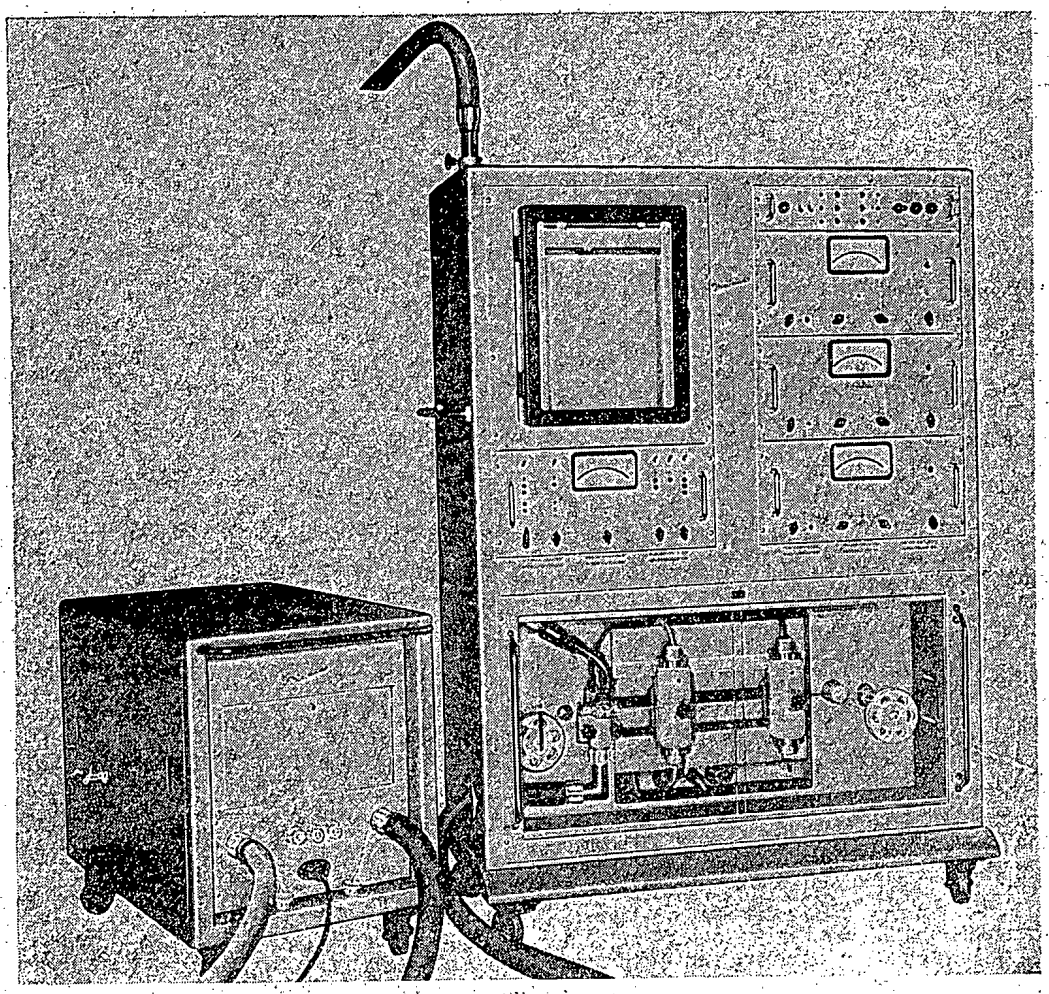

Fig. 2. VA-T-81 air monitor facility.

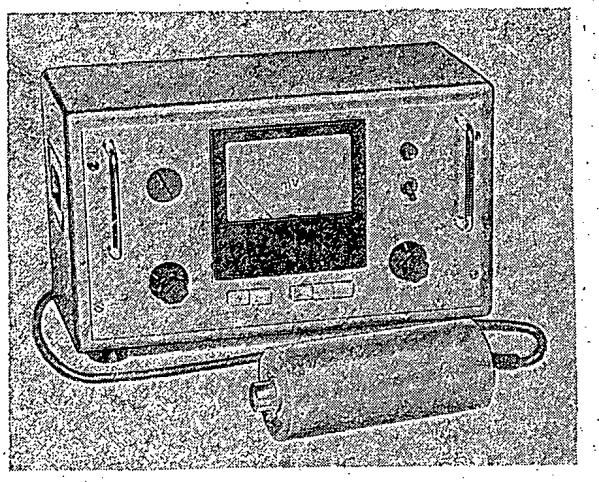

Fig. 3. VA-J-35 resistance, current, capacitance, and voltage measuring instrument.

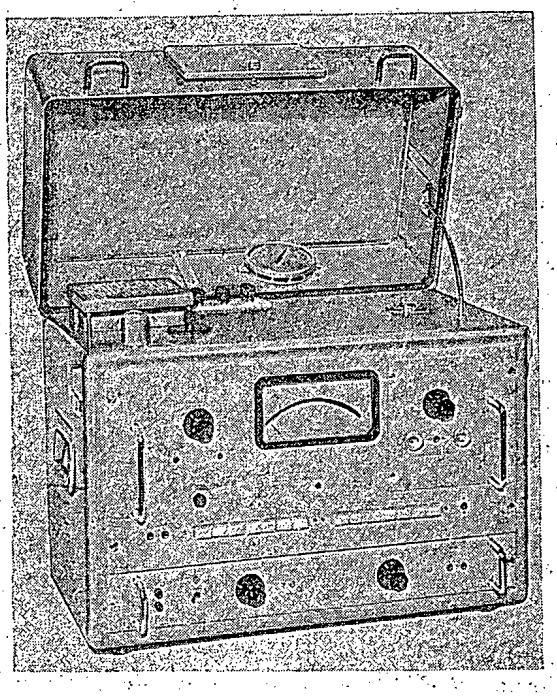

Fig. 4. VA-J-50 electrometer.

The VA-J-50 (Fig. 4) type dynamic condenser electrometer may be used to measure ionization-chamber currents, etc. The instrument has measurement ranges of 10, 30, 100, 300, and 1000 mV at an input resistance of 10^{15} ohms and capacitance of 30 mμF. Zero drift does not exceed 0.2 mV in 24 hours.

RESULTS OF PERSONNEL MONITORING IN POLAND *

Yu. V. Sivintsev

Translated from Atomnaya Énergiya, Vol. 14, No. 2,
p. 234, February, 1963

The Central Laboratory of Radiation Shielding attached to the Plenipotentiary Council of Ministers of the Polish Peoples Republic on Atomic Energy Affairs has published a report (by T. Musialowicz) on the results of systematic measurements of exposure doses during 1960 in personnel working with radioactive isotopes at various institutions. The centralized processing (development, photometric scanning, calibration) of personnel film badges for sensing ionizing radiations has made it possible to analyze dosage depending on the range of application of the radioisotopes, the age and sex of the person monitored, and to compare the results with similar totals for 1959.

TABLE 1. Distribution of Personnel Subjected to Exposures to Ionizing Radiations, According to Isotope Applications

Range of application	Number of persons	
	Men	Women
Research labs	285	99
Industrial plants	559	57
Medical institutions	82	357
Miscellaneous	33	3
Total	959	516

TABLE 2. Distribution of Personnel Subjected to Exposures to Ionizing Radiations, According to Isotope Application (taking into account the dose rate)

Range of application	Dose, rem				
	0.5	0.5 -1.5	1.5 -5.0	5.0 -12.0	> 12.0
Research labs	360	10	13	1	–
Industrial plants	437	77	79	21	2
Medical institutions	256	79	84	17	3
Miscellaneous	31	5	–	–	–
Total	1084	171	176	39	5

During 1960, the total number of persons who handled radioactive isotopes and were subjected to systematic monitoring almost doubled over the 1959 figure, to reach 1475 people in 61 institutions of all kinds. The distribution of personnel subjected to exposure to ionizing radiation is listed in Table 1. We learn from these data that over 65% of the jobs of this type at industrial plants and in research institutions are filled by men. At the same time, female personnel are found to predominate in medical institutions (over 80%) where, judging by the sizes of the doses registered (Table 2), radiation protection and health-physics services were less conscientiously organized than in the research laboratories.

The authors of the report turn most of their attention to the fact that the majority (66%) of the cases of exposure of persons to doses greater than the permissible 5 rem/year occurred in the case of persons who were of adult age (18-30 years) and occupied with work in medical institutions or in industrial plants. In 1960, not a single one of the persons monitored was exposed to any dose exceeding the tolerable limit set by the formula D = 5 (N-18), where N is the person's age in years, and D is the permissible dose in rem.

* T. Musialowicz et al. Personnel film monitoring service in Poland during 1960. GLOR-8. Warsaw, Poland (1961).

BRIEF COMMUNICATIONS

Translated from Atomnaya Énergiya, Vol. 14, No. 2,
pp. 234-235, February, 1963

East Germany. An apparatus has been built at the heavy machinery plant in Magdeburg for testing large parts by high-level x-radiography and gamma-radiography. A 15 MeV betatron of Czech fabrication is used in this job. A Co^{60} source of 1400 curie activity will be used for special tests and investigations.

NEW LITERATURE

Translated from Atomnaya Énergiya, Vol. 14, No. 2,
pp. 236-244, February, 1963

Books and Symposia. Books released by Gosatomizdat (Atom Press) Publications

S. Goudsmit. The Alsos Mission. Translated from the English, 1962, 189 pages. 45 kopeks.

R. Clark. The Birth of the Bomb. Translated from the English [Horizon Press, 1961]. 1962, 168 pages. 47 kopeks.

Quite a few items of memoir-type literature has been published in the west following the Second World War, directly or indirectly elucidating various curious details of the work on building the atomic weapon and on conducting atomic tests in the USA, Britain, France, and Germany. The Soviet reader is already acquainted with some of this genre: the book Atoms in Our Home by A. Fermi, and Brighter Than a Thousand Suns by R. Jung. The books Alsos Mission and Birth of the Bomb are two more in this line.

The Alsos Mission is devoted to the activities of a special American military team landed in France after the opening of the 1944 second front against the Germans by the Allies. This team was charged with the task of interning German nuclear physicists and evaluating the German "nuclear potential."

The book Birth of the Bomb renders an account of British and French efforts to build an atomic weapon immediately prior to the Second World War and during the war. It is perfectly understandable that the authors of books of this type insist on the priority of the country which they represent in nuclear matters. Thus, the author of Birth of the Bomb emphasizes repeatedly that British and French scientists had pursued their research in the area to a point far in advance of the American counterparts, up to a certain stage. And only the occupation of France and the onerous military situation of England constrained those nations to turn over the results of their work to the USA and to join and subordinate their efforts to the American program. It is demonstrated with sufficient clarity in the book how "pure nuclear physics" gradually became converted, in the hands of politicians, into a weapon of blackmail and terror. The alarm which swept through the most prominent scientists on seeing how the tremendous discovery of the 20th century – the chain reaction – was being used and what uses it was being put to serve is the subject of quite a few dramatic pages. Particularly characteristic in this regard are those spots in the book which deal with the work of the famous French physicist, the Communist Frederic Joliot-Curie, and his colleagues. This progressive scientist saw in the chain reaction not a means of destruction, but a new and powerful source of useful energy. He and his colleagues and pupils consequently insisted unflaggingly on the idea of peaceful use of the chain reaction by building a nuclear power reactor.

Yadernye reaktsii Vol. I . Translation of Nuclear Reactions, edited by P. Endt and M. Demeur. Translated from the English. 1962, 450 pages, 2 rubles, 24 kopeks.

This book, written by renowned foreign physicists, is devoted to a survey of theoretical and experimental papers on the physics of nuclear reactions. The book contains ten articles illuminating three basic trends: the theory of nuclear models, dynamics of nuclear reactions, and experimental research.

The chapters devoted to the first category include: The theory of the nucleus as a many-body system (I), the shell model (II), the statistical model of the nucleus (VII), and rotational motion of nuclei (X). The second category includes: Angular correlation and polarization (IV); resonance reactions, theoretical part (V). The third category includes: Heavy-ion reactions (III); resonance reactions, experimental part (VI); neutron resonances in heavy nuclei (VIII); and review of experiments on α-particle reactions and scattering (IX).

The book is written for graduate students and scientific workers in the field of nuclear physics.

Teoriya i raschet lineinykh uskoritelei. [Theory and design of linear accelerators]. Collection of articles. 1962, 348 pages. 1 ruble, 28 kopeks.

This collection contains 22 papers on the theory and design of linear accelerators, on the basis of which lie the designs of the proton and electron accelerators built or being built at the Physics and Engineering Institute (PTI) of the Academy of Sciences of the Ukrainian SSR.

The articles report on investigations into the basic problems of linear acceleration and the dynamics of accelerated particles; the method of acceleration by radiation pressure is discussed, as well as some problems in plasma acceleration of particles; various accelerating systems are described and the most effective design methods are presented.

The reference literature lists are appended to each chapter.

Kal'tsii. [Calcium]. N. A. Dorogin. 1962, 192 pages. 56 kopeks.

This book is devoted to problems in the extraction and metallurgy of calcium, a metal which is used in the production of rare refractory metals, and in the production of high-quality steel and cast iron.

The book presents the basic information on the raw material used in calcium production; it describes the method for winning calcium oxide by roasting lime, chalk, and marble; the fundamentals of the chemistry calcium and calcium compounds are presented; the production of calcium chloride anhydrate, used in the production of calcium metal by electrolysis was discussed, and the physico-chemical properties of the electrolyte are cited; a description is given of the method for obtaining calcium by electrolysis of calcium chloride in molten-cathode baths; vacuum distillation of calcium from a copper-calcium alloy is discussed; the metallothermic technique and the method of production of calcium metal by thermal dissociation of calcium carbide were described, as well as several possible miscellaneous techniques for winning calcium metal. A special chapter is devoted to the production of high-purity calcium. Concise recommendations are presented on the storage of calcium and calcium alloys. The appendixes list vapor pressure constants, rates of vaporization of metals, and the engineering parameters of pumps used in calcium production.

The literature reference list includes over 60 titles.

Spravochnik po toksikologii radioaktivnykh izotopov [Handbook on toxicology of radioactive isotopes]. D. I. Zakutinskii, Yu. D. Parfenov, and L. N. Selivanova. Moscow, Medgiz (Medical Press), 1962. 116 pp.

The handbook systematizes numerous data on the toxicology of radioactive substances. It starts off with determinations of the terms most frequently encountered; a brief account is rendered of radioactive isotopes, providing basic information (ranges of application, pathways of intake into the organism, toxicological properties); data presented on the physico-chemical properties of the elements, the decay characteristics of radioisotopes, and on resorption and secretion of radioactive isotopes from the organism. The handbook also includes information on the "standard" man and on experimental animals, as well as on the dosimetry of radioactive isotopes, background irradiation of the human body, and maximum tolerable concentrations of radioactive isotopes. The handbook may prove useful, not only to specialists working the field of radiobiology, but also to a broad circle of scientific workers dealing with radioactive isotopes.

Translated from Atomnaya Énergiya, Vol. 14, No. 2,
pp. 237-244, February, 1963

I. Nuclear Physics

Neutron physics and reactor physics. Physics of hot plasma and controlled fusion reactions. Physics of acceleration of charged particles.

Zhur. tekhn fiz. 32, No. 9 (1962)

V. N. Tsytovich, 1042-1049. On the structure of nonlinear waves in a plasma.

Yu. S. Azovskii et al., 1052-1054. Conical plasmoid source.

M. V. Samokhin, 1055-1062. Determination of transport coefficients in a plasma by the Grad method.

R. I. Khrapko, 1063-1071. Stationary quasi-one-dimensional magnetogasdynamic currents at finite conductivity.

L. I. Grechikhin, and L. Ya. Min'ko, 1072-1073. On the structure of a plasma jet in a pulsed discharge.

V. F. Kitaeva et al., 1084-1089. Structure of the column of an arc discharge in argon. I. Local electrical characteristics of the column.

V. N. Kolesnikov and N. N. Sobolev, 1090-1094. Structure of the column of an arc discharge in argon. II. On the radius of the column and the form of radial distributions.

K. V. Donskoi et al., 1095-1098. Electrical conductivity measurements in gas jets.

É. P. Zimin and V. A. Popov, 1099-1101. Experimental study of the conductivity of combustion products of methane-oxygen mixtures with alkali metal additives.

Zhur. éksptl. i teoret. fiz. 43, No. 3 (1962)

L. I. Dorman and Yu. M. Mikhailov, 752-62. Study of electromagnetic phenomena in flow around bodies in a conducting fluid in a magnetic field.

S. E. Kupriyanov et al., 763-64. Dissociation cross section of D_3^+ ions into D_2^+ and D^+ ions in collisions with deuterium molecules.

S. I. Andreev et al., 804-807. Investigation of the effects of an external magnetic field on the light characteristics of a pulsed discharge in helium.

A. P. Babichev et al., 881-85. Corkscrew instability of a toroidal discharge in a variable magnetic field.

Izv. vyssh. ucheb. zaved. Radiofizika, 5, No. 4 (1962)

V. V. Zheleznyakov and E. Ya. Zlotnik, 644-57. On the conversion of plasma waves to electromagnetic waves in an inhomogeneous isotropic plasma.

G. I. Svetozarova and V. N. Tsytovich, 658-70. On spatial dispersion of a relativistic plasma in a magnetic field.

Izv. vyssh. ucheb. zaved. Fizika, No. 4 (1962)

Yu. K. Petrov et al., 21-27. Correction of the radial topography of a magnetic field in cyclic accelerators.

Izv. Tomsk. politekhn. inst., 100 (1962).

A. A. Vorob'ev et al., 162-69. Waveguide electron cyclic accelerator.

Izv. Tomsk. politekhn. inst., 122 (1962)

A. K. Berzin et al., 21-26. Investigation of neutron background by nuclear photoemulsions at a 25-MeV betatron.

A. K. Berzin et al., 27-29. Use of Ya-2 type nuclear emulsions in the study of betatron neutron spectra.

B. Z. Kanter et al., 45-49. A 5-MeV microtron.

V. A. Moskalev et al., 50-53. Results of the commissioning and starting of the 25-MeV pulsed two-chamber stereobetatron.

P. A. Cherdantsev, 54-60. Note on a magnetic field with optimized focusing properties.

A. N. Didenko and A. S. Chumakov, 61-65. Radial-phase motion of electrons in a synchrotron.

A. S. Chumakov, 66-69. Note on electron bunching in a synchrotron.

B. N. Morozov et al., 80-88. Investigation of uniformly bent periodically iris-loaded waveguides for a cyclic electron accelerator.

A. G. Vlasov et al., 99-107. Vacuum systems for electron accelerators.

Pribory i tekhn. éksp., No. 5 (1962)

G. S. Kazanskii et al., 19-24. Methods for varying the duration of beam-target interaction in the 10-GeV proton synchrotron.

V. N. Logunov and S. S. Semenov, 35-37. Effect of injector focusing on the γ-ray intensity of a betatron.

V. P. Agafonov et al., 47-50. Determining of γ recording efficiency by monochromatization of a bremsstrahlung beam.

Kh. D. Androsenko and G. N. Smirenkin, 64-71. A simple isodose neutron counter.

A. Adam et al., 72-76. Ion chamber for measuring energy of fast neutrons.

A. E. Golovin et al., 77-79. Time-lag system using magnetostriction delay lines for time-of-flight neutron spectrometry.

L. Ozhdyani et al., 80-83. Use of spark techniques in scintillation counting.

T. A. Romanova and L. D. Chikil'dina, 88-93. Rational introduction of uranium salts in uranium plates sensitive to minimum ionization.

D. G. Fleishman, 98-102. Investigation of statistical processes in scintillation counters.

Yu. Ya. Stavisskii and A. V. Shapar', 177-78. CaF_2 crystal scintillation counter.

Atompraxis, 8, No. 8 (1962)

E. Danóczy and L. Tari, 285-88. Study of a 2π-geometry counter with a wide band of β-particle energies.

Comptes rendus Acad. sci., 255, No. 1 (1962)

M. Surdin, 82-84. On the propagation of ultrasound in a plasma.

J. Appl. Phys., 33, No. 8 (1962)

P. Hedvall, 2426-28. Properties of a plasma formed by an electron beam.

M. Ericson et al., 2429-34. Confinement of a plasma by high-frequency electric fields.

P. Mazur, 2653-54. Origin of oscillations in low-pressure thermionic energy converters.

J. Appl. Phys., 33, No. 9 (1962).

R. Evans et al., 2682-88. Interdiffusion of gases in low-permeability graphite at uniform pressure.

J. Wilcox et al., 2714-15. Eddy currents in a rotating plasma.

Kernenergie, 5, No. 9 (1962)

W. Stolz, 668-75. On the energy transport mechanism in liquid scintillation systems.

O. Hauser, 685-89. The Rossendorf Central Nuclear Physics Institute. Division of Materials and Solids.

Kerntechnik, 4, No. 8 (1962)

H. Mahnau, 321-32. Measuring device uses "fast" ionization chamber to determine α-activity.

J. Moritz and H. Tauffenbach, 349-50. Semiconductor detectors.

Nucl. Instrum. and Methods, 16, No. 2 (1962)

M. Cryzinskii and M. Sadowski, 129-34. Establishing magnetic fields in plasma research.

B. Collinge and F. Marciano, 145-52. Equipment for recording instrument readings in nuclear research.

J. Colard, J. Gal, 195-98. Calibration of solid-state p-n type detectors with the aid of high-energy α particles and heavy particles.

P. Polly, 214-20. Transistorized single-channel kicksorter.

P. Polly, 221-26. Transistorized pulse generator.

R. Stein et al., 240-46. Study of discrimination of charged particles by the ionographic method.

Nucleonics, 20, No. 10 (1962)

A. Cameron, 50-54. Missions for nuclear instruments in space.

R. Heacock, 55-57. Problems in space instrument design.

J. Wolff and R. Ravanesi, 58-60. Multichannel analyzers in space.

W. Corliss, 61-63. Power sources for nuclear space instruments.

A. Metzger et al., 64-66. Ranger γ -ray spectrometer.

C. Schrader et al., 67-68. Instrument package for analyzing lunar surface.

C. Schrader et al., 69. High-energy γ -ray telescope.

C. Schrader et al., 70. Cosmic-ray detection and analysis.

V. Parsegian, 104, 106-107. Versatile accelerator facility for research and training.

Physics Today, 15, No. 8 (1962)

R. Thomas, 38-40, 42. Third Rochester symposium on magnetohydrodynamics.

II. Nuclear Power Engineering

Nuclear reactor design and calculations. Reactor design. Performance of nuclear reactors and reactor power stations.

Zhur. Vychislit. matem. i matem. fiz. 2, No. 4 (1962)

L. V. Maiorov, 635-51. On the distribution of thermal neutrons in a medium with a planar source.

Inzhener.-fiz. zhur., 5, No. 10 (1962)

I. I. Sidorova, 53-57. Analog simulation of reactor dynamics with a feedback loop.

Atomkernenergie, 7, No. 9 (1962)

R. Prushchek, 305-11. Effect of temperature dependence of coolant characteristics on the temperature field in a flow of coolant at the reactor core exit.

H. Schludi, 312-18. Resonance absorption integral of a fuel-element cluster.

J. Clauss, 319-20. On the possibility of building fast reactors having small concentrations of fissionable material.

J. Cockroft, 332-36. Results and outlook of the British nuclear power development program.

Atompraxis, 8, No. 9 (1962)

U. Rombusch et al., 339-44. Thermodynamic properties of heavy water.

K. Eto et al., 351-57. Japan's first swimming-pool reactor.

Energia nucleare, 9, No. 8 (1962)

G. Casini et al., 455-61. Critical experiments with heavy-water lattices using uranium oxide and organic coolant.

G. Zorzoli, 462-66. Computing the effective resonance surface.

Energia nucleare, 9, No. 9 (1962)

G. Zorzoli, 497-502. Temperature of fuel-element neutrons.

P. Bonnaure, 529-34. Design and experimental testing program of the ECO reactor.

Énergie nucléaire, 4, No. 4 (1962)

Y. Sousselier, 253-59. The present conjuncture in the production of atomic energy.

M. Guéron, 260-65. Euratom and the status of atomic power development in the member-nations of Euratom.

A. Baude, 266-77. Organization of the control of the Saclay nuclear reactor Ulysse.

Kernenergie, 5, No. 8 (1962)

B. Köhler, 606-10. Burnup and service life of burnable poisons.

Kerntechnik, 4, No. 8 (1962)

B. Löfblad, 334-38. Preparation and monitoring of corrosion-resistant tubing for a heat exchanger with D_2O-H_2O coolant.

H. Droscha, 339-40. Fabrication of the Kahl reactor pressure vessel.

A. Fackelmeyer, 341-43. Hoist cranes and other hoisting devices in nuclear power facilities.

L. Rule, 343. Reactor power stations in Britain.

A. Meichner, 344. On fires occurring in glove boxes.

Nucl. Sci. and Engng., 13, No. 4 (1962)

C. Mills, 301-305. Reactors with reflectors of moderator material.

D. Parks et al., 306-324. Thermal neutron spectra in graphite.

J. Ream and R. Varnes, 325-37. Transitional heat-transfer regime in UO_2 experimental fuel elements in a sodium-cooled experimental reactor.

G. György, 338-44. Effect of modal interaction on xenon poisoning instability.

Y. Fukai, 345-54. Comparison of computations of flux ratio in lattices by means of integral transport theory.

R. Cooper, 355-65. Fast-reactor rocket engines: critical size.

Nucleonics, 20, No. 10 (1962)

R. Cooper, 92. How Brookhaven inspects medical reactor control rods.

T. Ruane, 94, 96, 98. Measuring effective delayed-neutron fractions.

III. Nuclear Fuel and Nuclear Materials

Nuclear geology and primary ore technology. Nuclear metallurgy and secondary ore technology. Chemistry of nuclear materials.

Geokhimiya, No. 8 (1962)

L. V. Dmitriev and L. L. Leonova, 665-72. Uranium and thorium in granitoids of the Kaib massive (central Kazakhstan).

Geokhimiya, No. 9 (1962)

A. K. Lisitsyn, 763-69. On the forms of uranium occurrence in underground waters and in precipitations in the form of UO_2.

E. M. Es'kova et al., 770-77. Uranium and thorium in Ural alkaline rocks.

Doklady Akad. Nauk SSSR, 145, No. 1 (1962)

A. F. Kuzina et al., 106-108. Acetone extraction of technetium-99.

Zhur. anal. khim., 17, No. 4 (1962)

N. I. Udal'tsova, 476-80. Application of the ampermetric titration technique with two indicator electrodes in uranium determinations.

A. A. Nemodruk and I. E. Vorotnitskaya, 481-85. Extraction-luminescent technique for determining uranium in soils, silt, plants, and animal tissues.

T. S. Dobrolyubskaya, 486-88. Effect of hydrogen ion concentration in luminescent determinations of hexavalent uranium in uranyl nitrate solutions.

P. N. Palei and Z. K. Karalova, 528-29. Effect of fluorides on uranium determination in the presence of beryllium.

Izv. vyssh. ucheb. zaved. Tsvetnaya metallurgiya, No. 4 (1962)

A. F. Bessonov and V. G. Vlasov, 137-42. Kinetics of oxidation of uranium in air, oxygen, and carbon dioxide gas.

Izv. Sibirsk. otdel. akad. nauk SSSR, No. 6 (1962)

A. V. Nikolaev et al., 102-105. Extraction of uranyl nitrate by diluted TBP in laboratory columns.

Issledovaniya po zharoprochnym splavam, 8 (1962)

N. S. Alferova et al., 172-77. Electron-microscope studies of the structure of ductile fracture in 1Kh18N9T stainless steel.

A. I. Parshin and I. E. Kolosov, 230-42. Nature of the anomalous behavior of 1Kh18N9T steel in long-term strength tests.

Trudy inst. geol. rudn. mestrozh., petrografii, mineralogii i geokhimii, No. 70 (1962)

S. G. Batulin, 15-19. On some features of uranium geochemistry in seas and lakes.

Trudy inst. geol. rud. m. petro., mineral. i geokhim., No. 82 (1962)

N. P. Laverov, et al., 116-35. Geological structure of uraniferous hydrothermal deposits confined to vent facies of effusive rocks and to subvolcanic intrusives.

B. P. Khudyakov, 136-42. On structural-lithological control of uranium mineralization in veins of carbonate-pitch formations.

A. A. Chernikov, 162-81. Hypergenetic zoning on sulfide-uranium occurrences and the reasons for zonation.

Trudy Kishinev. sel'sko-khoz. inst., 26 (1962)

M. P. Pavlovskaya and I. M. Reibel', 53-63. Optical and potentiometric techniques in determination of composition of uranyl ion complex with orthohydroxyquinolin.

M. P. Pavlovskaya and I. M. Reibel', 65-71. Determination of composition of uranyl complexes with oxime (in 2.5 M CH_3COOH) in the presence of isoamyl alcohol.

M. P. Pavlovskaya and I. M. Reibel', 73-79. Determination of the composition of uranyl ion complex with sulfosalicylic acid by potentiometric titration.

Fizika metallov i metallovedenie, 14, No. 2 (1962)

V. M. Zhukovskii et al., 319-20. Electrical properties of a uranium-oxygen system in the U_3O_8-UO_2 composition range.

Atompraxis, 8, No. 9 (1962)

E. Schmid, 321-35. Effect of bombardment by particles on the properties of solids.

E. Berninger, et al., 336-39. Effect of irradiation on the plasticity of metal crystals.

P. Lõwenstein, 357-62. Use of beryllium metal in reactors. II.

Chem. and Process Engng., 43, No. 9 (1962)

D. Morris and D. Slater, 442-47. Production of radioisotopes by bombardment with positively charged particles.

Energia nucleare, 9, No. 8 (1962)

G. Arcelli et al., 472-80. Hot shielded cave for research on the analytic chemistry of radioactive materials.

Energia nucleare, 9, No. 9 (1962)

A. Bassi et al., 513-28. Electron-microscopic study of cracks in sintered uranium oxide.

Énergie nucléaire, 4, No. 4 (1962)

A. Level, 278-86. The role of fluorine in uranium chemistry.

J. Appl. Phys., 33, No. 9 (1962)

L. Ianniello and A. Burr, 2689-90. Effect of various rare earths on the transition of the hexagonal close-packed structure of zirconium to the body-centered cubic structure.

J. Appl. Phys, 33, No. 10 (1962)

K. Yamamoto and M. Tsuchiya, 3016-3020. Electrical characteristics of glass in viewing windows exposed to γ -rays.

L. Chadderton, 3021-22. Dislocation loops in lead iodide irradiated by fission fragments.

D. Mosedale, 3143-44. Effect of irradiation on creep in metals.

J. Nucl. Materials, 6, No. 3 (1962)

C. Cupp, 241-55. Effect of neutron irradiation on the mechanical properties of zirconium alloy containing 2.5% niobium.

G. Boisde et al., 256-64. Study of production of high-grade beryllium by electrolytic refining in fused salts.

D. Smith et al., 265-70. High-temperature crystallographic phase transformation of BeO.

R. Aubeau et al., 271-80. Metering of small amounts of oxygen and argon in a gas coolant, by chromatography.

C. Walter and L. Kelman, 281-90. Study of the rate of penetration of fused uranium and uranium-fission alloy into stainless steel.

J. Wanklyn and P. Jones, 291-329. Corrosive attack on reactor metals in water.

S. Carniglia, 330-31. Determination of internal stresses in BeO. (Comment on article "Diffraction of x-rays in BeO").

G. Bentle, 336-37. Room-temperature elasticity of BeO.

J. Leteurtre, 338-41. Dislocation mechanism in uranium.

J. Leteurtre and G. Brebec, 342-45. Study of krypton-containing uranium by an electron microscope.

J. Sci. and Industr. Res., 21, No. 7 (1962)

V. Athavale and C. Krishnan, 339-40. Determination of alkali in uranium.

Kernenergie, 5, No. 8 (1962)

H. Liebscher and C. Fischer, 616-17. On the wet method in uranium tetrafluoride production.

R. Dreyer, 618-21. Note on the mechanism of the isotope exchange reaction $PtCl_6^{=} + Cl^{-} \rightleftarrows PtCl_6^{=} + Cl^{-}$.*

Kernenergie, 5, No. 9 (1962)

H. Röllig, 641-68. Compatibility between nuclear metal fuel and the jacket.

Korntechnik, 4, No. 8 (1962)

W. Fleischmann, 327-33. Radiation effects on properties of structural materials.

Materials Research and Standards, 2, No. 8 (1962)

H. Kalisch and F. Litton, 638-39. Thermal expansion of fuel plates of stainless steel and uranium dioxide.

Memoires Sci. Rev. Metallurgie, 59, No. 3 (1962)

C. Sauve, 208-224. Hydraulic pressing of jackets for cladding of tubular uranium-zirconium fuel elements.

Mining Journal, 259, No. 6626 (1962)

C. Sauve, 151-52. Lithium: mineral resources, winning, and use.

Nature, 195, No. 4839 (1962)

N. Allen, 317-18. Reactor materials and radiation damage.

Nucl. Sci. and Engng., 13, No. 4 (1962)

H. Waldron, 366-73. Review of methods for determining hydrogen in uranium.

W. Kelley and B. Twitty, 374-77. Improved method for determining isotope ratio of U^{235} in unpurified materials.

E. Kovacic, et al., 378-84. Capsule irradiation of uranium alloy paste with 10 wt. % molybdenum powder in sodium-potassium.

T. Eastwood and R. Werner, 385-90. Resonance and self-shielding of thermal neutrons in foils and cobalt wire.

G. Cathers et al., 391-97. Laboratory-scale demonstration of the process of volatilization of fused salts.

Nucleonics, 20, No. 10 (1962)

G. Cathers et al., 74. Pinhole camera speeds fuel sample tests.

U. Upson and F. Roberts, 86, 88. An in-cell γ-analyzer.

R. Hardell and S. Nilsson, 108, 110-111. Titanium and electrolytic iron for reactor-irradiation containers.

IV. Nuclear Radiation Shielding

Radiation safety. Shielding against ionizing radiations.

Agrobiologiya, No. 4 (1962)

V. V. Bernard and I. T. Geller, 610-16. Effect of γ radiation on several groups of soil microflora.

Biokhimiya plodov i ovoshchei, Coll. No. 7 (1962)

L. V. Metlitskii et al., 5-50. Use of ionizing radiations to control dormancy of potato tubers during storage.

A. I. Grechushnikova and V. S. Serebrenikov, 51-59. Effect of γ irradiation of tubers on carbohydrate and protein turnover in potato plants.

Vestnik sel'sko-khoz. nauki, No. 8 (1962)

M. K. Mel'nikova et al., 128-31. Pathways for inhibiting uptake of radiostrontium in plants.

*It appears thus in the Russian text.

Vestnik sel'sko-khoz. nauki, No. 9 (1962)

S. I. Yanushkevich, 110-14. Effect of pre-sowing γ irradiation on fertilization capability of grass pollen.

Gigiena i sanitariya, No. 7 (1962)

S. P. Golenetskii, 33-42. Determination and continuous recording of content of short-lived radioisotopes in air of aerosols by the filter "saturation" method.

V. N. Gus'kova and A. N. Bragina, 103-105. Note on soil radioactivity. Report No. 2.

Zhur. prikladnoi khim., 35, No. 6 (1962)

Yu. A. Kokotov and R. F. Popova, 1242-45. Sorption of long-lived fission products on soils and clayey minerals.

Zapisi Leningrad. sel'sko-khoz. inst., 84 (1962)

E. I. Panteleeva et al., 143-51. Effect of radium, potassium, and uranium on plant development under conditions of soil contamination by strontium-90 and cesium-137.

L. L. Ruppert, 152-56. Note on phosphorus and nitrogen turnover in barley plants affected by radiostrontium and uranium.

Zashchita rastenii ot vreditelei i boleznei, No. 9 (1962)

S. V. Andreev et al., 25-26. γ radiation in the fight against plant pests.

Okeanologiya, 2, No. 4 (1962)

N. N. Sysoev and Yu. I. Kirilyuk, 743-45. Information on the radioactivity of Pacific Ocean waters.

Sbornik nauchn. rabot inst. okhrany truda VTsSPS, No. 2 (1962)

E. D. Chistov et al., 65-74. Radiation shielding of the general-purpose high-level γ irradiation facility K-60,000.

Soobshcheniya akad. nauk Gruz. SSR, 28, No. 5 (1962)

B. M. Kavteladze, 583-86. Note on investigation of natural radioactivity of some soils and plants in the Gruz. SSR.

Atomkernenergie, 7, No. 9 (1962)

W. Rentshler and H. Schreiber, 325-28. Measurement of artificial radioactivity of atmospheric fallout and dust.

Atompraxis, 8, No. 8 (1962)

R. Plesch, 297-303. Effect of absence of saturation conditions on measurement of uniformly distributed activity.

H. Dreiheller, 303-306. Measurement of low-level γ activity with a scintillation well counter.

K. H. Weber, 307-310. Sensitivity of Geiger-Muller counters to x-radiation and γ radiation. II.

Chem. and Engng. News, 40, No. 42 (1962)

K. H. Weber, 60. Use of matrices of solid sulfur for storage of radioactive wastes.

Kernenergie, 5, No. 8 (1962)

H. Moldenhawer, 585-600. Surface contamination and deactivation.

Z. Spurny, 611-15. A thermoluminescent dosimeter.

Kernenergie, 5, No. 9 (1962)

K. F. Poulheim, 675-77. Investigation of "hot" particulate matter in an atmospheric aerosol.

H. Reissig, 678-84. Effect of lime fertilizer on uptake of Sr^{90} isotope by crop plants, under field conditions.

Nucleonics, 20, No. 10 (1962)

E. Ballinger et al., 76, 78, 80, 82, 85. Determination of neutron dose in terms of body Na^{24} activity.

R. Begley, 100. Liquid sodium absorbs gaseous iodine.

V. Radioactive and Stable Isotopes

Izv. vyssh. ucheb. zaved. Khimiya i khim. tekhnologiya, 5, No. 3 (1962)

V. E. Panova and M. D. Nasyrova, 371-73. Radiometric determination of lead, using Cr^{51} isotope.

Izv. Timiryazev. sel'sko-khoz. akad., No. 3 (1962)

Kh. A. Yarvela, 171-84. Estimate of accuracy of measurement of humidity of soil ground by neutron techniques under field conditions.

Sadovodstov, Vinogradarstvo i vinodelie Moldavii, No. 9 (1962)

L. G. Parfenenko, 33-35. Radioisotopes in the study of grapevine root systems.

Trudy Vsesoyuz. inst. po proekt. i nauchn. issled. rabot. Giprotsement, No. 24 (1962)

E. I. Morozov, 103-118. Study of interaction between clinker components and refractories by the radiotracer technique.

Trudy Vsesoyuz. nauch.-issled. inst. gidrotekhniki i melioratsii, 38 (1962)

E. G. Petrov and V. A. Emel'yanov, 5-12. Results and outlook of applications of nuclear radiations and radioactive tracers in irrigation, and land reclamation studies.

V. A. Emel'yanov, 28-38. Improved γ survey technique for measuring soil density.

S. I. Shoikhet, 46-55. γ monitoring of consistency of pulp moving through dredge lines.

M. V. Preobrazhenskaya, 56-67. Application of γ monitoring to the determination of soil humidity in soil improvement studies.

Sun, Yun-cha, 68-71. Observations of moisture migration in a column of soil by γ scanning techniques.

L. I. Beskin and A. I. Zaitsev, 72-83. Neutron method for soil moisture determination.

L. I. Beskin, 89-96. Results of testing of a neutron moisture sensor for automatic water metering at concrete plants.

M. P. Volarovich et al., 97-115. Tracer applications in the study of structure, moisture transport processes, and water content in peat.

M. P. Volarovich et al., 119-131. Study of water transport processes in a peat deposit by radioactive tracer methods.

R. Čabart, 139-43. Radioisotope techniques in land improvement experiments in Czechoslovakia.

V. E. Nesterov, 144-49. The outlook for the use of β radiation in soil and land improvement studies.

Trudy gidrolog. inst., No. 87 (1962)

A. M. Dimaksyan, 27-45. Remote measurement of water budget in snow by means of nuclear radiations.

Trudy Grozn. neft. nauchno-issled. inst., No. 13 (1962)

É. V. Sokolovskii, 99-106. On the reliability of data obtained in establishing the quality of a cement ring with isotope tracers.

Trudy inst. yadernoi fiz. akad. nauk Kazakh. SSR, 5 (1962)

A. A. Arkhangel'skii and G. D. Latyshev, 117-27. Experience in the use of a scintillation γ-radiographic facility.

Trudy Sverdlovsk. gorn. inst., No. 41 (1962)

G. S. Vozzhenikov, 125-28. On the activation constants of some isotopes.

Trudy Khar'kov. avtomobil.-dorozhn. inst., No. 29 (1962)

Yu. A. Kal'ko, 118-26. Tracer laboratory for measuring resistance to wear of machine parts.

Yu. A. Kal'ko, 127-29. Facility for introducing radiozinc into babbitt alloy by a melting technique.

Khim. promyshlennost', No. 6 (1962)

Ya. D. Zel'venskii and V. A. Shalygin, 38-41. Radioisotope applications in the study of rectification and testing of rectification columns.

Atomkernenergie, 7, No. 9 (1962)

H. Moser et al., 321-24. Radioisotope applications in hydrology. V. Tracer measurement of rate of flow of open streams.

Energia nucleare, 9, No. 9 (1962)

B. Chinaglia et al., 503-512. Applications of short-lived isotopes in activation analysis.

Jaderná energie, No. 12 (1962)

V. Santholcer and V. Havlovic. Increase in radioactive fallout during spring of 1962, and mechanism of distribution of nuclear fragments in the atmosphere.

P. Kovanic and J. Rýhl. Neutron probe operates with pulse fission chamber and ferrite transformer.

M. Kyrš, L. Holeckova, and L. Heyman, Concentration and isolation of cesium-137 from mains water of river water by nitrobenzene solvent extraction of polyiodides.

J. Kubát. Level gage.

J. Dlouhy. Investigation of physical and chemical methods of measurement, and their uses.

M. Kyrš. Mechanism of solvent extraction of various cesium compounds from the aqueous phase into nitrobenzene.

Svetepa and Doksanský. Use of Ca^{45} to detect layers of steel corrosively attacked by water.

Spiro. Linear pulse differential amplifier.

Soviet Journals Available in Cover-to-Cover Translation

ABBREVIATION	RUSSIAN TITLE		TITLE OF TRANSLATION	PUBLISHER	TRANSLATION Vol.	Issue	BEGAN Year
AÉ	Atomnaya énergiya		Soviet Journal of Atomic Energy	Consultants Bureau	1	1	1956
Akust. zh.	Akusticheskii zhurnal		Soviet Physics – Acoustics	American Institute of Physics	1	1	1955
	Astronomicheskii zhurnal		Soviet Astronomy – AJ	American Institute of Physics	34	1	1957
Astr(on). zh(urn).	Avtomaticheskaya svarka		Automatic Welding	Br. Welding Research Assn. (London)	12	1	1959
Avto(mat). svarka	Avtomatika i Telemekhanika		Automation and Remote Control	Instrument Society of America	27	1	1956
	Biofizika		Biophysics	National Institutes of Health**	6	1	1961
	Biokhimiya		Biochemistry	Consultants Bureau	21	1	1956
Byull. éksp(erim). biol. (i med.)	Byulleten' éksperimental'noi biologii i meditsiny		Bulletin of Experimental Biology and Medicine	Consultants Bureau	41	1	1959
		Life Sciences	Doklady Biological Sciences Sections (includes: Anatomy, biochemistry, biophysics, cytology, ecology, embryology, endocrinology, evolutionary morphology, genetics, histology, hydrobiology, microbiology, morphology, parasitology, physiology, zoology)	National Science Foundation*	112	1	1957
		Life Sciences	Doklady Botanical Sciences Sections (includes: Botany, phytopathology, plant anatomy, plant ecology, plant embryology, plant physiology, plant morphology)	National Science Foundation*	112	1	1957
DAN (SSSR) Dokl(ady) AN SSSR	Doklady Akademii Nauk SSSR	Chemical Sciences	Proceedings of the Academy of Sciences of the USSR, Section: Chemical Technology	Consultants Bureau	106	1	1956
		Chemical Sciences	Proceedings of the Academy of Sciences of the USSR, Section: Chemistry	Consultants Bureau	106	1	1956
		Chemical Sciences	Proceedings of the Academy of Sciences of the USSR, Section: Physical Chemistry	Consultants Bureau	112	1	1957
		Earth Sciences	Doklady Earth Sciences Sections (includes: Geochemistry, geology, geophysics, hydrogeology, lithology, mineralogy, oceanology, paleontology, permafrost, petrography)	American Geological Institute	124	1	1959
		Earth Sciences	Proceedings of the Academy of Sciences of the USSR, Section: Geochemistry	Consultants Bureau	106-123	1-6	1956-1958
		Earth Sciences	Proceedings of the Academy of Sciences of the USSR, Section: Geology	Consultants Bureau	112-123	1-6	1957-1958
		Mathematics	Soviet Mathematics – Doklady	American Mathematical Society	130	1	1960
		Physics	Soviet Physics – Doklady (includes: Aerodynamics, astronomy, crystallography, cybernetics and control theory, electrical engineering, energetics, fluid mechanics, heat engineering, hydraulics, mathematical physics, mechanics, physics, technical physics, theory of elasticity sections)	American Institute of Physics	106	1	1956
	Elektrosvyaz'		Telecommunications	Am. Inst. of Electrical Engineers		1	1957
Entom(ol). oboz(r).	Entomologicheskoe obozrenie		Entomological Review	National Science Foundation**	37	1	1958
FMM	Fizika metallov i metallovedenie		Physics of Metals and Metallography	Acta Metallurgica	5	1	1957
FTT, Fiz. tv(erd). tela	Fizika tverdogo tela		Soviet Physics – Solid State	American Institute of Physics	1	1	1959
Fiziol. Zh(urn). SSSR	Fiziologicheskii zhurnal imeni I.M. Sechenov		Sechenov Physiological Journal USSR	National Institutes of Health**	47	1	1961
Fiziol(ogiya) rast.	Fiziologiya rastenii		Plant Physiology	National Science Foundation*	4	1	1957
	Geodeziya i aerofotosyemka		Geodesy and Aerophotography	American Geophysical Union			1962
	Geokhimiya		Geochemistry	The Geochemical Society	1	1	1956
Geol. nefti i gaza	Geologiya nefti i gaza		Petroleum Geology	Petroleum Geology	2	1	1958
	Geomagnetizm i aeronomiya		Geomagnetism and Aeronomy	American Geophysical Union	1	1	1961
	Iskusstvennye sputniki zemli		Artificial Earth Satellites	Consultants Bureau	1	1	1958
Izmerit. tekhn(ika)	Izmeritel'naya tekhnika		Measurement Techniques	Instrument Society of America	7	1	1958

The translation of this journal is published in sections

Izv. AN SSSR O(td). Kh(im). N(auk)	Izvestiya Akademii Nauk SSSR: Otdelenie khimicheskikh nauk	Bulletin of the Academy of Sciences of the USSR: Division of Chemical Science	Consultants Bureau	16	1	1952
Izv. AN SSSR O(td). T(ekhn). N(auk): Metall). i top.	(see Met. i top)					
Izv. AN SSSR Ser. fiz(ich).	Izvestiya Akademii Nauk SSSR: Seriya fizicheskaya	Bulletin of the Academy of Sciences of the USSR: Physical Series	Columbia Technical Translations	18	3	1954
Izv. AN SSSR Ser. geofiz.	Izvestiya Akademii Nauk SSSR: Seriya geofizicheskaya	Bulletin of the Academy of Sciences of the USSR: Geophysics Series	American Geophysical Union	7	1	1957
Izv. AN SSSR Ser. geol.	Izvestiya Akademii Nauk SSSR: Seriya geologicheskaya	Bulletin of the Academy of Sciences of the USSR: Geologic Series	American Geological Institute	23	1	1958
Iz. Vyssh. Uch. Zav., Tekh. Teks. Prom.	Izvestiya Vysshikh Uchebnykh Zavedenii Tekhnologiya Tekstil'noi Promyshlennosti	Technology of the Textile Industry, USSR	The Textile Institute (Manchester)	4	1	1960
Kauch. i rez.	Kauchuk i rezina	Soviet Rubber Technology	Palmerton Publishing Company, Inc.	18	3	1959
	Kinetika i kataliz	Kinetics and Catalysis	Consultants Bureau	1	1	1960
	Koks i khimiya	Coke and Chemistry, USSR	Coal Tar Research Assn. (Leeds, England)		8	1959
Kolloidn. zh(urn).	Kolloidnyi zhurnal	Colloid Journal	Consultants Bureau	14	1	1952
	Kristallografiya	Soviet Physics – Crystallography	American Institute of Physics	2	1	1957
Metallov. i term.	Metallovedenie i termicheskaya obrabotka metallov	Metals Science and Heat Treatment of Metals	Acta Metallurgica	6	1	1958
	Metallurg	Metallurgist	Acta Metallurgica		1	1957
Met. i top.(gorn.)	Metallurgiya i toplivo (gornoye delo)	Russian Metallurgy and Fuels(mining)	Scientific Information Consultants, Ltd.		1	1960
Mikrobiol.	Mikrobiologiya	Microbiology	National Science Foundation*	26	1	1957
	Ogneupory	Refractories	Acta Metallurgica	25	1	1960
OS, Opt. i spektr.	Optika i spektroskopiya	Optics and Spectroscopy	American Institute of Physics	6	1	1959
Paleontol. Zh(urn)	Paleontologicheskii Zhurnal	Journal of Paleontology	American Geological Institute		1	1962
	Pochvovedenie	Soviet Soil Science	National Science Foundation**	53	1	1958
	Poroshkovaya Metallurgiya	Soviet Powder Metallury and Metal Ceramics	Consultants Bureau	2	1	1962
	Priborostroenie	Instrument Construction	Taylor and Francis, Ltd. (London)	4	1	1959
Pribory i tekhn. éks(perimenta)	Pribory i tekhnika éksperimenta	Instruments and Experimental Techniques	Instrument Society of America	3	1	1958
Prikl. matem. i mekh(an).	Prikladnaya matematika i mekhanika	Applied Mathematics and Mechanics	Am. Society of Mechanical Engineers	22	1	1958
PTE	(see Pribory i tekhn. éks.)					
	Problemy Severa	Problems of the North	National Research Council of Canada		1	1958
	Radiokhimiya	Radiochemistry	Consultants Bureau	4	1	1962
Radiotekh.	Radioteknika	Radio Engineering	Am. Institute of Electrical Engineers	16	1	1961
Radiotekhn. i élektron(ika)	Radiotekhnika i électronika	Radio Engineering and Electronic Physics	Am. Institute of Electrical Engineers	6	1	1961
	Stal'	Stal (in English)	Iron and Steel Institute	19	1	1959
	Stanki i instrument	Machines and Tooling	Production Engineering Research Assoc.	30	1	1959
Stek. i keram.	Steklo i keramika	Glass and Ceramics	Consultants Bureau	13	1	1956
Svaroch. proiz-vo	Svarochnoe proizvodstvo	Welding Production	Br. Welding Research Assn. (London)	5	4	1959
Teor. veroyat. i prim.	Teoriya veroyatnostei i ee primenenie	Theory of Probability and Its Application	Soc. for Industrial and Applied Math.	1	1	1956
Tsvet. metally	Tsvetnye metally	The Soviet Journal of Nonferrous Metals	Primary Sources	33	1	1960
UFN	Uspekhi fizicheskikh nauk	Soviet Physics – Uspekhi (partial translation)	American Institute of Physics	66	1	1958
UKh, Usp. khimi	Uspekhi khimii	Russian Chemical Reviews	Chemical Society (London)	29	1	1960
UMN	Uspekhi matematicheskaya nauk	Russian Mathematical Surveys	Cleaver-Hume Press, Ltd. (London)	15	1	1960
Vest. mashinostroeniya	Vestnik mashinostroeniya	Russian Engineering Journal	Production Engineering Research Assoc.	39	4	1959
Vop. onk(ol).	Voprosy onkologii	Problems of Oncology	National Institutes of Health**	7	1	1961
Zav(odsk). lab(oratoriya)	Zavodskaya laboratoriya	Industrial Laboratory	Instrument Society of America	24	1	1958
ZhAKh, Zh. anal(it). Khim(ii)	Zhurnal analiticheskoi khimii	Journal of Analytical Chemistry	Consultants Bureau	7	1	1952
ZhETF Zh. éksperim. i teor. fiz.	Zhurnal eksperimental'noi i teoreticheskoi fiziki	Soviet Physics – JETP	American Institute of Physics	28	1	1955
ZhFKh Zh. fiz. khimii	Zhurnal fizicheskoi khimii	Russian Journal of Physical Chemistry	Chemical Society (London)	33	7	1959
ZhNKh Zh. neorg(an). khim.	Zhurnal neorganicheskoi khimii	Journal of Inorganic Chemistry	Chemical Society (London)	4	1	1959
ZhOKh Zh. obshch. khim.	Zhurnal obshchei khimii	Journal of General Chemistry USSR	Consultants Bureau	19	1	1949
ZhPKh Zh. prikl. khim.	Zhurnal prikladnoi khimii	Journal of Applied Chemistry USSR	Consultants Bureau	23	1	1950
ZhSKh Zh. strukt(urnoi) khim.	Zhurnal strukturnoi khimii	Journal of Structural Chemistry	Consultants Bureau	1	1	1960
ZhTF	Zhurnal tekhnicheskoi fiziki	Soviet Physics – Technical Physics	American Institute of Physics	26	1	1956
Zh. tekhn. fiz.	Zhurnal vychislitel'noi matematika i matematicheskoi fiziki	U.S.S.R. Computational Mathematics and Mathematical Physics	Pergamon Press, Inc.	1	1	1962
Zh. vyssh. nervn. deyat. (im. Pavlova)	Zhurnal vysshei nervnoi deyatel'nosti (im I. P. Pavlova)	Pavlov Journal of Higher Nervous Activity	National Institutes of Health**	11	1	1961

*Sponsoring organization. Translation published by Consultants Bureau.
**Sponsoring organization. Translation published by Scripta Technica.

SOVIET PROGRESS IN NEUTRON PHYSICS

Edited by **P. A. Krupchitskii**

A collection of 40 original and review papers by Soviet specialists, publication of which was deemed essential by the editorial board of the *Soviet Journal of Atomic Energy*. The collection includes 18 contributions on moderation, resonance absorption, and neutron diffusion; 12 on the interactions of fast neutrons with nuclei; 6 on fission, fragments, and secondary neutrons; and 4 papers on gamma-radiation in neutron capture. The abundance of new data on neutron physics is of great interest, as is the material on the shielding of nuclear reactors and that on theoretical physics. Included among the authors are such important researchers as *G. I. Marchuk, A. D. Galanin, A. V. Stepanov, V. V. Orlov, V. I. Popov* and *N. S. Lebedeva*.

Contents include:

Measurement of the Energy Dependence of the Cross Section of the Cl (n,γ) Reaction • Gamma-Radiation in Inelastic Interaction between Fast Neutrons and Atomic Nuclei • Spectra of γ-rays which Accompany the Capture of Thermal Neutrons by Mo, Nb, Ho, Tu, and La Nuclei • Inelastic Scattering of Neutrons with Energies from 3.2 to 4.5 Mev on Beryllium • Spatial Distributions of Neutrons in Mixtures of Boron Carbide with Iron and Lead • Fragment Yields in the Fission of U^{235} and U^{238} by Fast Neutrons • Yields of Certain Fragments in Th^{232} Fission by 14.3-Mev Neutrons • Effect of the Resonance Structure of Cross-Sections on Neutron Diffusion • Multigroup Method of Calculating the Energy-Space Distribution of Thermal-Neutron Flux, and the Application of the Perturbation Method • Neutron Scattering by Crystals in the Incoherent Approximation • Theory of Thermal Neutron Diffusion with Velocity Distribution Taken into Account

278 pages $40.00

PHOTONEUTRON METHOD OF DETERMINING BERYLLIUM

by **Kh. B. Mezhiborskaya**

***"of value to all analysts using the photoneutron method"*—Current Engineering Practice**

***"extremely useful...well presented"*—The Analyst**

The radioactivation or photoneutron method for the determination of beryllium in mineral raw materials and hydrometallurgical products has been widely used in the Soviet Union. One of the foremost Soviet scientists in this field, Kh. B. Mezhiborskaya, presents the results of more than eight years of research.

A highly efficient technique for determining beryllium, the photoneutron method is usually employed by analysts having little knowledge of nuclear physics methods. This report presents a detailed discussion of the fundamentals of the method, apparatus for determining and prospecting for beryllium, recording methods, analysis procedures, effects of interference, standards, etc.

In addition, PHOTONEUTRON METHOD OF DETERMINING BERYLLIUM deals with the safety problems which occur during the practical use of this nuclear analysis method. Complete instructions on safety precautions are given, including shielding materials, dosimetric checking, space and equipment requirements.

This technical report will be of value to all analysts using the photoneutron method, as well as to those medical researchers concerned with radiation hazards and their prevention.

A Consultants Bureau Special Report 16,000 words $12.50

CONSULTANTS BUREAU
227 W. 17 ST., NEW YORK 11, N. Y.

Declassified and Approved For Release 2013/09/25 : CIA-RDP10-02196R000600100002-6

spectroscopy

ANALYSIS INSTRUMENTATION 1963

edited by Dr. L. Fowler, R. D. Eanes, and T. J. Kehoe

An expertly written book drawing upon the skills of leaders in analytical and process instrumentation to present an up-to-the-minute picture of the current state of development of this fast-growing field, including a number of startling new instruments and systems never before reported. *272 pages, $12.50*

IR — THEORY AND PRACTICE OF INFRARED SPECTROSCOPY

by Dr. Herman A. Szymanski and Dr. Nelson L. Alpert

A unique text providing complete coverage of all aspects of infrared spectroscopy, from basic theoretical principles to the very latest practical applications. The instrument chapter, written by Dr. Alpert, deals with general principles of IR instrumentation applicable to present and future developments. The text, amply supplemented by illustrations, charts, and all-new high-resolution spectra, includes a chapter devoted to "The Spectral Library" describing documentation, abstracting and reference services. *est. 300 pages, $10.00*

INFRARED BAND HANDBOOK

by Dr. Herman A. Szymanski, Chairman, Chem. Dept., Canisius College

Over 8500 band positions of organic and inorganic compounds tabulated according to wavenumber of their IR spectral absorption bands. Data retrieval time is cut since all compounds with absorption at a given wavelength are listed sequentially, and the formula cross index lists all bands produced by compounds. Completely referenced. Sample pages upon request.

496 pages, $35.00; annual supplements, $7.50

DEVELOPMENTS IN APPLIED SPECTROSCOPY, Volumes 1-3

Proceedings of the Annual Mid-America Spectroscopy Symposia sponsored by the Society for Applied Spectroscopy

A convenient and comprehensive guide to the latest research and developments in the field. Complete contents upon request.

Volume 1: edited by W. D. Ashby, Picker X-Ray Corp. *270 pages, $9.00*

Volume 2: edited by J. R. Ferraro, Argonne National Laboratory, and J. S. Ziomek, Martin-Marietta Corp. *448 pages, $16.00*

Volume 3: edited by J. E. Forrette and E. Lanterman, Borg-Warner Corp. *in preparation*

PROGRESS IN INFRARED SPECTROSCOPY, Volumes 1 and 2

Proceedings of the Annual Infrared Spectroscopy Institutes, Canisius College

Volume 1: Instrumentation (*all* spectral regions) and instrument design; group theory; analytical applications of UV, visible, near-IR absorption spectroscopy; inorganic IR spectroscopy; high-resolution instrumentation; KBr disk techniques; quantitative analysis; Raman spectroscopy; incorporation of NMR spectroscopy into the IR laboratory. Includes all discussions and a very extensive bibliography. *452 pages, $16.00*

Volume 2: Compact, expert surveys of specialized phases of contemporary spectroscopic methods: Far infrared, Raman, polarized infrared, inorganic infrared, near infrared, ultraviolet and visible, theoretical, instrumentation. *in preparation*

INTERPRETED INFRARED SPECTRA

prepared by Dr. Herman A. Szymanski

Some 300 IR spectra of all common classes of organic compounds have been marked to identify the structural groups causing typical absorption peaks. Of wider application than correlation tables, as interfering and related bands can be seen at a glance. *est. 200 pages, about $7.50*

RESEARCH ON SPECTROSCOPY AND LUMINESCENCE

A series documenting original research carried out at the P.N. Lebedev Institute of Physics, Acad. Sci. USSR. Extensive bibliographies. Translated from Russian.

1. Calculation of Wave Functions and Oscillator Strengths of Complex Atoms, by L. A. Vainshtein. *50 pages, $12.50*
2. On the Broadening and Shift of Spectral Lines in the Plasma of a Gaseous Discharge, by M. A. Mazing. *66 pages, $15.00*
3. On Excitation Spectra in Spark Discharges, by N. K. Sukhodrev. *52 pages, $12.50*
4. The Radioluminescence Yield of Organic Substances, by Z. A. Chizhikova. *50 pages, $12.50*

special set price (parts 1-4): $40.00

further information and complete contents on request

PLENUM PRESS 227 West 17th Street, New York 11, New York